University at Buffalo
The State University of New York

Guidelines for Implementing Seismic Base Isolation in Advanced Nuclear Reactors - Revision 01

by

Faizan Ul Haq Mir, Ching-Ching Yu, Benjamin M. Carmichael, Brandon M. Chisholm, Jason Redd, Mohamed M. Talaat, Chandrakanth Bolisetti, and Andrew S. Whittaker

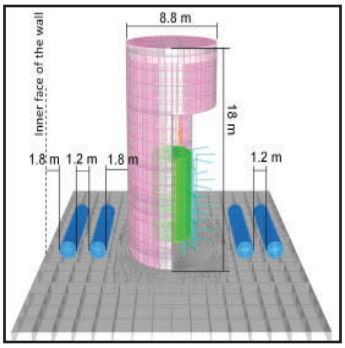

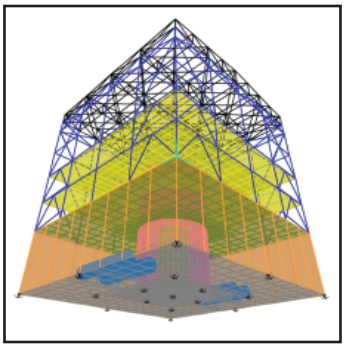
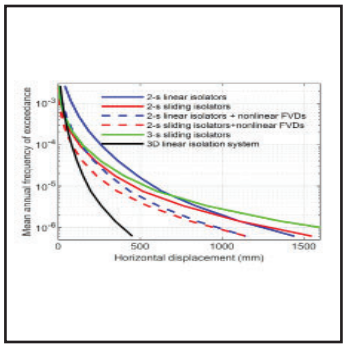

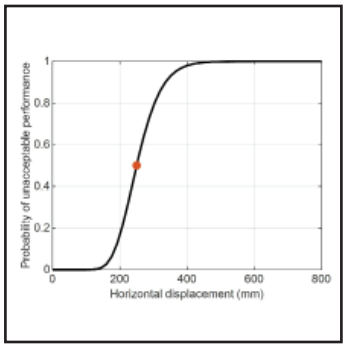

Technical Report MCEER-24-0001

Revision 01, March 7, 2025; originally published June 14, 2024

MCEER: Earthquake Engineering to Extreme Events

NOTICE

This report was prepared by the University at Buffalo, State University of New York, as a result of research sponsored by the Department of Energy under award number DE-FOA-0001817. Neither MCEER, associates of MCEER, its sponsors, University at Buffalo, State University of New York, nor any person acting on their behalf:

a. makes any warranty, express or implied, with respect to the use of any information, apparatus, method, or process disclosed in this report or that such use may not infringe upon privately owned rights; or

b. assumes any liabilities of whatsoever kind with respect to the use of, or the damage resulting from the use of, any information, apparatus, method, or process disclosed in this report.

Any opinions, findings, and conclusions or recommendations expressed in this publication are those of the author(s) and do not necessarily reflect the views of MCEER, the Department of Energy or other sponsors.

University at Buffalo
The State University of New York

Guidelines for Implementing Seismic Base Isolation in Advanced Nuclear Reactors – Revision 01

by

Faizan Ul Haq Mir[1], Ching-Ching Yu [2], Benjamin M. Carmichael[3], Brandon M. Chisholm[4], Jason Redd[5], Mohamed M. Talaat[6], Chandrakanth Bolisetti[7], and Andrew S. Whittaker[8]

Revision 01 Publication Date: March 7, 2025
Publication Date: June 14, 2024
Submittal Date: October 6, 2023

Technical Report MCEER-24-0001

Department of Energy
DE-FOA-0001817

1. Assistant Professor, Indian Institute of Technology Jammu, Jammu, JK, India (Formerly Postdoctoral Associate, Department of Civil, Structural and Environmental Engineering, University at Buffalo, The State University of New York)
2. Structural Analysis Engineer - Senior Vibration Engineer, TerraPower, Bellevue, WA (Formerly Postdoctoral Associate, Department of Civil, Structural and Environmental Engineering, University at Buffalo, The State University of New York)
3. Business Development Manager, Southern Company, Birmingham, AL
4. Advanced Nuclear R&D Engineer, Southern Company, Birmingham, AL
5. Project Engineer for Advanced Nuclear Power, Southern Nuclear, Birmingham, AL
6. Senior Project Manager, Simpson Gumpertz & Heger, Newport Beach, CA
7. Facility Risk Group Lead, Idaho National Laboratory, Idaho Falls, ID
8. SUNY Distinguished Professor, Department of Civil, Structural and Environmental Engineering, University at Buffalo, The State University of New York

MCEER: Earthquake Engineering to Extreme Events
University at Buffalo, The State University of New York
212 Ketter Hall, Buffalo, NY 14260
buffalo.edu/mceer

Preface

MCEER was originally established by the National Science Foundation in 1986 at the University at Buffalo, The State University of New York, as the first National Center for Earthquake Engineering Research (NCEER). In 1998, it became known as the Multidisciplinary Center for Earthquake Engineering Research (MCEER), from which the current name, MCEER, evolved.

Comprising a consortium of researchers and industry partners from numerous disciplines and institutions throughout the United States, MCEER's mission expanded in the early 2000s from its original focus on earthquake engineering to one which addresses the technical and socioeconomic impacts of a variety of hazards, both natural and man-made, on critical infrastructure, facilities, and society.

This report describes a pathway for an applicant to follow to develop, document and qualify a seismic isolation system for a U.S. nuclear power plant. The report presents a performance-based approach to implement a seismic isolation system and presents sample calculations for several systems to illustrate the pathway. An archetype reactor building, sited at Clinch River, East Tennessee, and ground motions derived using a seismic hazard calculator developed by the U.S. Geological Survey are used to illustrate the approach. Guidance is provided on the specification of seismic isolation systems and their commercial grade dedication.

Revision 01: This revision updates the discussion on the derivation of fragility functions (see Appendix C), moves the second approach for generating a seismic displacement demand curve from Section 5 to Appendix D (new), and revises some of the testing requirements in Section 6, with corresponding minor changes made elsewhere, including tabulated and plotted results.

ABSTRACT

Seismic isolation offers significant improvements to building and equipment performance where earthquake shaking is a design consideration. It has been applied to non-nuclear, mission-critical infrastructure in the United States for more than 40 years. A robust regulatory pathway can be useful for applicants seeking US Nuclear Regulatory Commission approval to incorporate seismic isolation in advanced nuclear power plants. This report, sponsored by the US Department of Energy under its Industry Opportunities for Advanced Nuclear Technology Development (Industry FOA), has been developed to present a pathway for review and consideration of endorsement by the NRC for an applicant to follow to develop, document, and qualify a seismic isolation system. The report presents a performance-based approach to implement a seismic isolation system for a reactor building and presents sample calculations for several systems to illustrate the pathway. The report does not propose a risk target for an isolation system but rather describes how a target value can be achieved. For demonstration purposes, an archetype reactor building is sited at Clinch River, East Tennessee, and ground motions are derived using a seismic hazard calculator developed by the US Geological Survey. Guidance is provided on the specification of seismic isolation systems and their commercial grade dedication.

ACKNOWLEDGEMENTS

The authors sincerely thank the US Department of Energy for funding the writing of this report under a grant to Southern Nuclear Development, LLC: Award No. DE-NE0008932.

Many individuals made important contributions to the preparation of the report for which the authors are most grateful: Dr. Matthew Denman and Mr. Brian Song of Kairos Power, Mr. Reid Zimmerman of KFPP, and Mr. Mark Peres of Peres Engineering. The authors thank members of the advisory committee formed at the beginning of the project to provide input to the process and to review the report, namely, Professors Jacopo Buongiorno and Koroush Shirvan of MIT, Mr. John Richards and Dr. Hasan Charkas of EPRI, Dr. Troy Morgan of Exponent, and Mr. Karl Fleming of KNF Consulting Services, LLC. The authors are also very grateful to members of the Nuclear Energy Institute's Advanced Reactor Regulatory Task Force who reviewed and commented on the final draft of this report, namely, Dr. Bob Iotti of ARC Clean Energy, Mory Diané of Oklo, Mr. Jim Kinsey of the Idaho National Laboratory, Ms. Amanda Spalding of Westinghouse Electric Company, Mr. Dennis Henneke of GE-Hitachi Nuclear, and Mr. Ian Gifford of TerraPower.

The authors acknowledge the seminal work by others on the application of seismic protective systems to mission-critical infrastructure. Three individuals deserve a special vote of thanks from the authors: Professor Emeritus James Kelly of UC Berkeley, Dr. Charles Kircher of Kircher and Associates, and Professor Michael Constantinou of the University at Buffalo.

TABLE OF CONTENTS

TABLE OF CONTENTS (CONT.)

TABLE OF CONTENTS (CONT.)

TABLE OF CONTENTS (CONT.)

TABLE OF CONTENTS (CONT.)

TABLE OF CONTENTS (CONT.)

TABLE OF CONTENTS (CONT.)

LIST OF FIGURES

LIST OF FIGURES (CONT.)

LIST OF FIGURES (CONT.)

LIST OF FIGURES (CONT.)

LIST OF TABLES

LIST OF TABLES (CONT.)

LIST OF TABLES (CONT.)

LIST OF ABBREVIATIONS

AASHTO	American Association of State Highway and Transportation Officials
ANS	American Nuclear Society
ASCE	American Society of Civil Engineers
ASME	American Society of Mechanical Engineers
BWR	Boiling water reactor
CDF	Core damage frequency
CEUS	Central and Eastern United States
CFR	Code of Federal Regulations
CGD	Commercial-grade dedication
CGI	Commercial-grade item
CLERP	Conditional large early release probability
CPEF	Conditional probability of an individual becoming a prompt (or early) fatality
CPLF	Conditional probability of an individual becoming a latent cancer fatality
DB	Design basis
DE	Dedicating entity
DOF	Degrees of freedom
DRS	Design response spectrum
EOR	Engineer of record
ETTP	East Tennessee Technology Park
EUS	Eastern United States
FMEA	Failure modes and effects analysis
FoS	Factor of safety
FVD	Fluid viscous damper
GMPE	Ground motion prediction equation

LIST OF ABBREVIATIONS (CONT.)

GW	Giga-watt
IAEA	International Atomic Energy Agency
IFOA	Industry funding opportunity announcement
ILR	Individual latent risk
ISO	International Organization for Standardization
ITAAC	Inspections, Tests, Analyses, and Acceptance Criteria
LDR	Low-damping rubber (bearing)
LERF	Frequency of a large early release capable of causing early fatalities
LLWR	Large light water reactor
LR	Lead-rubber (bearing)
LRFD	Load and resistance factor design
LWR	Light water reactor
MAFE	Mean annual frequency of exceedance
MCNP	Monte Carlo N-Particle
NEI	Nuclear Energy Institute
NIST	National Institute of Standards and Technology
NPP	Nuclear power plant
NRC	(US) Nuclear Regulatory Commission
PGA	Peak ground acceleration
PHX	Primary heat exchanger
PRA	Probabilistic risk assessment
PWR	Pressurized water reactor
QA	Quality assurance
QC	Quality control

LIST OF ABBREVIATIONS (CONT.)

QHO	Quantitative health objectives
RC	Reinforced concrete
RG	Regulatory Guide
RIPB	Risk-informed performance-based
RV	Reactor vessel
RVACS	Reactor vessel auxiliary cooling system
SDC	Seismic design category
SEI	Structural Engineering Institute
SER	Safety evaluation report
SF	Scale factor
SFP	Single concave friction pendulum (bearing)
SI	Seismic isolation
SPRA	Seismic probabilistic risk assessment
SRSS	Square root of the sum of the squares
SSCs	Structures, systems, and components
SSI	Soil-structure interaction
TFP	Triple friction pendulum (bearing)
TPG	Target performance goal
UHRS	Uniform hazard response spectrum
US	United States of America
USGS	United States Geological Survey
USNRC	United States Nuclear Regulatory Commission
VDD	Viscous damping device

LIST OF ABBREVIATIONS (CONT.)

WUS	Western United States

LIST OF NOTATIONS

A_R	Slope factor at a spectral period
C_d	Damping coefficient for a VDD or a system of VDDs
C_h	Damping coefficient for an isolation system in the horizontal direction
C_v	Damping coefficient for an isolation system in the vertical direction
DL	Average dead load on all isolators of a type and size
D_{DB}	Mean maximum resultant horizontal displacement for DB shaking on all isolators of a type and size
$D_{DB,v}$	Mean maximum vertical displacement for DB shaking on all isolators of a type and size
$D_{TPG,v}$	Mean maximum vertical displacement for TPG shaking on all isolators of a type and size
D^i	Maximum horizontal displacements corresponding to the i^{th} bin arranged as a vector
D^i_{mean}	Mean value of the entries in D^i
d_1	Yield displacement for an isolator (required in numerical analysis)
d^i_j	An element of the vector D^i
D_{50}	Median displacement of the fragility function to achieve the target performance goal (TPG)
E^i	Mean annual frequency of exceedance associated with the midpoint of the i^{th} bin on a seismic hazard curve
ΔE^i	Width of a bin on a hazard curve along the axis of mean annual frequency of exceedance (in linear space)
$\Delta E^i_{\log}$	Width of a bin on a hazard curve along the axis of mean annual frequency of exceedance (in log space)
F	Force

LIST OF NOTATIONS (CONT.)

$f_{iso,h}$	Horizontal isolation system frequency (i.e., reciprocal of $T_{iso,h}$)
$f_{iso,v}$	Vertical isolation system frequency (i.e., reciprocal of $T_{iso,v}$)
g	Gravitational acceleration
H_P	Mean annual frequency of exceedance (MAFE) equal to the TPG
K_{eff}	Effective (secant) horizontal stiffness of a bilinear isolation system, which is a function of horizontal displacement
$K_{iso,h}$	Horizontal stiffness of a linear isolator or linear isolation system, or the second-slope stiffness of the force-displacement relationship of a bi-linear isolator or a bilinear isolation system
$K_{iso,v}$	Vertical stiffness of a 3D isolation system
K_v	Vertical stiffness of a 2D (horizontal) isolation system
K_1	Stiffness of the elastic region of the force-displacement relationship of an isolator or an isolation system
LL	Average live load on all isolators of a type and size
m	Mass
n_{gm}	Number of ground motions in a bin
P_{DB}	Mean maximum earthquake-induced vertical load for DB shaking on all isolators of a type and size
P_{TPG}	Mean maximum earthquake-induced vertical load for TPG shaking on all isolators of a type and size
P_f	Target performance goal, expressed as a mean annual frequency (MAF) of unacceptable performance
Q	Zero-displacement force intercept on a bi-linear force-displacement relationship
R	Radius of curvature of a sliding surface
Sa or SA	Spectral acceleration

LIST OF NOTATIONS (CONT.)

SA^i	Spectral acceleration associated with bin number *i*
SA_{TPG}	Spectral acceleration associated with TPG shaking
T_{eff}	Effective horizontal period of a bilinear isolation system, calculated using K_{eff}
$T_{iso,h}$	Horizontal isolation-system period, calculated using $K_{iso,h}$
$T_{iso,v}$	Vertical isolation-system period, calculated using $K_{iso,v}$
u	Displacement
v	Velocity
W	Weight
β	Composite dispersion for the isolation-system fragility function
β_c	Dispersion in displacement capacity
β_d	Dispersion in displacement demand
β_f	Dispersion associated with model fidelity
β_{gm}	Dispersion associated with ground motions
β_i	Dispersion associated with mechanical properties of the isolation system
β_m	Dispersion associated with distribution of mass in the isolated superstructure
β_{mm}	Dispersion associated with variability in the two horizontal components of ground motion around the geometric mean
β_0	Dispersion associated with analysis using spectrally matched horizontal motions
δ	Velocity exponent used to define the *F-v* relationship of a VDD
μ	Coefficient of sliding friction
θ	Median displacement capacity used to define a fragility function for an isolation system

SECTION 1
PURPOSE, SCOPE, ORGANIZATION, AND SUMMARY

1.1 Purpose and Scope

The purpose of this report is to document and provide the technical justification for a process to select, analyze, design, and deploy a *passive* seismic isolation system beneath a reactor building.

Within the existing US Nuclear Regulatory Commission (NRC) nuclear power plant (NPP) licensing framework (i.e., Parts 50 and 52 of Title 10 of the Code of Federal Regulations), a risk-informed, performance-based (RIPB) methodology for identifying and evaluating licensing basis events, determining the safety classification of SSCs, and evaluating the adequacy of defense-in-depth was endorsed by the NRC in Regulatory Guide RG1.233 (USNRC 2020b). The process described in this report can be used in concert with the guidance provided on the evaluation of external hazards and the definition of Design Basis External Hazard Levels in NEI 18-04, Rev. 1 (NEI 2019), which is endorsed in RG1.233. Although a new RIPB NPP licensing framework is currently under development by the NRC (i.e., Part 53 of Title 10 of the Code of Federal Regulations), the proposed draft language for this rule (USNRC 2020a) currently indicates that ASCE/SEI 43-19 and/or the use of fragility models would be acceptable methods for showing that SSCs are able to withstand the effects of earthquakes. As such, the process documented in this report is one way to meet applicable regulatory requirements under the current and proposed US domestic NPP licensing frameworks. Alternate viable pathways to select, analyze, design, and deploy an isolation system that don't involve the performance (risk) calculations are not addressed, noting that for micro reactors classed as either Seismic Design Category 1 or 2 per ANS 2.26 (ANS 2017) and ASCE/SEI 43-19 (ASCE 2021), an applicant might propose to use ASCE/SEI 7-22 (ASCE 2022).

Recent experimental and numerical work (e.g., Mir *et al.* (2023b), Mir *et al.* (2023a), and Lal *et al.* (2023)) has demonstrated the viability of seismically isolating equipment. The process described in this report for the seismic isolation of reactor buildings could be easily adapted for safety-related equipment installed inside a reactor building, with additional steps needed to a) compute a seismic displacement demand curve with explicit considerations of the earthquake response of the building and equipment supports, b) integrate with ASME/IEEE standards, and c) address exposure to neutron and gamma radiation. The requirements for qualification, prototype, and production testing of isolators and dampers (Section 6), specifications (Section 7), with a treatment of neutron and photon fluence, as needed), and the process for commercial grade dedication of isolators and dampers (Section 8) should be broadly applicable to the seismic isolation of equipment.

Multiple seismic isolators and viscous damping devices (VDD) are addressed in the report, consistent with hardware in use in non-nuclear sectors and described in published standards of practice, all in the United States. No isolator or damper technology is preferred. Semi-active and active seismic isolation systems, which require external power and/or sensors to function and have not been deployed in the United States, are not included in the scope of this report.

Much of this report was prepared for submission to the NRC as a topical report for formal review and issuance of a safety evaluation report (SER). The US Nuclear Regulatory Commission Office Instruction, LIC-500, Topical report process power (USNRC 2018) defines a topical report as a stand-alone report containing technical information about a nuclear plant safety topic. A topical report provides the technical basis for a licensing action.

Topical reports are reviewed by the NRC staff with the intent of maximizing their scope of applicability consistent with current standards for licensing actions, compliance with the applicable regulations, and reasonable assurance that the health and safety of the public will not be adversely affected. Topical reports improve the efficiency of the licensing process by allowing the staff to review proposed methodologies, designs, operational requirements, or other subjects related to safety on a generic basis, so they may be implemented by reference by multiple US licensees once determined to be acceptable for use and verified by the NRC staff. By reviewing this information as a topical report, the NRC will reduce the review time for the technical bases by allowing applicants to reference the topical report and associated safety evaluation, rather than submitting it for review and approval on each application.

The review of the information provided in this topical report is intended to support reactor developers and other stakeholders by:

- Providing early acceptance and resolution of technical information and foundational information for industry to move forward with a degree of design and regulatory certainty
- Providing guidance on the numerical modeling of seismic isolators and VDDs
- Providing guidance on the benefits of alternate isolation systems, suitable for controlling accelerations and displacements in safety-class equipment inside a reactor building

In consultation with industry stakeholders, the adjective “performance-based” is used in this report instead of “risk-informed” or “risk-based”. Although the performance calculations and processes presented in this report seek to explicitly achieve a user-specified risk target, the sole focus herein is the seismic isolation system. The adjectives “risk-informed” and “risk-based” are generally applied to plant-level risk as determined by a probabilistic risk assessment. Herein, and as described later, the risk target for a seismic isolation system is defined as a *target performance goal* (TPG). The computed risk for the seismic isolation

system would be used as input to a plant-level seismic probabilistic risk assessment.

Although the scope of this document is focused on the use of seismic isolation of advanced reactor buildings, the process described in this report is technology-inclusive and could be applied to a wide variety of technologies and sizes of reactor, from large-light water reactors (LLWRs) at the GW scale to microreactors. It is possible that a user could apply this method to a different technology; however, it would be beneficial to engage in pre-application discussions with the NRC to provide information to the staff on the intended implementation of seismic isolation and the approach in this report.

The guidelines presented hereafter assume that the reader has a working knowledge of seismic isolation, isolators and dampers, and the prototype and production testing thereof, seismic hazard assessment and earthquake ground motion, numerical modeling, nonlinear dynamic analysis, fragility analysis, and risk assessment.

1.2 NRC Endorsement

The NRC staff was asked to endorse those sections of the report identified below:

- Isolation-system definitions per Section 1.4
- The role of seismic isolation solutions in ensuring adequate defense-in-depth per Section 1.5
- Earthquake shaking definitions for isolation-system design per Section 3.2
- Performance criteria for isolators and VDDs in a seismic isolation system per Section 3.3
- General requirements for isolation-system design per Section 3.4
- Requirements for seismic inputs to support performance calculations per Section 3.5
- Methods of dynamic analysis, and numerical models for isolators and VDDs per Section 3.6
- Requirements for design of connections for isolators and VDDs; isolation-system substructure; structures, systems, and components above the seismic isolation interface; systems and components crossing the seismic isolation interface; and clearance around the isolated building; all per Section 3.7
- Performance-based design of a seismic isolation system per Sections 5.1 through 5.4
- Minimum requirements for qualification, prototype, and production testing of isolators and dampers per Section 6
- Specifications for supply of isolators and VDDs per Section 7
- Plan for commercial grade dedication of isolators and VDDs per Section 8
- Process to establish a logarithmic standard deviation for the seismic fragility function of a seismic isolation system per Section C.2, to support performance calculations

- Derivation of a displacement demand curve spanning 4 decades of mean annual frequency of exceedance (MAFE) in log space and use of 11 bins of ground motions for performance calculations, equally spaced across the 4 decades, all per Section D.2
- Adjustment to the seismic displacement demand curve to address variability in ground shaking around the geometric mean and properties of the isolation system per Section D.3

The other parts of the report provide information and data to support those sections listed above.

1.3 Seismic Isolation Checklist

The checklist below applies to the analysis, design and delivery of seismic isolators and dampers for application to nuclear reactor buildings:

- Establish TPG for the seismic isolation system
- Generate seismic hazard curves, uniform hazard response spectra, and ground motion time series to establish an isolation-system-specific seismic displacement demand curve
- Determine the median displacement capacity of the isolation system required to achieve the TPG by convolution of the isolation-system fragility function and the seismic displacement demand curve
- Compute by dynamic analysis, for design basis (DB) and TPG shaking, displacements and forces for prototype and production testing of isolators and dampers
- Compute earthquake-induced demands on the basemat by the isolators and the VDDs, and design per industry practice, with considerations of all appropriate load combinations
- Compute earthquake-induced demands on the substructure supporting the isolators and the VDDs, and design per industry practice, with considerations of all appropriate load combinations
- Prepare specifications for supply of isolators and VDDs
- Prepare specifications for prototype and production testing of isolators and dampers
- Prepare a plan for commercial grade dedication of isolators and VDDs, if not previously approved
- Prepare requirements for maintenance, operation, and testing of isolators and VDDs.

1.4 Definitions

The following definitions apply to this report:

Bearing: the flexible structural element of a seismic isolator; used interchangeably here and in the literature with *isolator*.

Damper: the flexible structural element of a viscous or viscoelastic damping device that dissipates energy

caused by the relative motion between its ends.

Isolator: the complete assembly of isolator components, including the bearing and its mounting plates, if separate from the bearing; used interchangeably here and in the literature with *bearing*.

Seismic protective devices: isolators and/or viscous damping devices.

Seismic isolation interface: the boundary between the isolated superstructure and the non-isolated substructure and adjacent construction.

Seismic isolation system: the collection of structural elements, including all seismic isolators and viscous damping devices, and all connections of seismic isolators and viscous damping devices to structure above and below the isolation system.

Viscous damping device: a complete assembly of damper components, including the damper, its mounting brackets, and pins.

1.5 Role of Seismic Isolation Solutions in Defense-in-Depth

Sources of information on defense-in-depth can be found in IAEA (1996; 2005), Moe and Afzali (2020) and SECY-13-0132 (USNRC 2013).

Commission paper SECY-13-0132 describes the five facets of defense-in-depth (need, objective, approach to achieve, criteria for implementation, and sufficiency) and these are used here to frame a discussion of how seismic isolation interfaces with defense-in-depth.

Seismic isolation does not alter the need for defense-in-depth. Regardless of the use of seismic isolation as part of a reactor design, adequate defense-in-depth is still required through the design and operation of the facility to compensate for uncertainties and incompleteness inherent to the safety basis.

An evaluation of how seismic isolation supports the objective of defense-in-depth should include consideration of the reduction of the potential for severe accidents and damage to the plant in the event of severe earthquake shaking. In comparison to non-isolated designs, the implementation of seismic isolation for a nuclear facility substantially reduces earthquake demands on the reactor building and its safety-related equipment.

Seismic isolation contributes to the overall approach to achieve defense-in-depth by a) superior quality in design, construction, and operation of components of the isolation system, as described later in this report, b) ensuring reliable and predictable performance of the isolated building under the abnormal conditions of severe earthquake shaking, and c) the potential to supplement other layers of defense-in-depth (e.g.,

protective barriers) in the prevention of the initiation of certain incidents.

The implementation of seismic isolation systems does not affect the high-level criteria used to implement the approach or strategy of defense-in-depth. Similar to the preceding discussion of how use of this methodology contributes to the overall approach to achieve defense-in-depth, the rules for implementation of seismic isolation systems, as described in this report and the referenced consensus standards ASCE/SEI 4-16 (ASCE 2017) and 43-19 (ASCE 2021), reflect consideration of the criteria for implementation of defense-in-depth, by a) requiring physical testing of 100% of seismic isolators and dampers prior to installation, guaranteeing quality, b) including provisions for periodic testing of isolators and dampers exposed to the same environmental conditions as in-service devices, and c) being passive devices and not requiring either sensors or external power to function.

As discussed in SECY-13-0132, risk insights can be used as part of the evaluation to determine whether there is sufficient defense-in-depth. Herein, the capacity of the isolation system involves explicit probabilistic risk calculations, enabling the use of risk insights above the isolation interface for certain events (i.e., those events in which the approach for implementation of seismic isolation contributes to the prevention and/or mitigation of the specific facility of interest) and providing essential input to the comprehensive and systematic process used to ensure adequate defense-in-depth when considering the suite of available plant-specific capabilities and programmatic elements for all events of interest to a given design.

In summary, seismic base isolation offers an additional plant capability that will ultimately be evaluated in the context of the full suite of other plant capabilities and programmatic elements to ensure adequate defense-in-depth for a given nuclear plant design.

1.6 Report Organization

This report is organized into eight sections, a list of references, and seven appendices.

Section 2 introduces seismic isolation systems, which may include VDDs. Applications of seismic isolation, ranging from large mission-critical infrastructure to delicate, priceless sculpture are presented to demonstrate the wide range of applicability of the technology. The seismic isolators and dampers considered sufficiently mature to apply in the US nuclear industry are described. Codes, standards, and guidelines, used to implement the technology in nuclear and non-nuclear sectors, including a brief history of their development, are introduced.

Section 3 presents definitions of earthquake shaking for isolation-system design, performance expectations for seismically isolated reactor buildings, general design requirements for the isolation system and its

supporting structure, including monitoring and ITAAC, seismic inputs for isolation-system analysis, methods of nonlinear dynamic analysis, displacements and forces for design and testing of an isolation system and its supporting structure, and the minimum required clearance around the perimeter of an isolated reactor building.

To help demonstrate a process to implement a seismic isolation system, Section 4 introduces an archetype reactor building and sample safety-related equipment, and locates the isolators and VDDs. The finite element model of the isolated building and the two-degree-of-freedom model used in Section 5 for performance calculations are presented. The seven isolation systems that are used in different sections of this report are introduced and characterized, and numerical models for them are presented. A sample site for the archetype building is identified, and its seismic hazard is characterized for two site classes representing different near-surface geologies. Details of the hazard computations are presented in Appendix A.

A performance-based process to establish the median displacement capacity of an isolation system, sufficient to achieve a user-specified TPG is presented in Section 5, including the development of isolator-specific seismic displacement demand curves and isolation-system fragility functions. The process is demonstrated for two isolation systems. Calculations for the other isolation systems identified in Section 4 are presented in Appendix C.

Section 6 presents recommendations for qualification, prototype, and production testing of seismic isolators and dampers. Acceptance criteria are presented.

Sample specifications and a plan for commercial grade dedication of isolators and VDDs are presented in Section 7 and Section 8, respectively.

A list of the references cited in this report is presented in Section 9. For an exhaustive list of references on seismic isolation published prior to 2019, see Whittaker *et al.* (2017) and Whittaker *et al.* (2018).

Appendix A presents seismic hazard data for the hypothetical site introduced in Section 4, together with sets of ground motion triplets used for dynamic analysis in Section 5 and the appendices. The seismic hazard computations use online data developed by the US Geological Survey (USGS 2018), which is not an NRC-approved approach to characterize ground motion.

Two levels of earthquake shaking are used to design a seismic isolation system: 1) target performance goal (TPG), and 2) design basis (DB). Consistent with the approach of Table 1-1 of ASCE/SEI 43-19 (ASCE 2021), given a seismic design category (SDC), the DB spectrum at a period is computed as the product of a scale factor (SF) and the uniform hazard response spectrum with a mean annual frequency of exceedance

at the TPG. The SF is calculated for SDC 3, SDC 4, and SDC 5 and eight hypothetical sites for NPPs across the US in Appendix B. This calculation process utilizes seismic hazard data per Appendix A. The near-surface geology is assumed to be rock or stiff soil, represented by site classes BC and CD, respectively, per ASCE/SEI Standard 7-22 (ASCE 2022). The appendix presents recommendations for the SF, suitable for inclusion in the next revision of ASCE/SEI 43.

Appendix C presents a technical basis for the calculation of a logarithmic standard deviation for an isolation-system fragility function. The appendix also presents performance calculations for seismic isolation systems not considered in Section 5.

Appendix D provides information on the selection of ground motion intensities to support response-history analysis and performance calculations, and the generation of a displacement demand curve for a specific isolation system.

The purpose of Appendix E is to illustrate isolation-system options available to engineers and analysts, and how a type of isolation system could be selected for a NPP. The finite element model of the archetype reactor building and the numerical models of the isolators and dampers, all reported in Section 4, are exercised for two levels of ground shaking. Results are reported for seven monitoring locations, including the basemat, reactor head, and the points of attachment of the reactor cavity cooling system and the bridge crane. The cost of the isolation system is not addressed.

Appendix F introduces considerations for inspections, tests, analyses, and acceptance criteria (ITAAC) for seismic isolation devices and the seismic isolation system to support a combined license under 10 CFR Part 52.

Appendix G presents information of possible use in the preliminary selection of a TPG for a seismic isolation system.

The topical report submitted to the NRC for formal review and issuance of a SER included eight sections, a reference list, and five appendices. Table 1.1 presents a mapping of appendices in this report and the topical report submitted to the NRC.

Table 1.1. Mapping of Appendices in this report and the topical report submitted to the NRC

Appendix/section in this report		Corresponding appendix/section in the topical report submitted to the NRC
Appendix A		Appendix A
Appendix B		Not included in the topical report
Appendix C	Sections C.1 through C.4 and C.6	Appendix B
	Section C.5	Not included in the topical report
Appendix D	Sections D.1 through D.3 and D.6	Appendix C
	Sections D.4 and D.5	Not included in the topical report
Appendix E		Appendix E
Appendix F		Appendix D
Appendix G		Not included in the topical report

SECTION 2
SEISMIC ISOLATION SYSTEMS: TECHNOLOGY, USE, AND GUIDELINES

2.1 Introduction

This section of the report presents introductory information on seismic isolation, implemented isolation systems, available seismic isolator and damper technologies, and published US codes, standards, and guidelines.

2.2 Seismic Isolation Systems

Seismic isolation systems are comprised of isolators (also termed bearings) and VDDs that are used to substantially reduce accelerations and deformations that develop in structures, systems, and components due to earthquake shaking. Figure 2.1, dating from the 1980s, characterizes the benefits of 2D (horizontal) seismic isolation, namely, reductions in acceleration (i.e., forces) in Figure 2.1a, the corresponding increase in displacements in Figure 2.1b, and how to mitigate the increase in displacement through added damping in Figure 2.1c. There are four important notes to attach to Figure 2.1: 1) nuclear power plant buildings are stiff structures, with a fundamental frequency in the range of 10 Hz; 2) adding a seismic isolation system can reduce accelerations (and forces) in the building by a factor of 3 and greater; 3) nearly all of the displacement in the isolated building occurs over the height of the isolators, which are physically tested to demonstrate adequate performance; and 4) damping can be added internal to the isolator via friction or a central lead core and/or external to the isolator via VDDs, as described later.

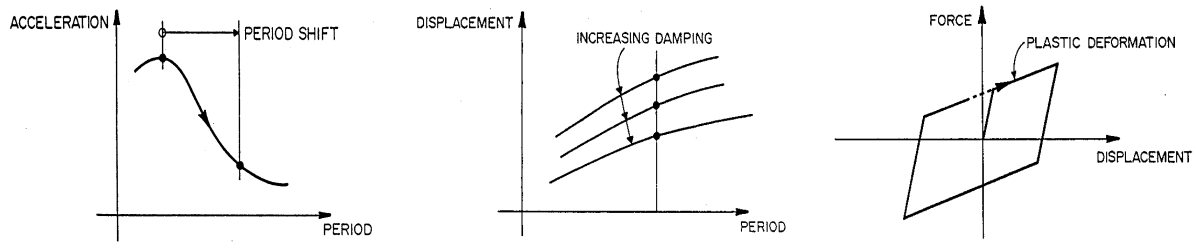

a) acceleration spectrum b) displacement spectrum c) added damping

Figure 2.1. Two-dimensional, horizontal seismic isolation (courtesy of DIS)

Seismic isolation systems can be implemented to protect assets across a broad range of sizes, from buildings and infrastructure, to large equipment such as reactor vessels, to small, priceless sculptures. Some sample applications of seismic isolation are presented in Figure 2.2: San Francisco City Hall, isolated after the 1989

Loma Prieta earthquake; a gas platform off Sakhalin Island, Russia, isolated with 4 bearings, in the early 2000s; the Statue of Hermes at Mt. Olympus, Greece, isolated with 4 bearings, in the early 2000s; and the new Apple Park, a $5B building for Apple Inc., in Cupertino, California. More than 10,000 buildings have been isolated worldwide, with nearly all applications involving the placement of seismic protective devices below the lowest occupied floor and above a foundation.

a) San Francisco City Hall

b) Sakhalin gas platform

c) Statue of Hermes

d) Apple Park

Figure 2.2. Sample isolated structures and sculpture

Kammerer *et al.* (2019) and Whittaker *et al.* (2018) discuss applications of seismic base isolation to non-nuclear and nuclear facilities through late 2017. Applications to operating nuclear facilities are limited to the Cruas nuclear power plant in France (early 1980s), the Koeberg nuclear power plant in South Africa (early 1980s), a spent fuel pool at Le Hague in France, and emergency operations buildings in some Japanese nuclear power plants (e.g., Kashiwazaki-Kariwa, Fukushima Daiichi, Fukushima Daiini, and Onagawa). The Jules Horowitz research fission reactor and the ITER fusion reactor, both under construction at the time of this writing in Caderache, France, are seismically isolated.

2.3 Seismic Isolators and Dampers

Seismic isolation systems can be configured to function in the horizontal plane (2D) or in both the horizontal and vertical planes (3D). Nearly all seismic isolation applications in the US have been 2D, achieved with

either elastomeric or spherical sliding (friction pendulum) isolators. Three-dimensional (3D) building seismic isolation has been proposed in the US (Nielsen *et al.* 2020), but it has not yet been implemented. There are applications of 3D isolation in Europe.

Early work on seismic isolation in the modern era can be traced to New Zealand in the early 1970s with research beginning in earnest in the US in the mid-1970s. The focus of research and development on seismic isolation systems, and the writing of companion guidelines and consensus standards, has been 2D (horizontal) base isolation because, until recently, vertical shaking effects were assigned secondary importance for earthquake-resistant design and construction of buildings. A more recent focus on the seismic performance and protection of equipment, both ground-supported and inside buildings, is promoting interest in 3D isolation because some equipment is susceptible to damage due to vertical shaking.

Figure 2.3 presents seismic isolators (bearings) and dampers that are commercially available in the US. Figure 2.3a and Figure 2.3b are photographs of the single concave (SFP) and triple concave (TFP) friction pendulum bearings, manufactured by Earthquake Protection Systems[1], in Vallejo, California. These spherical sliding bearings provide 2D isolation and have been widely used in the US and abroad for a broad range of applications. Isolation is achieved by the articulated slider moving across the hemispherical sliding surface. The sliding and rotating surfaces are a high-load, low-friction composite bearing on stainless steel. Energy is dissipated by friction. The upper panel in Figure 2.3a is an assembled SFP bearing. The lower right panel in Figure 2.3a shows the articulated slider and the spherical sliding surface. The lower left panel in Figure 2.3a shows the housing plate for the slider in the lower right panel, which would be inverted for assembly into a completed bearing. A cross section through an assembled SFP bearing is shown in Figure 2.4a. The composite material is bonded to the housing plate, within which the slider rotates, and to the underside of the slider—see the thicker solid black lines in Figure 2.4a. The idealized 2D force-displacement relationship of a SFP bearing is bilinear per Figure 2.4b, where the zero-displacement force intercept, Q, is the product of the coefficient of sliding friction and the instantaneous normal (axial) load on the bearing, and the second-slope stiffness, $K_{iso,h}$, is inversely proportional to the radius of curvature of the sliding surface. The coefficient of sliding friction can be varied by adjusting the contact pressure on the SFP's articulated slider. Typical coefficients of sliding friction are between 0.03 and 0.09. Typical sliding (second slope) periods are 1.5 seconds to 4 seconds.

The TFP bearing is a derivative of the SFP bearing, with multiple sliding surfaces. The upper panel in Figure 2.3b is an assembled TFP bearing. Figure 2.5a is a cross section through an assembled TFP bearing,

[1] https://www.earthquakeprotection.com/

identifying the top and bottom concave plates, the inner slide plates, and the central slider. The thicker solid black lines identify the four sliding surfaces. The lower two panels of Figure 2.3b show the internal construction of the TFP bearing. An idealized 2D force-displacement relationship for the TFP bearing is shown in Figure 2.5b, with five possible regimes of response that are a function of the coefficients of sliding friction on the four sliding surfaces and their radii of curvature.

Information on SFP and TFP bearings can be found in Constantinou *et al*. (1990; 1993; 2007; 2011), Fenz *et al*. (2008a; 2008b; 2008c; 2008d), Kumar *et al.* (2015a; 2015d; 2019b), Mokha *et al.* (1988; 1990; 1991a; 1991b), Morgan and Mahin (2010; 2011), Mosqueda *et al.* (2004), Sarlis and Constantinou (2016), Tsopelas and Constantinou (1994), and Zayas *et al*. (1987; 1989; 1990). The TFP bearing is more compact than the SFP bearing for a given displacement capacity because sliding occurs (primarily) on the two outer concave surfaces.

Figure 2.3c is a cut-away view of a lead-rubber (LR) isolator, composed of mounting plates and a bearing, where the bearing is comprised of alternating layers of low damping natural rubber bonded to carbon steel shims and a central cylindrical lead core. The lead-rubber bearing is manufactured by Dynamic Isolation Systems[2] of Sparks, Nevada. Isolation is achieved by shear deformation of the elastomer. Energy is dissipated primarily by yielding of the confined lead core, and secondarily by the elastomer. The idealized 2D force-displacement relationship of a LR bearing is bilinear per Figure 2.1c and Figure 2.4b, where the zero-displacement force intercept, Q, is a function of the area and dynamic yield stress of the lead core, and the second-slope stiffness, $K_{iso,h}$, is a function of the bonded area of the elastomer, the shear modulus of the elastomer, and the total thickness of elastomer in the bearing. The low-damping rubber (LDR) bearing is identical to LR bearing except there is no central lead core. Information on LR and LDR bearings can be found in Constantinou *et al*. (2007; 2011), Eidinger and Kelly (1978), Ishida *et al*. (1991a; 1991b), Kalpakidis *et al.* (2010), Kelly *et al.* (1980), Kelly (1991a; 1991b; 1993), Kumar *et al*. (2014; 2015b; 2015c; 2018; 2019a), and Tajirian *et al.* (1989). The diameter of the lead core varies between 1/6 and 1/3 of the bonded diameter of the bearing. The force Q in a LR bearing is generally between $0.06W$ and $0.09W$, where W is the supported weight. Typical isolated periods are between 1.5 seconds and 3 seconds.

[2] http://www.dis-inc.com/

a) SFP isolator

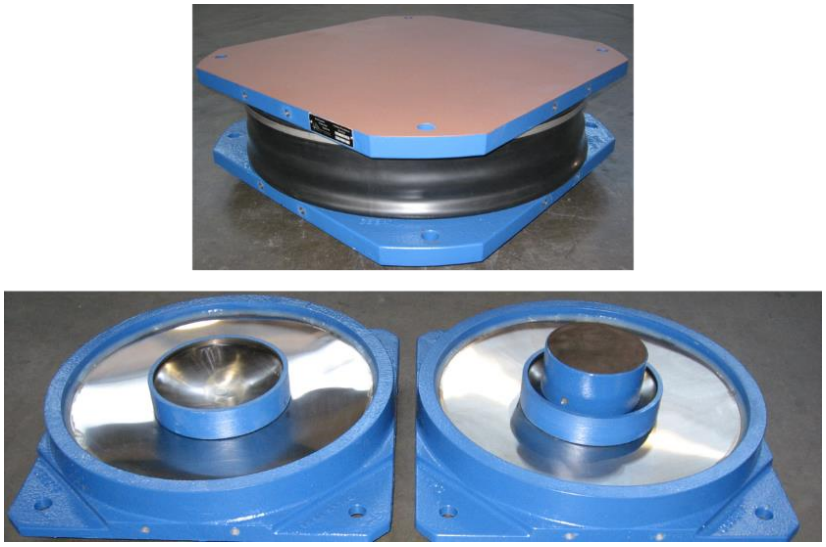

b) TFP isolator

Figure 2.3. Seismic isolators and dampers suitable for nuclear applications

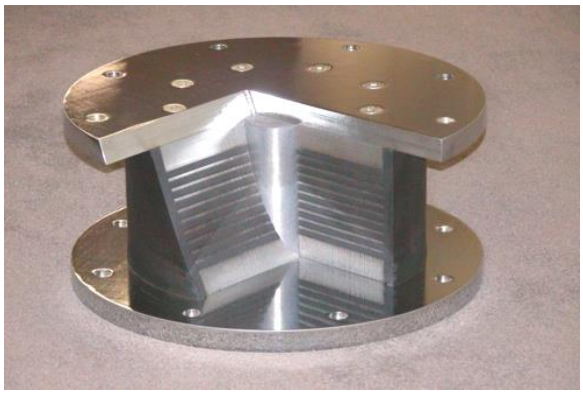

c) lead-rubber isolator

d) coil-spring isolator

e) machined springs for vertical isolation

f) 1D fluid viscous damper

g) 3D viscoelastic damper

Figure 2.3. Seismic isolators and dampers suitable for nuclear applications (cont.)

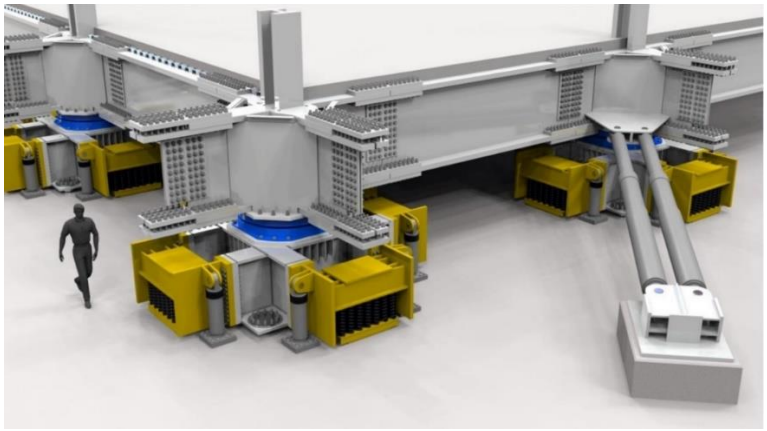

h) 3D hybrid isolator (Nielsen *et al.* 2020)

Figure 2.3. Seismic isolators and dampers suitable for nuclear applications (cont.)

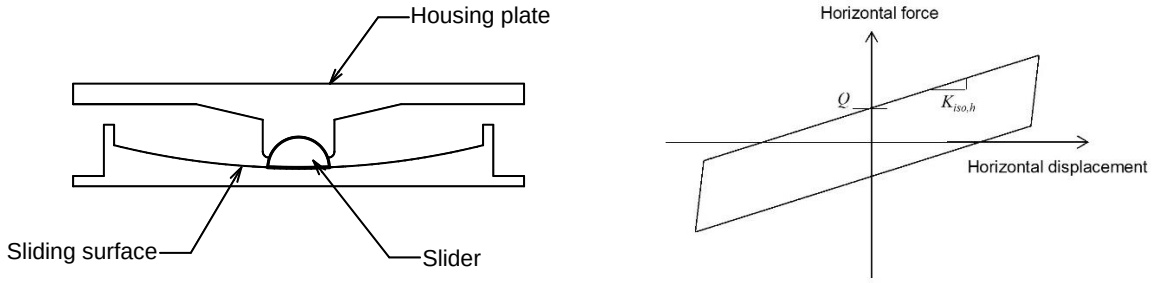

a) cross section b) 2D force-displacement hysteresis

Figure 2.4. SFP bearing

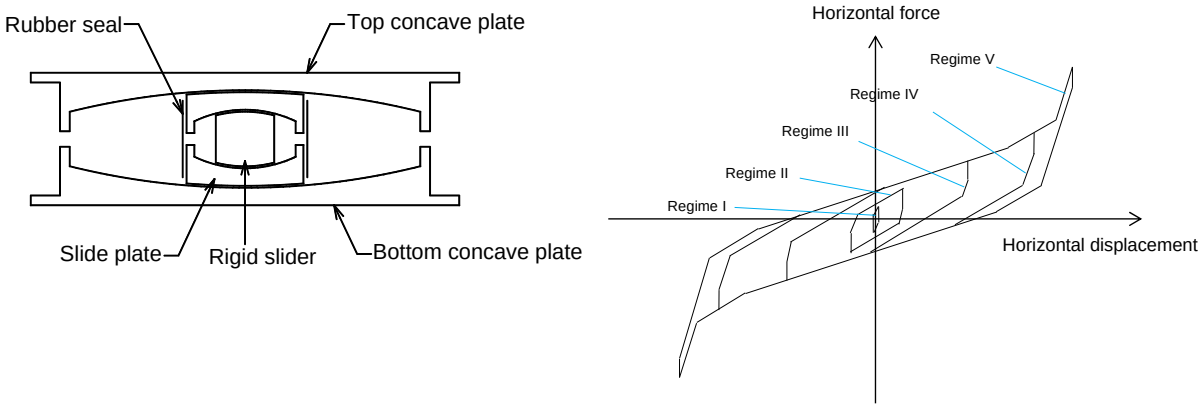

a) cross section b) 2D force-displacement hysteresis

Figure 2.5. TFP bearing

The spring isolator of Figure 2.3d offers vertical isolation, and if horizontal motion is not restricted, 3D isolation. Manufactured by GERB[3], Germany, this linear isolator is installed together with the 3D viscoelastic damper of Figure 2.3g. (LISEGA[4], also based in Germany, manufactures coil-spring isolators and 3D viscoelastic dampers, with applications to piping systems.) Isolation is achieved by the vertical and horizontal flexibility of the coil springs in the nested assembly. Typical horizontal and vertical isolation periods reported by GERB are 1.1 second and 0.4 second, respectively. No damping is assigned to the coil-spring assembly. The 3D damper is viscoelastic, with damping to complement the undamped coil-spring isolators. The damper fluids are highly viscous. Damping ratios in the horizontal and vertical directions, reported by GERB, are approximately 25% and 8% of critical, respectively, but these values are dependent on loading frequency. Information on the GERB isolators and dampers can be found in Nawrotzki (2009) and Nawrotzki *et al.* (2019). Makris and Constantinou (1990; 1992) provide information on dynamic testing of GERB hardware, together with recommendations for numerical modeling for dynamic analysis.

An alternative to the coil springs of Figure 2.3d is machined springs, such as those presented in Figure 2.3e, from Taylor Devices[5], North Tonawanda, New York. Such linear springs, used for US defense, aerospace, and civilian applications offer design flexibility not possible with coil springs, including materials other than carbon and alloy steels, enhanced corrosion resistance, package envelope size, and weight. Because isolator sizing is not addressed in this report, machined springs are not discussed further.

The uniaxial fluid viscous damper of Figure 2.3f from Taylor Devices has its roots in US defense and aerospace applications dating to the 1950s. Typically configured as a nonlinear damper, with a velocity exponent of approximately 0.3 to maximize energy dissipation and to enable capacity protection of connection hardware and support framing, these dampers have been applied to 750 buildings and bridges worldwide and included in 35 seismic isolation systems to complement the hysteretic isolation systems introduced previously, and reduce horizontal displacements. Dampers with force ratings of 3,000 kN and strokes of ±1,000 mm have been deployed in seismic isolation systems. The damper end-fixtures are equipped with spherical bearings to accommodate off-axis movements. Information on fluid viscous dampers can be found in Black and Makris (2007), Chang *et al.* (2002), Constantinou and Symans (1992), HITEC (1990), Makris (1998), Makris *et al.* (1998), and Nielsen *et al.* (2020).

The 3D hybrid isolator of Figure 2.3h (Nielsen *et al.* 2020) achieves horizontal isolation using the spherical

[3] https://www.gerb.com/

[4] https://www.lisega.de/en/

[5] https://www.taylordevices.com/

sliding bearing of Figure 2.3a installed atop an assembly of spring isolators of Figure 2.3d. The spring isolators are guided by low-friction pins, not seen in the image, to ensure the springs track vertically. (The elastomeric bearing of Figure 2.3c could be substituted for spherical sliding bearing in this hybrid isolator.) Horizontal isolation is achieved using the spherical sliding bearing to achieve a lower horizontal isolated frequency than is possible with a spring isolator. Hysteretic damping is achieved in the horizontal direction via friction in the spherical bearing. Viscous damping is achieved in the horizontal direction via the long-stroke, nonlinear fluid viscous dampers (see Figure 2.3f). Damping in the vertical direction is viscous, provided by short-stroke, nonlinear fluid viscous dampers.

The seismic isolators and 3D viscoelastic damper introduced above are axisymmetric devices in the horizontal plane and not planar (e.g., a reinforced concrete shear wall or moment-resisting frame). The maximum horizontal displacement response of these devices will be affected by both horizontal components (e.g., H1 and H2) of a ground motion triplet (e.g., H1, H2, and V), with peak response along an axis aligned with neither H1 nor H2 that is typically greater than the maximum responses along H1 and H2. This outcome is explicitly addressed in the calculations of displacement response in Section 5. The 1D fluid viscous damper of Figure 2.3f is a unidirectional device.

2.4 Codes, Standards, and Guidance

Guidance for the implementation of seismic isolation in buildings was first published in the US in 1986 (SEAONC 1986) and for damping devices in 1993 (Whittaker *et al.* 1993). Mandatory language and commentary for implementing seismic isolation was further developed in the late 1980s, with the *Uniform Building Code* (ICBO 1991) adopting guidance developed by the Structural Engineers Association of California (SEAOC) in late 1990. The 1994 *NEHRP Recommended Provisions for Seismic Regulations for New Buildings* (FEMA 1995) adopted the SEAOC/UBC seismic isolation provisions of late 1993, in Section 2.6, with guidance provided on analysis, design, and testing of seismic isolation systems and isolators. An appendix to Chapter 2 of the 1994 NEHRP provisions introduced passive energy dissipation (or damping) systems. The ASCE standard *Minimum Design Loads for Buildings and Other Structures*, ASCE/SEI 7, adopted provisions for seismic isolation in 2002 (ASCE 2002), drawing from the NEHRP provisions. Standard ASCE/SEI 7, which is re-issued every 5 to 6 years, is the primary pathway for introducing new information on seismic isolation (Chapter 17) and damping systems (Chapter 18); ASCE/SEI 7-22 (ASCE 2022) is the current version of this consensus standard.

The American Association of State Highway and Transportation Officials (AASHTO) published a guide specification for the seismic isolation design of highway bridges in 1990. This guide specification was updated in 1999 and 2010, and the latest and fourth edition was published in 2014 (AASHTO 2014).

Guidance for implementing seismic isolation in LLWRs was submitted to the USNRC in the early 2010s and published as NUREG/CR-7253 in 2019 (Kammerer *et al.* 2019). The technical considerations for seismic isolation presented in the Contractor Report represented the state of practice in the buildings sector in the late 2000s and addressed issues unique to the nuclear industry, including maintenance and inspection. The seismic-isolation provisions and commentary of ASCE/SEI 7-10 were a primary resource for this NUREG/CR. Two companion Contractor Reports, NUREG/CR-7254 and NUREG/CR-7255, were published in 2019, both state-of-the-art, with one focused on the behavior and modeling of spherical sliding bearings per Figure 2.3a (Kumar *et al.* 2019b), and the other addressing behavior and modeling of elastomeric bearings per Figure 2.3c (Kumar *et al.* 2019a). Both Kumar *et al.* reports developed numerical tools for modeling seismic isolators under extreme seismic loading environments.

2.5 Seismic Isolation Bibliography

Whittaker *et al.* (2017; 2018) includes an exhaustive list of references on seismic isolation of nuclear and non-nuclear facilities. A subset of those references is presented in Section 9 of this report. The 2017 bibliography lists seminal contributions to seismic isolation in the modern era, including work in the 1980s and 1990s that investigated the application of seismic isolation to both large light water and advanced reactors.

SECTION 3
EARTHQUAKE SHAKING DEFINITIONS, PERFORMANCE EXPECTATIONS, AND OTHER REQUIREMENTS

3.1 Introduction

This section of the report provides earthquake-shaking definitions for isolation-system design (Section 3.2), performance expectations for seismically isolated reactor buildings (Section 3.3), general design requirements for the isolation system and supporting structure (Section 3.4), and descriptions of seismic inputs for analysis of an isolated building (Section 3.5). Section 3.6 provides guidance on dynamic analysis of seismically isolated reactor buildings. Section 3.7 identifies displacements and forces for design of the isolation system and the SSCs, and the minimum required clearance between the isolated building and adjacent construction.

3.2 Earthquake Shaking Definitions for Design of a Seismic Isolation System

Dynamic analysis of a 3D numerical model of the isolated reactor building is performed for DB and TPG earthquake shaking to design a seismic isolation system and test components of the isolation system. Geomean horizontal and vertical uniform hazard response spectra are generated for a return period equal to the reciprocal of the TPG (e.g., if TPG = 10^{-4}, return period = 10,000 years). Consistent with the approach of Table 1-1 of ASCE/SEI 43-19 (ASCE 2021), a DB spectrum is generated as the product of the TPG spectrum and period-dependent scale factors, SF. (The value of SF is approximately equal to 0.5: see Appendix B or Yu and Whittaker (2024) for details.) Seed motions are spectrally matched to the DB and TPG spectra for dynamic analysis, consistent with US nuclear industry practice.

Fragility analysis is performed to determine the median horizontal displacement capacity of the isolation system required to achieve the TPG ($= D_{50}$), as described in Section 5.

3.3 Performance Criteria for Isolators and Dampers in a Seismic Isolation System

Table 3.1 lists performance criteria for isolators and dampers in a seismic isolation system.

Results of dynamic analysis of the 3D numerical model for DB shaking, including isolator and damper displacements, and axial forces in isolators, are used for *production* testing per Section 6.

Results of dynamic analysis of the 3D numerical model for TPG shaking, including axial forces in isolators, are used for *prototype* testing per Section 6. The horizontal displacement used for prototype testing of

isolators and dampers, D_{50}, is obtained from fragility analysis per Section 5.

Table 3.1. Performance criteria for isolators and dampers in a seismic isolation system

	DB shaking	@TPG
Use	Production testing of isolators and dampers	Prototype testing of isolators and dampers
Isolator and damper displacement	D_{DB}	D_{50}
Acceptance criteria	Production testing of each isolator with tests and acceptance criteria per Section 6.5	Prototype testing of three isolators of each type and size with tests and acceptance criteria per Section 6.4
	Production testing of each damper with tests and acceptance criteria per Section 6.5	Prototype testing of three dampers of each type and size with tests and acceptance criteria per Section 6.4
	No damage to isolators	Damage to isolators is acceptable but load-carrying capacity for gravity loading is maintained
	No damage to dampers	Damage to dampers is acceptable

3.4 General Requirements

3.4.1 Isolation system

3.4.1.1 General

The design of a seismic isolation system shall account for the effects of gravity loads, loadings induced by earthquake shaking and extreme winds, and other effects as appropriate, including operating temperature, humidity, and radiation. Sufficient shielding for neutron and gamma radiation is assumed, with the isolators and dampers installed below a reinforced concrete basemat.

The seismic isolation system shall be adequately protected from the effects of wildfire, flooding, wind-borne missiles, and other natural hazards. Depending on site and/or design-specific characteristics, different hazards may need to be addressed. References for identifying initiating events, including external hazards, include the ASME/ANS non-LWR PRA Standard, ASME/ANS RA-S-1.4-2021 (ASME 2021), as

endorsed by RG1.247 (USNRC 2022a) and Appendix A of NRC Draft Regulatory Guide (DG)-1413, Technology-Inclusive Identification of Licensing Events for Commercial Nuclear Plants (USNRC 2022b).

3.4.1.2 Plan distribution of seismic isolators and dampers

The effects of natural torsion shall be minimized using an appropriate plan distribution of seismic isolators and dampers. For DB shaking, the average maximum displacement of any isolator shall be no greater than 1.15 times the average maximum displacement at the center of rigidity. Eleven sets of ground motions, generated per Section 3.5, shall be used for analysis of the 3D model of the isolated building to compute these displacements.

Accidental eccentricity, which was introduced into seismic design standards for conventional, non-nuclear building construction to penalize torsionally flexible and/or weak lateral force-resisting systems, need not be addressed for seismically isolated nuclear power plants because a) the distribution of dead load and equipment loads are well defined and explicitly addressed in the numerical model, and b) the isolators are distributed across the footprint of the building.

3.4.1.3 Vertical load resistance

Each isolator in the isolation system shall be designed to suffer no permanent damage under loads and displacements associated with DB shaking.

Each isolator in the isolation system shall be designed to resist mean maximum and minimum loads associated with TPG shaking at a horizontal displacement equal to D_{50}.

3.4.1.4 Minimum lateral restoring force

The aggregated horizontal force-displacement relationship of the isolators in the isolation system shall be such that the force at D_{DB}, is at least $0.025W$ greater than the force at displacement $0.5D_{DB}$, where W is the building weight supported by the isolation system, similar to the requirement for non-nuclear buildings per ASCE/SEI 7 (ASCE 2022).

3.4.1.5 Wind loads

A seismically isolated nuclear power plant shall resist the effects of design wind loading in accordance with requirements for non-isolated plants. Design wind loads shall not damage either the isolators or the VDDs.

3.4.1.6 Operating conditions

The space containing the isolation system, referred to by some as the seismic vault, shall be enclosed and

maintained at a temperature between 5°C and 30°C at low humidity. A greater range for operating temperature is acceptable if it can be shown that the mechanical properties of the isolators and dampers in the isolation system do not vary by more than ±20% from the values used for analysis and design, for the expected lifetime of the isolation system.

3.4.1.7 Inspection, device replacement, and monitoring

The design shall provide access for inspection and replacement of all isolators and VDDs in the isolation system.

A program for monitoring the isolation system and inspection of all isolators and VDDs shall be prepared and implemented. Two spare isolators and VDDs of each type used in the isolation system shall be stored next to installed devices. Prototype isolators and VDDs, if not damaged by testing, may be used for this purpose. These spare isolators and VDDs shall be retested, at an interval not to exceed 10 years, with the same or a similar test machine and protocol used for the production tests described in Section 6. The requirement for storage and re-testing of spare devices may be tailored to specific technologies based on the availability of relevant, long-term performance data. For example, storage and periodic re-testing of elastomeric isolators, spherical sliding isolators, and fluid viscous dampers may not be necessary based on prior US experience by certain suppliers to non-nuclear sectors. If the requirement for storage and re-testing of spare devices is tailored or waived, a justification shall be documented that identifies the rationale and the data used in the decision-making process.

A program for inspection and maintenance of a) all systems and components crossing the isolation interface, and b) the clearance between the isolated building and horizontally adjacent construction, shall be prepared and implemented to ensure the unrestricted movement of the isolation system in the event of earthquake shaking.

3.4.1.8 Basemat and foundation designs

The basemat and the foundation shall be sufficiently stiff to engage all isolators and VDDs in resisting earthquake-induced loadings, ensuring horizontal diaphragm action above and below the isolation plane.

3.4.1.9 Systems and components crossing the isolation interface

All systems and components that cross the isolation interface shall be designed and detailed to provide negligible resistance to the horizontal and vertical seismic response of the isolated building.

3.4.1.10 Seismic monitoring

Three-component digital seismic monitoring equipment shall be placed at a minimum of 3 locations around the perimeter of the basemat to capture the acceleration response of the isolated superstructure. Instrumentation in the free field, on the foundation, and over the height of the isolated superstructure shall conform with Regulatory Guide 1.12 (USNRC 2017a). If a user selects an alternate approach to implement seismic instrumentation, the user shall justify the applicability of that approach.

3.4.2 Isolators and viscous damping devices

3.4.2.1 Mechanical properties

The mechanical properties of the isolators and VDDs shall not vary over the lifespan of the isolation system by more than ±20% from the values used for analysis and design, for the expected lifetime of the isolation system, accounting for variations in material properties at the time of device construction, changes in material properties with time (if any), operating temperature, and exposure to radiation. A greater expected percentage change in the mechanical properties of the isolation system must be supported by bounding analysis of the isolation system and the isolated SSCs to support design and risk calculations.

3.4.2.2 Quality control and quality assurance

Quality control and assurance for the testing and construction of isolators and VDDs shall be realized via either commercial grade dedication per Section 8 or by conforming with the most recent version of ISO 9001 (ISO 2015) or approved equivalent.

3.5 Seismic Inputs

3.5.1 Introduction

The isolation system shall be analyzed and designed using a minimum of 11 sets of three-component ground motions. The three components of translational motion, two horizontal and one vertical, shall be input at the boundaries of the mathematical model of the isolated building. The horizontal translational components of motion shall align with the principal horizontal axes of the building.

The sets of motions shall be matched to target vertical and geomean horizontal spectra for a) calculations per Section 3.7, including displacements and forces for prototype and production testing of isolators and dampers, b) performance (risk-type) calculations per Section 5 to determine the required horizontal median displacement capacity of the isolation system, D_{50}, and displacements for prototype testing, and c) design calculations for SSCs in the isolated superstructure assigned to Seismic Design Categories with target

performance goals different from that assigned to the isolation system.

3.5.2 Sets of ground motions for dynamic analysis

The minimum number of 11 sets of ground motions is based on requirements for nonlinear dynamic analysis of commercial buildings in ASCE/SEI Standard 7-22 (ASCE 2022) and FEMA P-58-1 (FEMA 2012), based on the theory presented in Appendix C of Huang *et al.* (2008). Fewer than 11 sets of motions can be used if justified per the theory of Huang *et al*. The procedure used to account for variability in the two horizontal components of ground motion around the geometric mean, used for the performance calculations of Section 5, is documented in Huang *et al.* (2009) and Huang *et al.* (2013), and is summarized in Appendix A.4.

3.6 Dynamic Analysis

3.6.1 General

Section 12.4.1 of ASCE/SEI 4-16 (ASCE 2017) presents three methods for analysis of seismically isolated nuclear structures, namely 1) time domain, 2) frequency domain, and 3) multistep. This report exclusively implements time-domain.

Soil-structure-interaction analysis is not addressed in this report. Such interaction may be important for the response of structures, systems, and components, if the building structure is both very stiff and massive or it is embedded. The introduction of a flexible isolation system beneath a stiff building will reduce the negative impacts (e.g., increased in-structure acceleration demand) of soil-structure interaction, if any. Lal *et al.* (2024) presents data that shows soil-structure-interaction analysis is insignificant for base-isolated reactor buildings and equipment supported therein.

3.6.2 Time-domain analysis

3.6.2.1 Introduction

Time-domain analysis of three-dimensional finite element models for DB and TPG shaking shall utilize three translational components of ground motion (i.e., one ground motion set) applied simultaneously. (A 2DOF model is used for the performance-based calculations of Section 5.) Commercial finite element software such as SAP2000[6], LS-DYNA[7], and ABAQUS[8] enable nonlinear dynamic analysis of seismic

[6] https://www.csiamerica.com/products/sap2000

[7] https://www.ansys.com/en-in/products/structures/ansys-ls-dyna

[8] https://www.3ds.com/products/simulia/abaqus

isolation systems and SSCs.

3.6.2.2 Finite element modelling

The modeling of the isolated building, basemat, and foundation, including element choices and mesh sizes, shall conform to current practice for non-isolated nuclear power plants. The in-plane and out-of-plane flexibility of the basemat and the foundation shall be modeled.

Seismic isolators and VDDs shall be explicitly modeled for analysis of the isolated building for DB and TPG shaking. Three dimensional models shall be used for seismic isolators and 3D VDDs. Uni-directional models shall be used for 1D fluid viscous dampers. Mathematical models of seismic isolators and dampers shall follow Section 3.6.3.

3.6.3 Mathematical modeling of isolators and dampers

Numerical models of isolators and VDDs are available in most commercial finite element codes (see above) and some open-source codes, including MASTODON[9] (Veeraraghavan *et al.* 2020). Such models should be verified using theory and validated using data from high-speed dynamic testing of prototype devices. Examples of verification and validation are presented in Kumar *et al.* (2019b) for spherical sliding (e.g., SFP) isolators and Kumar *et al.* (2019a) for LDR and LR bearings. Guidance on commercial grade dedication of seismic isolators and 1D fluid viscous damper elements can be found in Doulgerakis *et al.* (2021).

Nonlinear models should be used for analysis of seismic isolators and VDDs unless device response is linear elastic for the forces and displacements calculated for the imposed intensity of shaking. A model of a seismic isolator shall include axial force-displacement relationships in compression (and tension if developed) and a coupled bilinear horizontal force-displacement relationship, and must address coupling of vertical and horizontal force-displacement responses. Examples for SFP and elastomeric bearings can be found in Kumar *et al.* (2019b) and Kumar *et al.* (2019a), respectively.

A model of a 1D fluid viscous damper of Figure 2.3f and 2.3h shall include force-velocity-displacement relationships along its axis of action, and the effect, if any, of proximity to the device end-of-travel. For the 3D viscoelastic damper of Figure 2.3g, force-velocity-displacement relationships shall be provided along each axis of action, and shall address the frequency dependence of response, coupling of vertical and horizontal responses, and the effect, if any, of proximity to the device end-of-travel.

[9] https://mooseframework.inl.gov/mastodon/

3.7 Displacements and Forces for Design

3.7.1 General

This section of the report discusses the calculation of forces for design of connections of isolators and VDDs to the superstructure and the substructure. The design and detailing of SSCs in the isolated structure and of systems and components crossing the isolation interface shall conform with industry requirements for non-isolated structures, as noted in Section 3.7.4. The required horizontal clearance to adjacent construction is identified in Section 3.7.5.

3.7.2 Seismic isolators and dampers

3.7.2.1 DB shaking

Dynamic analysis of a 3D finite element of the isolated building shall be performed for DB shaking using 11 sets of ground motion triplets per Section 3.5.

For each type and size of isolator and/or damper in the isolation system, the following data shall be collected and processed for each DB ground motion triplet: 1) maximum resultant horizontal displacement, 2) maximum absolute earthquake-induced axial force, and 3) for 1D vertical and 3D isolation systems, the maximum absolute earthquake-induced vertical displacement. From 1), compute the mean (of 11) maximum resultant horizontal displacement. From 2), compute the mean (of 11) maximum earthquake-induced axial force. From 3) compute the mean (of 11) maximum earthquake-induced axial displacement. These forces and displacements are used for production testing per Section 6.5.

3.7.2.2 TPG shaking

Dynamic analysis of a 3D finite element of the isolated building shall be performed for TPG shaking using 11 sets of ground motion triplets per Section 3.5.

For each type and size of isolator and/or damper in the isolation system, the following data shall be collected and processed for each TPG ground motion triplet: 1) maximum absolute earthquake-induced axial force, 2) maximum absolute earthquake-induced axial force in the damper, and 3) for 1D vertical and 3D isolation systems, the maximum absolute earthquake-induced vertical displacement. From 1), compute the mean (of 11) maximum earthquake-induced axial force. From 2), compute the mean (of 11) maximum earthquake-induced damper force. From 3), compute the mean (of 11) maximum earthquake-induced vertical displacement. The mean maximum isolator axial forces and isolator vertical displacements shall be used for the prototype tests of Section 6.

The connections of each isolator to the structure above (i.e., basemat) and below (i.e., foundation) shall be designed to remain elastic for the mean maximum earthquake-induced axial force acting in compression or tension and co-existing gravity loads factored per materials standards, and the horizontal force in the isolator associated with displacement D_{50}, applied simultaneously.

The connections of each damper to the structure above (i.e., basemat) and below (i.e., foundation) shall be designed to remain elastic for the mean maximum earthquake-induced damper force acting in compression or tension and co-existing dead load factored per materials standards.

3.7.3 Structure below the isolation interface

The foundation and pedestals below each isolator and damper shall be designed to remain elastic for the mean maximum earthquake-induced axial force per Section 3.7.2.2 acting in compression or tension and co-existing gravity loads factored per materials standards, and the horizontal forces in the isolator associated with displacement D_{50} and the mean maximum damper force, applied simultaneously.

3.7.4 Systems and components crossing the isolation interface

The systems and components that cross the isolation interface shall be designed and detailed for shaking consistent with their assigned SDC, recognizing that significant relative horizontal displacements might develop between points of support on and *off* the isolated building, where *off* refers to both the foundation below the isolation interface and horizontally adjacent construction (i.e., the retaining wall of Figure 4.3).

3.7.5 Clearance to adjacent construction

The horizontal clearance to adjacent construction must be sufficient to permit unrestricted movement of the isolated building to achieve the TPG assigned to the isolation system. A minimum horizontal clearance equal to $1.15\,D_{50}$ along each principal axis of the isolated building shall be provided. (See Section 5.4 for details).

SECTION 4
ARCHETYPE REACTOR BUILDING, SAMPLE EQUIPMENT, AND SITING

4.1 Introduction

An archetype reactor building, safety-related equipment, and a hypothetical site are used in this report to demonstrate a process to select, analyze, design, and deploy a seismic isolation system. The building and its equipment are loosely based on an early version of a fluoride salt-cooled reactor plant being developed by Kairos Power of Alameda, CA. The building is sited in a region of moderate seismic hazard in the Central and Eastern United States. To demonstrate the utility of seismic isolation and the importance of correctly characterizing the local soil conditions, two different soil domains are considered: soft rock and stiff soil.

The building and its equipment are modeled in SAP2000 (CSI 2020) for the purpose of dynamic analysis. Soil-structure interaction is ignored since the building's footprint and mass are small, and it is base isolated.

Section 4.2 introduces the archetype nuclear reactor building and the assumed safety-related equipment. Finite element models for the building and equipment are prepared and key dynamic properties are reported. Section 4.3 presents the layout of the base isolation system. Section 4.4 presents information on the candidate isolation systems considered in this report. The two degree-of-freedom model used for the isolation-system performance calculations is introduced in Section 4.5. The hypothetical site is identified in Section 4.6.

All SAP2000 models and seismic inputs described in this report are available on DesignSafe; see Yu *et al.* (2023).

4.2 Reactor Building and Safety-related Equipment

4.2.1 Finite element models

Figures 4.1a, b, and c present the reactor building in three views, the global coordinate system, and key dimensions. The building includes four floors: a reinforced concrete (RC) basemat (grey), a suspended RC floor (green), and two composite floors (yellow). The RC basemat and the suspended floor slabs are 1.2 m thick. The composite floors are 76 mm of concrete on a 76 mm-deep metal deck; an average concrete thickness of 114 mm is modelled but the deck is not.

The suspended RC floor is supported around its perimeter by 1.2 m-thick RC walls (orange). The two composite floors are supported by structural beams (blue). The floor-to-floor heights vary: basemat to suspended RC floor = 8.6 m, suspended RC floor to lower composite floor = 5 m, and lower to upper composite floors = 4.6 m, as noted in Figure 4.1b. The reactor shield is a RC cylindrical wall (shaded pink) that is supported by the basemat. The RC shield wall and its circular head are 1.2-m thick. The outer diameter of the shield structure is 8.8 m, and its overall height is 18 m, as noted in Figure 4.1d. The suspended RC floor and the composite floor framing are pinned to the cylindrical shield wall. The building is framed in structural steel above the upper composite floor, shown in blue. The out-to-out plan dimensions of the building are 25 m x 25 m, and the height from the basemat (grade level) to the ridge is 33 m. The part of the building below the top of the suspended RC floor and reactor shield head is assumed to be safety related and houses safety-related equipment. The building above the suspended RC floor, namely, the steel framing and the composite floors, is assumed to be non-safety related. The design and analysis for the safety-related parts of the building follow nuclear standards including ASCE/SEI 4-16 (ASCE 2017), ASCE/SEI 43-19 (ASCE 2021), ACI 349-13 (ACI 2013), and ANSI/AISC N690 (AISC 2018). The non-safety-related part of the building is designed as a commercial building for loads defined in ASCE/SEI 7-22 (ASCE 2022), adopting non-nuclear standards such as ACI 318-19 (ACI 2019), ANSI/AISC 360-22 (AISC 2022), and ANSI/AISC 341-16 (AISC 2016).

The building is modeled in SAP2000 using elastic shell and line elements. The basemat, suspended RC floor, composite floors, walls, and reactor shield are modeled using shell elements with a thickness of 1.2 m, 1.2 m, 114 mm, 1.2 m, and 1.2 m, respectively. The structural steel framing is modeled using line elements. Table 4.1 presents the mechanical properties assumed for the numerical model.

A gantry crane is installed on the steel frame at the level of the grey dashed lines on the two *y-z* faces shown in Figure 4.1a. The mass of the crane is 27 tonnes, and it is assumed to be evenly distributed to the steel columns for dynamic analysis and represented by the grey solid circles shown in Figure 4.1a. Distributed masses of 75 kg/m^2 and 50 kg/m^2 are applied to the top faces of the roof and the outer faces (+*x*, -*x*, +*y*, and -*y* sides) of the steel frame, respectively, to address the mass of the sheeting, insulation, and sundry equipment, using lumped masses at nodes on the steel purlins and columns. Distributed masses of 500 kg/m^2, 250 kg/m^2, and 125 kg/m^2, representing the sum of the superimposed dead load and live load, are applied to the basemat, suspended RC floor, and the two composite floors, respectively.

The mass of the building is 8511 tonnes, including the reactor shield, gantry crane, and the assigned distributed and lumped masses, but excluding the explicitly modeled equipment (introduced in Figure 4.2). Table 4.2 lists the weight of each component of the reactor building.

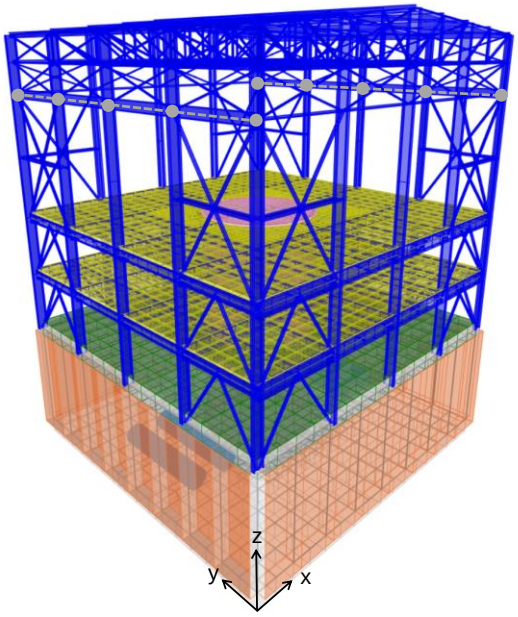

(a) building, isometric view

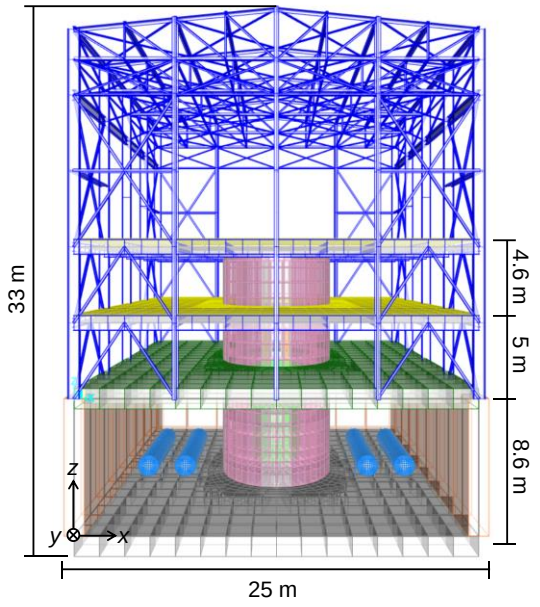

(b) building, *x*-*z* perspective view (reinforced concrete wall on the +*y* face removed from view)

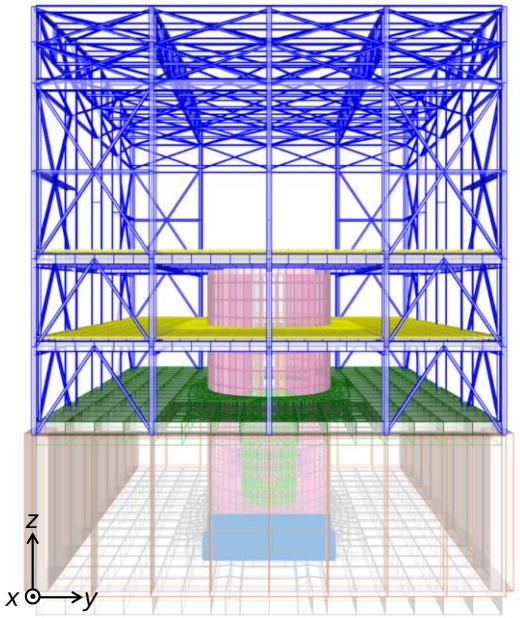

(c) building, *y*-*z* perspective view

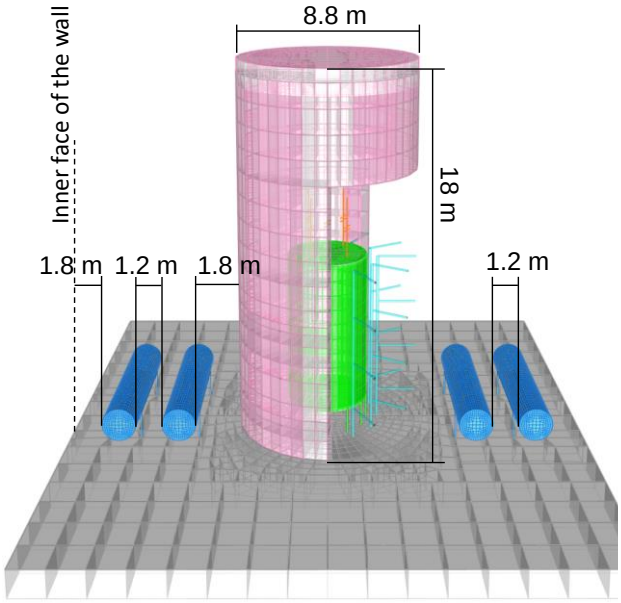

(d) basemat, reactor shield, and equipment, *x*-*z* perspective view (part of reactor shield removed)

Figure 4.1. Finite element models for the reactor building and its equipment

Table 4.1. Assumed mechanical properties for the reactor building framing

Concrete	Density (kg/m^3)	2403
	Compressive strength (MPa)	28
	Poisson's ratio	0.2
	Elastic modulus (N/m^2)	2.5×10^{10}
Structural steel	Density (kg/m^3)	7850
	Yield strength (N/m^2)	420
	Poisson's ratio	0.3
	Elastic modulus (N/m^2)	2×10^{11}

Table 4.2. Component masses in the building model

Component	Superimposed mass	Total mass[1] (tonne)
Basemat (grey)	500 kg/m^2	2032
Suspended RC floor (green)	250 kg/m^2	1700
Two composite floors (yellow)	125 kg/m^2	426 (213 each)
Four RC walls (orange)	--	2368 (592 each)
Steel frame (blue)	27 tonnes for the crane 75 kg/m^2 on the roof 50 kg/m^2 on the 4 outer faces	443
Reactor shield and head (pink)	--	1544

1. Sum of the self-weight of the component and the superimposed mass listed in the second column

Six pieces of safety-class equipment of three types are included in the model: one reactor vessel (RV), one reactor vessel auxiliary cooling system (RVACS), and four primary heat exchangers (PHXs). They are assumed to be manufactured using stainless steel and filled with molten salt with a density of 1940 kg/m^3.

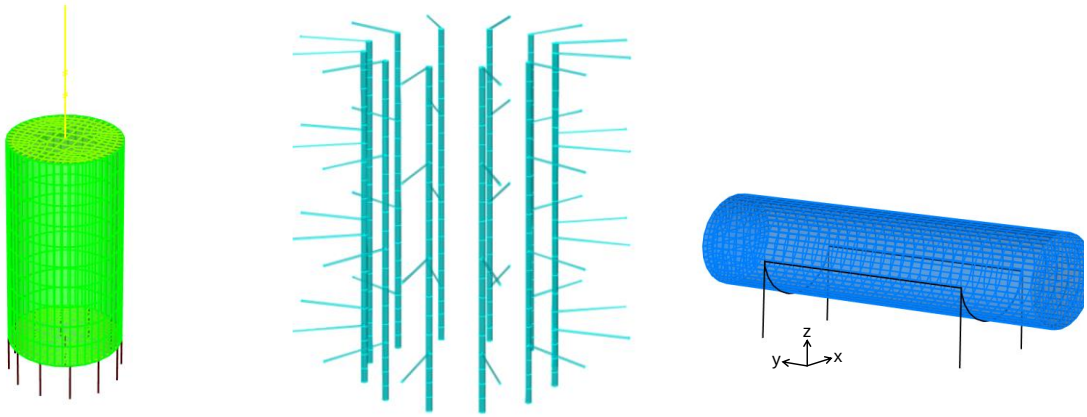

(a) reactor vessel (RV) (b) reactor vessel auxiliary cooling system (RVACS) (c) primary heat exchanger (PHX)

Figure 4.2. Finite element models of safety-related equipment

The RV is a cylindrical tank located inside the shield wall (pink) and supported on the basemat with vertical line elements, as shown in Figure 4.2a. The diameter of the RV is 3.8 m; its height, excluding the supporting elements, is 7.2 m, and its wall thickness is 25 mm. The tank is modeled using shell elements. The supporting elements are rigid, fixed at the basemat, and pinned at the bottom of the tank. The mass of the molten salt is 158 tonnes and it is included in the model using lumped masses distributed on the tank wall and base. Since the hydrodynamic pressure of the molten salt is normal to the inner surfaces of the tank, the wall (base) is assigned *x*- and *y*-directional (*z*-directional) distributed masses of 158 tonnes. There are 2 two-degree-of-freedom oscillators attached to the RV head to represent equipment, with horizontal frequencies of 10 and 20 Hz. The mass of each oscillator is 0.1 tonne. A distributed mass of 15 tonnes is assigned to the vessel head to address the weight of some head-mounted equipment submerged in the molten salt. The total mass of the RV is 216 tonnes.

The RVACS, shown in bright blue in Figures 4.1d and 4.2b, is located between the reactor and shield wall. The RVACS is modeled using twelve 8 m-long vertical tubes, with a diameter of 152 mm and a wall thickness of 6 mm. Each tube is supported by horizontal rigid line elements at four levels: at the top end of the pipe and 2.3 m, 4.6 m, and 6.6 m below the top end. These line elements are fixed at the shield wall and pinned at the tube. The top pinned support constrains the pipe in both the horizontal and vertical directions (*x*, *y*, and *z*), and the lower three pinned supports constrain the horizontal directions (*x* and *y*). The total mass of the 12 units is 71 tonnes.

There are 4 PHXs (shaded blue) in the reactor building. Each PHX is a horizontally oriented cylindrical tank simply supported by a rigid frame on the basemat; see Figure 4.2c. The diameter of the vessel is 1.5 m, its length is 7.3 m, and its wall thickness is 16 mm. The molten salt in each tank weighs 26 tonnes. The

total weight of each PHX is 30 tonnes. The mass of the reactor building, including the RV, RVACS, and PHXs, is 8918 tonnes.

4.2.2 Dynamic properties

Eigen modes are calculated for the finite element model of the reactor building (including the equipment) shown in Figure 4.1, assuming all basemat nodes to be fixed. The building and equipment respond in many modes. More than 500 modes are required to capture 90% of the total mass in the *x*, *y*, and *z* directions. The third column of Table 4.3 presents the frequencies of the modes that contribute the greatest modal effective mass in each direction. These modes are associated with displacements of the safety-related parts of the building. The listed *x*- and *y*-directional modes are associated with lateral displacements along the height of the building, including the RC walls, suspended RC floor, and reactor shield. The *z*-directional mode involves vertical displacements of the suspended RC floor, axial extension of the reactor shield wall, and breathing of the RC walls. The fourth, fifth, and sixth columns of Table 4.3 present the first modal frequencies for the equipment in the conventionally founded reactor building.

Table 4.3. Key modal properties of the conventionally founded reactor building, reactor vessel (R V), reactor vessel auxiliary cooling system (RVACS), and primary heat exchangers (PHXs)

		Reactor building[1]	RV	RVACS	PHXs
Frequency (Hz)	x	10 (28%)	12	7	11
	y	10 (25%)	12	7	24
	z	24 (21%)	37	27	18

1. Effective mass for each mode shown in parentheses

4.3 Seismic Isolation System: Layout of Isolators and Viscous Damping Devices

Figure 4.3 locates the isolation plane in the archetype reactor building. The isolators are shown installed on reinforced concrete pedestals, below the basemat and above the foundation. The VDDs are not shown in Figure 4.3. The isolation system provides horizontal and/or vertical flexibility between the basemat and the foundation, which substantially mitigates the effects of earthquake ground shaking on the building and the equipment.

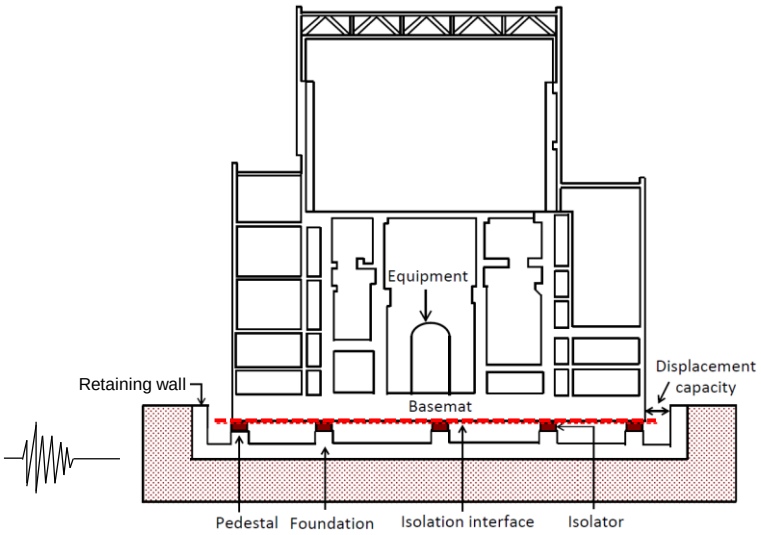

Figure 4.3. Base-isolated reactor building (adapted from Kammerer et al. (2019))

Figure 4.4a shows the finite element model of the reactor building supported by an isolation system. Each isolator is modeled explicitly at the underside of the basemat at the locations shown in Figures 4.4a and 4.4b.

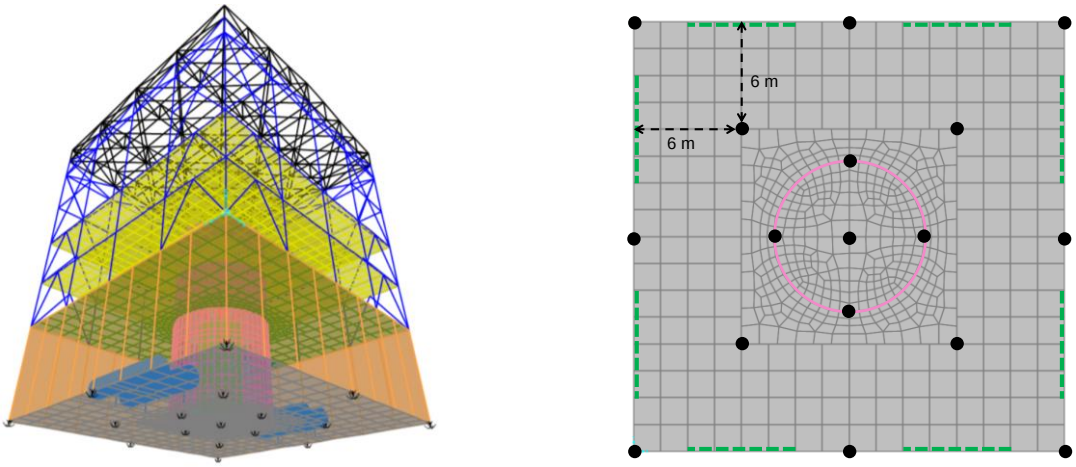

(a) building supported by isolators modeled using black elements below the basemat

(b) isolators (17) located by black solid circles and dampers (8) by dashed green lines[10]

Figure 4.4. Base isolation systems for the reactor building

There are 17 isolators, shown as black solid circles: at the center, 4 corners, middle of the 4 edges, 6 m from the edges of the basemat, and at the 4 sides of the bottom of the shield wall, which is identified by a pink

[10] Appropriate nodal connectivity in the basemat mesh is achieved using the *area edge constraint* command in SAP2000.

circle. This layout is used for the 2D (2H) and 3D (2H and 1V) isolation systems introduced in Section 4.4. Supplemental horizontal 1D fluid viscous dampers, which are deployed in two of the isolation systems considered below, are located by the dashed green lines in Figure 4.4b: four along each horizontal axis of the building. Supplemental vertical 1D fluid viscous dampers and 3D viscoelastic (pot) dampers, which are not identified in Figure 4.4b, are used in the 3D isolation systems, and located adjacent to each of the 17 isolators.

The layout of Figure 4.4b is not optimized for any of the isolation systems. Considerations for locating isolators and VDDs should include a) limiting the number of device sizes, b) similar maximum gravity loads on individual isolators, and c) distributing isolators in plan to minimize torsional response.

4.4 Isolation Systems Considered

4.4.1 Introduction

The seven isolation systems of Table 4.4 are considered in this report. The list is not exhaustive but includes isolation systems available for deployment in the US at the time of this writing. Of the seven systems, five provide horizontal (2D) isolation: 1) 2-sec linear elastomeric (LDR) isolators, 2) 2-sec nonlinear SFP isolators, 3) 2-sec linear elastomeric (LDR) isolators and uniaxial (1D) horizontal nonlinear fluid viscous dampers (FVDs), 4) 2-sec nonlinear SFP isolators and 1D horizontal nonlinear FVDs, and 5) 3-sec SFP isolators. The other two systems provide three-directional (3D) isolation. System 6 is identified as a 3D linear system herein and is composed of 3D spring isolators and 3D viscoelastic dampers. The 3D hybrid system 7 is composed of 2-sec SFP isolators functioning in the horizontal plane and guided spring isolators and 1D nonlinear FVDs in the vertical direction. In Table 4.4, H1 and H2 are the principal horizontal axes of the building, aligning with the x and y axes, respectively, of Figure 4.1a. A LR isolation system is not analyzed herein solely because the force-displacement properties of the bearings are bilinear and like that of the SFP bearing; near identical outcomes would be reported.

Systems 1 and 3 are considered for the performance calculations of Section 5. Systems 2, 4, 5, and 6 are considered for the supplemental performance calculations of Appendix C. All seven isolation systems are addressed in Appendix E.

Table 4.4. Isolators and VDDs used in the seven candidate isolation systems for the reactor buildin g, horizontal (H1, H2) and vertical (V) directions

System	Isolation direction	Isolators		VDDs	
		H1, H2	V	H1, H2	V
1	2D	2-sec linear	--	--	--
2	2D	2-sec nonlinear	--	--	--
3	2D	2-sec linear	--	1D nonlinear FVDs	--
4	2D	2-sec nonlinear	--	1D nonlinear FVDs	--
5	2D	3-sec nonlinear	--	--	--
6	3D	3D linear; 1.1 sec for H and 0.4 sec for V		3D viscoelastic dampers	
7	3D	2-sec nonlinear	1D linear; 0.4 sec for V	--	1D nonlinear FVDs

Section 4.4.2 presents the mechanical properties of the seven isolation systems. Numerical modeling in SAP2000 (CSI 2020) for an isolation system, an isolator, and a damper is described in Section 4.4.3.

4.4.2 Mechanical properties of the isolation systems

System 1: 2-sec linear

System 1 is a lightly damped 2D linear system composed of 17 identical LDR isolators with a horizontal force-displacement (*F*-*u*) relationship shown in Figure 4.5. The *F*-*u* relationship for the isolation system is defined by a horizontal stiffness, $K_{iso,h}$, and a viscous damping ratio, characterizing the area of the hysteresis loop. Given the isolation period $T_{iso,h} = 2$ seconds and a superstructure mass *m* = 8,920 tonnes, the horizontal stiffness, $K_{iso,h}$, of the isolation system is 8.8×10^4 kN/m. (Information on the design of the elastomeric and sliding isolators can be found in Constantinou *et al.* (2007; 2011). Isolators were sized but that information is not reported in this section.) The vertical stiffness, K_v, of the isolation system is 2.4×10^8 kN/m. Assuming the superstructure to be rigid, the vertical frequency is 26 Hz (period = 0.04 sec). Assuming 5% damping in the elastomer, the damping coefficients are $C_h = 2800$ kN-s/m and $C_v = 1.5 \times 10^5$ kN-s/m in the horizontal and vertical directions, respectively.

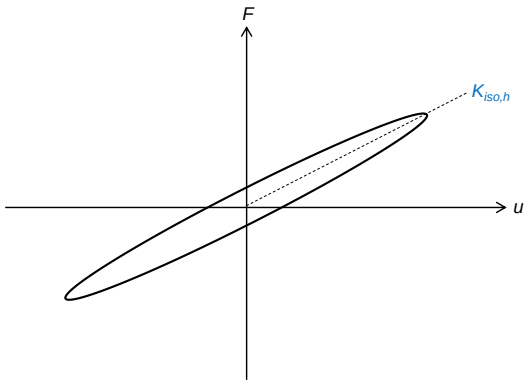

Figure 4.5. Force-displacement (F-u) relationship of system 1, linear isolators, horizontal directions

System 2: 2-sec nonlinear

System 2 is a 2D nonlinear system composed of 17 identical SFP isolators. The idealized horizontal *F-u* relationship of the system is presented in Figure 4.6. The *F-u* relationship is characterized by a zero-displacement force intercept, Q, and a second-slope stiffness, $K_{iso,h}$, which defines the isolation period $T_{iso,h}$. The parameters d_1 and K_1 are introduced to enable numerical modeling; see the second footnote to Table 4.5. The value of Q is the product of the coefficient of sliding friction, μ, and the instantaneous vertical load on the isolation system; Q changes by time step with the vertical earthquake shaking. The coefficient of sliding friction, μ, is assumed to be 0.06, which is an often-used value. In the absence of vertical shaking and for *m* = 8,920 tonnes (W = 8.75×10^4 kN), Q = 5,250 kN. The second-slope stiffness $K_{iso,h}$ is inversely proportional to the radius, R, of the curvature of the concave sliding surface; $K_{iso,h}$ = mg/R, where g is gravitational acceleration. For $T_{iso,h}=2$ seconds and *m* = 8,920 tonnes, $K_{iso,h}=8.8\times10^4$ kN/m and $R=1$ m. The *F-u* response of each isolator along each horizontal axis of the building, H1 and H2, is coupled, namely, *F-u* response along direction H1 is affected by displacement response along H2, and vice versa. The coupled hysteresis is addressed explicitly in SAP2000.

The axial stiffness of a SFP isolator in compression is a function of the geometry of the articulated slider. (The axial stiffness in tension is zero.) Herein, the superstructure gravity load is distributed equally to each isolator and the assumed contact pressure is set equal to 34 MPa, resulting in a slider radius of 217 mm. Assuming 17 identical articulated sliders and a vertical stiffness per isolator equal to 20% of the axial stiffness of a carbon steel cylinder with a radius and height equal to 217 mm, the vertical compressive stiffness, K_v, of the isolation system is 4.6×10^8 kN/m. Assuming the superstructure to be rigid, the vertical frequency = 36 Hz (period = 0.03 second). Assuming a damping ratio of 2% in the vertical direction, C_v = 8.1×10^4 kN-s/m.

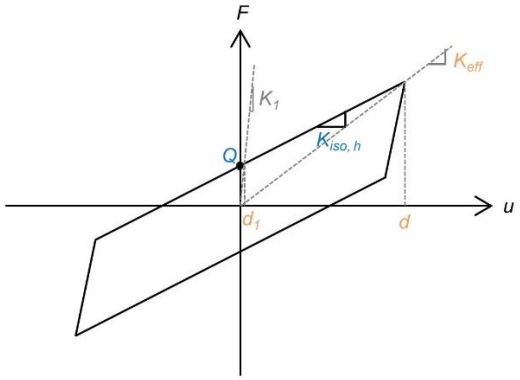

Figure 4.6. Force-displacement (*F-u*) relationship of systems 2, 5, and 7, nonlinear isolators, horizontal directions

System 3: 2-sec linear and 1D nonlinear FVDs

System 3 is a 2D isolation system composed of the 2-sec linear isolators of system 1 and uniaxial (1D), nonlinear FVDs in the two horizontal directions. The F-u relationship for the 2-sec linear system is shown in Figure 4.5, and the parameters are $K_{iso,h} = 8.8 \times 104$ kN/m, $K_v = 2.4 \times 108$ kN/m, $C_h = 2800$ kN-s/m, and $C_v = 1.5 \times 105$ kN-s/m, as described for system 1. Figure 4.7a presents the force-velocity (F-v) relationship for the nonlinear FVDs, defined by a damping coefficient, C_d and a velocity exponent, δ, less than 1. Herein, $\delta = 0.3$ and $C_d =$ 5,000 kN-(s/m)0.3 along each horizontal axis of the building. The composite F-u relationship for system 3 is the sum of those shown in Figure 4.5 (linear isolators) and Figure 4.7b (a nonlinear FVD subjected to sinusoidal loading).

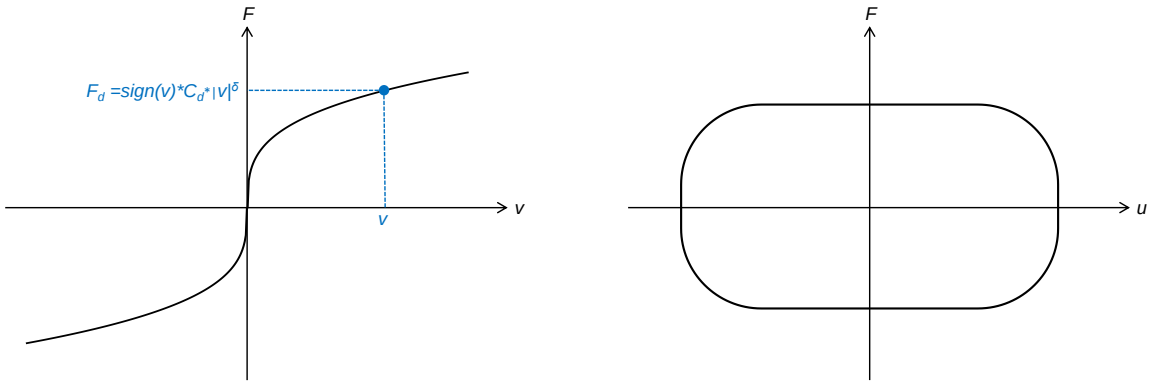

(a) *F-v* relationship **(b) *F-u* relationship**

Figure 4.7. Force-velocity (*F-v*) and force-displacement (*F-u*) relationships for uniaxial FVDs, horizontal directions for systems 3 and 4, vertical direction for system 7

System 4: 2-sec nonlinear and 1D nonlinear FVDs

System 4 is composed of the 2-sec SFP isolators of system 2 and the nonlinear FVDs used for system 3. The *F-u* relationship of system 4 is the sum of those shown in Figure 4.6 (SFP isolators) and Figure 4.7b (nonlinear FVDs).

System 5: 3-sec nonlinear

System 5 is composed of 3-sec SFP isolators. The idealized horizontal *F-u* relationship is shown in Figure 4.6. Given $T_{iso,h} = 3$ seconds and m = 8,920 tonnes, $K_{iso,h} = 3.9 \times 10^4$ kN/m and $R = mg / K_{iso,h}$ = 2.2 m. Other parameters are set to those for the 2-sec sliding isolators of system 2, namely, $Q = 5{,}250$ kN, K_v = 4.6×10^8 kN/m, and $C_v = 8.1 \times 10^4$ kN-s/m.

System 6: 3D linear (viscoelastic)

System 6 is composed of 3D spring isolators (see Figures 2.3d and 2.3e) and 3D viscoelastic dampers. The spring isolators are assumed to have linear stiffness and negligible damping in each of the three directions. Coupling of horizontal and vertical responses is ignored[11]. The 3D viscoelastic dampers are assumed to be viscous for the analysis presented below and elsewhere in this report[12]. The *F-u* relationship of the isolation system in each direction is shown in Figure 4.8 and is linear viscoelastic. The dynamic properties assumed for analysis are $T_{iso,h} = 1.1$ seconds, $T_{iso,v} = 0.4$ second, 25% damping in the horizontal directions, and 8% damping in the vertical direction: $K_{iso,h} = 2.9 \times 10^5$ kN/m, $K_{iso,v} = 2.2 \times 10^6$ kN/m, $C_h = 2.5 \times 10^4$ kN-s/m, and $C_v = 2.2 \times 10^4$ kN-s/m.

[11] Coupling must be addressed for project-specific calculations.

[12] These 3D dampers exhibit viscoelastic behavior, namely, both elastic and viscous characteristics, and can be modelled using fractional derivatives, as described in Makris and Constantinou (1990; 1991). The frequency-dependent response of the viscoelastic dampers must be captured for project-specific calculations.

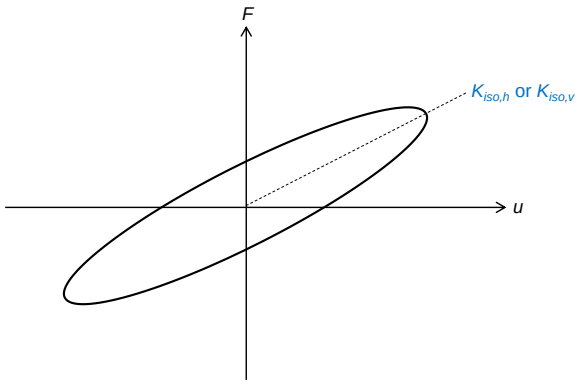

Figure 4.8. Force-displacement (*F*-*u*) relationship of the 3D linear viscoelastic isolation system

System 7: 3D hybrid

System 7 is a hybrid system composed of 2-sec SFP isolators in the horizontal plane and 1D *guided* spring isolators and 1D nonlinear FVDs in the vertical direction. (This hybrid system is like that shown in Figure 2.3h except for the horizontal FVDs.) The 2-sec nonlinear isolators of system 2 are used in system 7. The stiffness of the spring isolators in the vertical direction is linear; the damping is negligible. The vertical period, $T_{iso,v}$, of the spring isolators is set to 0.4 second (identical to system 6), and so the aggregate vertical stiffness, including the flexibility of the sliding isolators, is $K_{iso,v} = 2.2 \times 10^6$ kN/m. The aggregated mechanical properties of the vertically oriented 1D nonlinear FVDs in system 7 are identical to those for systems 3 and 4 and are $\delta = 0.3$ and $C_d = 5{,}000$ kN-(s/m)$^{0.3}$. The *F*-*u* relationship of system 7 in the vertical direction is the sum of Figure 4.9a for the spring isolators and Figure 4.9b for the nonlinear FVDs.

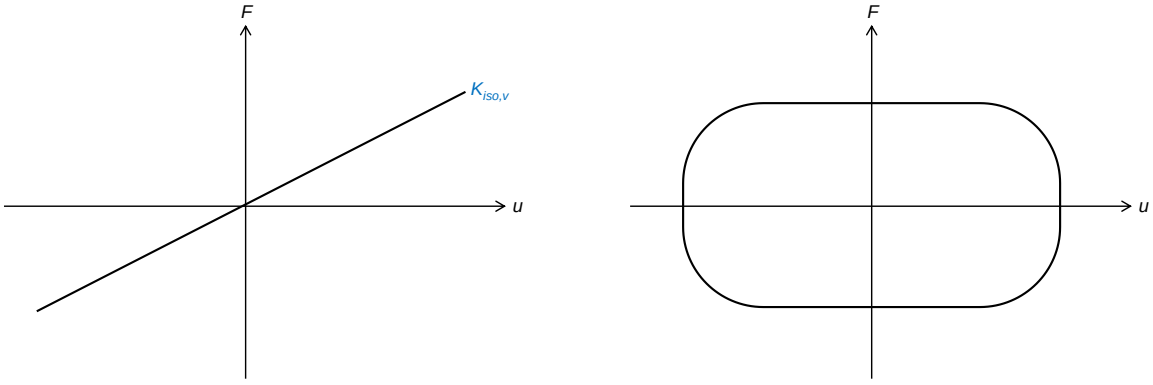

(a) coil-spring isolators (b) uniaxial nonlinear fluid viscous dampers

Figure 4.9. Force-displacement (*F*-*u*) relationships of the 3D hybrid isolation system in the vertical direction

The properties of the seven isolation systems are summarized in Table 4.5.

Table 4.5. Properties of seven isolation systems, superstructure mass, *m* = 8,920 tonnes, horizontal (H1, H2) and vertical (V) directions, super structure assumed to be rigid

System	Isolation direction	Period* (sec)		Frequency* (Hz)		Isolators†		Dampers‡	
		H1, H2	V	H1, H2	V	H1, H2	V	H1, H2	V
1	2D	2	0.04	0.5	26	$K_{iso,h} = 8.8 \times 10^4$ kN/m; C_h =2800 kN-s/m	$K_v = 2.4 \times 10^8$ kN/m; C_v =1.5×10^5 kN-s/m	--	--
2	2D	2*	0.03	0.5*	36	$\mu = 0.06$; R = 1 m; $K_{iso,h}$ = 8.8×10^4 kN/m; $K_1 = 5.3 \times 10^6$ kN/m§	$K_v = 4.6 \times 10^8$ kN/m; $C_v = 8.1 \times 10^4$ kN-s/m	--	--
3	2D	2	0.04	0.5	26	$K_{iso,h} = 8.8 \times 10^4$ kN/m; C_h =2800 kN-s/m	$K_v = 2.4 \times 10^8$ kN/m; C_v =1.5×10^5 kN-s/m	δ = 0.3; C_d = 5,000 kN-(s/m)$^{0.3}$	--
4	2D	2*	0.03	0.5*	36	$\mu = 0.06$; R = 1 m; $K_{iso,h}$ = 8.8×10^4 kN/m; $K_1 = 5.3 \times 10^6$ kN/m§	$K_v = 4.6 \times 10^8$ kN/m; $C_v = 8.1 \times 10^4$ kN-s/m	δ = 0.3; C_d = 50,00 kN-(s/m)$^{0.3}$	--
5	2D	3*	0.03	0.33*	36	$\mu = 0.06$; R = 2.2 m; $K_{iso,h} = 3.9 \times 10^4$ kN/m; $K_1 = 5.3 \times 10^6$ kN/m§	$K_v = 4.6 \times 10^8$ kN/m; $C_v = 8.1 \times 10^4$ kN-s/m	--	--
6	3D	1.1	0.4	0.91	2.5	$K_{iso,h} = 2.9 \times 10^5$ kN/m	$K_{iso,v} = 2.2 \times 10^6$ kN/m	C_h = 2.5 × 10^4 kN-s/m†	C_v = 2.2 × 10^4 kN-s/m†
7	3D	2*	0.4	0.5*	2.5	$\mu = 0.06$; R = 1 m; $K_{iso,h} = 8.8 \times 10^4$ kN/m; $K_1 = 5.3 \times 10^6$ kN/m§	$K_{iso,v} = 2.2 \times 10^6$ kN/m	--	δ = 0.3; C_d = 5,000 kN-(s/m)$^{0.3}$

* Periods and frequencies calculated using the superstructure mass m = 8,920 tonnes, and $K_{iso,h}$ and K_v for the 2D systems or $K_{iso,h}$ and $K_{iso,v}$ for the 3D systems; superstructure assumed to be rigid; for sliding isolation systems 2, 4, 5, and 7, the effective period T_{eff}, associated with K_{eff} shown in Figure 4.6, changing with the displacement and less than the listed isolation period

§ Defined to enable numerical modeling for sliding isolation systems: see Section 4.4.3 for details; K_1 calculated using Q = 5,250 kN at d_1 = 1 mm; period T_1, associated with K_1, is 0.26 second

† $K_{iso,h}$, C_h, K_1, $K_{iso,v}$, K_v, and C_v are the aggregated properties of 17 identical isolators located by the solid black circles in Figure 4.4b

‡ For systems 3 and 4, C_d is the aggregated coefficient for the 4 dampers (i.e., C_d /4 for each) along a horizontal axis (H1 or H2), identified as dashed green lines in Figure 4.4b; for systems 6 and 7, C_h, C_v, and C_d are the aggregated damper coefficients at the 17 locations (i.e., C_h /17, C_v /17, and C_d /17 for each) identified by the solid black circles in Figure 4.4b

† See footnote 12 in Section 4.4.2 regarding the viscoelastic behavior of the 3D damper.

4.4.3 Numerical modeling of the isolation systems in SAP2000

For the performance calculations of Section 5 and Appendix C, macro models are used to simulate the isolation *systems*, introduced in Section 4.5, with aggregated properties along the horizontal axes (H1, H2) of the building per Table 4.5. For the calculations of Appendix E, the isolators and VDDs are modeled explicitly per Figure 4.4a, with properties back-calculated from the aggregated values of Table 4.5 (see footnotes † and ‡ of the table). The elements used to model the isolation system (in the macro model) and each isolator (and damper, if used, in the finite element model) are identical. The elements used for the seven systems are described below.

The 2D linear isolators in systems 1 and 3, and the 3D linear isolation system 6 are simulated using the *linear* link in SAP 2000 with the stiffnesses and damping coefficients for the three translational degrees of freedom: $K_{iso,h}$, K_v or $K_{iso,v}$, C_h, and C_h listed in Table 4.5. The degrees of freedom are independent, namely, the responses of the linear isolation systems in the 3 directions are decoupled. The SFP isolators of systems 2, 4, 5, and 7 are simulated using the *friction isolator* link in SAP2000 for nonlinear horizontal response and linear vertical response. The horizontal and vertical degrees of freedom of the link are dependent. The horizontal force, Q, at zero displacement in the *F-u* relationship (Figure 4.6) changes with the vertical compressive load on the friction isolator link, which varies due to the vertical shaking. The horizontal sliding response of isolation systems 2, 4, 5, and 7 is simulated using the two stiffnesses, K_1 and $K_{iso,h}$, as identified in Figure 4.6. The first-slope stiffness, K_1, is set to 5.3×10^6 kN/m, which is calculated using $Q = 5{,}250$ kN at an assumed displacement d_1 of 1 mm. The period, T_1, associated with K_1 is 0.26 second. For the 2D systems 2, 4, and 5, $K_{iso,h}$, K_1, μ, R, K_v, and C_v listed in Table 4.5 are assigned to the friction isolator link. For the 3D isolation system 7, $K_{iso,h}$, K_1, μ, R, and $K_{iso,v}$ per Table 4.5 are assigned to the friction isolator link, where $K_{iso,v}$ is the stiffness of the vertical coil-spring isolators. The vertical stiffness, K_v or $K_{iso,v}$, is associated with axial compression.

The 1D nonlinear FVDs used in systems 3, 4, and 7 are simulated using the *damper-exponential* link in SAP2000, with δ and C_d listed in Table 4.5 . The link has two horizontal degrees of freedom for the 2D systems 3 and 4, and one vertical degree of freedom for the 3D system 7. The damper-exponential link and the isolator link are placed in parallel in the model for systems 3, 4, and 7.

Eigen modes are calculated for the isolated buildings using the finite element model of Figure 4.4a. For all seven isolation systems, the first mode in each horizontal axis (H1 and H2) is associated with nearly 100%

of the superstructure mass at the frequency of the isolation system, namely, 0.5 Hz for systems 1, 2, 3, 4, and 7; 0.3 Hz for system 5; and 0.9 Hz for system 6. For the 2D systems 1 to 5, the vertical modes are associated with the coupled responses of the isolation system and the superstructure. Due to the vertical flexibility of the superstructure (e.g., a mode at 24 Hz for 21% of mass per Table 4.3), the vertical frequencies of the isolated building are lower than those listed in Table 4.5, for which the superstructure is assumed to be rigid: 26 Hz and 36 Hz for the linear and bilinear isolation systems, respectively. Much of the vertical mass in the isolated building is associated with modes around 18 Hz for the linear isolation systems 1 and 3 (=58%) and around 20 Hz for the nonlinear isolation systems 2, 4, and 5 (=43%). For the 3D systems 6 and 7, the first vertical mode is at the isolation frequency (=2.5 Hz), with a modal effective vertical mass of 100%.

4.4.4 Response-history analysis in SAP2000

The Fast Nonlinear Analysis (FNA) algorithm in SAP2000 is used for the response-history analysis of the isolated buildings. Ritz modes are used for modal decomposition in FNA. Per Sarlis and Constantinou (2010), near-zero modal damping is assigned for the purely isolated modes (i.e., H1 and H2 for the 2D systems, and H1, H2, and V for the 3D systems), and 4% damping is assigned to the mixed and higher modes.

4.5 Two-Degree-of-Freedom Model for Performance Calculations

A two-degree-of-freedom (2DOF) model of the base-isolated reactor building is developed here to support the performance calculations for isolation systems presented in Section 5, Appendix C, and Appendix D. The required performance of the isolation system is the unrestricted horizontal displacement sufficient to achieve the user-specified TPG. A numerical model with two orthogonal horizontal degrees of freedom is sufficient to compute the maximum horizontal displacement of an isolation system because fluctuating axial load due to vertical shaking and overturning has no meaningful effect, as shown by Mosqueda *et al.* (2004).

Figure 4.10 presents the 2DOF model: an oscillator composed of a mass and a link element(s) fixed at the ground. This model assumes that the building is rigid, and the dynamic responses are characterized using one mode in each horizontal direction. The mass is 8,920 tonnes, including those of the building, basemat, and equipment described in Section 4.2.1. The isolation system supporting the building shown in Figure 4.4 is simulated using the orange link element(s), which accommodates the composite response of the 17 isolators and damping devices. The model for systems 1, 2, 5, and 6 uses one link element to simulate the isolation system, including the isolators and linear viscoelastic dampers, if used. The model for systems 3, 4, and 7 uses two link elements to simulate the isolators and nonlinear FVDs separately. The link is placed

vertically in the model and has 6 degrees of freedom at each end. The model of Figure 4.10 is described as a 2DOF model because it is used in Section 5, Appendix C, and Appendix D to generate horizontal responses for performance calculations; the vertical responses are not used for the reason given above. The 3 rotational degrees of freedom are restrained.

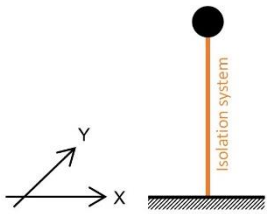

Figure 4.10. Two-degree-of-freedom model; orange links used to simulate the isolation system

4.6 Hypothetical Site for the Reactor Building

To demonstrate a calculation process in Section 5, the reactor building is assumed to be sited in the Central and Eastern United States at the East Tennessee Technology Park (ETTP) in Oak Ridge, Tennessee (TN), near Clinch River. The assumed (latitude, longitude) pair for the site is (35.94°N, 84.40°W). Two different near-surface soil profiles are considered, to demonstrate the utility of seismic isolation over a wide range of soil conditions. The soft rock site (stiff soil site) is represented by the boundary between site classes B and C (C and D) per ASCE/SEI Standard 7-22 (ASCE 2022). The average shear wave velocities in the upper 30 m of the soil column for site classes BC and CD are approximately 760 m/sec and 360 m/sec, respectively.

To enable seismic analyses of the reactor building, seismic hazard curves, uniform hazard response spectra (UHRS), and ground motions for the Clinch River site are generated using data provided by the US Geological Survey (USGS 2018). Figure 4.11 presents seismic hazard curves at the Clinch River site for spectral periods of 0 (PGA), 0.1 second, and 2 seconds, 5% damping, and site classes BC and CD. Figure 4.12 presents 5%-damped, geomean, horizontal UHRS for return periods of 1,000, 10,000, and 25,000 years and the two site classes. Details on the generation of the seismic hazard curves and UHRS are presented in Appendix A.

Soil-structure interaction analysis is not performed herein for the reason given in Section 3.6.1 and shown in Lal *et al.* (2024). Ground motions matched to a surface free field spectrum are used as input for the dynamic analysis. Possible reductions in the surface free-field spectral ordinates associated with base-slab averaging, ground motion incoherence, and embedment are ignored.

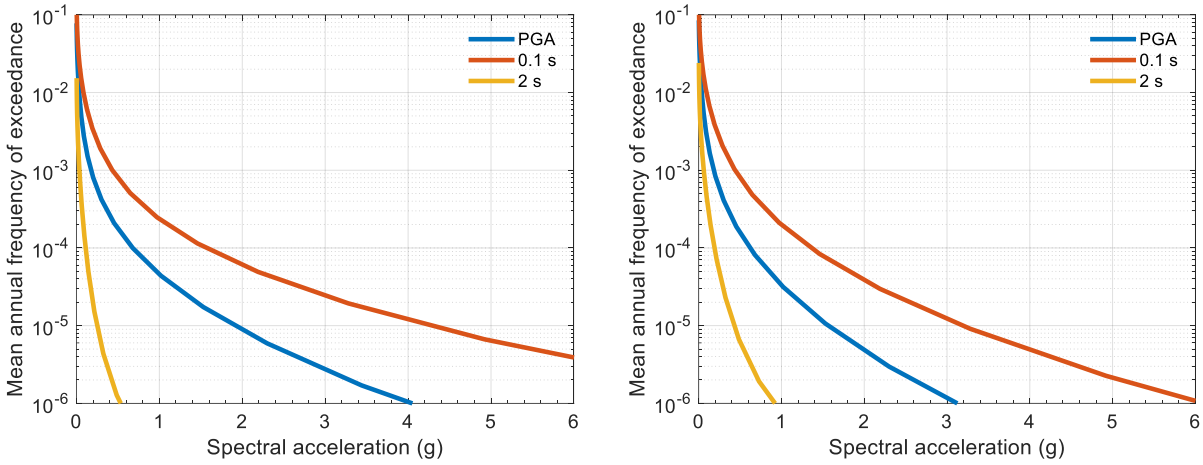

(a) BC (b) CD

Figure 4.11. Seismic hazard curves, geomean horizontal shaking, Clinch River site, BC and CD soils, 5% damping

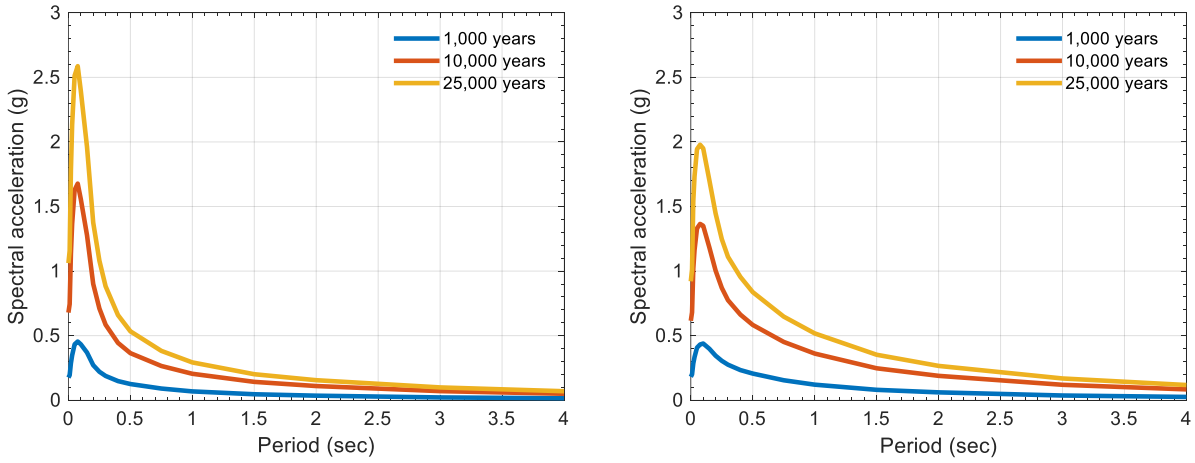

(a) BC (b) CD

Figure 4.12. Uniform hazard response spectra (UHRS), geomean horizontal shaking, 1,000, 10,000, and 25,000 years, Clinch River site, BC and CD soils, 5% damping

SECTION 5
PERFORMANCE-BASED DESIGN OF A SEISMIC ISOLATION SYSTEM

5.1 Introduction

Figure 4.3 illustrated the implementation of a seismic isolation system for a nuclear power plant, and it is repeated below as Figure 5.1 to support the presentation in this section. The isolators and VDDs are installed below a basemat and above a foundation. The isolators are shown installed on reinforced concrete pedestals. The isolation interface separates the isolated superstructure from a conventional substructure. The retaining wall shown in the figure represents horizontally adjacent, non-safety-related construction, which may not be present. Sufficient clearance (noted as displacement capacity in the figure) between the isolated superstructure and horizontally adjacent structure, along both horizontal axes of the building, must be provided to allow unrestricted movement of the isolation system during earthquake shaking.

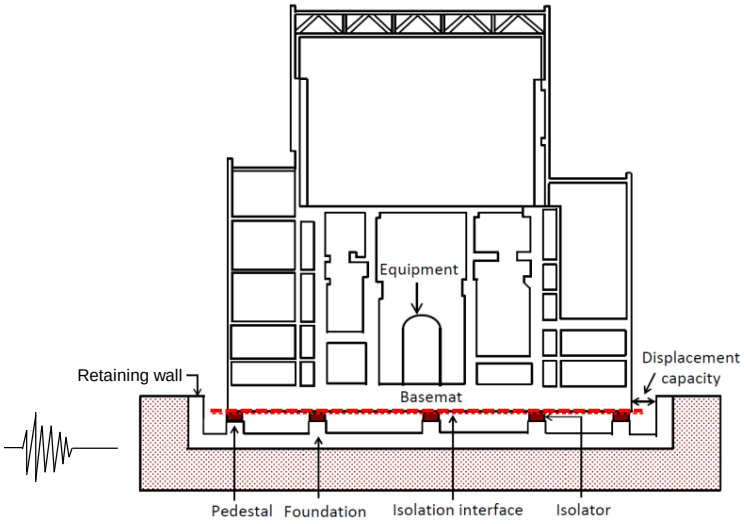

Figure 5.1. Base-isolated reactor building, adapted from Kammerer *et al.* (2019)

This section of the report provides the steps to be followed to determine a) the median horizontal displacement, D_{50}, of an isolation system to achieve a user-specified target performance goal (TPG) (Section 5.2), b) the minimum stroke of 1D and 3D VDDs (Section 5.3) , and c) the minimum clearance along each horizontal axis of the building between the isolated building and any adjacent construction (Section 5.4). Section 5.5 presents performance calculations to illustrate the process presented in Section 5.2.

5.2 Achieving a Target Performance Goal for a Seismic Isolation System

5.2.1 Introduction

In this report, the required performance of an isolation system is unrestricted horizontal displacement sufficient to achieve the TPG.

To demonstrate compliance, the required horizontal displacement capacity of an isolation system is determined using a) a seismic displacement demand curve, and b) a fragility function for the isolation system. The fragility function is integrated over the demand curve to compute the MAFE, and the median value is adjusted until the TPG is reached. Figure 5.2 presents the workflow.

5.2.2 Seismic displacement demand curve

The horizontal seismic displacement demand curve is determined by dynamic analysis of the chosen isolation system and building model for incremented levels of two-component horizontal ground shaking. A 2DOF model (1DOF in each horizontal direction) is sufficient to compute isolation-system displacements, wherein the building reactive mass (i.e., dead load and permanent live load) above the isolation interface is lumped at the level of the basemat. The 2DOF model was introduced in Section 4.5; best-estimate properties are used to define the force-displacement hysteresis of the isolation system.

The displacement demand curve, which is specific to a user-selected isolation system, is generated in 6 steps:

1. Generate uniform hazard response spectra (UHRS) for the site for geometric mean horizontal shaking for 11 return periods (i.e., reciprocal of MAFE) spanning 4 decades[13], centered on the TPG
2. Generate 11 sets of ground motion acceleration time-series, for each of the 11 return periods, that are spectrally matched to the geometric mean UHRS
3. Analyze the two degree-of-freedom model of the user-selected seismic isolation system for each ground motion pair (H1, H2) in the set of 11 in a bin and calculate the mean maximum resultant horizontal displacement in a bin
4. Repeat step 3 for all 11 bins

[13] See Appendix D for the technical basis for 4 decades. Four decades centered on the TPG cover a range on mean annual frequency between TPG/100 and 100×TPG.

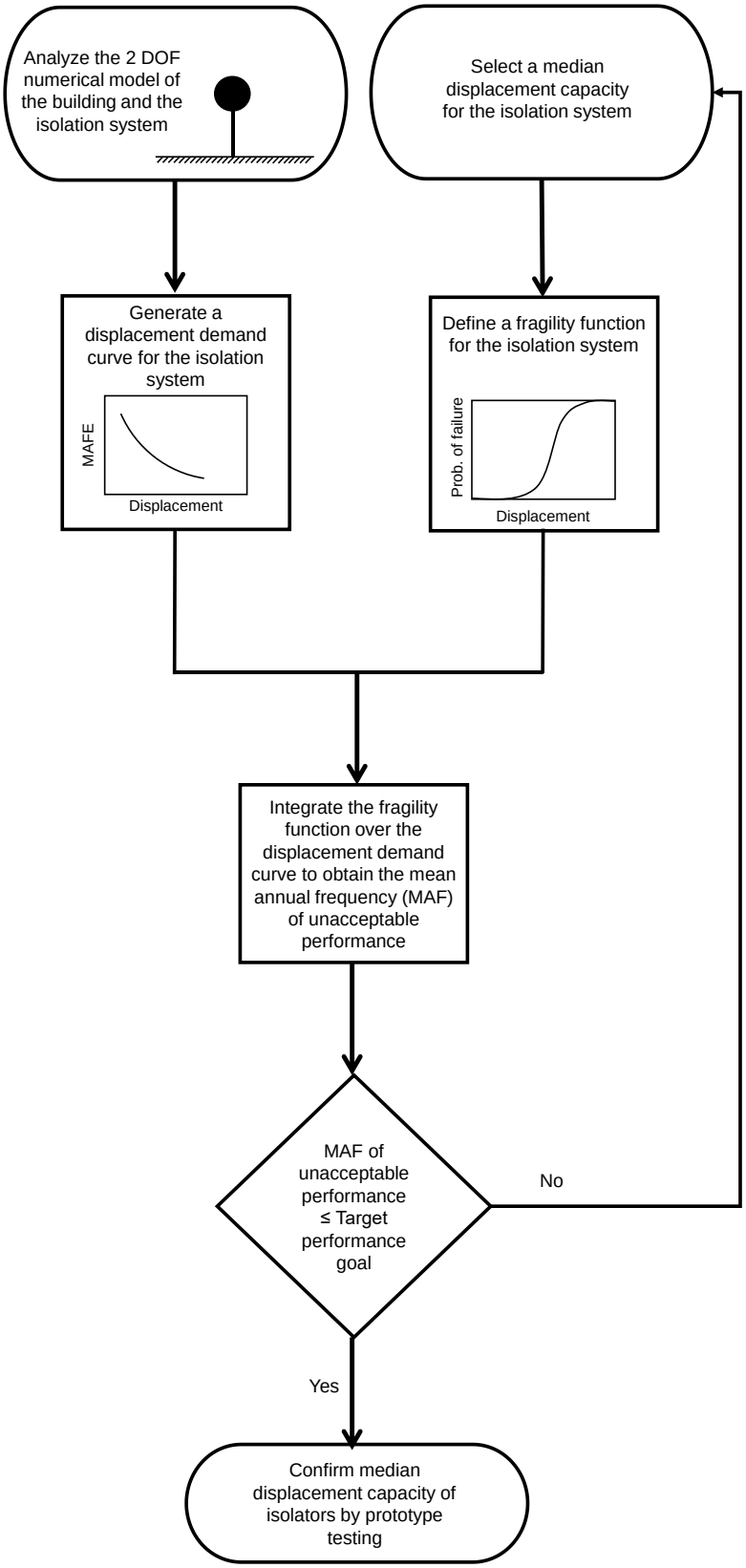

Figure 5.2. Achieving a target performance goal for an isolation system, workflow diagram

5. Increase the 11 horizontal displacements from step 4, calculated using spectrally matched motions, by a factor of 1.2 per Section C.2.2 and D.3 to address the variability in a) the horizontal components of ground motion, H1 and H2, around the geometric mean, and b) the mechanical properties of the isolators and dampers, and
6. Generate the displacement demand curve using the mid-point MAFE for each bin from step 1 and the corresponding displacement from step 5

Appendix D presents information on the derivation of a seismic displacement demand curve and the basis for using 11 intensity levels (or bins) centered on the TPG. Eleven sets of motions provide a stable estimate of the median displacement in each bin, as adopted in Section 5.2.2 of FEMA P-58-1 (FEMA 2012) for intensity-based assessments and documented in Appendix C.3 of Huang *et al.* (2008). Section D.5 reproduces the relevant material from Appendix C.3 of Huang *et al*. The process used herein to generate the spectrally matched motions is presented in Appendix A.3.

Accordingly, a seismic displacement demand curve is generated using 121 simulations: 11 intensity levels and 11 sets of ground motions per intensity level.

The displacement demand curves presented in Section 5, Appendix C, and Appendix D are generated using 30 sets of motions per bin because a) the ground motions were available for the Clinch River site and the two soil types from another project, and b) 30 sets of motions are used in Appendix C to compute dispersions in each bin, used to develop a default value of logarithmic standard deviation for isolation-system fragility functions.

5.2.3 Isolation system fragility function

The isolation-system fragility function is defined by a median displacement capacity and a logarithmic standard deviation. The logarithmic standard deviation and median capacity are independent. The median displacement capacity is confirmed by prototype testing per Section 6.

The composite logarithmic standard deviation for the isolation-system fragility function is computed with considerations of uncertainty and variability in ground motion (β_{gm}), mechanical properties of the isolation system (β_i), distribution of mass in the isolated superstructure (β_m), and model fidelity (β_f):

$$\beta = \sqrt{\beta_{gm}{}^2 + \beta_i{}^2 + \beta_m{}^2 + \beta_f{}^2} \tag{5.1}$$

The default value for β is 0.35, as established in Appendix C, noting that a smaller value could likely be justified on a project- and site-specific basis for linear isolation systems and isolation systems supported on firm soil or rock sites.

Performance calculations are presented in Section 5.5 for two isolation systems to illustrate the six-step process summarized above: 1) 2-second linear isolation system, and 2) 2-second linear isolation system with supplemental 1D nonlinear FVDs. Additional calculations are presented in Appendix C for the other four isolation systems.

5.3 Minimum Stroke of 1D and 3D Damping Devices

Seismic isolators are produced using high quality processes and controls on materials and manufacturing, with quality confirmed by a) prototype testing of three units of each type and size for seismic demands consistent with the horizontal displacement D_{50}, and b) production testing of all units to a horizontal displacement consistent with DB shaking. See Section 6 for details. Accordingly, the variability in isolator properties is more narrowly constrained than in conventional materials for building construction.

Similarly, the 1D and 3D damping devices identified in this report have force-velocity-displacement, and force-frequency-displacement relationships, respectively, that must also be confirmed by prototype and production testing per Section 6. Unlike seismic isolators, the horizontal displacement capacity of these devices is limited by two end caps for the 1D FVDs, and the vessel containing the highly viscous fluid for the 3D viscodamper. These displacement capacities are known to millimeters, and they too must be confirmed by prototype testing per Section 6.

For a seismic isolation system with a displacement capacity defined by a median D_{50} and a logarithmic standard deviation of 0.05 (0.10) per Section C.2.3, a damper stroke of $\pm 1.15\,D_{50}$ is sufficient to ensure with 99% (92%) confidence that it will not reach its stroke capacity before the seismic isolators.[14]

[14] At a displacement of $1.15D_{50}$, the cumulative distribution function of a lognormal distribution with median D_{50} and logarithmic standard deviation of ξ equals $\Phi((\ln(1.15D_{50}) - \ln(D_{50})) / \xi)$, where Φ denotes the cumulative distribution function (CDF) of a normal distribution. $\Phi((\ln(1.15D_{50}) - \ln(D_{50})) / 0.05) = \Phi(2.79) = 0.99$ and $\Phi((\ln(1.15D_{50}) - \ln(D_{50})) / 0.1) = \Phi(1.4) = 0.92$.

Accordingly, the unrestricted horizontal displacement of a 1D fluid viscous damper around the installed position, prior to engaging the end caps, shall be $\pm$ 1.15 D_{50}. The unrestricted radial displacement of a 3D viscoelastic damper in any horizontal direction, around the installed position, prior to engaging the wall of the vessel shall be $\pm$ 1.15 D_{50}.

5.4 Minimum Clearance to Adjacent Construction

The minimum clearance between an isolated building and any adjacent construction, along each horizontal axis, shall be no less than 1.15 D_{50}, as drawn in Figure 5.3. The justification for the multiplier of 1.15 on D_{50} is presented in Section 5.3.

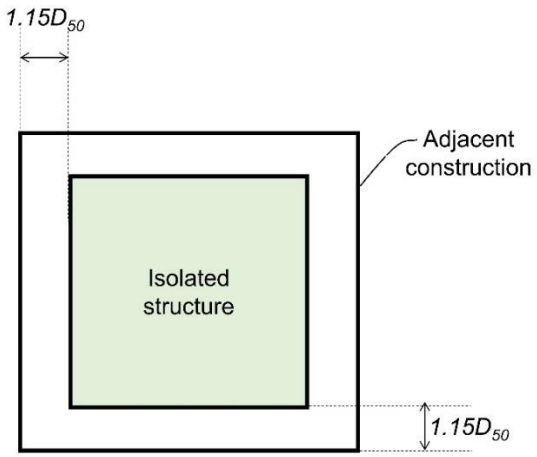

Figure 5.3. Horizontal clearance around a seismically isolated nuclear power plant

5.5 Performance Calculations

5.5.1 Introduction

This section provides performance calculations to demonstrate a) the derivation of displacement demand curves, b) calculations of mean annual frequency of unacceptable performance, and c) how a TPG could be achieved for different isolation systems (Section 5.5.4). Calculations of a) and b) are presented for the Clinch River site and v_{s30} = 760 m/sec (Section 5.5.2) and v_{s30} = 360 m/sec (Section 5.5.3).

5.5.2 Performance calculations, Clinch River, TN, v_{s30} = 760 m/sec

For the purpose of demonstrating the calculation process, the seismic hazard at the Clinch River site is generated using data developed by the US Geological Survey (USGS 2018). The database provides mean annual frequencies of exceedance for geometric mean (or geomean) accelerations at different spectral

periods (or frequencies) for 5% of critical damping. Detailed information on the seismic hazard at the Clinch River site is presented in Appendix A. Figure 5.4a presents seismic hazard curves (i.e., geomean spectral acceleration as a function of MAFE) at periods of 0 (PGA), 0.1, and 2 seconds, for the Clinch River site (latitude = 35.94, longitude = -84.40) assuming soft rock (site class BC per Table 20.2-1 of ASCE/SEI 7-22 (ASCE 2022)), which is characterized here by an average shear wave velocity in the upper 30 m of the soil column, v_{s30}, of 760 m/sec.

Seismic hazard curve ordinates, at a given MAFE, at specified frequencies, are used to generate a UHRS. Figure 5.4b, previously presented as Figure 4.12a and repeated here for convenience, presents geomean horizontal acceleration response spectra for return periods (reciprocal of MAFE) of 1,000, 10,000, and 25,000 years and 5% critical damping, for the Clinch River site and $v_{s30} = 760$ m/sec. Two-component horizontal ground motions (i.e., H1, H2) are spectrally matched to the 25,000-year geomean UHRS. The process used herein to generate the spectrally matched motions is presented in Section A.3.

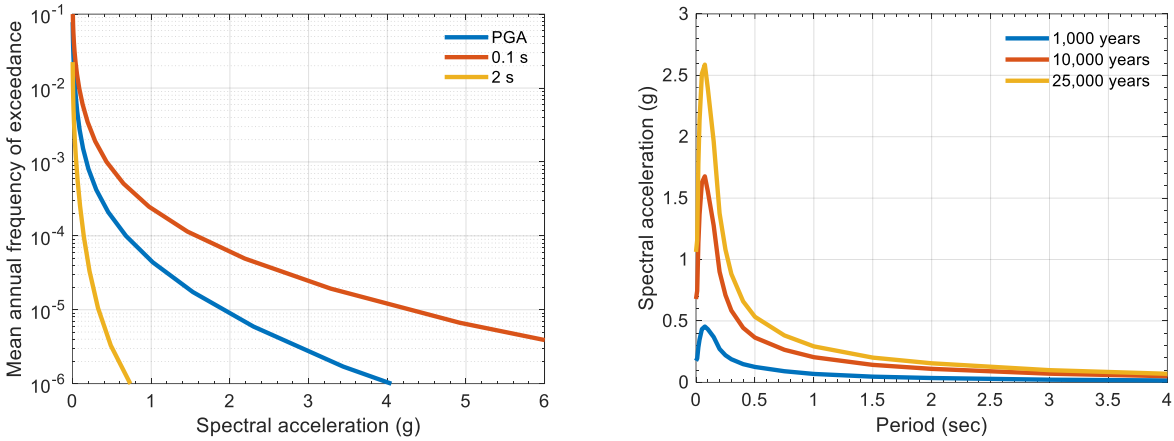

(a) 0, 0.1-, and 2-second seismic hazard curves (b) uniform hazard response spectra (UHRS)

Figure 5.4. Seismic hazard data, geomean horizontal, 5% critical damping, Clinch River, BC soil (identical to Figure A.1a and Figure A.2a)

The 2-second seismic hazard curve is used here to calculate scale factors for the spectrally matched motions for other return periods (or MAFE). The process is explained in detail in Appendix D and is summarized here. Figure 5.5 presents the 2-second hazard curve for BC soil to demonstrate the process for a TPG of 4×10^{-5}. The logarithm of the TPG is marked on the vertical axis of the plot and the corresponding spectral acceleration is marked as SA_{TPG} on the horizontal axis. The vertical axis is divided into eleven segments (or *bins*) of equal width in log space between (log(TPG) – 2) and (log(TPG) + 2), spanning 4 decades of frequency, centered on the TPG (i.e., span = 4 in Figure 5.5). The scale factor for motions in a particular

bin is the ratio of the 2-second spectral acceleration at the center of the bin (SA^i) to SA_{TPG} and the corresponding exceedance frequency is the MAFE at the center of the bin (E^i).

The use of ground motions that are spectrally matched to the 25,000-year geomean UHRS and scale factors for other return periods that are derived from the 2-second seismic hazard curve implies that the same spectral shape is used for all return periods. This is a simplification. The ground motions in a particular bin should be spectrally matched to the UHRS corresponding to the return period associated with that bin. Although one spectral shape may suffice for many (or all) of the 11 bins, this would have to be substantiated on a project-specific basis.

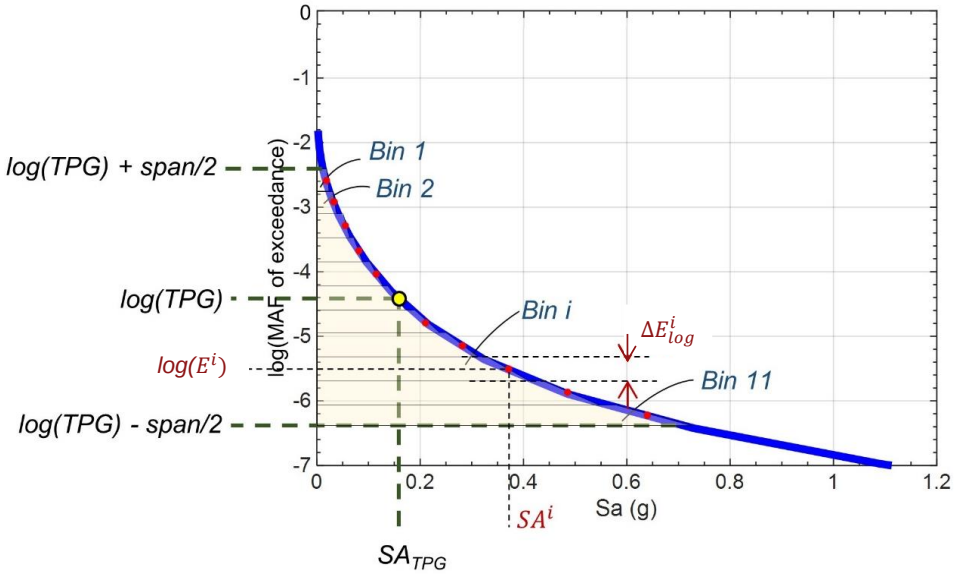

Figure 5.5. 2-second hazard curve, BC soil, calculation of scale factors for return periods other than 25,000 years, TPG is 4 × 10^{-5}, $\Delta E^i_{\log}$ is the width of a bin along the MAFE axis in log space

A 2DOF model of each isolation system is analyzed for each ground motion in a set of 30, and the analysis is carried out for all eleven bins. That is, the model is analyzed for 30 × 11 motions in total. For each bin, the average of the maximum resultant horizontal displacements is computed and multiplied by a factor of 1.2, as noted in Section 5.2.2. This displacement, and the corresponding MAFE at the center of the bin, defines one coordinate on the displacement demand curves. Eleven coordinates, one per bin, are used to define the displacement demand curve.

Figure 5.6 illustrates the performance calculation. Figure 5.6a presents the MAFE (ordinate) of mean maximum horizontal seismic displacement in mm (abscissa) for a 2-second, 5%-damped, linear elastomeric isolation system, system 1 of Table 4.4 and Table 4.5, sited at Clinch River. Figure 5.6b presents two

isolation-system fragility functions, both with β = 0.35 and a median displacement capacity of 200 and 250 mm.

The displacement demand curve of Figure 5.6a and the fragility functions of Figure 5.6b are discretized into 50 increments of horizontal displacement. The two fragility functions are numerically integrated over the displacement demand curve in 50 increments, resulting in MAFs of unacceptable performance of 6.6×10^{-5} and 3.6×10^{-5}, respectively. Increasing the median displacement capacity reduces the risk. Figure 5.6c presents the contributions to the MAF of unacceptable performance for the two median displacement capacities (200 mm and 250 mm), as risk density plots.

Adding FVDs to an isolation system is a proven strategy in non-nuclear sectors to reduce horizontal displacements in seismic isolation systems subjected to extreme ground shaking. Adding FVDs will adjust the seismic displacement demand curve, and for a given median isolation-system capacity, achieve a more demanding (lower) seismic risk target. To demonstrate the process, eight nonlinear FVDs are added to the 2-sec linear isolation system introduced above at the locations shown by the dashed green lines in Figure 4.4b: system 3 per Table 4.4 and Table 4.5. The force-velocity relationship for the nonlinear FVDs is $F = C_d v^{\delta}$, where C_d is the damping coefficient and set equal to 5,000 kN-(s/m)$^{0.3}$ along each horizontal axis of the building, v is the relative velocity across the damper, and δ is the velocity exponent, taken as 0.3. The damping coefficient for each of the 8 dampers shown in Figure 4.4 is 1,250 kN-(s/m)$^{0.3}$. Results are presented in Figure 5.7. The displacement demand curve of Figure 5.7a, which is established by nonlinear dynamic analysis for incremented levels of ground shaking, is different from that in Figure 5.6a. The isolation-system fragility functions in Figures 5.6b and 5.7b are identical. Convolving the fragility functions of Figure 5.7b over the displacement curve of Figure 5.7a results in MAFs of unacceptable performance of 1×10^{-5} and 6×10^{-6}, respectively; the reduction in risk associated with the addition of the nonlinear FVDs is approximately a factor of 6.

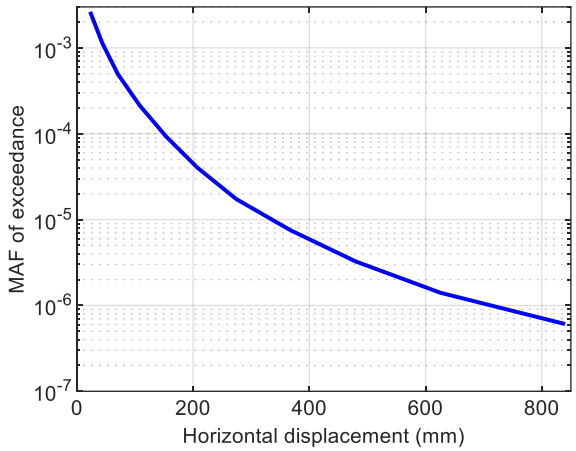

(a) displacement demand curve

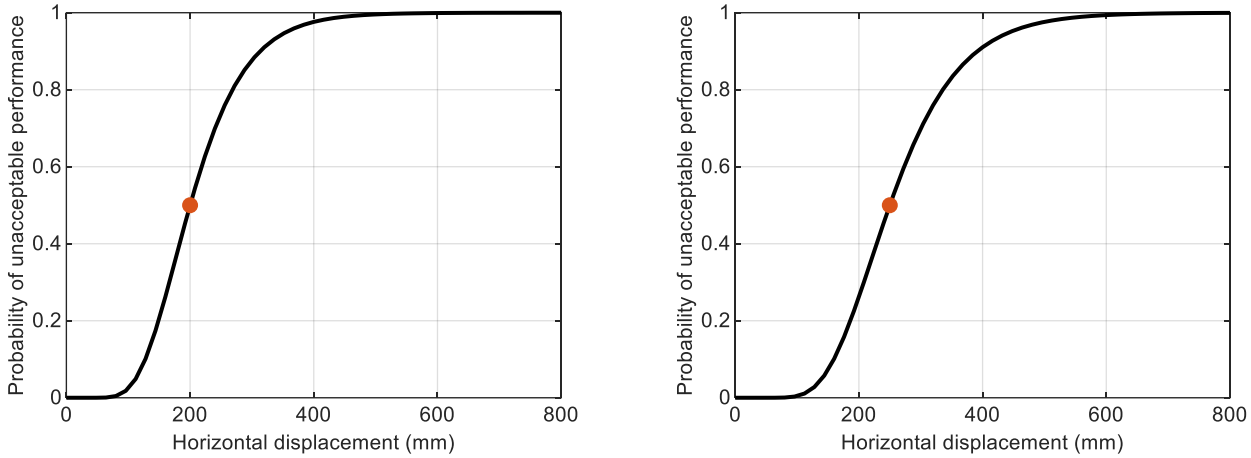

(b) isolation-system fragility functions, β = 0.35

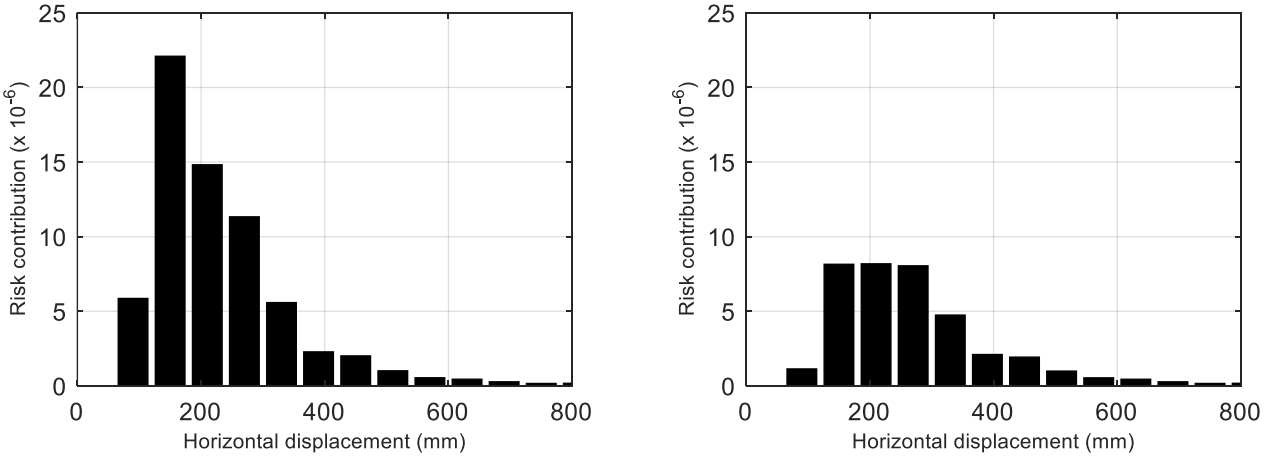

(c) risk density

Figure 5.6. Steps toward achieving a target performance goal: 2-sec linear isolation system, Clinch River, BC soil

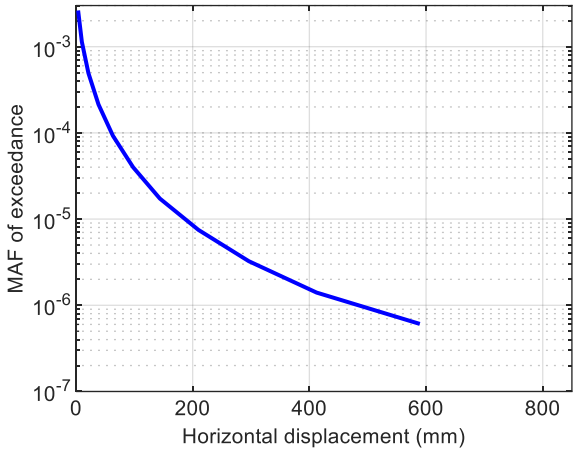

(a) displacement demand curve

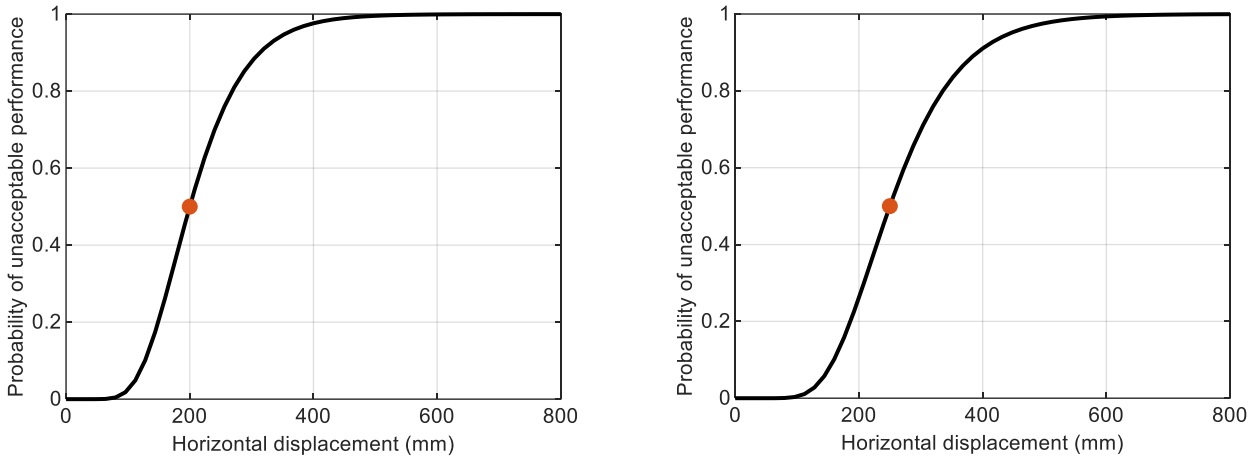

(b) isolation-system fragility functions, $\beta = 0.35$

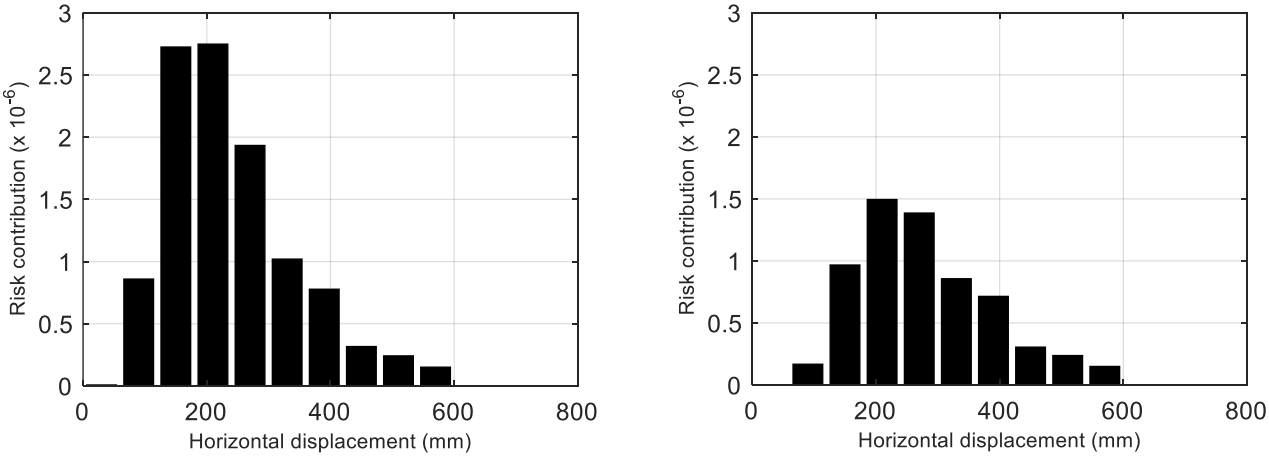

(c) risk density

Figure 5.7. Steps toward achieving a target performance goal: 2-sec linear isolation system with supplemental nonlinear FVDs, Clinch River, BC soil

5.5.3 Performance calculations, Clinch River, TN, v_{s30} = 360 m/sec

The performance calculations of Section 5.5.2 are repeated here but for an average shear wave velocity in the upper 30 m of the soil column of 360 m/sec: dense sand or very stiff clay (site class CD per Table 20.2-1 of ASCE/SEI Standard 7-22). Figure 5.8a presents seismic hazard curves at periods of 0, 0.1, and 2 seconds. Figure 5.8b, previously presented as Figure 4.12b and repeated here for convenience, presents geomean horizontal acceleration response spectra for return periods of 1,000, 10,000, and 25,000 years for the Clinch River site and $v_{s30} = 360$ m/sec. Thirty sets of two-component horizontal ground motions are spectrally matched to the 25,000-year spectrum (see Section A.3). The spectrally matched motions are amplitude scaled using scale factors derived using the 2-second seismic hazard curve shown in Figure 5.8a using the process described in Section 5.5.2 for BC soil. Figure 5.9 presents the displacement demand curves for the two isolation systems considered in Section 5.5.2 for CD soil, again including the multiplier of 1.2 to correct displacements computed using spectrally matched motions for variability in those components around the geometric mean.

To illustrate the importance of soil type on the performance calculation, the fragility functions of Figure 5.6b, used earlier for the calculations assuming site class BC, are used here. Results are presented in Table 5.1. The MAF of unacceptable performance increases with the change to CD soil, which is intuitive given the change in spectral demands. See Figure 5.10, which presents the 10,000- and 25,000-year UHRS for the two site classes: spectral demands for a given return period are greater for site class CD, for periods greater than 0.3 second.

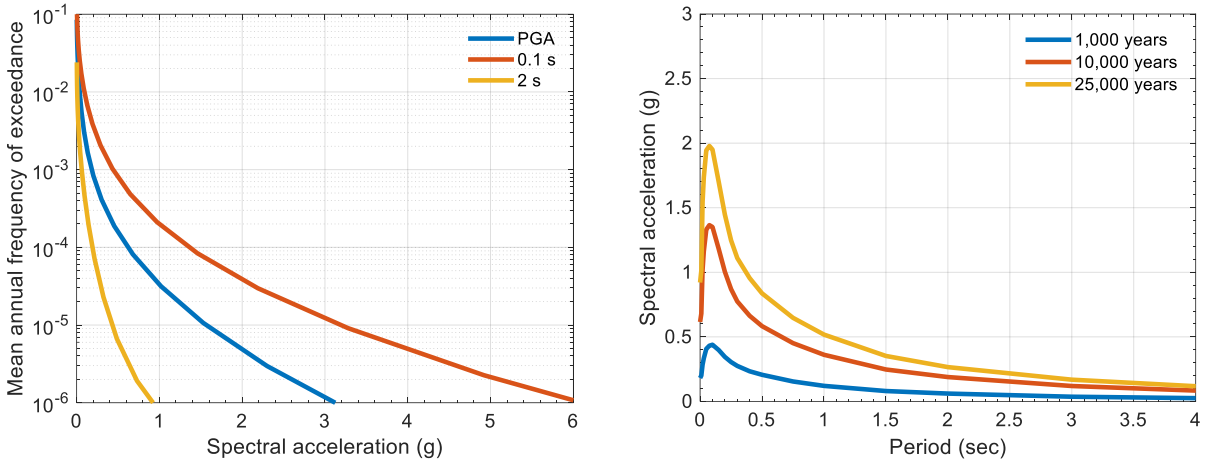

(a) 0, 0.1-, and 2-second seismic hazard curves (b) UHRS

Figure 5.8. Seismic hazard data, geomean horizontal, 5% critical damping, Clinch River, CD soil

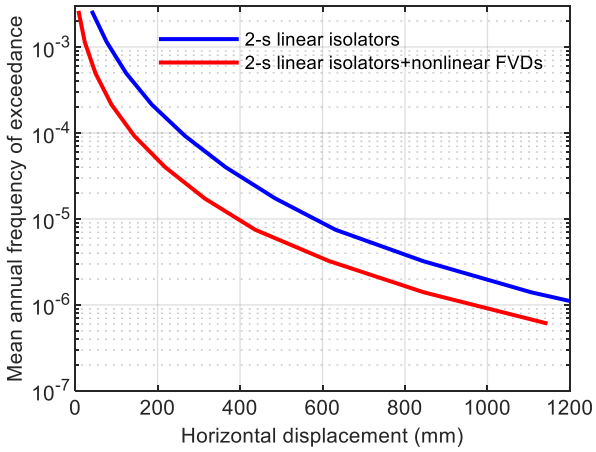

Figure 5.9. Displacement demand curves, two isolation systems, Clinch River, CD soil

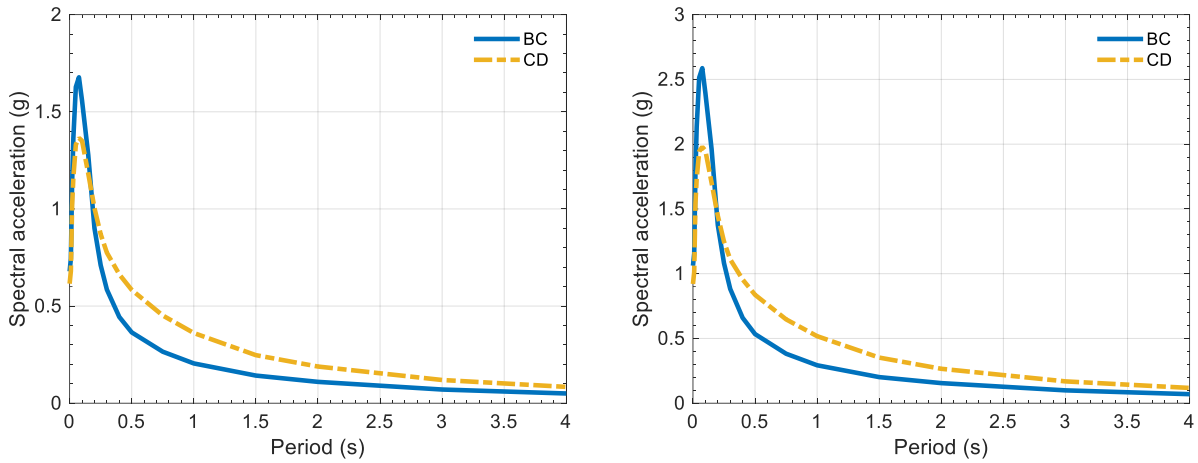

(a) 10,000-year return period (b) 25,000-year return period

Figure 5.10. Geomean horizontal UHRS, two return periods, Clinch River, BC and CD soils

Table 5.1. Performance calculations, Clinch River, BC and CD soils, β = 0.35

	Median displacement capacity (mm)	MAF of unacceptable performance	
		BC soil	CD soil
2-sec linear isolation system[1]	200	6.6×10^{-5}	2.4×10^{-4}
	250	3.6×10^{-5}	1.5×10^{-4}
2-sec linear isolation system incl. nonlinear FVDs[2]	200	1.1×10^{-5}	6.0×10^{-5}
	250	6.3×10^{-6}	3.8×10^{-5}

1. Isolation system 1 per Table 4.4 and Table 4.5

2. Isolation system 3 per Table 4.4 and Table 4.5

5.5.4 Achieving a target performance goal with different isolation systems

Table 5.2 presents the required median displacement capacities, for each of the isolation systems to achieve TPGs of 1×10^{-4} (1/10,000 years), 4×10^{-5} (1/25,000 years), and 2×10^{-5} (1/50,000 years). For the calculations presented in this table, the displacement demand curve is generated using one spectral shape, as noted above. For a given risk target, the median displacement capacity, D_{50}, varies significantly, with larger displacements typically translating to larger accelerations on the basemat, albeit all much smaller than the peak horizontal ground acceleration. All the median displacements in Table 5.2 are substantially smaller than the peak displacement capacities of elastomeric and sliding isolators, and 1D nonlinear fluid viscous dampers, installed in mission-critical buildings in the US in regions of high seismic hazard.

Table 5.2. Median displacement capacity, D_{50}, to achieve different TPGs, $\beta = 0.35$, Clinch River, BC and CD soils

	Median displacement capacity[1], D_{50} (mm)					
	BC soil			CD soil		
	Target performance goal			Target performance goal		
Risk target	1×10^{-4}	4×10^{-5}	2×10^{-5}	1×10^{-4}	4×10^{-5}	2×10^{-5}
2-sec linear isolation system[2]	170	242	310	294	424	542
2-sec linear isolation system incl. nonlinear FVDs[3]	68	110	152	152	244	334

1. The risk calculations for different TPGs presented in this table use the same demand curve: i.e., the curve attached to motions matched to a target spectrum corresponding to a return period of 25,000 (TPG = 4×10^{-5}). So, the risk numbers for TPGs other than 4×10^{-5} are approximate.

2. Isolation system 1 per Table 4.4 and Table 4.5

3. Isolation system 3 per Table 4.4 and Table 4.5

SECTION 6
QUALIFICATION, PROTOTYPE, AND PRODUCTION TESTING

6.1 Introduction

This section of the report provides guidance on qualification, prototype, and production testing of seismic isolators and dampers.

Qualification tests are intended to demonstrate basic performance characteristics of devices and systems, independent of a project application. Such tests shall be completed, and results reported prior to consideration for a project. Prototype and production testing are project specific, requiring results of analysis for TPG and DB shaking, respectively.

Minimum requirements for each type of test are identified below in Sections 6.3 (qualification), 6.4 (prototype), and 6.5 (production). The requirements for 2D isolators are based on Chapter 12 of ASCE/SEI 4-16 (ASCE 2017) and Chapter 9 of ASCE/SEI 43-19 (ASCE 2021) (which repeats the testing requirements of 4-16, nearly verbatim). Minimum requirements for 1D and 3D isolators are adapted from those for 2D isolators. Minimum requirements for 1D FVDs are adapted from Chapter 18 of ASCE/SEI Standard 7-22 and three decades of US practice in non-nuclear sectors. Minimum requirements for 3D viscoelastic dampers, which have not been deployed to date in the US, are derived from those for 1D FVDs, recognizing that the response of the 3D dampers is dependent on frequency and displacement. Adaptations made in this section to the requirements from industry standards are informed by lessons learned and additional experience gained from implementation of these devices since the development of the original requirements for nuclear facilities in the early 2010s. These adaptations are expected to be reflected in upcoming revisions to these nuclear industry standards.

The scope of each testing program described below may be augmented by project-specific requirements.

6.2 Notation

The notation used in Sections 6.4 and 6.5 is defined at the front of this report and repeated below. Notation specific to one type of isolator or damper is defined in the corresponding section.

C_d Damping coefficient for a device

DL Average dead load on all isolators of a type and size

D_{DB} Mean maximum resultant horizontal displacement for DB shaking on all isolators of a type and size

$D_{DB,v}$ Mean maximum vertical displacement for DB shaking on all isolators of a type and size

$D_{TPG,v}$ Mean maximum vertical displacement for TPG shaking on all isolators of a type and size

D_{50} Median displacement of the fragility function to achieve the target performance goal (TPG)

$f_{iso,h}$ Horizontal isolation system frequency (i.e., reciprocal of $T_{iso,h}$)

$f_{iso,v}$ Vertical isolation system frequency (i.e., reciprocal of $T_{iso,v}$)

LL Average live load on all isolators of a type and size

P_{DB} Mean maximum earthquake-induced vertical load for DB shaking on all isolators of a type and size

P_{TPG} Mean maximum earthquake-induced vertical load for TPG shaking on all isolators of a type and size

$T_{iso,h}$ Horizontal isolation-system period calculated using $K_{iso,h}$

$T_{iso,v}$ Vertical isolation-system period calculated using $K_{iso,v}$

6.3 Qualification Tests

The seven tasks listed below, all project independent, shall be performed and successfully completed prior to prototype testing of project-specific devices for a nuclear power plant application:

1. Dynamic testing of full-scale (prototype) isolators for compressive and tensile axial loads and bidirectional horizontal motion at amplitudes of displacement expected for design basis (DB) ground motions in regions of moderate to high seismic hazard for non-nuclear structures
2. Development of verified and validated numerical models capable of predicting results of dynamic testing of prototype isolators
3. Demonstration through basic chemistry, laboratory tests and field applications that the mechanical properties of the isolators do not change by more than 20% over their design life in the temperature range of 5°C to 30°C
4. System-level testing of the isolation system on a 6DOF earthquake simulator using three simultaneously applied translational components of earthquake ground motion

5. Verification and validation of numerical tools and code to predict the response of the isolation system to three simultaneously applied translational components of earthquake ground motion
6. Deployment of the isolation system in U.S., non-nuclear, mission-critical structures in regions of moderate to high seismic hazard
7. If components of the isolation system are subjected to significant radiation dose, the qualification shall include demonstration via basic chemistry, laboratory tests, and MCNP-type simulations (mcnp.lanl.gov) that the cumulative change over their design life, including task 3 above, is no more than 20%

Accelerated aging tests shall not be used in task 3 to characterize the evolution of mechanical properties of elastomeric bearings per Constantinou *et al.* (2007).

Qualification tests 1a, 2a, 3a, and 7a shall *also* be performed for 1D FVDs that form a part of the isolation system as follows:

1a. Dynamic uniaxial testing of full-scale (prototype) dampers at amplitudes of displacement, velocity, and force expected for DB ground motions in regions of moderate to high seismic hazard for non-nuclear structures

2a. Development of verified and validated numerical models capable of predicting results of dynamic testing of prototype dampers

3a. Demonstration through basic chemistry, laboratory tests and field applications that the mechanical properties of the dampers do not change by more than 20% over their design life in the temperature range of 5°C to 30°C

7a. If the dampers are subjected to significant radiation dose, the qualification shall include demonstration via basic chemistry, laboratory tests, and MCNP-type simulations that the cumulative change over their design life, including task 3a above, is no more than 20%.

Qualification tests 1b, 2b, 3b, and 7b shall also be performed for 3D viscoelastic dampers that form part of the isolation system as follows:

1b. Dynamic 3D testing of full-scale (prototype) dampers at amplitudes of displacement, frequency, velocity, and force expected for DB ground motions in regions of moderate to high seismic hazard for non-nuclear structures

2b. Development of verified and validated numerical models capable of predicting results of dynamic testing of prototype dampers, including frequency dependence

3b. Demonstration through basic chemistry, laboratory tests and field applications that the mechanical properties of the dampers do not change by more than 20% over their design life in the temperature

range of 5°C to 30°C

7b. If the dampers are subjected to significant radiation dose, the qualification shall include demonstration via basic chemistry, laboratory tests, and MCNP-type simulations that the cumulative change over their design life, including task 3b above, is no more than 20%.

Tasks 1, 2, 3, 4, 5 and 7 above, including 1a, 1b, 2a, 2b, 3a, 3b, 7a, and 7b shall be performed by experienced persons independent of the device manufacturer.

Three types of 2D seismic isolators, from two suppliers, have been used in US construction practice for 30+ years and are considered pre-qualified for use in seismically isolated nuclear power plants, aside from task 7: low-damping (natural) rubber (LDR) isolators and lead-rubber (LR) isolators from Dynamic Isolation Systems[15] of Sparks, Nevada, and Friction Pendulum (or spherical sliding) (FP) bearings from Earthquake Protection Systems[16] of Vallejo, California. All three isolators are described in Section 2.

One type of FVD, from one supplier, has been used as part of US seismic isolation systems for 30+ years and is considered qualified for use in seismically isolated nuclear power plants, namely, the 1D fluid viscous damper from Taylor Devices[17] of North Tonawanda, New York. The damper is described in Section 2.

6.4 Prototype Tests

6.4.1 Introduction

Prototype tests of isolators and dampers are performed on *three* devices of each type and size planned for use in the isolation system. Prototype devices shall not be used for construction but may be used, if not damaged by testing, to support a maintenance and inspection program.

Forces, velocities, and displacements shall be digitally recorded at a sampling rate of no less than 200 Hz for each cycle of each prototype test.

All tests shall be performed at an ambient air temperature of 20°C ± 5°C (68°F ± 9°F). Ambient temperature shall be logged.

[15] http://www.dis-inc.com/

[16] https://www.earthquakeprotection.com/

[17] https://www.taylordevices.com/

6.4.2 2D elastomeric and spherical sliding isolators

6.4.2.1 Introduction

This section addresses low damping rubber, lead-rubber, and spherical sliding bearings (see Figure 2.3a, b, and c). The testing protocol and acceptance criteria provided below are *minimum* requirements.

Each prototype isolator shall have a target horizontal (shearing) force-displacement relationship that is either linear (low damping rubber) or bilinear (lead-rubber or spherical sliding) and a target range for vertical stiffness.

6.4.2.2 Testing protocol

The following sequence of four tests shall be performed on each prototype isolator:

1. Three cycles of loading between minimum and maximum vertical force
2. One hundred fully reversed cycles of horizontal loading corresponding to the design wind force
3. Three fully reversed cycles of loading to a horizontal displacement equal to D_{DB}
4. Three fully reversed cycles of loading to a horizontal displacement equal to D_{50}

For test 1, the imposed vertical load shall vary between 1) DL + 0.25LL + P_{TPG}, and 2) DL - P_{TPG}. The frequency of the loading for test 1 shall be 0.1 Hz or less.

For tests 2 and 3, the imposed vertical load shall equal DL + LL. The frequency of loading for test 2 shall be 0.1 Hz or less. The frequency of loading for test 3 shall be equal to $f_{iso,h}$.

Test 4 will be performed twice, for an imposed vertical load of 1) DL + 0.25LL + P_{TPG}, and 2) DL - P_{TPG}. The frequency of loading for test 4 shall be $f_{iso,h}$. The value of P_{TPG} shall be determined per Section 3.7.2.2

6.4.2.3 Acceptance criteria

Acceptance criteria shall be project specific. As a minimum:

1. For test 1, the vertical stiffness shall fall within the range assumed for analysis and design
2. For tests 2 and 3, the horizontal force-displacement relationship shall have positive stiffness on the loading segments of each cycle
3. For test 3, the horizontal force-displacement relationship shall be within ±20% of the target at 25%, 50%, and 100% of the maximum displacement in all cycles of loading

4. For test 3, the energy dissipated per cycle of horizontal loading shall be no less than 80% of the value computed using the target force-displacement relationship
5. For test 4, the horizontal force-displacement relationship shall be within ±20% of the target at 50% and 100% of the maximum displacement in all cycles of loading
6. For test 4, the energy dissipated per cycle of horizontal loading shall be no less than 80% of the value computed using the target force-displacement relationship
7. For test 4, the isolator shall sustain the imposed vertical load
8. The prototype isolator shall suffer no damage in tests 1, 2 and 3. Damage is acceptable in test 4.

If a prototype isolator fails to meet the acceptance criteria, it shall be rejected, and a new isolator shall be built and tested.

The data from test 3 can be used to develop isolator-specific acceptance criteria for production testing.

6.4.3 1D *guided* spring isolators

6.4.3.1 Introduction

This section addresses *vertically guided* 1D linear spring isolators per Figure 2.3h, of the type shown in Figure 2.3d (coil) and Figure 2.3e (machined), offering isolation in the vertical direction only. The testing protocol and acceptance criteria provided below are *minimum* requirements. Not addressed below are testing requirements for the pins and sleeves that form the 1D vertical guide, which must resist horizontal force.

Each prototype spring isolator shall have a target linear vertical (axial) force-displacement relationship.

6.4.3.2 Testing protocol

The following test shall be on each prototype isolator:

1. Three fully reversed cycles of loading between the minimum and maximum vertical force

For test 1, the vertical load shall vary between 1) DL + 0.25LL + P_{TPG} , and 2) DL - P_{TPG} The frequency of the loading for test 1 shall be 0.1 Hz or less because the behavior of these devices is not dependent on loading rate. The value of P_{TPG} shall be determined per Section 3.7.2.2.

6.4.3.3 Acceptance criteria

Acceptance criteria shall be project specific. As a minimum:

1. For test 1, the vertical stiffness shall be within ±10% of the target

2. For test 1, the vertical stiffness shall be linear
3. The prototype isolator shall suffer no damage in test 1.

If a prototype isolator fails to meet the acceptance criteria, it shall be rejected, and a new isolator shall be tested. Spring isolators may be re-built and re-tested.

The data from test 1 can be used to develop isolator-specific acceptance criteria for production testing.

6.4.4 3D spring isolators

6.4.4.1 Introduction

This section addresses 3D linear spring isolators such as those shown in Figure 2.3d and Figure 2.3e. The testing protocol and acceptance criteria provided below are *minimum* requirements.

Each prototype 3D spring isolator shall have target vertical and horizontal force-displacement relationships. Coupling between vertical and horizontal responses shall be characterized and used to inform the acceptance criteria for tests 3 and 4.

6.4.4.2 Testing protocol

The following tests shall be performed on each prototype isolator:

1. Three fully reversed cycles of loading between the minimum and maximum vertical force.
2. One hundred fully reversed cycles of horizontal loading corresponding to the design wind force
3. Three fully reversed cycles of loading to a horizontal displacement equal to D_{DB}
4. Three fully reversed cycles of loading to a horizontal displacement equal to D_{50}

For test 1, the imposed vertical load shall vary between 1) DL + 0.25LL + P_{TPG}, and 2) DL - P_{TPG}. The frequency of the loading for test 1 shall be 0.1 Hz or less because the behavior of these devices is not dependent on loading rate. The value of P_{TPG} shall be determined per Section 3.7.2.2.

For tests 2 and 3, the imposed vertical load shall equal DL + 0.25LL on all isolators of that type and size. The frequency of loading for tests 2 and 3 shall be 0.1 Hz or less.

Test 4 will be performed twice, for an imposed vertical load of 1) DL + 0.25LL + P_{TPG}, and 2) DL - P_{TPG}. The frequency of loading for test 4 shall be $f_{iso,h}$. The value of P_{TPG} shall be determined per Section 3.7.2.2.

6.4.4.3 Acceptance criteria

Acceptance criteria shall be project specific. As a minimum:

1. For test 1, the vertical stiffness shall be within ±10% of the target
2. For test 1, the vertical stiffness shall be linear
3. For tests 2 and 3, the horizontal force-displacement relationship shall have positive stiffness on the loading segments of each cycle
4. For test 3, the horizontal force-displacement relationships shall be within ±20% of the target at 25%, 50%, and 100% of the maximum horizontal displacement in all cycles of loading
5. For test 4, the axial and horizontal force-displacement relationships shall be within ±20% of the target at 50% and 100% of the maximum horizontal displacement in all cycles of loading
6. The prototype isolator shall suffer no damage in tests 1, 2, 3, and 4.

If a prototype isolator fails to meet the acceptance criteria, it shall be rejected, and a new isolator shall be tested. Spring isolators may be re-built and re-tested.

The data from test 3 can be used to develop isolator-specific acceptance criteria for production testing.

6.4.5 1D fluid viscous dampers

6.4.5.1 Introduction

This section addresses 1D FVDs (see Figure 2.3f). The testing protocol and acceptance criteria provided below are *minimum* requirements.

Each prototype FVD shall have a target force-velocity relationship.

6.4.5.2 Testing protocol

For horizontal installations, the following sequence of tests shall be performed on each prototype damper:

1. Three fully reversed cycles of loading to the minimum contraction and maximum extension (i.e., full stroke) of the damper
2. One hundred fully reversed cycles of horizontal loading corresponding to the design wind force and the corresponding horizontal displacement
3. Three fully reversed cycles of sinusoidal loading to a horizontal displacement equal to D_{DB} at a frequency equal to $f_{iso,h}$
4. Three fully reversed cycles of sinusoidal loading to a horizontal displacement equal to D_{50} at a frequency equal to $f_{iso,h}$

The frequency of the loading for tests 2 and 3 shall be 0.1 Hz or less.

For vertical installations per Figure 2.3h, prototype dampers shall be subjected to test 1 above and:

5. Three fully reversed cycles of sinusoidal loading to a vertical displacement equal to $D_{DB,v}$ at a frequency equal to $f_{iso,v}$
6. Three fully reversed cycles of sinusoidal loading to a vertical displacement equal to $D_{TPG,v}$ at a frequency equal to $f_{iso,v}$

6.4.5.3 Acceptance criteria

Acceptance criteria shall be project specific. As a minimum:

1. For tests 1, 2, 3, and 5, no evidence of leakage, before, during, or after testing from the damper
2. For tests 1, 2, 3, and 5, no evidence of binding, yielding, or permanent deformation in any part of the damper
3. For tests 1, 2, 3, and 5, no evidence of damage or degradation of the seals in the damper
4. For tests 3, 4, 5, and 6, the force shall range between ±20% of the target
5. For tests 3, 4, 5, and 6, the energy dissipated per cycle of loading shall be no less than 80% of the theoretical value determined using the target force-velocity relationship
6. For tests 3 and 5, the force output in one direction of travel shall neither be less than 90% nor greater than 110% of the force output in the opposite direction, for a given piston-head location and velocity.

If any prototype damper fails to meet the acceptance criteria, it shall be rejected, and another damper tested. Dampers may be re-built and re-tested.

The data from tests 3 (horizontal installation) or 5 (vertical installation) can be used to develop isolator specific acceptance criteria for production testing.

6.4.6 3D viscoelastic dampers

6.4.6.1 Introduction

This section addresses 3D viscoelastic dampers (see Figure 2.3g). The testing protocol and acceptance criteria provided below are *minimum* requirements.

The force outputs (2H, 1V) from a 3D viscoelastic damper are generally dependent on frequency and displacement. Horizontal and vertical force outputs may be coupled and shall be characterized, including the effect of plunger proximity to the wall of the vessel containing the fluid. Each prototype 3D viscoelastic

damper shall have a target force-frequency-displacement relationships.

6.4.6.2 Testing protocol

The following sequence of tests shall be performed on each prototype damper:

1. Three fully reversed horizontal cycles of loading to the wall of the vessel, along two perpendicular horizontal axes of the damper (i.e., no less than $\pm 1.15 D_{50}$)
2. One hundred fully reversed cycles of horizontal loading corresponding to the design wind force and the corresponding horizontal displacement
3. Three fully reversed cycles of sinusoidal loading to a horizontal displacement equal to D_{DB} at frequencies equal to $4 f_{iso,h}$, $2 f_{iso,h}$, and $f_{iso,h}$
4. Three fully reversed cycles of sinusoidal loading to a vertical displacement equal to $D_{DB,v}$ at frequencies equal to $4 f_{iso,v}$, $2 f_{iso,v}$, and $f_{iso,v}$
5. Three fully reversed cycles of sinusoidal loading to a horizontal displacement equal to D_{50} at a frequency equal to $f_{iso,h}$.
6. Three fully reversed cycles of sinusoidal loading to a vertical displacement equal to $D_{TPG,v}$ at a frequency equal to $f_{iso,v}$.

The frequency of the loading for tests 1 and 2 shall be 0.1 Hz or less.

6.4.6.3 Acceptance criteria

Acceptance criteria shall be project specific. As a minimum:

1. For tests 1 through 4, no evidence of leakage, before, during, or after testing from the damper
2. For tests 1 through 4, no evidence of binding, yielding, or permanent deformation in any part of the damper
3. For tests 1 through 4, no evidence of damage or degradation of the seals in the damper
4. For tests 3, 4, 5, and 6, the force shall range between ±20% of the target
5. For tests 3, 4, 5, and 6, the energy dissipated per cycle of loading shall be no less than 80% of the theoretical value determined using the target force-frequency-displacement relationship
6. For tests 3 and 4, the force output in one direction of travel, vertical or horizontal, shall neither be less than 90% nor greater than 110% of the force output in the opposite direction, for a given plunger location and velocity.

If a prototype damper fails to meet the acceptance criteria, it shall be rejected, and another damper tested. Dampers may be re-built and re-tested.

The data from tests 3 and 4 can be used to develop isolator-specific acceptance criteria for production testing.

6.5 Production Tests

6.5.1 Introduction

Production tests are performed on all devices planned for use in the isolation system.

Production devices shall be fabricated identically to the corresponding prototype devices.

Forces, velocities, and displacements shall be digitally recorded at a sampling rate of no less than 200 Hz for each cycle of each production test.

All tests shall be performed at an ambient air temperature of 20°C ± 5°C (68°F ± 9°F). Ambient temperature shall be logged.

6.5.2 2D elastomeric and spherical sliding isolators

6.5.2.1 Introduction

This section addresses LDR, LR, and spherical sliding bearings: see Figure 2.3a, b, and c. The testing protocol and acceptance criteria provided below are *minimum* requirements.

Each production bearing shall have a target horizontal (shearing) force-displacement relationship that is either linear (LDR) or bilinear (LR or spherical sliding).

6.5.2.2 Testing protocol

The following test shall be performed on each production isolator:

1. Three fully reversed cycles of loading to a horizontal displacement equal to D_{DB}

For test 1, the vertical load shall equal the average dead load plus one quarter of the average live load for the type and size of isolator. The loading shall be either 1) dynamic at the frequency used for prototype testing, or 2) slow, at a frequency of 0.1 Hz or less. If slow-speed tests are performed, the isolator mechanical properties at slow speed shall be correlated to the dynamic properties using full-scale test data.

6.5.2.3 Acceptance criteria

Acceptance criteria shall be project specific. As a minimum:

1. For test 1, the horizontal force-displacement relationship shall have positive stiffness on the loading segments of each cycle
2. For test 1, the horizontal force-displacement relationship shall be within ±20% of the target at 50% and 100% of the maximum displacement in all cycles of loading
3. For test 1, the energy dissipated per cycle of horizontal loading shall be no less than 80% of the value computed using the target force-displacement relationship
4. For test 1, the isolator shall suffer no damage

6.5.3 1D *guided* spring isolators

6.5.3.1 Introduction

This section addresses *vertically guided* 1D linear spring isolators per Figure 2.3h, offering isolation in the vertical direction only. The testing protocol and acceptance criteria provided below are *minimum* requirements. Not addressed below are testing requirements for the pins and sleeves that form the 1D vertical guide, which must resist horizontal force.

Each production spring isolator shall have a target linear vertical (axial) force-displacement relationship.

6.5.3.2 Testing protocol

The following test shall be performed on each production isolator:

1. Three fully reversed cycles of loading between the minimum and maximum vertical force.

For test 1, the imposed vertical load shall vary between 1) DL + 0.25LL + P_{DB} , and 2) DL – P_{DB} . The frequency of the loading for test 1 shall be 0.1 Hz or less because the behavior of these devices is not dependent on loading rate. The value of P_{DB} shall be determined per Section 3.7.2.1.

6.5.3.3 Acceptance criteria

Acceptance criteria shall be project specific. As a minimum:

1. For test 1, the vertical stiffness shall be within ±10% of the target
2. For test 1, the vertical stiffness shall be linear
3. For test 1, the isolator shall suffer no damage

6.5.4 3D spring isolators

6.5.4.1 Introduction

This section addresses 3D, linear spring isolators such as that shown in Figure 2.3d and Figure 2.3e. The testing protocol and acceptance criteria provided below are *minimum* requirements.

Each production 3D spring isolator shall have target vertical and horizontal force-displacement relationships.

6.5.4.2 Testing protocol

The following tests shall be performed on each production isolator:

1. Three fully reversed cycles of loading between the minimum and maximum vertical force
2. Three fully reversed cycles of loading to a horizontal displacement equal to D_{DB}

For test 1, the imposed vertical load shall vary between 1) DL + 0.25LL + P_{DB}, and 2) DL – P_{DB}. The frequency of the loading for test 1 shall be 0.1 Hz or less because the behavior of these devices is not dependent on loading rate. The value of P_{DB} shall be determined per Section 3.7.2.1.

For test 2, the imposed vertical load shall equal DL + 0.25LL. The frequency of the loading for test 2 shall be 0.1 Hz or less.

6.5.4.3 Acceptance criteria

Acceptance criteria shall be project specific. As a minimum:

1. For test 1, the vertical stiffness shall be within ±10% of the target
2. For test 1, the vertical stiffness shall be linear
3. For test 2, the horizontal force-displacement relationship shall have positive stiffness on the loading segments of each cycle
4. For test 2, the horizontal force-displacement relationships shall be within ±20% of the target at 50%, and 100% of the maximum horizontal displacement in all cycles of loading
5. The production isolator shall suffer no damage in tests 1 and 2

6.5.5 1D fluid viscous dampers

6.5.5.1 Introduction

This section addresses 1D FVDs: see Figure 2.3f. The testing protocol and acceptance criteria provided

below are *minimum* requirements.

Each production FVD shall have a target force-velocity relationship.

6.5.5.2 Testing protocol

For horizontal installations, the following sequence of tests shall be performed on each production damper:

1. One fully reversed cycle of loading to the minimum contraction and maximum extension of the damper
2. Three fully reversed cycles of sinusoidal loading to a horizontal displacement equal to D_{DB} at a frequency equal to $f_{iso,h}$

For vertical installations per Figure 2.3h, prototype dampers shall be subjected to test 1 and:

3. Three fully reversed cycles of sinusoidal loading to a vertical displacement equal to $D_{DB,v}$ at a frequency equal to $f_{iso,v}$

The frequency of the loading for test 1 shall be 0.1 Hz or less.

6.5.5.3 Acceptance criteria

Acceptance criteria shall be project specific. As a minimum:

1. For tests 1 through 4, no evidence of leakage, before, during, or after testing from the device
2. For tests 1 through 4, no evidence of binding, yielding, or permanent deformation in any part of the device
3. For tests 1 through 4, no evidence of damage or degradation of the seals in the device
4. For tests 3 and 4, the force shall range between ±20% of the target
5. For tests 3 and 4, the energy dissipated per cycle of loading shall be no less than 80% of the theoretical value determined using the target force-velocity relationship
6. For tests 3 and 4, the force output in one direction of travel shall neither be less than 90% nor greater than 110% of the force output in the opposite direction, for a given piston-head location and velocity.

6.5.6 3D viscoelastic dampers

6.5.6.1 Introduction

This section addresses 3D viscoelastic dampers (see Figure 2.3g). The testing protocol and acceptance

criteria provided below are *minimum* requirements.

Each production 3D viscoelastic damper shall have target force-frequency-displacement relationships.

6.5.6.2 Testing protocol

The following sequence of tests shall be performed on each production damper:

1. Three fully reversed horizontal cycles of loading to the wall of the vessel, along two perpendicular horizontal axes of the damper (i.e., no less than $\pm 1.15 D_{50}$)
2. Three fully reversed cycles of sinusoidal loading to a horizontal displacement equal to D_{DB} at a frequency equal to $f_{iso,h}$
3. Three fully reversed cycles of sinusoidal loading to a vertical displacement equal to $D_{DB,v}$ at a frequency equal to $f_{iso,v}$

The frequency of the loading for test 1 shall be 0.1 Hz or less.

6.5.6.3 Acceptance criteria

Acceptance criteria shall be project specific. As a minimum:

1. For tests 1 through 3, no evidence of leakage, before, during, or after testing from the damper
2. For tests 1 through 3, no evidence of binding, yielding, or permanent deformation in any part of the damper
3. For tests 1 through 3, no evidence of damage or degradation of the seals in the damper
4. For tests 2 and 3, the force shall range between ±20% of the target
5. For tests 2 and 3, the energy dissipated per cycle of loading shall be no less than 80% of the theoretical value determined using the corresponding target force-frequency-displacement relationship
6. For tests 2 and 3, the force output in one direction of travel, vertical or horizontal, shall neither be less than 90% nor greater than 110% of the force output in the opposite direction, for a given plunger location and velocity.

SECTION 7
SPECIFICATIONS FOR THE SUPPLY OF ISOLATORS AND VISCOUS DAMPING DEVICES

7.1 Introduction

This section of the report presents draft specifications for the supply of 2D seismic isolators and 1D FVDs. These specifications utilize language and requirements used to procure 2D seismic isolators and 1D FVDs in non-nuclear sectors in the United States, over the past few decades. Three-dimensional isolation systems are not addressed. Resistance to gamma and neutron radiation is not addressed.

Each specification includes three parts: I, II, and III. Text (i.e., [abc]) or numbers (i.e., [123]) highlighted in yellow would be replaced in a project-specific specification.

7.2 2D Seismic Isolators

-o-

Part I. General

I.1 Related documents

A. Drawings and general provisions of the Contract, including General and Supplementary Conditions and Division [123], apply to this section.

I.2 Summary

A. This section includes the following:

1. Engineering design, design calculations and shop drawings of seismic isolators and temporary locking assemblies
2. Fabrication of seismic isolators and temporary locking assemblies
3. Prototype and production testing of bearings
4. Delivery, storage, and handling of all materials to the site
5. Installation of seismic isolators

B. Related sections include the following:

1. Section [123] “Structural Steel”

2. Section [123] “Exterior Painting and Coating”, section [456] “Interior Painting and Coating” and section [789] "High-Performance Coatings" for surface preparation and priming requirements.

I.3 Definitions

A. Elastomeric bearing: a bearing composed of alternating layers of bonded natural rubber and carbon steel shims.

B. Friction pendulum bearing: a bearing composed of between one and four nested spherical surfaces of varying radii, separated by high-load low-friction composite liners; also known as a spherical sliding bearing.

C. Lead-rubber bearing: an elastomeric bearing with a central lead plug.

D. Production bearing: a bearing to be used for construction.

E. Prototype bearing: a bearing used for prototype testing in accordance with this section. Prototype bearings shall not be used for construction without the prior approval of the Dedicating Entity (DE).

F. Seismic isolator: the complete assembly of isolator components, from bottom mounting plate to top mounting plate, including the bearing. (The mounting plates may be an integral part of a spherical sliding bearing.)

G. Seismic isolator components: The individual elements comprising the isolator, including:

1. For elastomeric bearings and lead-rubber bearings, the anchors to the structure above and below, the top and bottom mounting plates, rubber layers, steel shims, and lead core, if provided.

2. For friction pendulum bearings, the anchors to structure above and below, the concave plate(s), inner slider(s), composite sliding material, and seals.

H. Target mechanical properties: The vertical and horizontal force-displacement relationships assumed for the analysis and design of the isolators in the seismic isolation system.

I. Temporary locking assembly: Hardware that prevents relative movement of the components of a seismic isolator during transportation and installation.

I.4 Action submittals

A. Design calculations: Submit calculations bearing the signature and seal of the Engineer of Record (EOR), who must be a licensed structural engineer registered in the United States. The DE

shall approve the design calculations for the prototype and production isolators prior to the manufacture of any bearings.

B. Isolator drawings: Submit isolator drawings bearing the signature and seal of the EOR. The DE shall approval the drawings of the prototype and production isolators prior to their manufacture. Isolator drawings shall include, but not be limited to, fabrication drawings, installation drawings, setting diagrams, bolting templates, schedules of materials and the following:

1. For each type and size of isolator, dimensions, weights, material types, and hole locations.

2. All components and temporary locking assemblies

3. Method of corrosion protection for all components

C. Product data: Submit product data including, but not limited to, that listed below. The DE shall approve the product data prior to the start of bearing manufacture.

1. Manufacturer's specifications. Clearly identify any proprietary processes that are part of the fabrication process. Include manufacturer's literature and data on any adhesive and paint used for isolator components.

2. Manufacturer's quality assurance program.

D. Proposed test procedures: Submit annotated and drafted illustrations of the proposed test apparatus and the procedures for the prototype and production tests required by this section. The DE shall approve the procedures prior to the start of testing.

E. Test reports: Submit the following reports, signed by Manufacturer's testing engineer, for approval by the DE.

1. Prototype bearing test reports: Submit test data, including plots, for each prototype bearing tested. The DE shall approve these reports prior to the manufacture of any production bearings.

2. Production bearing test reports: Submit test data, including plots, for each production bearing within fourteen (14) calendar days of completing the last production test.

3. Final bearing test report: Submit a final report summarizing the test results for all prototype and production bearings within thirty (30) calendar days of completing the last production test.

F. Bearing dimensions: Submit external dimensions for each production bearing, measured after production testing, to the DE, to show compliance with the tolerances specified in this section.

G. Provide documentation that describes requirements for all jobsite storage, handling, and installation requirements, for prior approval by the DE.

H. Operations and maintenance manual: Provide an Operations and Maintenance Manual, for approval by the DE, that shall include, as a minimum:

1. Procedure for removal and reinstallation of seismic isolators.

2. Instructions for inspection and maintenance requirements for a period of twenty-five years[18], including:

a. Visual inspection in the event of a fire.

b. Visual inspection in the event of flooding, with standing water within 6 inches (152 mm) of the bottom mounting plate.

c. Visual inspection of all seismic isolators after an earthquake producing shaking at the site with a peak horizontal acceleration of 0.2g.

I.5 Informational submittals

A. Product durability data: Submit technical data in accordance with Section [123].

B. Certifications: Submit the following documents:

1. Certification signed by an approved independent testing agency that all testing equipment has been calibrated by appropriate standards for the purpose of this specification. Certification shall be deemed current if issued within the preceding 12 months and shall be maintained for the duration of the Manufacturer's testing activities for the project.

2. Certified mill test reports signed by an approved independent testing agency for all steel to be used as components of the seismic isolators.

3. Certification signed by the Manufacturer's representative stating that the prototype and production seismic isolators meet all requirements of applicable codes and standards, and this section. Submit the certification within fourteen (14) calendar days of completing all

[18] A user can modify this requirement based upon relevant data and operating experience.

testing.

I.6 Manufacturers

A. Approved manufacturers, with no need to execute the qualification tests of Section II.5B of this specification, are:

1. ABC

    a. Acceptable for elastomeric bearings and lead-rubber bearings

2. ABC

    a. Acceptable for friction pendulum (spherical sliding) bearings

B. Seismic isolator manufacturers not listed above may be considered acceptable after submission of qualification data per Section II.5.B of this specification and approval by the DE.

I.7 Quality assurance

A. Seismic isolators shall be manufactured under an established and maintained quality assurance program by the Manufacturer, including written process specifications and procedures. The system must ensure that manufacturing, process, inspection, and testing are accomplished in accordance with the following:

1. Manufacturing control: Maintain a system that complies with the requirements of the commercial grade dedication program approved by the DE, ISO 9001, or an equivalent approved by the DE.

2. Process control: Maintain a system that includes, as a minimum, all the following

    a. Specific raw material traceability

    b. Special process certification traceability

    c. Detailed manufacturing instructions that identify the work performed by operation and machine

    d. Inspection instructions

    e. In-process and final detail component inspection instructions with actual dimensions

3. Change control: Any change or substitution of material, dimensions, processes, or other characteristics, after either design approval or hardware delivery, whichever occurs first,

must be approved by the DE prior to incorporation.

4. Calibration control: All devices used to measure, gauge, test, inspect or otherwise examine items to determine compliance with specification and/or contractual requirements shall be calibrated to a measurement standard traceable to the National Institute of Standards and Technology (NIST), or approved equivalent.

Part II. Products

II.1 Seismic isolator components

A. All seismic isolators

1. Threaded anchor bolts: ASTM F1554, Grade 105.

2. Paint: Manufacturer's standard zinc-rich primer and finish coat intended for an exterior environment.

3. Corrosion protection, if other than Manufacturer's standard primer and finish coat.

B. Elastomeric and lead-rubber isolators

1. Top and bottom mounting plates: ASTM A572 Grade 50, ASTM A36, or ASTM A570.

2. Inner steel laminate plates: ASTM A-1011-00-SS Grade 36 Type 1.

3. Elastomer: Base polymer shall be natural rubber. Required elastomer mechanical properties include:

a. Heat resistance per ASTM D573 (160°F (71°C) for seven (7) days).

1. Maximum permissible change in tensile strength: -25%

2. Maximum permissible change in ultimate elongation: -25%

3. Maximum permissible change in durometer hardness: +10 points

b. Compression set per ASTM D395 Method B (160°F (71°C) for twenty-two (22) hours): Maximum permissible set is 50%.

c. Ozone resistance of elastomer exposed to the environment: Ozone resistance shall be determined by tests on strips of representative material mounted per Method A of ASTM D518. The tests shall be performed by ASTM D1149 at an ozone concentration of 50 ± 5 parts per hundred million at 20% strain at 100±2°F (38±1°C) for 100 hours. The ozone resistance shall be regarded as satisfactory if

on conclusion of a test no cracks are visible using 7x magnification.

d. Bond of elastomer to steel laminate: Peel strength tests shall be performed per ASTM D429 Method B. The failure type shall be 100% elastomer tear.

e. Tensile strength and ultimate elongation of elastomer: Minimum tensile strength and ultimate elongation tests shall be performed per ASTM D412. The minimum tensile strength shall be 2250 psi (15.5 MPa) and the minimum ultimate elongation shall be 600%.

f. Hardness of elastomer: The durometer hardness at 70 ± 10°F (21 ± 5°C) shall be determined per ASTM D2240 and reported.

g. Shear modulus at 50% shear strain of elastomer: The shear modulus of the elastomer at 50% shear strain shall be determined by ASTM D4014 and reported. The tangent modulus shall be determined and reported.

4. Lead: Lead shall be 99.9% pure per ASTM E37.

C. Friction pendulum isolators

1. Liner material: Non-metallic and self-sacrificing, and able to provide satisfactory, repeatable performance for energy dissipation rate and heat resistance with a minimum strength of 80000 psi (550 MPa).

2. Concave plates, housing plates, and sliders: ASTM A536, ASTM A576, ASTM A572, ASTM A108, ASTM A36, or approved equivalent.

3. Concave spherical surfaces: ASTM A240 Grade 304 or Grade 316 stainless steel.

4. Seals: Ethylene propylene.

II.2 Product life and maintenance

A. Durability: Isolator mechanical properties shall not change by more than 20%, from the target values used for design, over their design life in an environment like that of the installation, including operating temperature, relative humidity, exposure to moisture and radiation, aging, and creep.

B. Environmental protection: All materials subject to corrosion shall be protected. All materials sensitive to ultraviolet light, ozone or moisture shall be protected by a seal or a cover layer of elastomeric material.

C. Installation: Seismic isolators shall be constructed such that removal and replacement, if needed,

shall not require special tools or methods.

D. Fire protection: The seismic isolators shall be protected by appropriate fire suppression systems (e.g., operating fire sprinklers), as determined by relevant plant specific analyses (e.g., Plant Fire Hazards Analysis).

II.3 Design criteria

A. Elastomeric or lead-rubber bearings

1. Shear strain due to lateral deformation, calculated as D_{50} divided by the total thickness of rubber in the isolator, shall not exceed 300%.

2. Strain due to axial loads shall be calculated considering the overlap area for D_{50}.

3. Strain due to a rotation of no less than 0.003 radians shall be calculated.

4. Total shear strain at D_{50} shall not exceed 600%.

5. The overlap area at D_{50} shall be used to calculate buckling capacity.

B. Friction pendulum bearings

1. Axial stiffness shall be calculated at zero horizontal displacement.

2. Retainer rings, if present, shall not engage at a displacement less than $1.5\,D_{50}$.

II.4 Design calculations

A. Variables, formulas, and assumptions shall be reported in the design calculations.

B. For design calculations, the following load combinations apply, where for each type and size of each bearing, D = maximum dead load, L = maximum live load, S = maximum snow load, E = maximum earthquake-induced axial force due to horizontal and vertical TPG shaking:

1. Vertical load combination 1: 1.0D+0.5L; co-existing horizontal displacement = 0.

2. Vertical load combination 2: Maximum of 1.4D, 1.2D+1.6L+0.5S, and 1.2D+1.6S+0.5L; co-existing horizontal displacement = 0.

3. Vertical load combination 3: 1.2D+0.5L+0.2S+E; co-existing horizontal displacement = D_{50}.

4. Vertical load combination 4: 0.9D-E; co-existing horizontal displacement = D_{50}.

C. Calculations for each type and size of each bearing to resist the forces resulting from Section II.4.B of this specification, with the corresponding factors of safety (FoS):

1. FoS = 3.0

2. FoS = 2.0

3. FoS = 1.1

4. FoS = 1.1

D. LRFD calculations per AISC 360 for mounting plates and threaded anchor rods to resist the forces resulting from Section II.4.B of this specification.

E. Calculations for each type and size of each bearing for the verification of vertical stiffness in accordance with the requirements of this section.

F. Calculations for each type and size of each bearing for the verification of the horizontal force-displacement relationship in accordance with the requirements of this section.

G. LRFD calculations per AISC 360 for temporary locking assemblies to resist 5 kips (22 kN) of horizontal load applied in any horizontal direction at each seismic isolator.

II.5 Testing

A. Testing, reporting, and acceptance criteria shall be in accordance with this section.

B. Qualification testing

1. See Section 6.3 of this report for purpose.

2. A waiver of qualification testing based on available test results for a similar or identical isolators in an isolation system requires prior written approval by the DE.

3. See Section 6.3 of this report for testing requirements.

C. Prototype testing

1. See Section 6.4.1 of this report for purpose.

2. A waiver of prototype testing based on available test results for a similar or identical bearings requires the prior written approval by DE.

3. See Section 6.4.2.2 of this report for testing requirements.

4. See Section 6.4.2.3 of this report for acceptance criteria.

5. See Section 6.4.2.3 of this report for required actions if acceptance criteria are not met.

D. Production testing

1. See Section 6.5.1 of this report for purpose.

2. See Section 6.5.2.2 of this report for testing requirements.

3. See Section 6.5.2.3 of this report for acceptance criteria.

Part III. Execution

III.1 Fabrication and manufacturing

A. All seismic isolators

1. Plates with drilled holes: All plates requiring holes shall be drilled using a template.

2. Tolerances after manufacture and prior to testing:

a. External plan dimensions: ± 0.50 in (12.7 mm).

b. Overall height: ± 0.25 in (6.4 mm).

c. Horizontal offset between top and bottom mounting plates: ± 0.25 in (6.4 mm).

d. Flatness of top and bottom mounting plates: ≤ 0.10 in (2.5 mm). at all points measured from straight edge laid in any direction across entire plate length or width.

e. Out of parallel of top and bottom mounting plates: ≤ 0.005 radians with respect to the other

3. Exposed steel surfaces shall be blasted in accordance with SSPC-SP-6 and painted with the Manufacturer's zinc-rich primer and finish paint, unless additional corrosion protection is required.

B. Elastomeric and lead-rubber bearings

1. All plate surfaces to be bonded to the elastomer shall be sandblasted and cleaned of oils, water, surface coating, rust, and mill scale, before bonding. All edges on plate surfaces to be bonded shall be rounded. All plan corners of plate surfaces to be bonded shall have a minimum radius of 0.25 in (6.4 mm).

2. All molds shall have standard shop-practice mold finish.

3. After fabrication, all elastomeric layers shall have equal thickness with no more than 0.10 in (2.5 mm). variation over the bonded diameter of the bearing.

4. The central hole of each bearing shall be pre-formed and smooth, and neither drilled nor machined.

C. Friction pendulum bearings

1. All plate surfaces to be bonded to bearing liner material shall be sandblasted and cleaned of oils, water, surface coating, rust, and mill scale before bonding.

2. The bearing liner material shall be bonded to the steel concave plates and slider under controlled temperature, pressure, and time, as specified by the Manufacturer. The final liner shall be free of bubbles, show no sign of delamination, and be fully bonded.

III.2 Identification

A. Unique serial numbers shall be assigned to each seismic isolator.

B. Each bearing shall be permanently marked with its unique serial number on two equally spaced locations on the vertical faces of the bearing. The serial number shall also be marked on two faces of the protective packaging used for freight and handling.

III.3 Delivery, storage, and handling

A. Delivery: The isolators shall be delivered to the jobsite in protective packaging, with temporary locking assemblies installed.

B. Handling: The isolators shall be handled to prevent damage, breaking, denting, gouging, and scratching. Damaged bearings will be rejected and must be replaced at the Manufacturer's expense.

C. Storage: The isolators shall be stored in a clean, dry place prior to installation, protected from dirt, fumes, construction debris, and physical damage.

III.4 Installation

A. Comply with the requirements of Section [456] "Structural Steel Framing".

B. Carefully install isolators to prevent damage, breaking, denting, gouging, or scratching. Damaged isolators will be rejected and must be replaced at the Manufacturer's expense.

C. Welding of steel in contact with a bearing shall be performed to avoid heat transfer into the bearing. The temperature of the mounting plates immediately adjacent to a bonded interface shall not exceed the lesser of 200°F (93°C) and the temperature specified by the Manufacturer.

D. Remove temporary locking assemblies in accordance with the Manufacturer's instructions but not before substantial completion of the construction of the building.

E. Clean the area around each isolator of all debris and construction materials.

F. Confirm the clearance (i.e., no obstructions or debris) in the final condition such that the seismic isolators can displace no less than D_{50} in any horizontal direction.

7.3 1D Fluid Viscous Dampers

-o-

Part I. General

I.1 Related documents

A. Drawings and general provisions of the Contract, including General and Supplementary Conditions and Division [123], apply to this section.

I.2 Summary

A. This section includes the following:

1. Engineering design, design calculations and shop drawings of 1D fluid viscous dampers
2. Fabrication of 1D fluid viscous fluid dampers
3. Prototype and production testing of 1D fluid viscous fluid dampers
4. Delivery, storage, and handling of materials to the site
5. Installation of 1D fluid viscous dampers

B. Related sections include the following:

1. Section [123] "Structural Steel"
2. Section [456] "Topic 2"

I.3 Definitions

A. Damper: an energy dissipating element, including a pressure vessel, a piston rod, viscous fluid medium, seals, and housing.

B. Production damper: a damper to be used for construction.

C. Prototype damper: a damper used for prototype testing in accordance with this section.

Prototype damper may be rebuilt for construction, subject to successful production testing and the prior approval of the Dedicating Entity (DE).

D. Viscous damping device (VDD): a damper together with mounting brackets. The components of a VDD include the damper, clevis plates, spherical bearings, and pins and fasteners necessary to connect the individual elements in accordance with the Contract Documents.

E. Force-velocity relationship: The relationship between the damping force in the VDD and the relative velocity between the ends of the VDD, as determined by testing specified in this section.

F. Target mechanical properties: The force-velocity relationships assumed for the analysis and design of the VDDs in the seismic isolation system.

I.4 Action submittals

A. Design calculations: Submit calculations bearing the signature and seal of the Engineer of Record (EOR), who must be a licensed structural engineer registered in the United States. The DE shall approve the design calculations for the prototype and production damper units prior to the manufacture any damper units.

B. VDD drawings: Submit VDD drawings bearing the signature and seal of the EOR. The DE shall approve the drawings of the prototype and production dampers prior to their manufacture. The VDD drawings shall include, but not be limited to fabrication drawings, installation drawings, setting diagrams, bolting templates and schedules of materials, and the following:

1. For each type and size of VDD, dimensions, weights, and material types.

2. All VDD components, including mounting and connection hardware.

3. Method of corrosion protection for all VDD components.

C. Product data: Submit product data including, but not limited to, that listed below. The DE shall approve the product data prior to the start of damper manufacture.

1. Manufacturer’s specifications: Clearly identify any proprietary processes that are part of the fabrication process. Include manufacturer’s literature and data on any seals and coatings used in VDD components.

2. Manufacturer’s quality assurance program.

D. Proposed test procedures: Submit annotated and drafted illustrations of the proposed test apparatuses and the procedures for the prototype and production tests required by this section. The

DE shall approve the procedures prior to the start of testing.

E. Test reports: Submit the following reports, written and signed by the Manufacturer's testing engineer, for approval by the DE.

1. Prototype damper test reports: Submit test data, including plots, for each prototype VDD tested. The DE shall approve these reports prior to the manufacture of any production dampers.

2. Production damper test reports: Submit test data, including plots, for each production VDD within fourteen (14) calendar days of completing the last production test.

3. Final test report: Submit a final report summarizing the test results for all prototype and production dampers within thirty (30) calendar days of completing the last production test.

F. Damper dimensions: Submit external dimensions for each production damper, measured after production testing, to the DE, to show compliance with the tolerances specified in this section.

G. Provide documentation that describes requirements for all jobsite storage, handling, and installation requirements, for prior approval by the DE.

H. Operations and maintenance manual: Provide an Operations and Maintenance Manual, for approval by the DE, that shall include, as a minimum:

1. Procedure for removal and reinstallation of VDDs.

2. Instructions for inspection and maintenance requirements for a period of twenty-five years[19], including.

a. Visual inspection in the event of a fire.

b. Visual inspection in the event of flooding, with standing water within 6 inches (152 mm) of the underside of the VDD.

c. Visual inspection of all VDDs after an earthquake producing shaking at the site with a peak horizontal acceleration of 0.2g.

[19] A user can modify this requirement based upon relevant data and operating experience.

I.5 Informational submittals

A. Product durability data: Submit technical data in accordance with Section [123].

B. Certifications: Submit the following documents:

1. Certification signed by an approved independent testing agency that all testing equipment has been calibrated by appropriate standards for the purpose of this specification. Certification shall be deemed current if issued within the preceding 12 months and shall be maintained for the duration of the Manufacturer's testing activities for the project.

2. Certified mill test reports signed by an approved independent testing agency for all metals to be used as components of the VDDs.

3. Certification signed by the Manufacturer's representative stating that the prototype and production VDDs meet all requirements of applicable codes and standards, and this section. Submit the certification within fourteen (14) calendar days of completing all testing.

I.6 Manufacturers

A. Approved VDD manufacturers, with no need to execute the qualification tests of Section II.5B of this specification, are:

1. ABC

B. Viscous damper manufacturers not listed above may be considered acceptable after submission of qualification data per Section II.5.B of this specification and approval by the DE.

I.7 Quality assurance

A. Dampers shall be manufactured under an established and maintained quality assurance program by the Manufacturer, including written process specifications and procedures. The system must ensure that manufacturing, process, inspection, and testing are accomplished in accordance with the following:

1. Manufacturing control: Maintain a system that complies with the requirements of the commercial grade dedication program approved by the DE, ISO 9001, or an equivalent approved by the DE.

2. Process control: Maintain a system that includes, as a minimum, all the following

a. Specific raw material traceability

b. Special process certification traceability

c. Detailed manufacturing instructions that identify the work performed by operation and machine

d. Inspection instructions

e. In-process and final detail component inspection instructions with actual dimensions

3. Change control: Any change or substitution of material, dimensions, processes, or other characteristics, after either design approval or hardware delivery, whichever occurs first, must be approved by the DE prior to incorporation.

4. Calibration control: All devices used to measure, gauge, test, inspect or otherwise examine items to determine compliance with specification and/or contractual requirements shall be calibrated to a measurement standard traceable to the National Institute of Standards and Technology (NIST), or approved equivalent.

Part II. Products

II.1 VDD components

A. All VDD components

1. Threaded anchor bolts: ASTM F1554, Grade 105.

2. Paint: Manufacturer's standard zinc-rich primer and finish coat intended for an exterior environment.

3. Corrosion protection, if other than Manufacturer's standard primer and finish coat.

B. Dampers:

1. Pressure vessels: The pressure vessel components of the damper shall not be of tie-rod type construction and shall not include externally supported heads or end caps.

2. Castings: Castings are prohibited for pressure vessel parts, or any other parts subjected to tensile or bending stresses, except for parts such as covers, handles, etc., the failure of which would not affect the structural integrity or performance characteristics of the damper.

3. Piston rods: Base metal shall be wrought or forged steel only and shall be either stainless steel or chrome plated.

4. Fluid viscous medium: The fluid viscous media used in the dampers shall be chemically inert, OSHA-approved, non-toxic, non-corrosive, and non-flammable. Petrochemical materials shall not be used.

5. Seals: The damper's seals shall not leak or weep under operating conditions.

6. Piston rod protection: The VDD shall be designed to prevent dusting, scratching, dinging or otherwise marring of the piston rod surface. If a protective cover is used, it shall be fitted with an inspection hatch to allow easy inspection of the damper unit seals and piston rod.

7. Reservoirs and plumbing: External reservoirs, external plumbing and/or viscous medium level indicators are not permitted.

C. VDD components other than the damper:

1. Spherical bearings shall have an inner ring with a spherical outer surface and an outer ring with a spherical inner surface. Bearings shall be fabricated with stainless or high alloy steel and may be of the lined type with non-metallic liners.

2. Pins shall be machined and hardened to be compatible with design requirements of the clevis plates and spherical bearings.

3. Clevis plates shall be ASTM A36, ASTM A572, or approved equivalent.

D. Finish requirements:

1. The damper casing exterior surfaces shall either be nickel plated or painted with a primer coat. A finish coat of paint shall be applied on top of the nickel plating or primer coat.

a. Primer paint: Manufacturer's standard, complying with all limitations of the DE. Coating thickness shall be no less than 0.0001 inch (25 microns).

b. Finish paint: In accordance with manufacturer's standards. Coating thickness shall be no less than 0.0001 inch (25 microns).

II.2 Product life and maintenance

A. Damper mechanical properties shall not change by more than 20%, from the target values used for design, over their design life in an environment like that of the installation, including operating temperature, relative humidity, exposure to moisture and radiation, aging, and creep. Damper units shall be maintenance-free for their design life, where maintenance-free means that refilling of the fluid or replacement of parts is not required.

B. Environmental protection: All materials subject to deterioration or corrosion shall be protected, by methods including, but not limited to, coating, plating, and painting.

C. Installation: The VDDs shall be constructed such that installation, and removal and replacement, if necessary, shall not require any special tools or methods.

D. Fire protection: The VDDs shall be protected by appropriate fire suppression systems (e.g., operating fire sprinklers), as determined by relevant plant specific analyses (e.g., Plant Fire Hazards Analysis).

II.3 Design criteria

A. The damper shall be designed for a target force-velocity (F-v) relationship:

$$F = C_d v^{\delta}$$

where C_d is a damping coefficient and δ is a velocity exponent.

B. The VDD shall be designed for the operating conditions of Section II.3.D below and for the extreme loads imposed by DB and TPG ground motions. Extreme load response of damper units is evaluated by prototype and production testing per Section II.5.C and II.5.D.

C. Operating conditions: The VDD shall be designed for the operational loadings below, capable of performing according to the target force-velocity relationship of Section II.3.B when operating at the temperatures, installed duration, wind and seismic duty cycles, and other environmental conditions specified herein, without degradation of performance, as measured by Section II.3.E.

1. Annual wind duty cycles: ±0.abc inch amplitude at 0.de Hz for fghi cycles.

2. Annual seismic duty cycles: ±k.l inch amplitude at 0.mn Hz for 5 cycles.

3. Ambient operating temperature: Ambient temperatures ranging from +23°F to +120°F (-5°C to 50°C).

4. Humidity: Relative humidity up to 100 percent, including condensation due to temperature change.

D. The force developed by the damper shall be within the following tolerances, when cycled about any point under any loadings associated with operating and non-operating conditions:

1. Force: The damper force output shall be no less than 85% and no more than 115% of the value given by the target F-v relationship of Section II.3.B.

2. Cyclic force difference: The force output developed by the damper in one direction of travel shall be no less than 90% and no more than 110% of the force developed in the opposite direction of travel for a given piston-rod position, velocity, and temperature.

E. The VDD shall be designed and detailed to accommodate the following:

1. The VDD shall include provisions for overall length adjustment. The minimum length adjustment provided shall be ±0.25 inch (6 mm) from the neutral position. Slotted bolted holes shall not be used to provide the required length adjustment.

2. Total stroke: The VDD shall have a total stroke sufficient to allow a complete cycle of displacement as shown on the structural drawings. The complete cycle of displacement shall be measured from the installed, at-rest position.

3. Articulation: The end attachments of the VDD shall accommodate rotations of ±20° in the plane of isolation and a minimum of ±3° in the perpendicular plane.

F. No leakage: The dampers shall not leak under either operating conditions or extreme loads consistent with DB and TPG shaking, as demonstrated by production and prototype testing per Sections II.5.C and II.5.D, respectively.

II.4 Design calculations

A. Variables, formulas and assumptions shall be reported in the design calculations.

B. Stresses in metallic VDD components shall be less than yield for the following loadings:

1. Simultaneous application of $2V_{TPG}$ and a lateral acceleration of 1g, at any piston-rod position, under any of the requirements in Section II.5, with a factor of safety on yield of 2.

2. Application of an internal pressure of 200% of maximum operating pressure, but not less than 20000 psi (138 MPa), with a factor of safety on yield of 1.1.

II.5 Testing

A. Testing, reporting, and acceptance criteria shall be in accordance with this section.

B. Qualification testing

1. See Section 6.3 of this report for purpose.

2. A waiver of qualification testing based on available test results for similar or identical dampers in an isolation system requires prior written approval by the DE.

3. See Section 6.3 of this report for testing requirements.

C. Prototype testing

1. See Section 6.4.1 of this report for purpose.

2. A waiver of prototype testing based on available test results for similar or identical dampers requires the prior written approval by DE.

3. See Section 6.4.5.2 of this report for testing requirements.

4. See Section 6.4.5.3 of this report for acceptance criteria.

5. See Section 6.4.5.3 of this report for required actions if acceptance criteria are not met.

D. Production testing

1. See Section 6.5.1 of this report for purpose.

2. See Section 6.5.5.2 of this report for testing requirements.

3. See Section 6.5.5.3 of this report for acceptance criteria.

Part III. Execution

III.1 Fabrication and manufacturing

A. Unless suitably protected against electrolytic corrosion, dissimilar materials shall not be used in contact with each other. Dissimilar metal joints shall not be permitted without a non-metallic separator or gasket with a thickness of no less than 0.06 inch (1.5 mm). The use of aluminum, aluminum alloys, magnesium, magnesium alloys, and beryllium and beryllium alloys is prohibited.

B. The damper shall contain provisions to limit internal positive or negative pressures as may be caused by thermal expansion and/or contraction of the hydraulic medium and that would otherwise result in seal failure, and leakage or damage to the VDD.

C. Non-filled cavities of the damper shall be sealed against external contamination and moisture and shall be constructed of materials protected against corrosion.

D. Only non-nutrient materials shall be used in the VDD.

E. All non-metallic packings, seals, wipers, or gaskets shall be of non-age sensitive materials.

III.2 Identification

A. Unique serial numbers shall be assigned to each VDD. The individual numbers shall be assigned according to the Manufacturer's standard practice unless otherwise specified in the purchase order or contract.

B. Each damper shall be permanently marked with its unique serial number on a vertical face on each side of the unit. The serial number shall also be marked on two faces of the protective packaging used for freight and handling.

III.3 Delivery, storage, and handling

A. Delivery: Each VDD shall be delivered to the jobsite in protective packaging, with temporary locking assemblies, if any, installed.

B. Handling: Each VDD shall be handled to prevent damage, breaking, denting, gouging, and scratching. Damaged VDDs will be rejected and must be replaced at the Manufacturer's expense.

C. Storage: Each VDD shall be stored in a clean, dry place prior to installation, protected from dirt, fumes, construction debris, and physical damage.

III.4 Installation

A. Comply with the requirements of Section [456] "Structural Steel Framing".

B. Carefully install VDDs to prevent damage, breaking, denting, gouging, or scratching. Damaged production VDDs will be rejected and must be replaced at the Manufacturer's expense.

C. Welding of steel in contact with a VDD is not permitted.

D. Remove temporary locking assemblies, if any, in accordance with the Manufacturer's instructions but not before substantial completion of the construction of the building.

E. Clean the area around each VDD of all debris and construction materials.

F. Confirm the clearance (i.e., no obstructions or debris) in the final condition such that the VDDs can displace no less than $1.15D_{50}$ in any horizontal direction.

SECTION 8
COMMERCIAL GRADE DEDICATION OF SEISMIC ISOLATORS AND DAMPERS

8.1 Background

Commercial-grade dedication (CGD) is a process by which a commercial-grade item (CGI) is designated for use as a basic component in a nuclear power plant. This acceptance process is undertaken to provide reasonable assurance that a CGI to be used as a basic component will perform its intended safety function and, in this respect, is deemed equivalent to an item designed and manufactured under a 10 CFR Part 50, Appendix B, quality assurance program and thus may be used in structures, systems, and components that have been designated as safety-related. This assurance is achieved by identifying the critical characteristics of the item and verifying their acceptability by inspections, tests, or analyses by the purchaser or third-party dedicating entity.

8.2 Purpose

For the application of seismic isolation (SI) to US nuclear power plants, the most common elements to be considered for CGD are elastomeric bearings, spherical sliding bearings, and 1D FVDs—hardware produced and widely used in the US for non-nuclear applications. Although the presentation below focuses on this U.S.-manufactured hardware and points to specifications in Section 7 that address them, the plan could be extended to 1D guided and 3D spring isolators and 3D viscoelastic dampers, described elsewhere in this report.

This section of the report provides a template for performing the technical evaluation tasks required by 10 CFR 21 (USNRC 2004a) and 10 CFR 50 Appendix B (USNRC 2004b) for CGD.

The entirety of a Licensee or Supplier's CGD process is beyond the scope of this document. This document addresses the technical evaluation process described in Section 4 of EPRI (2014).

8.3 Regulatory Guidance

In June 2017, the NRC published Regulatory Guide 1.164 Rev. 0 "Dedication of commercial grade items for use in nuclear power plants" (USNRC 2017b). This RG endorses, in part, the Electric Power Research Institute (EPRI) report 3002002982, Rev. 1 to EPRI NP-5652 and TR-102260, "Plant engineering: guideline for the acceptance of commercial-grade items In nuclear safety-related applications" (EPRI 2014).

8.4 Industry Guidance

As endorsed by USNRC (2017b), EPRI (2014) is the basis for the model plan for CGD presented below.

8.5 Plan for Commercial Grade Dedication

The model plan for CGD of seismic isolators and dampers reflects the guidance of EPRI (2014). References to steps or section numbers map to that EPRI document. This model plan makes a series of assumptions for steps 1, 2, and 3 for the scope of SI components considered. Key to the entire CGD process is the formal Technical Evaluation, Acceptance Plan, and Acceptance Activities.

This model plan is agnostic to the type of seismic isolation technology. As the different types of seismic isolation hardware (e.g., isolators, dampers, 1D, 2D, or 3D) have different technical attributes, practical implementation of this model plan will need to address the unique characteristics of the hardware under consideration.

8.5.1 Step 1: identify the item being procured

This model CGD plan considers the following components, which are both manufactured in the US and used in non-nuclear sectors at this time:

- Elastomeric isolators: LDR and LR
- Spherical sliding isolators: SFP and TFP
- 1D FVDs

Other isolators and VDDs, as identified in Section 8.2, should follow this model plan, with necessary adjustments. In a practical application of the EPRI (2014) guidance, the component identification characteristics such as the part number, model number, original shop order number, and drawing number should be specified, as required per Sections 7.2 and 7.3 of this report for 2D isolators and 1D FVDs, respectively.

As described further in Section 5.2 of EPRI (2014), USNRC regulations prohibit certain items from being accepted using the CGD process. For nuclear power plant applications, the main reason a component would be ineligible for CGD is if it must comply by law with specific codes and standards (e.g., a reinforced concrete shear wall). Although standards are used for the analysis and design of isolators and dampers, this regulation does not apply because the standards a) do not prescribe how to design and detail the hardware, unlike, for example, a reinforced concrete shear wall, and b) mandate physical testing for design basis (production items) and beyond-design-basis (prototype items) shaking.

8.5.2 Step 2: determine if the item performs a safety function

The reactor plant designer designates which structures, systems, and components (SSCs) perform a safety function needed for the protection of the public and environment. For the purposes of this model CGD plan, the seismic isolation components are presumed to perform a safety function.

The safety functions of seismic isolation components will likely include the following:

- Structural integrity: Being installed between a foundation and a basemat, seismic isolators will form part of the gravity load path from the safety-related components, such as the reactor vessel, to the building structure to the ultimate foundation during both normal static (operating) conditions and during a dynamic event such as earthquake shaking.
- Protection from earthquake shaking: The seismic isolation devices mitigate the effects of strong ground shaking on the supported building and its safety-related components, limiting accelerations and displacements to values within the design basis.

8.5.3 Step 3: determine if the item will be procured as a commercial grade item

Because there is no market demand at the time of this writing, there are no suppliers of nuclear safety-related seismic isolators and dampers in the U.S., nor have suppliers announced plans to either produce or qualify nuclear safety-related isolators and dampers on an ongoing basis. Thus, for application of seismic isolators and dampers to a nuclear safety-related function, the components must be purchased as a CGI and appropriately dedicated.

8.5.4 Step 4: identify and document safety function(s) and the FMEA

The preparer of the CGD technical evaluation process must clearly define and document 1) safety function(s), and 2) either the detailed design information or the failure modes and effects analysis (FMEA) for the components. For 2) and application to seismic isolators and dampers, detailed design information shall be provided, as listed in Sections 7.2 and 7.3, for 2D isolators and 1D FVDs, respectively. As stated in EPRI (2014), the technical evaluation must provide the basis for:

- The logic behind the selection of the critical characteristics
- How critical characteristics are related to safety function(s)
- How critical characteristics are related to either 1) detailed design information, or 2) the postulated failure modes and mechanisms that could prevent the item from performing its intended safety-related function(s). (Option 1 is followed here because detailed design information is provided for every isolator and damper, as noted above.)

Isolators and VDDs have been implemented in non-nuclear buildings (e.g., hospitals) and infrastructure (e.g., offshore platforms, liquid storage tanks) for more than three decades. These decades of in-service operation paired with both academic and industrial testing provides a robust technical body of knowledge to select critical characteristics and tie those critical characteristics to the nuclear safety functions.

The use of seismic isolation devices in US nuclear power plants will be in new construction for which design information for both the entire nuclear island and the individual SI components will be available to the supplier/dedicating entity. As described in EPRI (2014) Section 4.5, when such design information is known, the critical characteristics can be derived from that design information in lieu of failure modes and effects analysis.

8.5.5 Step 5: identify and document critical characteristics

Critical characteristics of a component considered for CGD for use in a nuclear power plant are defined in 10 CFR 21.3 *Definitions* (USNRC 2004a) as "those important design, material, and performance characteristics of a commercial grade item that, once verified, will provide reasonable assurance that the item will perform its intended safety function."

The critical characteristics identified during the technical evaluation, for isolators and dampers via design information, are those that are then verified and/or validated during the acceptance process.

Critical characteristics for 2D isolators and 1D FVDs include:

- Elastomeric isolators
    - Isolator geometry per the Action Submittal of Section 7.2 of this report
    - Number of internal rubber layers and thickness
    - Lead core diameter, if provided
    - Axial load capacity per the Action Submittal of Section 7.2 of this report
    - Force-displacement relationships for design-basis shaking per the testing requirements of Section 6.5.2 of this report
- Spherical sliding isolators
    - Isolator external geometry per the Action Submittal of Section 7.2 of this report
    - Isolator internal geometry, including sliding surfaces, sliders, and thickness of liner
    - Axial load capacity per the Action Submittal of Section 7.2 of this report
    - Coefficient(s) of friction on sliding surfaces
    - Force-displacement relationships for design-basis shaking per Section 6.5.2 of this report

- 1D FVDs
    - Element geometry, including pin-to-pin distance, per the Action Submittal of Section 7.3 of this report
    - Stroke per the Action Submittal of Section 7.3 of this report
    - Proof pressure capacity per Section 6.4.5 of this report
    - Force-velocity-displacement relationships for design-basis shaking per Section 6.5.5 of this report

8.5.6 Step 6: select acceptance criteria methods and develop and document acceptance criteria

Section 4.6 of EPRI (2014) identifies four Acceptance Criteria Methods as listed below:

- Special tests and inspection (Method 1)
- Commercial-grade surveys (Method 2)
- Source verification (Method 3)
- An acceptable item and supplier performance record (Method 4)

Each of these methods is recognized as an acceptable means of satisfying the USNRC regulations regarding CGD. Two or more methods may be combined to provide reasonable assurance that the subject component will perform its safety function. As described below, some of these methods are better suited to seismic isolators and dampers for future nuclear power plants than others, for a variety of technical, administrative, and practical reasons. Below, the methods are introduced, and nuances associated with the CGD of seismic isolators and dampers are identified.

Method 1 – special tests and inspection

Method 1 is the most straight-forward means of accepting any physical component. This method involves the physical inspection, testing, and verification of the critical characteristics of the component to be dedicated after the item is received.

For isolator and VDD critical characteristics that are readily checked by exterior physical inspection and measurement, this method is readily applicable. However, validating some of the critical characteristics associated with high forces and large displacements requires special testing equipment that no dedicating entity (DE) will possess. In non-nuclear sectors, this is addressed by requiring 1) independent observation of all prototype and production tests (see Sections 7.2 and 7.3 of this report for 2D isolators and 1D FVDs, respectively) and reporting of supplier (manufacturer) generated test data to the DE, 2) supplier submission of all test reports (see Sections 7.2 and 7.3 of this report for 2D isolators and 1D FVDs, respectively), and

3) acceptance of all test reports by the DE, before any production devices are shipped to the jobsite. This three-step process, which has been used for seismic isolators and dampers in non-nuclear sectors in the US for more than 30 years, is an expanded version of Method 3, as introduced below.

Method 2 – commercial-grade survey

EPRI describes this method as "…a performance-based assessment of a supplier conducted to determine the adequacy of supplier quality controls that are directly related to ensuring that the critical characteristics of the product being dedicated are acceptable."

Reputable domestic US manufacturers of isolators and VDDs, as identified in Section 2 of this report, have extensive and long-running Quality Control (QC) programs with detailed records. These suppliers provide components for mission-critical infrastructure, such as hospitals and long-span bridges, owned by both public agencies and private companies, which, while not the same as Nuclear Quality Assurance programs under 10 CFR 50 Appendix B (USNRC 2004b), have their own demanding procurement requirements including for supplier QC. Per all US standards for seismic isolators and dampers, including ASCE/SEI 7-22 (ASCE (2022), buildings), ASCE/SEI 4-16 (ASCE (2017), nuclear structures), and ASCE/SEI 43-19 (ASCE (2021), nuclear structures), each production isolator and VDD is tested for DB loadings and must be shown to perform adequately before it is shipped to the jobsite (see the discussion on Method 1). One example of past and present rigorous regulator review of seismic isolators and dampers and design of seismic isolation systems for mission-critical infrastructure is by the State of California Department of Health Care Access and Information (HCAI, formerly the Office of Statewide Health Planning and Development, OSHPD) for applications of the technology to hospitals.

The DE will prepare a survey plan of the manufacturer, based on the previously identified component critical characteristics, which includes the programmatic and process controls necessary to provide assurance that the subject isolators and dampers will perform their intended safety functions.

Method 3 – source verification

For this acceptance method, the DE performs verification of critical characteristics during the manufacture and testing of the subject component. Under this method, the DE either independently performs the verification actions or witnesses the performance of measurements and testing executed by the component manufacturer during the production process (see Method 1 above).

Method 4 – item/supplier performance record

The long-term performance of the product and manufacturer in similar applications may be considered as an acceptance method and is fully expected by NRC to be considered by the DE in selecting and

implementing the other acceptance methods. Although isolators and VDDs have not been used in domestic US nuclear applications, the technology has a long service history in the US, with similar or more aggressive environmental conditions (e.g., bridge and marine applications) and seismic demands (i.e., installations at sites of very high seismic hazard).

8.5.7 Step 7: conduct acceptance activities

The acceptance activities, performed in accordance with one or more of the Methods described above, are performed by the DE. Once the DE has determined that the critical characteristics of the isolators and/or dampers are satisfactory and the appropriate documentation completed, the DE is responsible for ensuring that the components are marked in an identifiable manner and tracked according to the dedicating entity's processes and procedures such that traceability is maintained—see Sections 7.2 and 7.3 of this report, for 2D isolators and 1D FVDs, respectively.

Among the four methods defined by EPRI (2014), none are excluded from the CGD of seismic isolators and VDDs. However, the methods will play different roles, as recommended below:

- Method 1, augmented by Method 3 as noted above, should form the backbone of CGD of isolators and VDDs, with all visual inspections and measurements, all physical testing performed, and all isolators and VDDs accepted for construction, before the devices are shipped to the jobsite.
- Method 2 alone cannot be used for project-specific CGD. However, the proven quality procedures demanded of a supplier (or manufacturer) of hardware to mission-critical sectors (e.g., hospitals in California, as regulated by the CA HCAI; defense applications) in regions of high seismic hazard in the US, could be applied directly to nuclear power plants.
- Method 4 alone cannot be used for project specific CGD. However, the performance record of a supplier (or manufacturer) of hardware to non-nuclear sectors in the US is part of the mandated qualification process identified in Section 6.3 of this report.

Note that the DE may delegate the performance of some or all acceptance activities to a service provider with the appropriate competencies and capabilities to perform the acceptance activities under a QA program, which satisfies 10 CFR 50 Appendix B (USNRC 2004b).

SECTION 9
REFERENCES

American Association of State Highway and Transportation Officials (AASHTO) (2014). "Guide specifications for seismic isolation design." 4th edition, AASHTO, Washington D.C.

American Concrete Institute (ACI) (2013). "Code requirements for nuclear safety-related concrete structures and commentary." *ACI 349-13*, ACI, Farmington Hills, IL

American Concrete Institute (ACI) (2019). "Building code requirements for structural concrete and commentary." *ACI 318-19*, ACI, Farmington Hills, IL

American Institute of Steel Construction (AISC) (2016). "Seismic provisions for structural steel buildings." *ANSI/AISC 341-16*, AISC, Chicago, IL

American Institute of Steel Construction (AISC) (2018). "Specification for safety-related steel structures for nuclear facilities." *ANSI/AISC N690-18*, AISC, Chicago, IL

American Institute of Steel Construction (AISC) (2022). "Specification for structural steel buildings." *ANSI/AISC 360-22*, AISC, Chicago, IL

American Nuclear Society (ANS) (2017). "Categorization of nuclear facility structures, systems, and components for seismic design." *ANSI/ANS-2.26-2004 (R2017)*, ANS, La Grange Park, IL

American Society of Civil Engineers (ASCE) (2002). "Minimum design loads for buildings and other structures." *ASCE/SEI 7-02*, ASCE, Reston, VA

American Society of Civil Engineers (ASCE) (2017). "Seismic analysis of safety-related nuclear structures and commentary." *ASCE/SEI 4-16*, ASCE, Reston, VA

American Society of Civil Engineers (ASCE) (2021). "Seismic design criteria for structures, systems, and components in nuclear facilities." *ASCE/SEI 43-19*, ASCE, Reston, VA

American Society of Civil Engineers (ASCE) (2022). "Minimum design loads and associated criteria for buildings and other structures." *ASCE/SEI 7-22*, ASCE, Reston, VA

American Society of Mechanical Engineers (ASME) (2021). "Probabilistic risk assessment standard for advanced non-light water reactor nuclear power plants." *ASME/ANS RA-S-1.4-2021*, ASME/ANS, New York, NY

Black, C. J., and Makris, N. (2007). "Viscous heating of fluid dampers under small and large amplitude

motions: experimental studies and parametric modeling." *Journal of Engineering Mechanics*, 133(5), 566-577.

Chang, S. P., Makris, N., Whittaker, A. S., and Thompson, A. C. (2002). "Experimental and analytical studies on the performance of hybrid isolation systems." *Earthquake Engineering and Structural Dynamics*, 31(2), 421-443.

Computers and Structures (CSI) (2020). "SAP2000 Version 22.1.0." CSI, Walnut Creek, CA.

Constantinou, M. C., Mokha, A., and Reinhorn, A. M. (1990). "Teflon bearings in base isolation II: modeling." *Journal of Structural Engineering*, 116(2), 455-474.

Constantinou, M. C., and Symans, M. (1992). "Experimental and analytical investigation of seismic response of structures with supplemental fluid viscous dampers." *NCEER-92-0032*, University at Buffalo, Buffalo, NY

Constantinou, M. C., P. Tsopelas, Y-S Kim, and Okamoto, S. (1993). "NCEER-Taisei Corporation research program on sliding seismic isolation systems for bridges: experimental and analytical study of friction pendulum system (FPS)." *NCEER-93-0020*, University at Buffalo, Buffalo, NY

Constantinou, M. C., Whittaker, A. S., Kalpakidis, Y., Fenz, D. M., and Warn, G. P. (2007). "Performance of seismic isolation hardware under service and seismic loading." *MCEER-07-0012*, University at Buffalo, Buffalo, NY

Constantinou, M. C., Kalpakidis, I. V., Filiatrault, A., and Lay, R. A. E. (2011). "LRFD-based analysis and design procedures for bridge bearings and seismic isolators." *MCEER-11-0004*, University at Buffalo, Buffalo, NY

Doulgerakis, N., Tehrani, P. K., Talebinejad, I., Kosbab, B. K., Cohen, M., and Whittaker, A. S. (2021). "Software commercial grade dedication guidance for nonlinear seismic analysis." *DE-NE0008857*, US Department of Energy, Washington, D.C.

Eidinger, J. M., and Kelly, J. (1978). "Experimental results of an earthquake isolation system using natural rubber bearings." *UCB/EERC-78/03*, Earthquake Engineering Research Center, University of California, Berkeley, CA

Electric Power Research Institute (EPRI) (2014). "Plant engineering: guideline for the acceptance of commercial-grade items in nuclear safety-related applications: revision 1 to EPRI NP-5652 and TR-102260." *3002002982*, EPRI, Charlotte, N.C

Federal Emergency Management Agency (FEMA) (1995). "NEHRP recommended provisions for seismic

regulations for new buildings." *FEMA P-2082-1*, FEMA, Washington, D.C.

Federal Emergency Management Agency (FEMA) (2012). "Seismic performance assessment of buildings, volume 1-methodology." *FEMA P-58-1*, FEMA, Washington, D.C.

Fenz, D. M., and Constantinou, M. C. (2008a). "Modeling triple friction pendulum bearings for response-history analysis." *Earthquake Spectra*, 24(4), 1011-1028.

Fenz, D. M., and Constantinou, M. C. (2008b). "Spherical sliding isolation bearings with adaptive behavior: experimental verification." *Earthquake Engineering and Structural Dynamics*, 37(2), 185-205.

Fenz, D. M., and Constantinou, M. C. (2008c). "Spherical sliding isolation bearings with adaptive behavior: theory." *Earthquake Engineering and Structural Dynamics*, 37(2), 163-183.

Fenz, D. M., and Constantinou, M. C. (2008d). "Mechanical behavior of multi-spherical sliding bearings." *MCEER-08-0007*, University at Buffalo, Buffalo, NY

Highway Innovation Technology Evaluation Center (HITEC) (1990). "Summary of evaluation findings for the testing of seismic isolation and energy dissipating devices." American Society of Civil Engineers (ASCE), Reston, VA

Huang, Y.-N., Whittaker, A. S., and Luco, N. (2008). "Performance assessment of conventional and base-isolated nuclear power plants for earthquake and blast loadings." *MCEER-08-0019*, University at Buffalo, Buffalo, NY

Huang, Y.-N., Whittaker, A. S., Kennedy, R. P., and Mayes, R. L. (2009). "Assessment of base-isolated nuclear structures for design and beyond-design basis earthquake shaking." *MCEER-09-0008*, University at Buffalo, Buffalo, NY

Huang, Y. N., Whittaker, A. S., Kennedy, R. P., and Mayes, R. L. (2013). "Response of base‐isolated nuclear structures for design and beyond‐design basis earthquake shaking." *Earthquake Engineering and Structural Dynamics*, 42(3), 339-356.

International Atomic Energy Agency (IAEA) (1996). "Defense in depth nuclear safety." *INSAG-10*, IAEA, Vienna, Austria

International Atomic Energy Agency (IAEA) (2005). "Assessment of defence in depth for nuclear power plants." *Safety Reports Series No. 46*, IAEA, Vienna, Austria

International Conference of Building Officials (ICBO) (1991). "Uniform Building Code." ICBO, Whittier, CA

International Organisation for Standardisation (ISO) (2015). "Quality management systems — requirements." *ISO 9001:2015*, Geneva, Switzerland

Ishida, K., Shiojiri, H., Ilzuka, M., Mizukoshi, K., and Takabayashi, K. (1991a). "Failure tests of laminated rubber bearings." *Proceedings, 11th International Conference on Structural Mechanics in Reactor Technology (SMiRT-11)*, Tokyo, Japan.

Ishida, K., Shiojiri, H., Kobayashi, Y., and Terazaki, H. (1991b). "Shaking table test on base isolated FBR plant model: part 2 - simulation analysis." *Proceedings, 11th International Conference on Structural Mechanics in Reactor Technology (SMiRT-11)*, Tokyo, Japan.

Kalpakidis, I. V., Constantinou, M. C., and Whittaker, A. S. (2010). "Modeling strength degradation in lead-rubber bearings under earthquake shaking." *Earthquake Engineering and Structural Dynamics*, 39(13), 1533-1549.

Kammerer, A. M., Whittaker, A. S., and Constantinou, M. C. (2019). "Technical considerations for seismic isolation of nuclear facilities." *NUREG/CR-7253 (ML19050A422)*, US Nuclear Regulatory Commission, Washington, D.C.

Kelly, J. M., Skinner, M. S., and Beucke, K. E. (1980). "Experimental testing of an energy-absorbing base isolation system." *UCB/EERC-80/35*, Earthquake Engineering Research Center, University of California, Berkeley, CA

Kelly, J. M. (1991a). "Dynamic and failure characteristics of Bridgestone isolation bearings." *UCB/EERC-91/04*, Earthquake Engineering Research Center, University of California, Berkeley, CA

Kelly, J. M. (1991b). "Shake table tests of long period isolation system for nuclear facilities at soft-soil sites." *Proceedings, 11th International Conference on Structural Mechanics in Reactor Technology (SMiRT-11)*, Tokyo, Japan.

Kelly, J. M. (1993). *Earthquake-resistant design with rubber*, Springer, New York, NY.

Kumar, M., Whittaker, A. S., and Constantinou, M. C. (2014). "An advanced numerical model of elastomeric seismic isolation bearings." *Earthquake Engineering and Structural Dynamics*, 43(13), 1955-1974.

Kumar, M., Whittaker, A. S., and Constantinou, M. (2015a). "Seismic isolation of nuclear power plants with sliding bearings." *MCEER-15-0006*, University at Buffalo, Buffalo, NY

Kumar, M., Whittaker, A. S., and Constantinou, M. C. (2015b). "Response of base-isolated nuclear structures to extreme earthquake shaking." *Nuclear Engineering and Design*, 295, 860-874.

Kumar, M., Whittaker, A. S., and Constantinou, M. C. (2015c). "Seismic isolation of nuclear power plants with elastomeric bearings." *MCEER-15-0008*, University at Buffalo, Buffalo, NY

Kumar, M., Whittaker, A. S., and Constantinou, M. C. (2015d). "Characterizing friction in sliding isolation bearings." *Earthquake Engineering and Structural Dynamics*, 44(9), 1409-1425.

Kumar, M., and Whittaker, A. S. (2018). "Cross-platform implementation, verification and validation of advanced mathematical models of elastomeric seismic isolation bearings." *Engineering Structures*, 175, 926-943.

Kumar, M., Whittaker, A. S., and Constantinou, M. C. (2019a). "Seismic isolation of nuclear power plants using elastomeric bearings." *NUREG/CR-7255 (ML19063A541)*, US Nuclear Regulatory Commission, Washington D.C.

Kumar, M., Whittaker, A. S., and Constantinou, M. C. (2019b). "Seismic isolation of nuclear power plants using sliding bearings." *NUREG/CR-7254 (ML19158A513)*, US Nuclear Regulatory Commission, Washington D.C.

Lal, K. M., Whittaker, A. S., and Sivaselvan, M. V. (2023). "Mid-height seismic isolation of equipment in nuclear power plants: Numerical simulations and design recommendations." *Nuclear Engineering and Design*, 408, 112286.

Lal, K. M., Whittaker, A. S., Vahdani, S., Kosbab, B. D., Shirvan, K., and Parsi, S. S. (2024). "Considerations of soil-structure-interaction for seismically isolated nuclear reactor buildings." *MCEER-24-0003*, University at Buffalo, Buffalo, NY

Makris, N., and Constantinou, M. C. (1990). "Viscous dampers: testing, modeling, and application in vibration and seismic isolation." *NCEER-90-0028*, University at Buffalo, Buffalo, NY

Makris, N., and Constantinou, M. C. (1991). "Fractional-derivative Maxwell model for viscous dampers." *Journal of Structural Engineering*, 117(9), 2708-2724.

Makris, N., and Constantinou, M. C. (1992). "Experimental study and analytical prediction of response of spring-viscous damper isolation system." *Proceedings, 10th World Conference on Earthquake Engineering*, Madrid, Spain.

Makris, N. (1998). "Viscous heating of fluid dampers. I: Small-amplitude motions." *Journal of Engineering Mechanics*, 124(11), 1210-1216.

Makris, N., Roussos, Y., Whittaker, A. S., and Kelly, J. M. (1998). "Viscous heating of fluid dampers. II: Large-amplitude motions." *Journal of Engineering Mechanics*, 124(11), 1217-1223.

Mir, F. U. H., Tilow, K., Nguyen, N., Song, B., Clavelli, M., Kosbab, B. D., and Whittaker, A. S. (2023a). "Earthquake response of head-mounted equipment in advanced nuclear reactors." *Earthquake Spectra*, 39(4), 1967-1991.

Mir, F. U. H., Whittaker, A. S., Kosbab, B. D., and Nguyen, N. (2023b). "Characterizing the seismic response of a molten salt nuclear reactor." *Earthquake Engineering & Structural Dynamics*, 52(7), 2025-2046.

Moe, W. L., and Afzali, A. (2020). "Modernization of technical requirements for licensing of advanced non-light water reactors: risk-informed and performance-based evaluation of defense-in-depth adequacy." *INL/EXT-20-57941*, Idaho National Laboratory, Idaho Falls, ID

Mokha, A., Constantinou, M. C., and Reinhorn, A. M. (1988). "Teflon bearings in aseismic base isolation: experimental studies and mathematical modeling." *NCEER-88-0038*, University at Buffalo, Buffalo, NY

Mokha, A., Constantinou, M. C., and Reinhorn, A. M. (1990). "Teflon bearings in base isolation I: testing." *Journal of Structural Engineering*, 116(2), 438-454.

Mokha, A., Constantinou, M. C., and Reinhorn, A. M. (1991a). "Further results on frictional properties of teflon bearings." *Journal of Structural Engineering*, 117(2), 622-626.

Mokha, A., Constantinou, M. C., Reinhorn, A. M., and Zayas, V. A. (1991b). "Experimental study of friction-pendulum isolation system." *Journal of Structural Engineering*, 117(4), 1201-1217.

Morgan, T. A., and Mahin, S. A. (2010). "Achieving reliable seismic performance enhancement using multi‐stage friction pendulum isolators." *Earthquake Engineering and Structural Dynamics*, 39(13), 1443-1461.

Morgan, T. A., and Mahin, S. A. (2011). "The use of base isolation systems to achieve complex seismic performance objectives." *PEER 2011/06*, Pacific Earthquake Engineering Research Center (PEER), University of California, Berkeley, CA

Mosqueda, G., Whittaker, A. S., and Fenves, G. L. (2004). "Characterization and modeling of friction pendulum bearings subjected to multiple components of excitation." *Journal of Structural Engineering*, 130(3), 433-442.

Nawrotzki, N. (2009). "Earthquake protection strategies for power plant equipment." *Proceedings, ASME Power Conference 2009*, Alburquerque, NM.

Nawrotzki, P., Siepe, D., and Salcedo, V. (2019). "Seismic protection of NPP structures using 3-D base

control systems." *Proceedings, 25th International Conference on Structural Mechanics in Reactor Technology (SMiRT-25)*, Charlotte, NC.

Nielsen, G., Rees, S., Zekioglu, A., Sarebanha, A., Biscombe, L., Shao, B., and Dong, B. (2020). "A 3-D seismic isolation system to protect the Loma Linda University Hospital from near-fault earthquakes." *Proceedings, 17th World Conference on Earthquake Engineering*, Sendai, Japan.

Nuclear Energy Institute (NEI) (2019). "Risk-informed performance-based technology inclusive guidance for non-light water reactor licensing basis development." *Technical report 18-04*, NEI, Washington D.C.

Sarlis, A. A., and Constantinou, M. (2010). "Modeling of triple friction pendulum isolators in program SAP2000." *Supplement to MCEER Report 05-009*, University at Buffalo, Buffalo, NY, <https://figshare.com/articles/presentation/Modeling_triple_friction_pendulum_isolators_in_program_SAP2000/25139669>.

Sarlis, A. A., and Constantinou, M. C. (2016). "A model of triple friction pendulum bearing for general geometric and frictional parameters." *Earthquake Engineering and Structural Dynamics*, 45(11), 1837-1853.

Structural Engineers Association of Northern California (SEAONC) (1986). "Tentative seismic isolation design requirements." *Seminar and workshop on base isolation and passive energy dissipation, ATC-17*, Applied Technology Council (ATC), San Francisco, CA.

Tajirian, F. F., Kelly, J. M., and Gluekler, E. L. (1989). "Testing of seismic isolation bearings for the PRISM advanced liquid metal reactor under extreme loads." *Proceedings, 10th International Conference on Structural Mechanics in Reactor Technology (SMiRT-10)*, Anaheim, CA.

Tsopelas, P., and Constantinou, M. C. (1994). "NCEER-Taisei Corporation research program on sliding seismic isolation systems for bridges: experimental and analytical study of a system consisting of sliding bearings and fluid restoring force/damping devices." *NCEER-94-0014*, University at Buffalo, Buffalo, NY

US Geological Survey (USGS) (2018). "Hazard curves for the 2018 update of the U.S. National Seismic Hazard Model." <https://www.sciencebase.gov/catalog/item/5d559795e4b01d82ce8e3fef>. (Feb, 2021).

US Nuclear Regulatory Commission (USNRC) (2004a). "Part 21—reporting of defects and noncompliance." USNRC, Rockville, MD

US Nuclear Regulatory Commission (USNRC) (2004b). "Part 50—domestic licensing of production and utilization facilities." USNRC, Rockville, MD

US Nuclear Regulatory Commission (USNRC) (2013). "U.S. Nuclear Regulatory Commission staff recommendation for the disposition of recommendation 1 of the Near-Term Task Force report." *SECY-13-0132 (ML13277A413)*, USNRC, Rockville, MD

US Nuclear Regulatory Commission (USNRC) (2017a). "Nuclear power plant instrumentation for earthquakes." *Regulatory Guide RG1.12 (ML17094A831)*, USNRC, Rockville, MD

US Nuclear Regulatory Commission (USNRC) (2017b). "Dedication of commercial grade items for use in nuclear power plants." *Regulatory Guide RG1.164 (ML17041A206)*, USNRC, Washington, D.C

US Nuclear Regulatory Commission (USNRC) (2018). "Office instruction: topical report process." *LIC-500, Rev. 6 (ML18016A217)*, Office of Nuclear Reactor Regulation, Rockville, MD

US Nuclear Regulatory Commission (USNRC) (2020a). "Risk-informed, technology-inclusive regulatory framework for advanced reactors." *Proposed rule (ML21162A102)*, USNRC, Rockville, MD

US Nuclear Regulatory Commission (USNRC) (2020b). "Guidance for a technology-inclusive, risk-informed, and performance-based methodology to inform the licensing basis and content of applications for licenses, certifications, and approvals for non-light-water reactors." *Regulatory Guide RG1.233 revision 0 (ML20091L698)*, USNRC, Rockville, MD

US Nuclear Regulatory Commission (USNRC) (2022a). "Acceptability of probabilistic risk assessment results for non-light-water reactor risk-informed activities." *Regulatory Guide RG1.247 (ML21235A008)* USNRC, Rockville, MD

US Nuclear Regulatory Commission (USNRC) (2022b). "Technology-inclusive identification of licensing events for commercial nuclear plants." *Draft regulatory guide DG1.254, revision 0 (ML22272A042)* USNRC, Rockville, MD

Veeraraghavan, S., Bolisetti, C., Slaughter, A., Coleman, J., Dhulipala, S., Hoffman, W., , Kim, K., Kurt, E., Spears, R., and Munday, L. (2020). "MASTODON: An open-source software for seismic analysis and risk assessment of critical infrastructure." *Nuclear Technology*, 207(7), 1073-1095

Whittaker, A. S., Aiken, I. D., Bergman, D., Clark, P., Cohen, J., Kelly, J. M., and Scholl, R. (1993). "Code requirements for the design and implementation of passive energy dissipation devices." *Seminar on Seismic Isolation, Passive Energy Dissipation, and Active Control, ATC-17-1*, San Francisco, CA.

Whittaker, A. S., Sollogoub, P., and Kim, M.-K. (2017). "Seismic isolation of nuclear structures: past, present and future." *Proceedings, 24th International Conference on Structural Mechanics in Reactor Technology (SMiRT-24)*, Busan, Korea.

Whittaker, A. S., Sollogoub, P., and Kim, M.-K. (2018). "Seismic isolation of nuclear structures: past, present, and future." *Nuclear Engineering and Design*, 338, 290-299.

Yu, C.-C., Mir, F. U. H., and Whittaker, A. S. (2023). "Design options and risk calculations for seismic isolation systems in advanced nuclear reactors." *Implementing Seismic Base Isolation in Advanced Nuclear Reactors*, DesignSafe-CI, https://doi.org/10.17603/ds2-15y1-dg79 v1.

Yu, C.-C., and Whittaker, A. S. (2024). "Generating seismic design basis spectra for US nuclear energy facilities." *Nuclear Engineering and Design*, 426, 113333.

Zayas, V. A., Low, S. S., and Mahin, S. A. (1987). "The FPS earthquake resisting system: experimental report." *UCB/EERC-87/01*, Earthquake Engineering Research Center, University of California, Berkeley, CA

Zayas, V. A., Low, S. S., and Mahin, S. A. (1989). "Seismic isolation using the friction pendulum system." *Proceedings, 10th International Conference on Structural Mechanics in Reactor Technology (SMiRT-10)*, Anaheim, CA.

Zayas, V. A., Low, S. S., and Mahin, S. A. (1990). "A simple pendulum technique for achieving seismic isolation." *Earthquake Spectra*, 6(2), 317-333.

APPENDIX A
SEISMIC HAZARD AND GROUND MOTION DEVELOPMENT

A.1 Introduction

This appendix presents the process used to develop seismic hazard curves, response spectra, and ground motion time series for a hypothetical site to enable dynamic analysis of a base-isolated nuclear power plant (NPP). This process utilizes seismic hazard data developed by the United States Geological Survey (USGS). Given that the site is hypothetical, and that one goal of the analysis was to demonstrate the utility of seismic isolation for a wide range of soil conditions, a SSHAC-type process per NUREG-2213 (USNRC 2018) was not followed to generate seismic demands.

The seismic hazard and ground motion is developed for a site in the Central and Eastern United States (CEUS) at the East Tennessee Technology Park in Oak Ridge, Tennessee (TN), near Clinch River. The near-surface geology is assumed to be soft rock or stiff soil. The soft rock site (stiff soil site) is represented by the boundary between site classes B and C (C and D) and characterized by an average shear wave velocity of 760 m/sec (360 m/sec) in the upper 30 m of the soil column, per ASCE/SEI 7-22 (ASCE 2022)[20]. Three-component ground motion time series are spectrally matched to UHRS at the Clinch River site. The spectrally matched motions are used for dynamic analysis of the base-isolated reactor building introduced in Section 4.

Section A.2 presents seismic hazard calculations and the derivation of UHRS at the Clinch River site. Section A.3 describes the generation of spectrum-compatible ground motion time series for dynamic analysis of 3D models of the NPP building per US nuclear industry practice. Section A.4 addresses variability in ground shaking between two orthogonal horizontal components of motion in an (H1, H2) pair, used in Appendix C to develop a composite logarithmic standard deviation for a fragility function for a seismic isolation system, and in Section D.3 to adjust a seismic displacement demand curve derived using spectrally matched ground motions.

[20] Section 3.7.1-2 of Revision 4 of the Standard Review Plan (USNRC 2014) identifies competent material, suitable for founding a nuclear power plant, as soil with a shear wave velocity of 1,000 feet/sec (305 m/sec) and higher. The shear wave velocity of 360 m/sec, consistent with a CD site per ASCE/SEI 7-22, is close to the lower bound identified in the Standard Review Plan.

A.2 Seismic Hazard and Response Spectra

Seismic hazard curves for the Clinch River site are generated using the database for the National Seismic Hazard Model developed by the United States Geological Survey (USGS 2018). The USGS database provides seismic hazard for assumed locations in the US, defined using a latitude-longitude pair and a site class that characterizes near-surface geology. The seismic hazard data present mean annual frequencies of exceedance (MAFE) for spectral accelerations of geomean horizontal shaking at numerous periods ranging between 0 (peak ground acceleration, PGA) and 10 seconds, for 5% critical damping. The data enable the generation of uniform hazard response spectra (UHRS).

The (latitude, longitude) pair for the Clinch River site is assumed to be (35.94°N, 84.40°W). The near-surface geology is assumed to be soft rock and stiff soil, represented by BC and CD soil, respectively. The average shear wave velocities in the upper 30 m of the soil column for BC and CD soils are 760 m/sec and 360 m/sec, respectively, per ASCE/SEI 7 (ASCE 2022). Figure A.1 presents seismic hazard curves at the Clinch River site generated using the USGS database for spectral periods of 0 (PGA), 0.1 second, and 2 seconds and the two soils (or site classes).

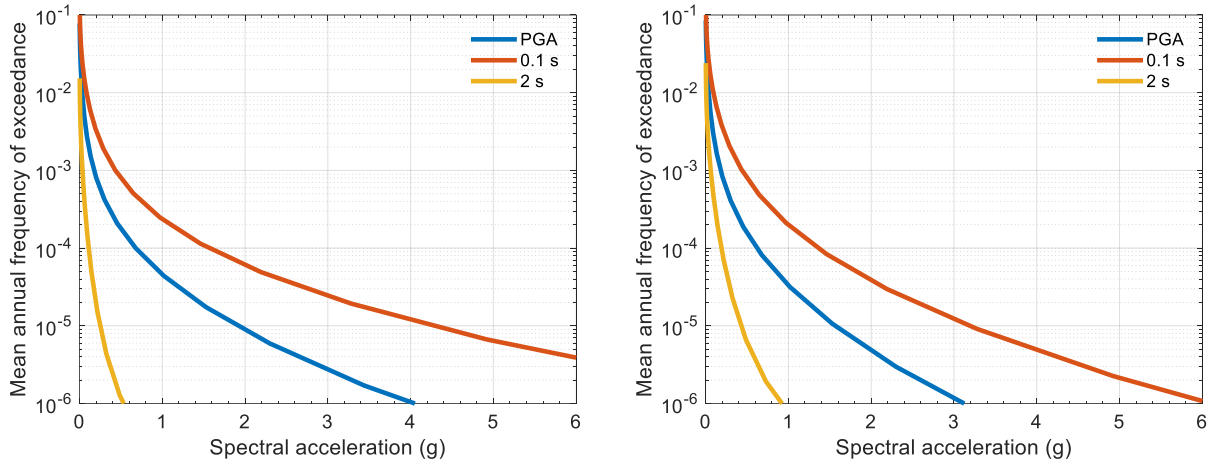

(a) BC (b) CD

Figure A.1. Seismic hazard curves, geomean horizontal shaking, Clinch River, BC and CD soils, 5% damping

The ordinates of the seismic hazard curves at a given MAFE for eighteen periods are used to generate a UHRS. Figure A.2 presents geomean horizontal acceleration response spectra for return periods (reciprocal of MAFE) of 1,000, 10,000, and 25,000 years, 5% critical damping, and BC and CD soil. Table A.1 lists the ordinates of the UHRS of Figure A.2. For a given return period, spectral ordinates for soil BC are greater for short periods (0 to 0.2 second) and those for soil CD are greater for long periods (0.2 to 4 seconds).

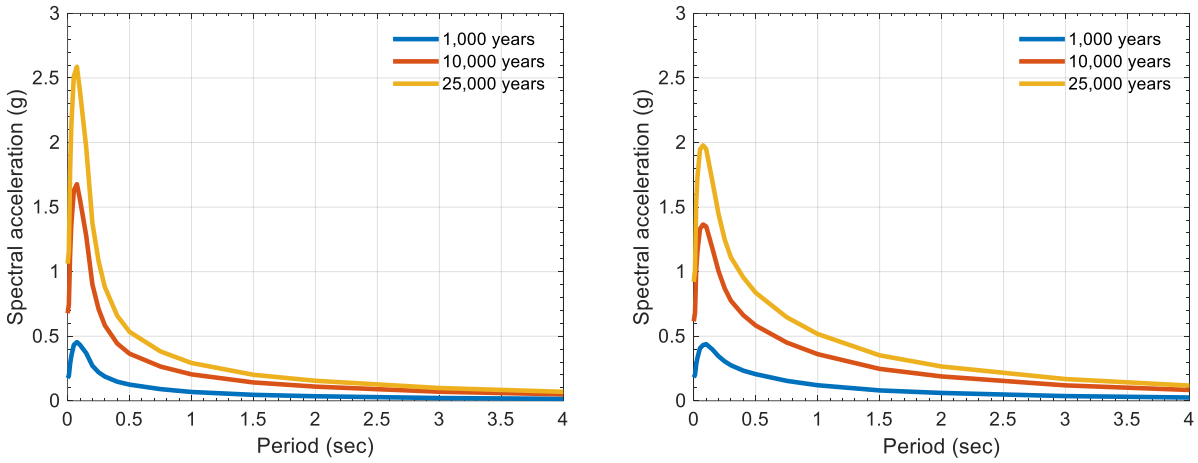

(a) BC (b) CD

Figure A.2.Uniform hazard response spectra (UHRS), return period of 1,000, 10,000, and 25,000 years, geomean horizontal shaking, Clinch River, BC and CD soils, 5% damping

Table A.1. Ordinates of the UHRS shown in Figure A.2, return periods of 1,000, 10,000, and 25,000 years, geomean horizontal shaking, Clinch River, BC and CD soils, 5% critical damping

(a) 1,000 years, BC

Period (sec)	0	0.01	0.02	0.03	0.05	0.075	0.1	0.15	0.2
Spectral acceleration (g)	0.18	0.19	0.29	0.35	0.43	0.45	0.43	0.37	0.27
Period (sec)	0.25	0.3	0.4	0.5	0.75	1	2	3	4
Spectral acceleration (g)	0.22	0.19	0.15	0.13	0.09	0.07	0.04	0.02	0.02

(b) 10,000 years, BC

Period (sec)	0	0.01	0.02	0.03	0.05	0.075	0.1	0.15	0.2
Spectral acceleration (g)	0.68	0.74	1.13	1.37	1.63	1.68	1.56	1.28	0.90
Period (sec)	0.25	0.3	0.4	0.5	0.75	1	2	3	4
Spectral acceleration (g)	0.71	0.58	0.44	0.36	0.27	0.20	0.11	0.07	0.05

(c) 25,000 years, BC

Period (sec)	0	0.01	0.02	0.03	0.05	0.075	0.1	0.15	0.2
Spectral acceleration (g)	1.06	1.16	1.78	2.13	2.51	2.59	2.40	1.96	1.38
Period (sec)	0.25	0.3	0.4	0.5	0.75	1	2	3	4
Spectral acceleration (g)	1.08	0.88	0.66	0.53	0.38	0.29	0.16	0.10	0.07

(d) 1,000 years, CD

Period (sec)	0	0.01	0.02	0.03	0.05	0.075	0.1	0.15	0.2
Spectral acceleration (g)	0.18	0.20	0.28	0.33	0.41	0.43	0.44	0.40	0.34
Period (sec)	0.25	0.3	0.4	0.5	0.75	1	2	3	4
Spectral acceleration (g)	0.31	0.28	0.23	0.21	0.15	0.12	0.06	0.04	0.03

(e) 10,000 years, CD

Period (sec)	0	0.01	0.02	0.03	0.05	0.075	0.1	0.15	0.2
Spectral acceleration (g)	0.62	0.68	1.02	1.16	1.33	1.37	1.35	1.18	1.00
Period (sec)	0.25	0.3	0.4	0.5	0.75	1	2	3	4
Spectral acceleration (g)	0.87	0.77	0.66	0.58	0.45	0.36	0.19	0.12	0.08

(f) 25,000 years, CD

Period (sec)	0	0.01	0.02	0.03	0.05	0.075	0.1	0.15	0.2
Spectral acceleration (g)	0.92	1.01	1.54	1.73	1.94	1.98	1.95	1.70	1.45
Period (sec)	0.25	0.3	0.4	0.5	0.75	1	2	3	4
Spectral acceleration (g)	1.25	1.11	0.96	0.84	0.65	0.52	0.27	0.17	0.12

The UHRS for vertical shaking are generated by scaling the ordinates of the corresponding horizontal spectrum using a factor (V/H) of 2/3 (=0.67) per ASCE/SEI 7-22 (ASCE 2022) for the CEUS. Figure A.3 presents the 5%-damped UHRS at 25,000 years for horizontal and vertical shaking at the Clinch River, and BC and CD soil.

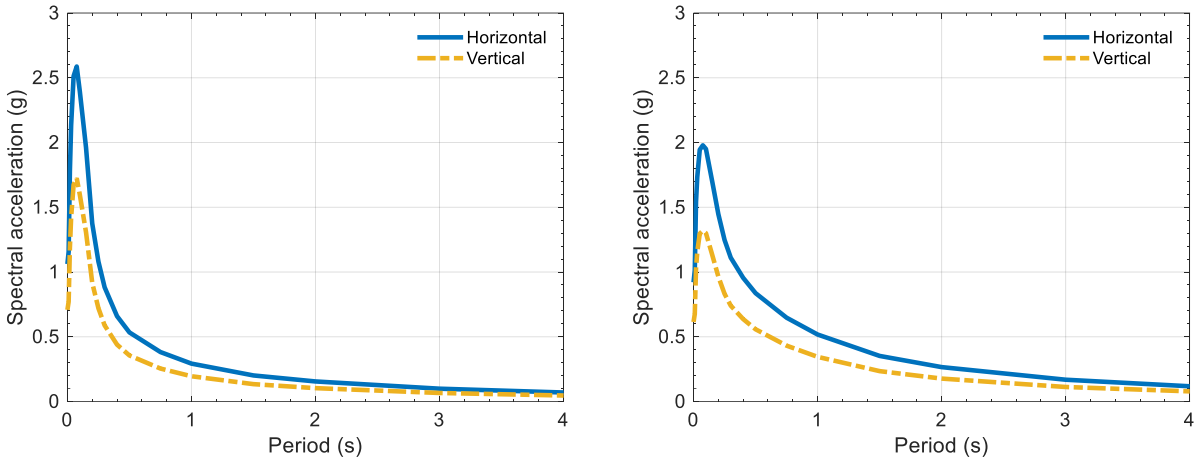

(a) BC (b) CD

Figure A.3. UHRS for a return period of 25,000 years, geomean horizontal and vertical shaking, V/H=0.67, Clinch River, BC and CD soils, 5% damping

A.3 Generation of Spectrum Compatible Ground Motion Time Series

Three-component ground motion time series, compatible with the 25,000-year UHRS for the Clinch River site, shown in Figure A.3, are generated for dynamic analysis of 3D building models. The seed motions are extracted from the ground motion database provided by the Pacific Earthquake Engineering Research Center (PEER 2021). Thirty[21] seed-motion triplets are selected based on a disaggregation of the seismic hazard at Clinch River into magnitude-distance (M , r_{Rup} [22]) pairs.

Figure A.4 presents disaggregation data generated using the USGS unified hazard tool (USGS 2021) for the 1-sec spectral acceleration, MAF of exceedance of 10^{-4}, and site class BC, at the Clinch River site. The bins represent the contribution of earthquakes for different (M , r_{Rup}) pairs. The spectral period of 1 second is representative of the seismically isolated reactor building. Disaggregation data for site class CD or MAFE

[21] Thirty sets of three-component ground motions are used in Appendix C.2.2.2 to establish dispersions, consistent with the number used in Huang *et al.* (2009).

[22] r_{Rup} = closest distance from the site to the fault rupture plane

smaller than 10^{-4} are not available. The (M , r_{Rup}) pair of (6.1, 12 km), identified by an orange arrow in Figure A.4, is the peak contributor and representative of the surrounding data cluster. This pair is used for selecting seed-motion triplets for the two site classes. (The tall bin identified by a green arrow in Figure A.4 is an (M , r_{Rup}) pair of (7.8, 448 km). The site-to-source distance of 448 km is great and the contribution of this bin to the total hazard at 1 second is not significant. Consequently, this (M , r_{Rup}) pair is not considered further.) Table A.2 presents the PEER record numbers and (M , r_{Rup}) pairs of the 30 selected seed-motion triplets for the BC and CD sites. All listed (M , r_{Rup}) pairs are close to that of the peak bin (6.1, 12 km) shown in Figure A.4.

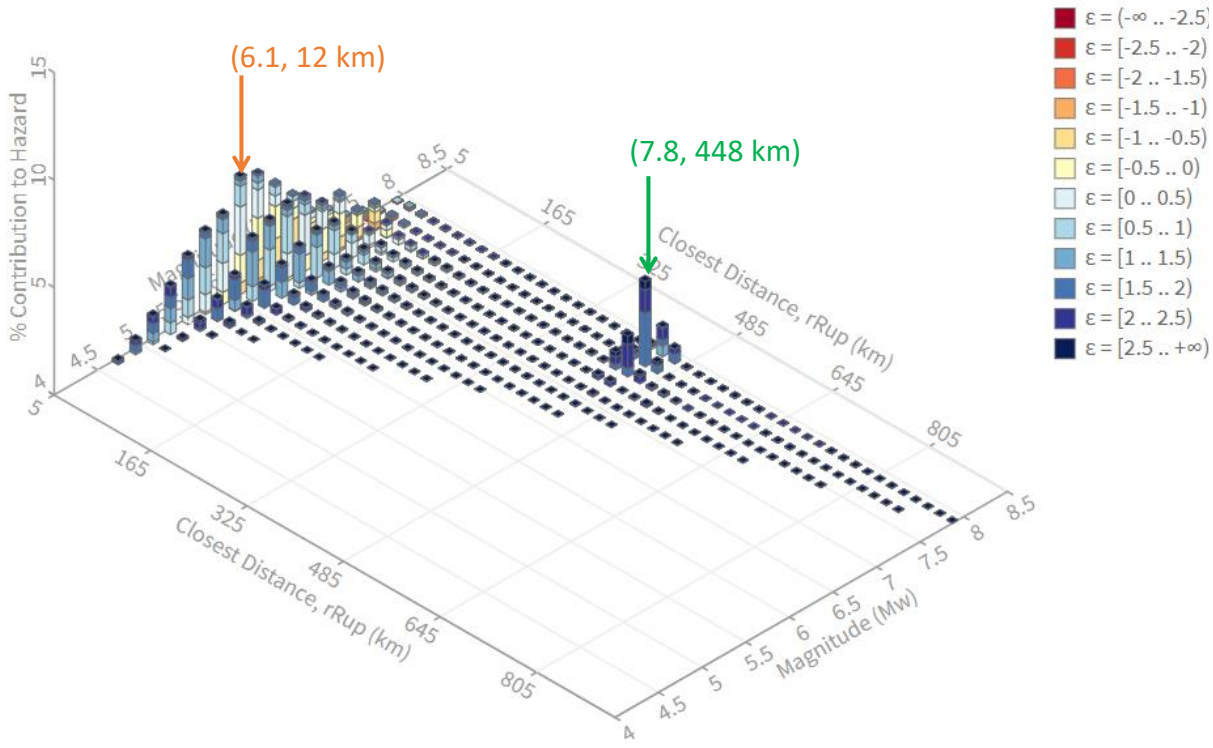

Figure A.4. Disaggregation data, 1-sec spectral acceleration, MAF of exceedance of 10^{-4}, BC soil

The time-domain procedure of RSPMatch2005 (Hancock *et al.* 2006) is used to match the seed-motion triplets listed in Table A.2 to the 25,000-year UHRS presented in Figure A.3 for horizontal and vertical shaking. For a given site class, the two horizontal components of each triplet are matched to the blue spectrum, and the vertical component is matched to the yellow spectrum shown in Figure A.3. Figure A.5 presents the 5%-damped acceleration spectra of the matched motions and the UHRS in the three directions (x = H1, y = H2, and z = V) for BC soil, with respect to a linear scale in period and a logarithmic scale in

frequency. There are 30 matched motion spectra (grey) in each panel. Figure A.6 presents the companion spectra for CD soil.

Section 2.6.2 of ASCE/SEI 4-16 (ASCE 2017) requires that the three orthogonal components in a ground motion triplet be statistically independent. The statistical independence is determined using a correlation coefficient between two components of each triplet. For a given set of ground motion triplets, the mean value of the coefficients for the set must be no greater than 0.16, with a maximum value for any one pair of 0.3. Table A.3 lists the correlation coefficients for any two components (*x*-*y*, *x*-*z*, and *y*-*z*) and the mean of the three coefficients for each matched motion triplet. The matched motions have correlation coefficients that comply with ASCE/SEI 4-16.

Table A.2. Record numbers (record sequence numbers, RSNs) and magnitude-distance pairs (M , r_{Rup}) for the 30 selected seed-motion sets from the PEER database, BC and CD soils

(a) BC

Set #	1	2	3	4	5	6	7	8	9	10
RSN	236	2391	2399	2632	2635	2658	31	405	4069	4085
M	5.9	5.9	5.9	6.2	6.2	6.2	6.2	5.8	6.2	6
r_{Rup} (km)	12.4	10.4	12.0	9.3	9.8	12.8	12.9	11.5	9.5	13
Set #	11	12	13	14	15	16	17	18	19	20
RSN	4129	4136	4138	4139	413	4140	4141	4143	4144	4145
M	6.0	6.0	6	6	5.8	6	6.0	6.0	6.0	6.0
r_{Rup} (km)	12.5	9.7	10.1	10	11.7	10	9.6	9.6	9.6	9.6
Set #	21	22	23	24	25	26	27	28	29	30
RSN	4146	4148	4149	4478	4513	460	527	8118	8124	8134
M	6	6.0	6.0	6.3	5.6	6.2	6.1	6.2	6.2	6.2
r_{Rup} (km)	9.1	9.5	9.4	11.2	11.2	12.1	12	9.1	9.4	11.3

(b) CD

Set #	1	2	3	4	5	6	7	8	9	10
RSN	130	136	1666	236	2386	2391	2632	2635	30	31
M	5.9	5.9	6.1	5.9	5.9	5.9	6.2	6.2	6.2	6.2
r_{Rup} (km)	11	12.2	11.3	12.4	10.7	10.4	9.3	9.8	9.6	12.9
Set #	11	12	13	14	15	16	17	18	19	20
RSN	3473	4069	4075	4085	408	4124	4129	4136	4138	4139
M	6.3	6.2	6	6	5.8	6	6	6	6	6
r_{Rup} (km)	11.5	9.5	10.8	13	11.1	11.5	12.5	9.7	10.1	10
Set #	21	22	23	24	25	26	27	28	29	30
RSN	4142	4144	4146	4148	4478	4513	460	527	8118	8134
M	6.0	6.0	6	6.0	6.3	5.6	6.2	6.1	6.2	6.2
r_{Rup} (km)	9.6	9.6	9.1	9.5	11.2	11.2	12.1	12	9.1	11.3

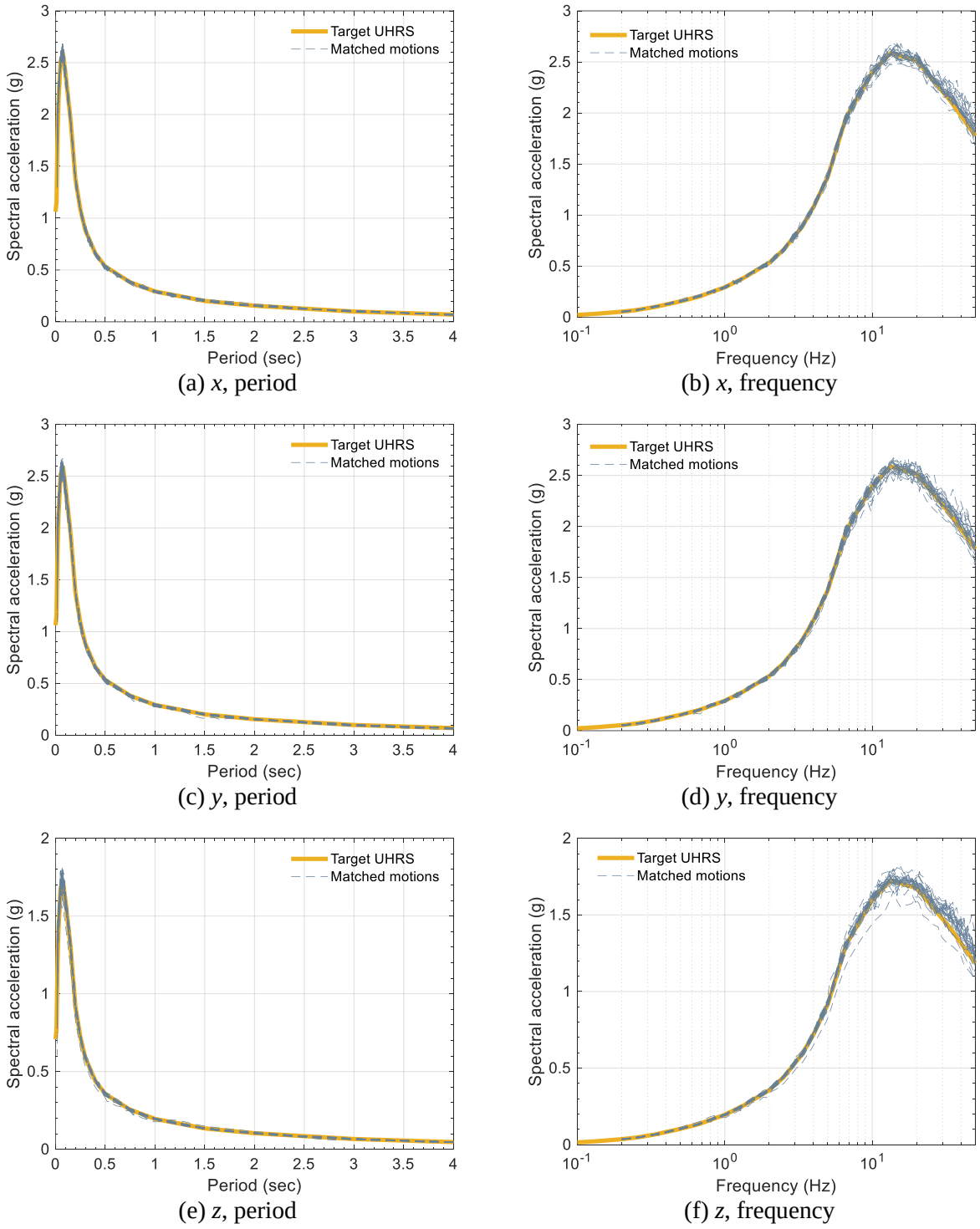

(a) *x*, period (b) *x*, frequency

(c) *y*, period (d) *y*, frequency

(e) *z*, period (f) *z*, frequency

Figure A.5. Response spectra of the matched motions and UHRS for 25,000 years, Clinch River, BC soil, three components, 5% damping

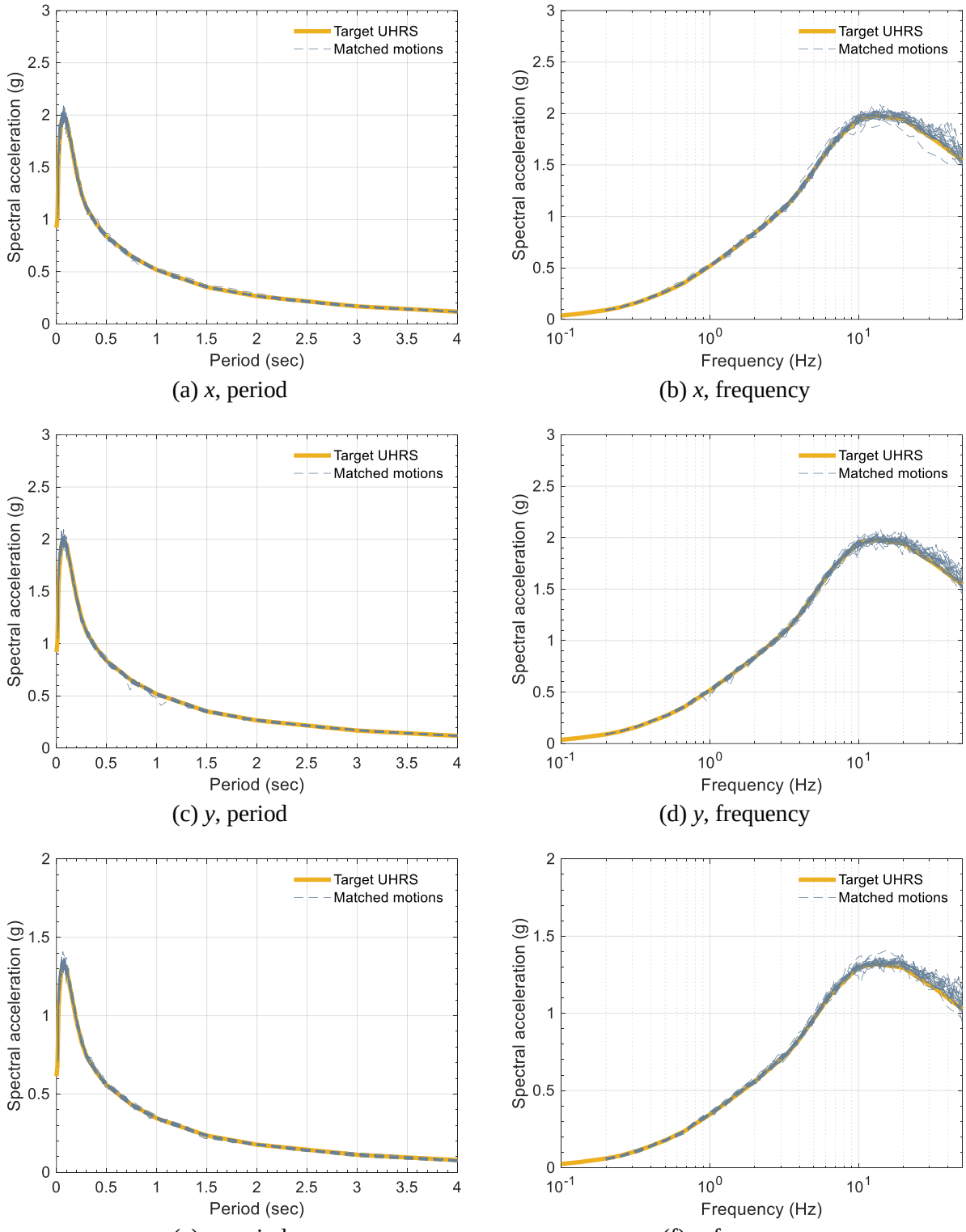

(a) *x*, period (b) *x*, frequency

(c) *y*, period (d) *y*, frequency

(e) *z*, period (f) *z*, frequency

Figure A.6. Response spectra of the matched motions and UHRS for 25,000 years, Clinch River, CD soil, three components, 5% damping

A.4 Variability in Horizontal Components of Shaking around the Geometric Mean Spectrum

In the US nuclear industry, both horizontal ground motions in a pair used for seismic analysis are generally matched to a horizontal geometric mean spectrum, which is the product of a seismic probabilistic hazard analysis. For a recorded pair of horizontal ground motion time series, H1 and H2, the geometric mean spectrum (Sa_{geo}) computed frequency by frequency as $Sa_{geo} = \sqrt{Sa_{H1} Sa_{H2}}$, where Sa_{H1} and Sa_{H2} are the spectra computed using the H1 and H2 time series. The two horizontal components can be rotated in plane to determine an axis of strongest shaking, termed maximum direction shaking by Huang *et al*. (2007, 2008, 2009a)[23]. The ordinates of the maximum direction spectrum are greater than those of the geometric mean spectrum. The ordinates of the minimum direction spectrum, on the orthogonal axis to the maximum direction spectrum are less than those of the geometric mean spectrum. The orientation of the maximum direction of shaking with respect to the causative fault is random for site-to-source distances of 5+ kilometers (Huang *et al*. 2009b).

The use of spectrally matched ground motions for seismic analysis of NPPs is appropriate given the planar framing (e.g., reinforced concrete shear walls) used in conventional nuclear power plants and the random orientation of the strongest horizontal shaking. Seismic input along a direction perpendicular to the axis of the planar framing will generally result in a small or negligible increase in component force demands (e.g., in-plane shear in a wall). Conversely, the seismic isolators and the 3D viscoelastic damper introduced in Section 2 are axisymmetric devices, with force-displacement hysteresis along one horizontal axis being dependent on the displacement response on the orthogonal horizontal axis, and the device guaranteed to experience the strongest shaking. The use of spectrally matched motions for dynamic analysis of a seismically isolated reactor building will underpredict maximum horizontal displacement demand on axisymmetric isolators and dampers, and that is explicitly addressed in this report. Coexisting axial loadings on isolators, delivered by planar framing above the isolation interface, can be computed using spectrally matched ground motions per current practice.

Huang *et al*. (2007, 2008) studied the ratio of maximum to geomean spectral demands using 147 pairs of ground motion records from earthquakes with moment magnitude of 6.5 and greater and a closest site-to-source distance of 15 km and less. Such shaking might be assigned to Western US sites only. In those studies, the maximum spectral demand at a given period was defined as the maximum of the spectral

[23] Huang *et al*. (2007, 2008, 2009a) provide the technical basis for maximum-direction ground motions and spectra, as implemented first in ASCE/SEI 7-10 (ASCE 2010) and subsequently in ASCE/SEI 7-16 (ASCE 2016) and ASCE/SEI 7-22 (ASCE 2022).

accelerations at orientations between 0° to 180° for a pair of two horizontal components of ground motions. Figure 3-7a of Huang *et al*. (2009a) presents the 16th, 50th (median) and 84th percentiles of the ratio of the maximum demand to GMRotI50, which is an orientation-independent geomean demand defined in Boore *et al*. (2006). The median (θ) of the ratio varies between 1.25 and 1.35 at periods greater than 0.4 second. Figure 3-7b of Huang *et al*. (2009a) presents the logarithmic standard deviation (β) of the ratio, varying between 0.10 and 0.13 at periods greater than 0.4 second.

Beyer and Bommer (2006) investigated the ratio of the maximum to recorded geomean spectral demands using 949 earthquake records with moment magnitude ranging between 4.2 and 7.9 and hypocentral distance ranging between 5 and 200 km. Such shaking could address Eastern US, Central US, and Western US sites. Beyer and Bommer reported that the median of the ratio varied between 1.2 and 1.3, depending on the period (the dotted line in Figure 3-7a of Huang *et al*. (2009a)): a very similar outcome to that of Huang *et al*. (2008).

Table A.3. Correlation coefficients between two components of each triplet, 30 matched motions, BC and CD soils

(a) BC

Triplet #	1	2	3	4	5	6	7	8	9	10
x-y	0.28	0.16	0.03	0.02	0.10	0.09	0.11	0.01	0.13	0.00
x-z	0.01	0.04	0.05	0.03	0.09	0.04	0.10	0.07	0.03	0.01
y-z	0.12	0.03	0.23	0.04	0.08	0.02	0.05	0.06	0.14	0.06
Mean	0.14	0.08	0.10	0.03	0.09	0.05	0.09	0.04	0.10	0.02
Triplet #	11	12	13	14	15	16	17	18	19	20
x-y	0.23	0.07	0.10	0.23	0.22	0.02	0.12	0.10	0.08	0.08
x-z	0.00	0.08	0.03	0.00	0.26	0.06	0.14	0.11	0.18	0.00
y-z	0.08	0.05	0.12	0.08	0.03	0.08	0.01	0.06	0.05	0.03
Mean	0.10	0.07	0.08	0.10	0.16	0.06	0.09	0.09	0.10	0.04
Triplet #	21	22	23	24	25	26	27	28	29	30
x-y	0.14	0.00	0.03	0.10	0.06	0.03	0.11	0.10	0.07	0.06
x-z	0.09	0.00	0.10	0.16	0.22	0.11	0.05	0.01	0.01	0.02
y-z	0.07	0.08	0.03	0.15	0.08	0.09	0.05	0.06	0.07	0.05
Mean	0.10	0.03	0.06	0.14	0.12	0.08	0.07	0.05	0.05	0.04

(b) CD

Triplet #	1	2	3	4	5	6	7	8	9	10
x-y	0.08	0.05	0.05	0.28	0.03	0.13	0.01	0.16	0.04	0.03
x-z	0.00	0.10	0.01	0.02	0.07	0.02	0.08	0.11	0.01	0.11
y-z	0.10	0.02	0.15	0.20	0.00	0.07	0.01	0.10	0.11	0.01
Mean	0.06	0.06	0.07	0.16	0.03	0.07	0.03	0.13	0.05	0.05
Triplet #	11	12	13	14	15	16	17	18	19	20
x-y	0.02	0.09	0.17	0.01	0.19	0.08	0.20	0.03	0.10	0.17
x-z	0.04	0.01	0.03	0.03	0.05	0.02	0.01	0.08	0.06	0.05
y-z	0.03	0.08	0.12	0.03	0.03	0.00	0.12	0.06	0.11	0.09
Mean	0.03	0.06	0.11	0.02	0.09	0.03	0.11	0.06	0.09	0.10
Triplet #	21	22	23	24	25	26	27	28	29	30
x-y	0.02	0.10	0.07	0.05	0.12	0.12	0.01	0.08	0.04	0.00
x-z	0.00	0.15	0.08	0.02	0.15	0.15	0.11	0.01	0.00	0.04
y-z	0.04	0.01	0.10	0.03	0.17	0.01	0.08	0.01	0.09	0.02
Mean	0.02	0.09	0.08	0.03	0.15	0.09	0.07	0.03	0.04	0.02

A.5 References

American Society of Civil Engineers (ASCE) (2010). "Minimum design loads for buildings and other structures." *ASCE/SEI 7-10*, ASCE, Reston, VA.

American Society of Civil Engineers (ASCE) (2016). "Minimum design loads and associated criteria for buildings and other structures." *ASCE/SEI 7-16*, ASCE, Reston, VA.

American Society of Civil Engineers (ASCE) (2017). "Seismic analysis of safety-related nuclear structures and commentary." *ASCE/SEI 4-16*, ASCE, Reston, VA.

American Society of Civil Engineers (ASCE) (2022). "Minimum design loads and associated criteria for buildings and other structures." *ASCE/SEI 7-22*, ASCE, Reston, VA.

Beyer, K., and Bommer, J. J. (2006). "Relationships between median values and between aleatory variabilities for different definitions of the horizontal component of motion." *Bulletin of the Seismological Society of America*, 96(4A), 1512-1522.

Boore, D. M., Watson-Lamprey, J., and Abrahamson, N. A. (2006). "Orientation-independent measures of ground motion." *Bulletin of the Seismological Society of America*, 96(4A), 1502-1511.

Hancock, J., Watson-Lamprey, J., Abrahamson, N.A., Bommer, J.J., Markatis, A., McCoyh, E., and Mendis, R. (2006). "An improved method of matching response spectra of recorded earthquake ground motion using wavelets." *Journal of Earthquake Engineering*, 10(spec01), 67-89.

Huang, Y.-N., Whittaker, A. S., and Luco, N. (2008) "Maximum spectral demands in the near-fault region." *Earthquake Spectra*, 24(1), 319-341.

Huang, Y.-N., Whittaker, A. S., Kennedy, R. P., and Mayes, R. L. (2009a). "Assessment of base-isolated nuclear structures for design and beyond-design-basis earthquake shaking." Technical Report MCEER-09-0008, Multidisciplinary Center for Earthquake Engineering Research, University at Buffalo, Buffalo, NY.

Huang, Y.-N., Whittaker, A. S., and Luco, N. (2009b) "Orientation of maximum spectral demand in the near-fault region." *Earthquake Spectra*, 25(3), 707-717.

Pacific Earthquake Engineering Research (PEER) (2021). "PEER ground motion database." <http://peer.berkeley.edu/peer_ground_motion_database>. (Feb, 2021).

US Geological Survey (USGS) (2018). "Hazard curves for the 2018 update of the U.S. National Seismic Hazard Model." <https://www.sciencebase.gov/catalog/item/5d559795e4b01d82ce8e3fef>. (Feb,

2021).

US Geological Survey (USGS) (2021). "Unified hazard tool (v4.2.0)." <https://earthquake.usgs.gov/hazards/interactive/>. (Feb, 2021).

US Nuclear Regulatory Commission (USNRC) (2014). "Standard review plan, Section 3.7.1." *NUREG-0800 (ML14198A460)*, USNRC, Rockville, MD.

US Nuclear Regulatory Commission (USNRC) (2018). "Updated implementation guidelines for SSHAC hazard studies." *NUREG-2213 (ML18282A082)*, USNRC, Rockville, MD.

APPENDIX B
SCALE FACTORS FOR DERIVING DESIGN BASIS SPECTRA

B.1 Introduction

Two levels of earthquake shaking are used to design a seismic isolation system: 1) target performance goal (TPG) shaking, and 2) design basis (DB) shaking. Consistent with the approach of Table 1-1 of ASCE/SEI 43-19 (ASCE 2021), given a seismic design category (SDC), the DB spectrum at a period is computed as the product of a scale factor (SF) and the uniform hazard response spectrum (UHRS) with a mean annual frequency of exceedance at the TPG. In this appendix, the SF is calculated for SDC 3, SDC 4, and SDC 5, eight sites of nuclear-energy facilities in the United States, and two soil types per site. The calculations utilize seismic hazard data developed by the United States Geological Survey (USGS 2018).

The eight sites are identified in Section B.2. Section B.3 provides calculations for the SF.

B.2 Sites of Nuclear-Energy Facilities

Figure B.1 (Kumar *et al.* 2017) identifies the eight sites considered in this appendix: 1) Diablo Canyon, 2) Hanford Site, 3) Idaho National Laboratory, 4) Los Alamos National Laboratory, 5) Oak Ridge National Laboratory, 6) Vogtle, 7) Summer, and 8) North Anna. The (latitude, longitude) pairs for the sites are listed in Table B.1. These sites include regions of low, moderate, and high seismic hazard. Two near-surface geologies are considered for each site, represented by site classes BC (soft rock) and CD (stiff soil) per ASCE/SEI 7-22 (ASCE 2022), for which the average shear wave velocity in the upper 30 m of the soil column is 760 m/sec and 360 m/sec, respectively. The (latitude, longitude) pairs and the site classes are used to extract seismic hazard data from the 2018 USGS database to generate the uniform hazard response spectra (UHRS) presented in Section B.3.

Figure B.1. Eight sites of nuclear-energy facilities (Kumar *et al.* 2017)

B.3 Scale Factor Calculations

Per Section 2.2 of ASCE/SEI 43-19 (ASCE 2021), given a seismic design category (SDC), the spectrum describing DB earthquake shaking, termed a design response spectrum (DRS), is computed as the product of SF and the UHRS at the TPG:

$$DRS = SF \times UHRS_{H_P} \tag{B.1}$$

where H_P is a mean annual frequency of exceedance (MAFE) equal to the TPG, and SF is calculated at each spectral period per Eqs. (2-3a) to (2-3d) in ASCE/SEI 43-19:

Table B.1. Latitude and longitude for eight sites of US nuclear facilities

Site	Latitude (°N)	Longitude (°W)
Diablo Canyon	35.21	120.86
Hanford Site	46.63	119.65
Idaho National Laboratory	43.52	112.05
Los Alamos National Laboratory	35.84	106.29
Oak Ridge National Laboratory	35.94	84.40
Vogtle	33.13	81.77
Summer	34.30	81.32
North Anna	38.06	77.79

$$SF = Maximum\ \ SF_1, SF_2, SF_3 \tag{B.2}$$

$$SF_1 = A_R^{-1} \tag{B.3}$$

$$SF_2 = 0.6 A_R^{-0.2} \tag{B.4}$$

$$SF_3 = 0.45 \tag{B.5}$$

where A_R is a slope factor at a spectral period, defined using the spectral ordinate, Sa, of the UHRS at H_P and H_D (=10 H_P):

$$A_R = \frac{Sa_{H_P}}{Sa_{H_D}} \tag{B.6}$$

For SDC 3, 4, and 5, the TPG are 10^{-4}, 4×10^{-5} and 10^{-5}, respectively, per Table 1-1 of ASCE/SEI 43-19. To compute the SF, the geomean horizontal UHRS at H_P (=TPG) and H_D (=10 H_P) are generated using the USGS Hazard Tool (USGS 2022) and the (latitude, longitude) pairs listed in Table B.1, for the eight sites and BC and CD soils. The 5%-damped UHRS at $H_P = 10^{-4}$, 4×10^{-5}, and 10^{-5} ($H_D = 10^{-3}$, 4×10^{-4}, and 10^{-4}), for SDC 3, 4, and 5, respectively, are presented in Figure B.2 using solid (dash-dotted) lines. Each panel in Figure B.2 presents the UHRS at the six MAFE (i.e., three values each of H_P and H_D) for a given location and site class.

Scale factors are calculated for 19 spectral periods ranging between 0 and 4 seconds using the ordinates of the presented UHRS. The SF at each spectral period is taken as the maximum of SF_1, SF_2, and SF_3. Table B.2 and Table B.3 present the SFs at 12 periods for BC and CD soil, respectively. The geomean horizontal DRS for 5% of critical damping can then be calculated per Eq. (B.1) using the SF and the UHRS at H_P (=TPG), shown as solid lines in Figure B.2.

The SF lies between 0.45 and 0.55, for the eight sites, three SDCs, and BC and CD soils. A value of 0.5 for the SF across all SDCs, soil types, and periods is a most reasonable assumption and so is used in this report with no loss of accuracy, given that DB analysis of the isolated building is performed solely to generate displacements and forces for production testing of isolators and dampers.

B.4 References

American Society of Civil Engineers (ASCE) (2021). "Seismic design criteria for structures, systems, and components in nuclear facilities." *ASCE/SEI 43-19*, ASCE, Reston, VA.

American Society of Civil Engineers (ASCE) (2022). "Minimum design loads and associated criteria for buildings and other structures." ASCE/SEI 7-22, ASCE, Reston, VA.

Kumar, M., Whittaker, A.S., Kennedy, R.P., Johnson, J.J., and Kammerer, A. (2017). "Seismic probabilistic risk assessment for seismically isolated safety-related nuclear facilities." *Nuclear Engineering and Design*, 313, 386-400.

US Geological Survey (USGS) (2018). "Hazard curves for the 2018 update of the U.S. National Seismic Hazard Model." <https://www.sciencebase.gov/catalog/item/5d559795e4b01d82ce8e3fef>. (Feb, 2021).

US Geological Survey (USGS) (2022). "Beta: NSHM Hazard Tool." <https://earthquake.usgs.gov/nshmp/>. (Nov, 2022).

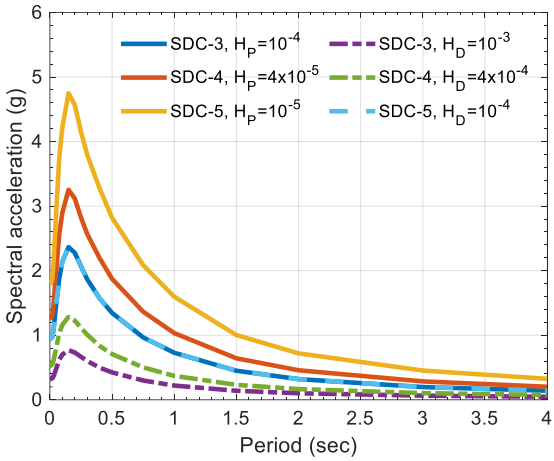

(a) Diablo Canyon, BC

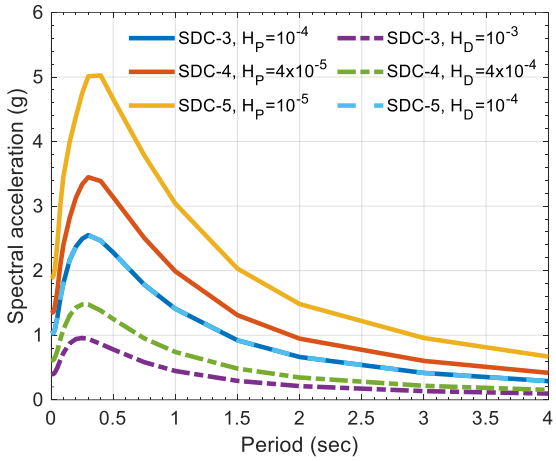

(b) Diablo Canyon, CD

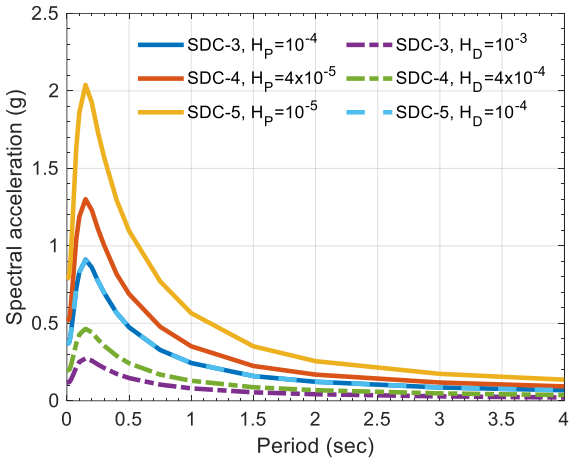

(c) Hanford Site, BC

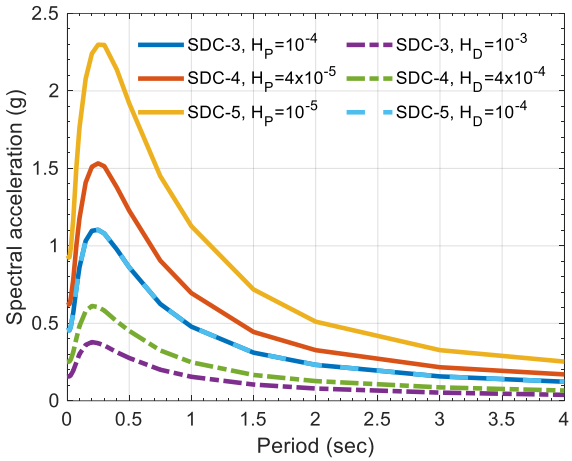

(d) Hanford Site, CD

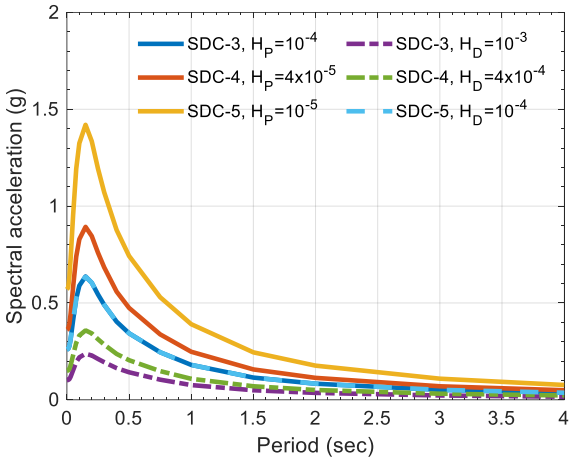

(e) Idaho National Laboratory, BC

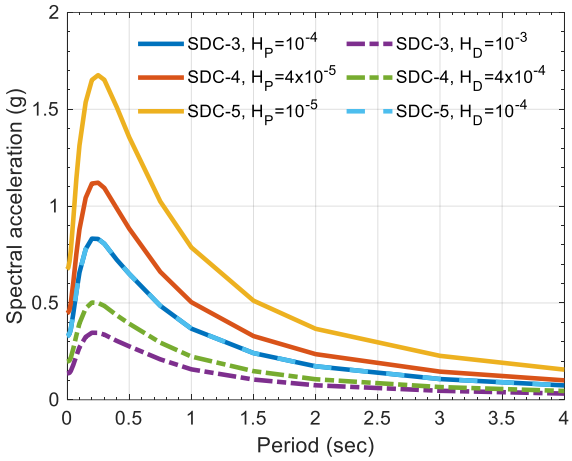

(f) Idaho National Laboratory, CD

Figure B.2. Uniform hazard response spectra at H_P = 10^{-4}, 4×10^{-5}, and 10^{-5}, H_D = 10^{-3}, 4×10^{-4}, and 10^{-4}, SDCs 3, 4, and 5, geomean horizontal shaking, BC and CD soils, 5% damping

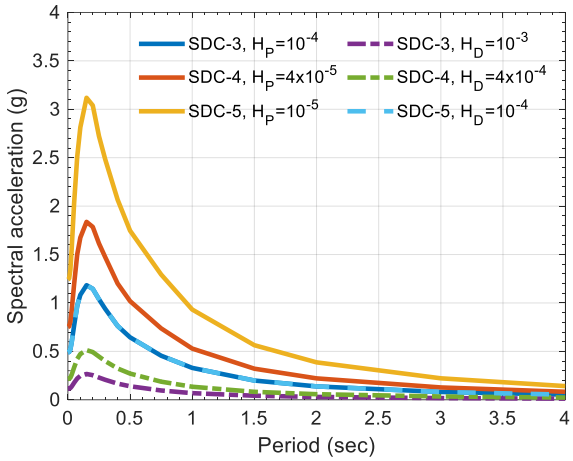

(g) Los Alamos National Laboratory, BC

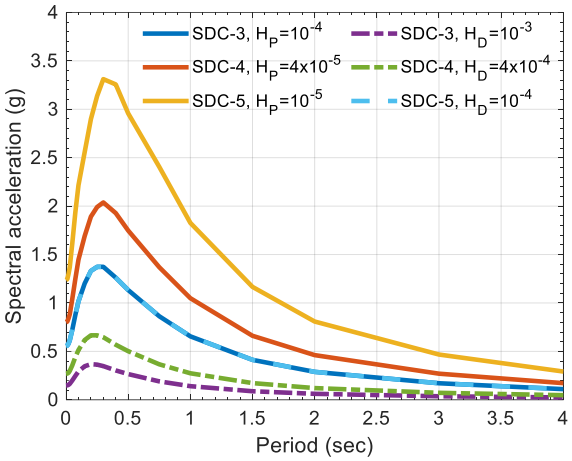

(h) Los Alamos National Laboratory, CD

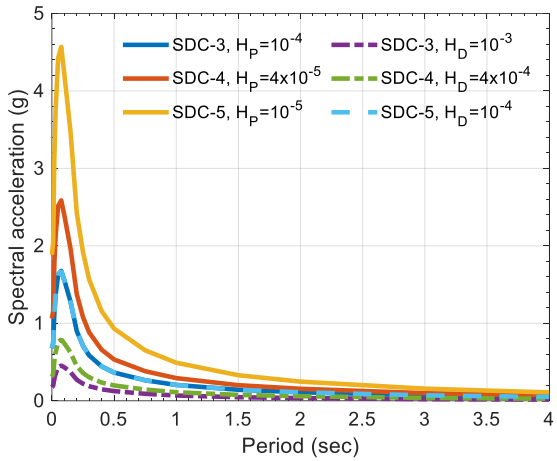

(i) Oak Ridge National Laboratory, BC

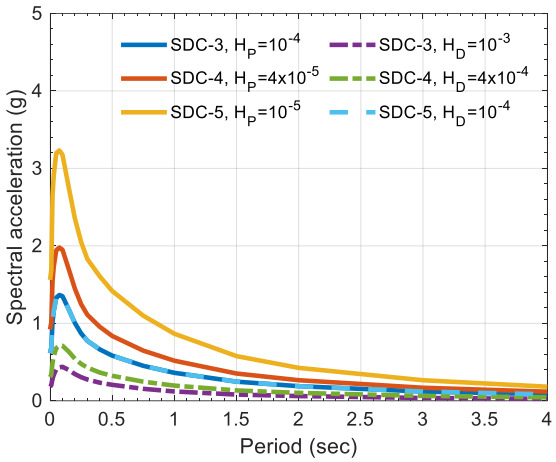

(j) Oak Ridge National Laboratory, CD

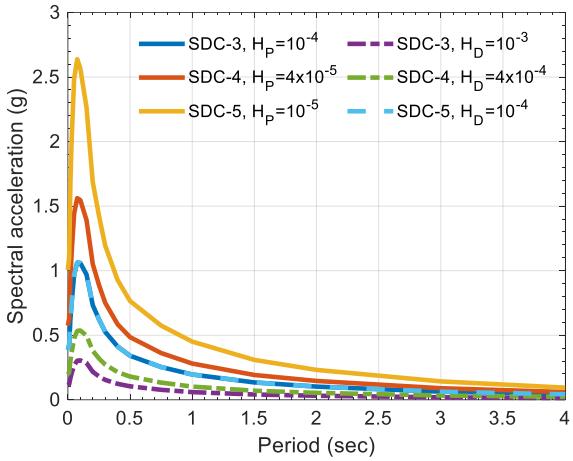

(k) Vogtle, BC

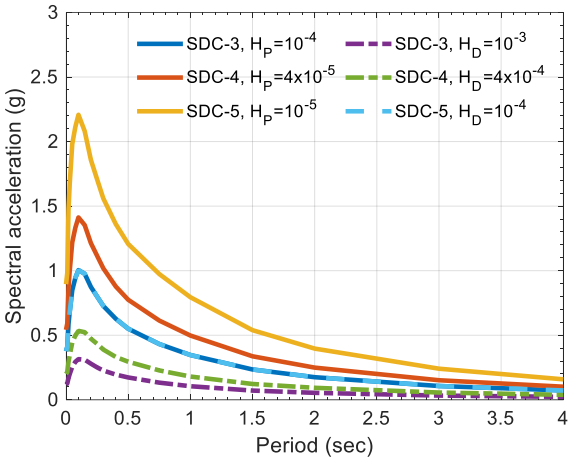

(l) Vogtle, CD

Figure B.2. Uniform hazard response spectra at H_P = 10^{-4}, 4×10^{-5}, and 10^{-5}, H_D = 10^{-3}, 4×10^{-4}, and 10^{-4}, SDCs 3, 4, and 5, geomean horizontal shaking, BC and CD soils, 5% damping (cont.)

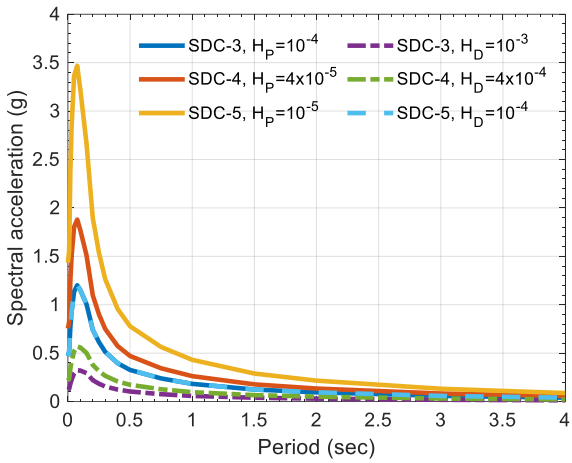

(m) Summer, BC

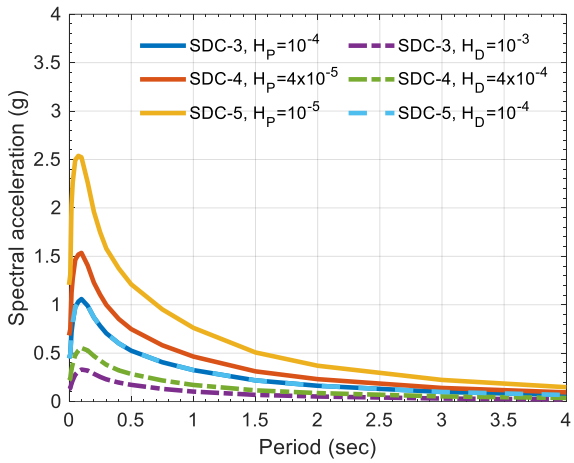

(n) Summer, CD

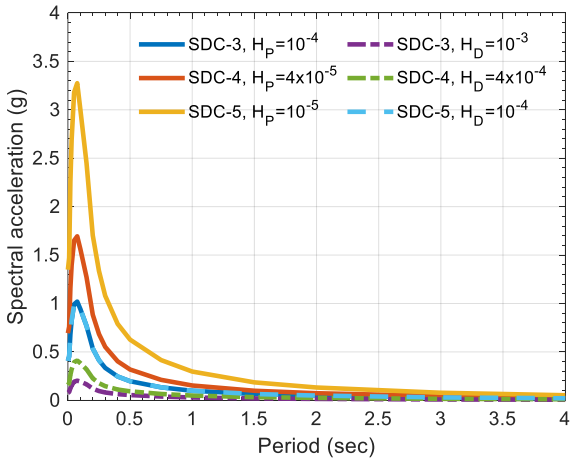

(o) North Anna, BC

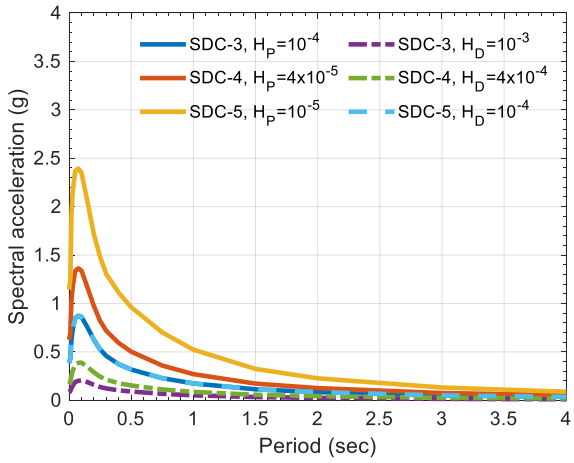

(p) North Anna, CD

Figure B.2. Uniform hazard response spectra at $H_P =$ 10^{-4}, 4×10^{-5}, and 10^{-5}, $H_D =$ 10^{-3}, 4×10^{-4}, and 10^{-4}, SDCs 3, 4, and 5, geomean horizontal shaking, BC and CD soils, 5% damping (cont.)

Table B.2. Scale factors for calculating design response spectra using the uniform hazard response spectra of Figure B.2, 5% damping, 12 spectral periods, SDC 3 ($H_P = 10^{-4}$), SDC 4 ($H_P = 4 \times 10^{-5}$) and SDC 5 ($H_P = 10^{-5}$), eight sites, BC soil

		Period (sec)											
		0	0.02	0.05	0.1	0.2	0.3	0.4	0.5	1	2	3	4
Site	SDC	Scale factor											
Diablo Canyon	3	0.48	0.48	0.48	0.48	0.48	0.48	0.48	0.48	0.47	0.48	0.48	0.48
	4	0.50	0.50	0.50	0.50	0.50	0.50	0.49	0.49	0.49	0.49	0.49	0.49
	5	0.53	0.53	0.52	0.52	0.52	0.52	0.52	0.52	0.51	0.51	0.51	0.51
Hanford	3	0.48	0.48	0.47	0.47	0.47	0.47	0.47	0.47	0.48	0.49	0.48	0.48
	4	0.49	0.49	0.49	0.49	0.49	0.49	0.49	0.49	0.49	0.50	0.50	0.50
	5	0.52	0.51	0.51	0.51	0.51	0.51	0.51	0.51	0.51	0.52	0.52	0.52
Idaho	3	0.50	0.50	0.49	0.49	0.49	0.50	0.50	0.50	0.50	0.51	0.51	0.51
	4	0.50	0.50	0.50	0.50	0.50	0.50	0.51	0.51	0.51	0.51	0.51	0.51
	5	0.51	0.51	0.51	0.51	0.51	0.51	0.51	0.51	0.51	0.52	0.52	0.52
Los Alamos	3	0.45	0.45	0.45	0.45	0.45	0.45	0.45	0.45	0.45	0.45	0.45	0.45
	4	0.47	0.47	0.47	0.47	0.46	0.46	0.46	0.46	0.46	0.46	0.46	0.47
	5	0.50	0.50	0.49	0.50	0.49	0.49	0.49	0.49	0.49	0.49	0.49	0.49
Oak Ridge	3	0.46	0.46	0.46	0.46	0.47	0.48	0.48	0.48	0.48	0.48	0.47	0.47
	4	0.47	0.47	0.47	0.47	0.48	0.48	0.49	0.49	0.49	0.50	0.49	0.49
	5	0.49	0.49	0.49	0.49	0.49	0.49	0.50	0.50	0.50	0.51	0.51	0.51
Vogtle	3	0.47	0.46	0.46	0.47	0.47	0.47	0.47	0.47	0.47	0.47	0.47	0.48
	4	0.48	0.48	0.48	0.49	0.49	0.49	0.49	0.49	0.49	0.49	0.49	0.50
	5	0.50	0.49	0.50	0.50	0.51	0.51	0.51	0.51	0.51	0.51	0.51	0.51
Summer	3	0.46	0.45	0.46	0.46	0.47	0.47	0.48	0.48	0.48	0.48	0.48	0.48
	4	0.47	0.46	0.47	0.48	0.48	0.49	0.49	0.49	0.49	0.49	0.49	0.50
	5	0.48	0.48	0.48	0.49	0.50	0.50	0.50	0.50	0.51	0.51	0.51	0.51
North Anna	3	0.45	0.45	0.45	0.45	0.45	0.45	0.46	0.46	0.47	0.47	0.47	0.47
	4	0.45	0.45	0.45	0.45	0.46	0.46	0.46	0.47	0.48	0.48	0.48	0.49
	5	0.47	0.47	0.48	0.48	0.48	0.47	0.48	0.48	0.48	0.49	0.50	0.50

Table B.3. Scale factors for calculating design response spectra using the uniform hazard response spectra of Figure B.2, 5% damping, 12 spectral periods, SDC 3 ($H_P = 10^{-4}$), SDC 4 ($H_P = 4\times10^{-5}$) and SDC 5 ($H_P = 10^{-5}$), eight sites, CD soil

		Period (sec)											
		0	0.02	0.05	0.1	0.2	0.3	0.4	0.5	1	2	3	4
Site	SDC	Scale factor											
Diablo Canyon	3	0.50	0.50	0.50	0.50	0.50	0.49	0.49	0.48	0.48	0.48	0.48	0.48
	4	0.51	0.51	0.51	0.51	0.51	0.51	0.50	0.50	0.49	0.49	0.49	0.49
	5	0.55	0.54	0.53	0.53	0.54	0.52	0.52	0.52	0.51	0.51	0.51	0.51
Hanford	3	0.48	0.49	0.48	0.49	0.49	0.48	0.48	0.48	0.48	0.48	0.48	0.48
	4	0.50	0.50	0.50	0.50	0.50	0.50	0.49	0.49	0.49	0.50	0.50	0.50
	5	0.52	0.52	0.52	0.52	0.52	0.52	0.51	0.51	0.51	0.51	0.52	0.52
Idaho	3	0.50	0.50	0.50	0.50	0.50	0.50	0.50	0.51	0.51	0.51	0.51	0.51
	4	0.51	0.51	0.51	0.51	0.51	0.51	0.51	0.51	0.51	0.51	0.51	0.51
	5	0.52	0.52	0.52	0.52	0.52	0.52	0.52	0.52	0.52	0.52	0.52	0.52
Los Alamos	3	0.46	0.46	0.46	0.47	0.46	0.46	0.45	0.45	0.45	0.45	0.45	0.45
	4	0.48	0.48	0.48	0.49	0.49	0.48	0.47	0.47	0.46	0.46	0.46	0.46
	5	0.51	0.51	0.51	0.51	0.51	0.50	0.50	0.50	0.49	0.49	0.49	0.49
Oak Ridge	3	0.47	0.46	0.47	0.48	0.48	0.49	0.49	0.49	0.48	0.48	0.47	0.47
	4	0.48	0.48	0.49	0.49	0.49	0.50	0.49	0.50	0.49	0.50	0.49	0.49
	5	0.50	0.50	0.50	0.51	0.51	0.51	0.50	0.50	0.50	0.51	0.51	0.51
Vogtle	3	0.47	0.47	0.47	0.48	0.48	0.48	0.48	0.48	0.47	0.47	0.47	0.48
	4	0.49	0.48	0.49	0.49	0.50	0.49	0.49	0.49	0.49	0.49	0.49	0.49
	5	0.50	0.50	0.51	0.51	0.52	0.52	0.51	0.51	0.51	0.51	0.51	0.51
Summer	3	0.47	0.46	0.47	0.48	0.48	0.48	0.48	0.48	0.48	0.48	0.48	0.48
	4	0.48	0.47	0.48	0.49	0.50	0.49	0.49	0.49	0.49	0.49	0.49	0.50
	5	0.49	0.49	0.50	0.50	0.51	0.51	0.51	0.51	0.51	0.51	0.51	0.51
North Anna	3	0.45	0.45	0.45	0.45	0.46	0.46	0.46	0.47	0.47	0.47	0.47	0.47
	4	0.46	0.46	0.46	0.47	0.47	0.47	0.47	0.47	0.48	0.48	0.48	0.49
	5	0.48	0.48	0.49	0.49	0.49	0.49	0.48	0.48	0.48	0.49	0.50	0.50

APPENDIX C
ACHIEVING A PERFORMANCE TARGET FOR A SEISMIC ISOLATION SYSTEM

C.1 Purpose

This appendix provides information on the derivation of a fragility function for an isolation system (Section C.2) and presents performance-related data for isolation systems (Section C.3) not addressed in Section 5. The sensitivity of the calculated risk to the chosen value of the composite logarithmic standard deviation is presented in Section C.4. Section C.5 investigates the change in risk associated with the truncation of the isolation-system fragility function based on data from production testing.

The terms *variability* and *uncertainty* are used interchangeable in this appendix without distinction between aleatory and epistemic sources since the composite dispersion of Section C.2 includes both sources.

Seismic risk is typically computed by integrating a fragility function over a seismic hazard curve. Herein, the target performance goal for the seismic isolation system is achieved by incrementing the median capacity of an isolation-system fragility function until the convolution of the fragility function and the seismic displacement demand curve produces a mean annual frequency of unacceptable performance equal to or lower than the TPG.

C.2 Deriving an Isolation-System Fragility Function

C.2.1 Introduction

The fragility function for an isolation system uses horizontal displacement as the demand parameter because performance is measured as the unrestricted horizontal movement of the base-isolated building, namely, no collision with adjacent construction or buildings. In the vertical direction, it is assumed that there is no restriction on upwards displacement of the isolated building.

Following conventional practice in the nuclear industry, the fragility function for an isolation system (including both isolators and VDDs) is assumed to be a cumulative lognormal distribution defined by a median displacement capacity, θ, and a logarithmic standard deviation, β. The median and logarithmic standard deviation are assumed to be independent.

The median horizontal displacement capacity of an isolator and/or a damper is confirmed by prototype testing, as described in Section 6.4. Given the acceptance criteria for prototype tests, which does not permit

device failure, median capacity will be underestimated by prototype testing, and perhaps by a wide margin. Further, the loss of horizontal stiffness in one isolator due to excessive displacement does not compromise the lateral stiffness of the isolation system, and so the median capacity of an isolation *system*, as judged by prototype testing of individual isolators for coexisting demands of displacement D_{50} and maximum axial loads, is likely conservatively biased, with the resultant risk being overestimated.

The logarithmic standard deviation β is a composite parameter, accounting for uncertainties in the isolation-system displacement capacity due to the device-to-device variability and differences between the field conditions and those assumed for analysis and device testing. Although a fragility function is used to describe the displacement capacity of the isolation system, those uncertainties in the response not addressed by the seismic displacement demand curve are included in β. The logarithmic standard deviation β is computed as

$$\beta = \sqrt{\beta_d^2 + \beta_c^2} \tag{C.1}$$

where β_d is the dispersion in the displacement demand and β_c is the dispersion in the displacement capacity. Dispersions β_d and β_c are calculated using the variables listed in Table C.1, which is adapted from EPRI (1994), and similar to the presentation in EPRI (2018).

Table C.1. Variables affecting demand and capacity (from EPRI (1994))

Demand	Capacity
1. Ground motion **2. Modeling** 3. Damping 4. Mode combination 5. Input time series 6. Foundation-structure interaction 7. Earthquake component combination	8. Strength 9. Inelastic energy absorption

C.2.2 Variability in demand

C.2.2.1. Introduction

Dynamic analysis of a base-isolated building is more straightforward and accurate than that for a conventional nuclear power plant (NPP) structure because response is dictated by the behavior of the seismic isolation system, whose materials (e.g., rubber, lead, stainless steel) and devices are well characterized, and the manufacturing of isolators and dampers is of high quality. The isolation-system

displacement response is accurately described using two horizontal modes, which is taken advantage of herein. Therefore, the demand-related discussion below focuses solely on the horizontal displacement response of the seismic isolation system.

Many of the variables listed in EPRI (1994) do not apply to the fragility analysis of an isolation system; these are numbered 3 through 9 in Table C.1. Descriptions of these variables can be found in Section 3 of EPRI (1994). The damping ratio (energy dissipated per cycle, #3) of isolators and VDDs is confirmed by prototype and production testing, variability is expected to be very small in production devices, based on US non-nuclear experience, and the force-displacement hysteresis (or damping) is included explicitly in the dynamic analysis. Importantly, since an isolation system will generally be composed of 10s to 100s of isolators and VDDs, system variability will be smaller than that of an individual device. Uncertainty associated with modal combinations (#4) is negligible because isolation-system response is dominated by one mode in each horizontal direction. Variability in the input time series (#5) is explicitly accounted for in the probabilistic demand curve using the acceleration time series ensemble. The variability in foundation-structure interaction (#6) is not considered because soil-structure-interaction is of no importance for isolated nuclear structures because its frequency is well removed from that of the supporting soil domain (Lal *et al*. 2024). Combining responses (#7) from shaking components (e.g., H1 and H2) is explicitly performed time step by time step and its variability is accounted for in the probabilistic demand curve. Variables numbered 8 and 9 in Table C.1 are described in Section C.2.3.

Variability in ground motion (#1) and modeling of isolator, damper, and structure (#2), bolded in Table C.1, affect the horizontal displacement demand, and must be addressed. The accuracy of modeling of the isolation system is related to the identification of its mechanical properties and supported mass, and uncertainty in the fidelity of the model[24]. Accordingly, the dispersion in the displacement demand β_d is associated with four sources and is calculated as:

$$\beta_d = \sqrt{\beta_{gm}^2 + \beta_i^2 + \beta_m^2 + \beta_f^2} \tag{C.2}$$

where β_{gm}, β_i, β_m, and β_f are the dispersions in the displacement demand due to the uncertainty and/or variability in ground motion, mechanical properties of the isolation system, distribution of mass in the isolated superstructure, and model fidelity, respectively.

[24] Uncertainty in fidelity of the model addresses the uncertainty in the model itself rather than its parameters: mode shape uncertainty per EPRI (2018)).

Dispersions are derived below for nonlinear systems, which include all isolation systems listed in Table 4.4, aside from System 1, which can be accurately modeled using a linear spring and a dashpot in parallel, with a damping coefficient that is independent of frequency, temperature, and displacement. Systems 2 and 6 of Table 4.4, which include 1D and 3D VDDs, respectively, are nonlinear, noting that the response of the 3D viscoelastic damper of system 6 is dependent on frequency, temperature, and displacement. There are insufficient data from which to derive a default dispersion for linear systems, which will be smaller than those for nonlinear systems. The dispersions developed for nonlinear systems can be applied to linear systems.

C.2.2.2. Derivation of dispersions

Variability in isolator displacement response[25] due to ground motion is due to the difference between the distribution of earthquake shaking and the inputs used for dynamic analysis. Herein, ground motions are matched to a target UHRS, which is developed by probabilistic seismic hazard assessment and addresses both variability and uncertainty in the calculation of spectral demands at each annual frequency of exceedance.

The dispersion in the horizontal displacement response of the isolation system due to ground motion is computed by parsing β_{gm} into β_0 and β_{mm} as:

$$\beta_{gm} = \sqrt{\beta_0^2 + \beta_{mm}^2}$$

where β_0 is the dispersion associated with analysis using spectrally matched horizontal motions and β_{mm} is the additional dispersion due to variability in the two horizontal components around the geometric mean (see Section A.4), denoted β_{mm}.

Equation C.2 can then be rewritten as:

$$\beta_d = \sqrt{\beta_0^2 + \beta_{mm}^2 + \beta_i^2 + \beta_m^2 + \beta_f^2} \quad \text{(C.3)}$$

Two sources of data were used to develop β_0 and β_{mm}. Data generated in the study that supported the writing of this report is used to determine β_0, building on the data presented in Huang *et al*. (2009, 2013). The data of Huang *et al*. (2009, 2013) is used to determine β_{mm}, for which a median of 1.3 and a logarithmic standard deviation of 0.13 was used to define the ratio of maximum to geomean spectral demands. These

[25] Variability in the vertical-to-horizontal V/H ratio per EPRI (2018), which supersedes the recommendations of EPRI (1994), is not considered here because it does not affect the horizontal displacement response of an isolation system.

studies used 30 sets of ground motions per bin to ensure that the sample dispersion approximates the population dispersion. (Eleven sets of motions can be used to ensure that the sample mean approximates the population mean.)

Huang *et al.* (2009, 2013) considered three sites of very different seismic hazard: 1) Eastern United States (EUS), North Anna, Virginia, 2) Central and Eastern United States (CEUS), Vogtle, Georgia, and 3) Western United States (WUS), Diablo Canyon, California. The ground motions developed for analysis were consistent with a design response spectrum (DRS) and 150% DRS for an SDC-5 nuclear power plant. All the input motions included two horizontal and one vertical components: see Huang *et al.* (2009, 2013) for details.

The Huang *et al*. studies utilized ground motions matched to a geometric mean UHRS. Thirty seed ground motion triplets were first selected from recorded ground motions in the PEER database. The two horizontal components in the triplet, H1 and H2, were then separately matched to the target geometric mean UHRS using the process described in Appendix A, producing two different acceleration times series: the G0 motions introduced next.

Huang *et al.* generated 4 datasets: 1) G0, spectrum compatible ground motions, best estimate model of the isolation system, 2) M0, maximum-minimum (max-min) ground motions, best estimate model of the isolation system, 3) M1, max-min ground motions, varied mechanical properties of the isolation system (± 10% of best estimate), and 4) M2, max-min ground motions, varied mechanical properties of the isolation system (± 20% of best estimate). The max-min ground motions for analysis set M0, M1, and M2 were generated by Huang *et al.* using maximum direction spectra, as introduced in Section A.4.

Table C.2 through Table C.4 present the median displacements and logarithmic standard deviations, extracted from Huang *et al.* (2013), for the three sites, different isolation systems, DRS and 150% DRS shaking, together with reference to specific tables in that paper. (The subscripts to θ and β in these tables denote the analysis sets.)

Table C.2. Compilation of data from Table III of Huang *et al.* (2013), Eastern United States, North Anna

Model[1]	DRS shaking								150% DRS shaking							
	θ_{G0} (mm)	θ_{M0} (mm)	θ_{M1} (mm)	θ_{M2} (mm)	β_{G0}	β_{M0}	β_{M1}	β_{M2}	θ_{G0} (mm)	θ_{M0} (mm)	θ_{M1} (mm)	θ_{M2} (mm)	β_{G0}	β_{M0}	β_{M1}	β_{M2}
LR_T2Q3	31	35	35	35	0.1	0.12	0.12	0.13	43	50	50	50	0.13	0.13	0.14	0.14
LR_T3Q3	35	40	40	40	0.11	0.13	0.13	0.14	50	58	58	58	0.13	0.17	0.17	0.18
LR_T4Q3	37	43	43	43	0.11	0.14	0.15	0.15	52	63	63	62	0.12	0.17	0.17	0.17
FP_T2Q3	9.4	11	11	11	0.18	0.25	0.24	0.25	18	23	23	23	0.19	0.23	0.23	0.25
FP_T3Q3	10	12	12	12	0.2	0.24	0.24	0.24	19	24	24	24	0.2	0.23	0.23	0.24
FP_T4Q3	11	13	13	13	0.21	0.23	0.23	0.24	20	25	25	25	0.21	0.23	0.23	0.25
LDR_T2	61	70	70	69	0.12	0.1	0.1	0.1	92	105	105	104	0.12	0.1	0.1	0.1
LDR_T3	63	72	72	72	0.11	0.1	0.1	0.1	94	109	109	108	0.11	0.1	0.1	0.1
LDR_T4	63	73	73	73	0.12	0.12	0.12	0.12	95	110	110	110	0.12	0.12	0.12	0.12

1. LDR = low damping rubber, LR = lead-rubber, FP = Friction Pendulum; T* =* second period, Q* = zero-displacement force-intercept normalized by supported weight

Table C.3. Compilation of data from Table V of Huang *et al.* (2013), Central and Eastern United States, Vogtle

Model[1]	DRS shaking								150% DRS shaking							
	θ_{G0} (mm)	θ_{M0} (mm)	θ_{M1} (mm)	θ_{M2} (mm)	β_{G0}	β_{M0}	β_{M1}	β_{M2}	θ_{G0} (mm)	θ_{M0} (mm)	θ_{M1} (mm)	θ_{M2} (mm)	β_{G0}	β_{M0}	β_{M1}	β_{M2}
LR_T3Q3	289	349	348	347	0.13	0.18	0.18	0.19	467	558	557	555	0.12	0.15	0.15	0.16
LR_T3Q6	204	264	263	263	0.16	0.24	0.23	0.24	368	456	455	454	0.15	0.21	0.21	0.22
LR_T4Q3	227	274	274	274	0.13	0.2	0.2	0.2	352	425	426	427	0.11	0.18	0.18	0.18
LR_T4Q6	195	238	238	238	0.15	0.23	0.23	0.23	309	373	374	374	0.16	0.23	0.23	0.23
FP_T3Q3	246	303	303	303	0.14	0.2	0.19	0.2	433	523	523	523	0.12	0.15	0.15	0.15
FP_T3Q6	140	190	190	189	0.21	0.3	0.3	0.31	308	391	391	391	0.18	0.25	0.24	0.25
FP_T4Q3	193	240	240	240	0.15	0.22	0.22	0.22	325	403	403	403	0.12	0.19	0.19	0.19
FP_T4Q6	128	168	168	168	0.20	0.29	0.28	0.29	255	319	319	319	0.18	0.26	0.25	0.26

1. LR = lead-rubber, FP = Friction Pendulum; T* =* second period, Q* = zero-displacement force-intercept normalized by supported weight

Table C.4. Compilation of data from Table X of Huang *et al.* (2013), Western United States, Diablo Canyon

Model[1]	DRS shaking								150% DRS shaking							
	θ_{G0} (mm)	θ_{M0} (mm)	θ_{M1} (mm)	θ_{M2} (mm)	β_{G0}	β_{M0}	β_{M1}	β_{M2}	θ_{G0} (mm)	θ_{M0} (mm)	θ_{M1} (mm)	θ_{M2} (mm)	β_{G0}	β_{M0}	β_{M1}	β_{M2}
LR_T2Q3	488	572	573	576	0.1	0.13	0.13	0.14	792	932	932	936	0.09	0.12	0.12	0.13
LR_T2Q6	401	473	473	472	0.14	0.2	0.2	0.21	678	797	797	798	0.12	0.16	0.16	0.17
LR_T2Q9	338	404	404	405	0.19	0.25	0.25	0.25	595	703	703	702	0.14	0.21	0.21	0.21
LR_T3Q6	494	584	585	585	0.19	0.26	0.25	0.25	862	1039	1039	1041	0.18	0.22	0.22	0.22
LR_T3Q9	404	471	472	472	0.2	0.28	0.28	0.28	729	863	864	865	0.2	0.26	0.26	0.26
LR_T4Q9	418	493	493	495	0.21	0.29	0.29	0.29	779	951	951	950	0.19	0.24	0.24	0.24
FP_T2Q3	492	571	571	572	0.11	0.14	0.14	0.14	819	953	953	953	0.11	0.13	0.13	0.13
FP_T2Q6	392	461	461	461	0.15	0.22	0.21	0.22	686	800	801	801	0.13	0.17	0.17	0.17
FP_T2Q9	321	385	385	384	0.21	0.26	0.26	0.27	593	697	697	697	0.16	0.22	0.22	0.22
FP_T3Q6	471	555	556	557	0.21	0.28	0.27	0.28	852	1006	1006	1007	0.18	0.23	0.23	0.23
FP_T3Q9	374	442	443	443	0.23	0.29	0.29	0.3	707	832	833	834	0.21	0.28	0.27	0.27
FP_T4Q9	382	462	462	463	**0.24**	0.31	0.31	0.31	756	925	925	928	0.2	0.24	0.23	0.24

1. LR = lead-rubber, FP = Friction Pendulum; T* =* second period, Q* = zero-displacement force-intercept normalized by supported weight

Derivation of β_0

The maximum dispersion in the horizontal displacement response of an isolation system for the G0 dataset, computed using data from Table C.2 through Table C.4, is 0.24 for the nonlinear systems: see the highlighted cell in Table C.4.

Analysis of the data generated in support of the writing of this report is focused on one site, two soil conditions (BC and CD per Section 4.6), six horizontal isolation systems (per Table 4.4), and a broader range of earthquake shaking than that considered in Huang *et al*., but also using spectrally matched motions, yielded a slightly greater maximum dispersion, as explained next.

Per Section 5.2, seismic hazard curves are parsed into 11 bins spanning 4 decades in MAFE. Dynamic analysis is performed for each ground motion pair (GM 1 to 30) in each bin to compute a maximum resultant horizontal displacement for isolation systems 1 through 6 in Table 4.4. The logarithmic standard deviation of the maximum resultant horizontal displacement is calculated for each bin. The average of the values in bins 5 through 8, is reported in Table C.5. The dispersions for bins 1 through 4 are set aside because a) the displacements are very small and of no significance to the risk calculation, and b) production testing of isolators and dampers will preclude device failure at small displacements. The dispersions for bins 9, 10, and 11 are set aside because a) the risk contributions are small for the associated AFE, and b) the values are smaller than those in the mid-range of the 11 bins, for the nonlinear systems: a conservatism. (Detailed results are tabulated in the annex to this appendix: see Table C.11 to Table C.22.) Dispersions are listed for BC and CD soils. The dispersions are the lowest for the lightly damped linear system (1) and highest for the nonlinear systems (2, 4, and 5). The dispersions for the heavily damped linear system (3) fall *midway* between those for the lightly damped linear and the nonlinear systems.

Table C.5. Values of β_0 for isolation systems 1 through 6 of Table 4.4

	Isolation system					
	1	2	3	4	5	6
BC soil	0.10	0.21	0.17	0.19	0.20	0.13
CD soil	0.10	0.22	0.19	0.28	0.24	0.17

Based on the data presented in Table C.5, β_0 is set equal to 0.28, in the absence of project- and site-specific calculations to support the use of a lower value, noting that such calculations might support the use of a substantially smaller value for a) linear isolation systems, and b) nonlinear systems on firm soil

or rock sites. Project-specific estimates of β_0 should be made with results of analysis using 30 sets of ground motions.

Derivation of β_{mm} and β_i

Huang *et al*. (2009, 2013) characterized the variability in the horizontal displacement response of an isolation system due to both ground motion orientation and the mechanical properties of the isolation system: the M2 dataset.

The mechanical properties of the isolation systems considered by Huang *et al.* were allowed to vary by up to 20% from the values used for analysis and design, which is the limit set in Section 9.2.2.1 of ASCE/SEI 43-19 (ASCE 2021) and Section 3.4.2.1 of this report. The mechanical properties of the isolation system were assumed to be distributed normally with a coefficient of variation (i.e., the ratio of the standard deviation to the mean) of 0.10 (Huang *et al.* 2009).

The additional dispersion introduced using max-min components of horizontal ground shaking for analysis (instead of spectrally matched components) and consideration of variability in the mechanical properties of the isolation system is computed using the data from Table C.2 through Table C.4 for the nonlinear systems. For each row in these tables, the value of $\sqrt{\beta_{mm}^2 + \beta_i^2} = \sqrt{\beta_{M2}^2 - \beta_{G0}^2}$ is calculated for DBE and 150% DBE shaking. The average of the 52 values is 0.14, and it is used hereafter.

Adjustment to mean displacement demand and derivation of associated dispersion β_r

The analysis performed in this report is analogous to analysis set G0 per Huang *et al.* (2013), that is, analysis of a best estimate model of an isolation system using ground motions spectrally matched to a geometric mean spectrum. Accordingly, adjustments are made to the displacement demand curve, based on the results of response-history analysis using spectrally matched motions, to partly account for the variability in ground shaking around the geometric mean and in the properties of the isolation system: see Section D.3. The remaining variability is addressed via the logarithmic standard deviation assigned to the fragility function.

The average values of the ratio of $\theta_{M2} / \theta_{G0}$ for DRS and 150% DRS shaking presented in Table C.2 through Table C.4 are reported in Table C.6. The average value of the ratio is 1.2. The logarithmic standard deviation of the distribution of the ratio, β_r, is 0.05, and it is included in the fragility function as follows:

$$\beta_d = \sqrt{\beta_0^2 + \beta_{mm}^2 + \beta_i^2 + \beta_m^2 + \beta_f^2} = \sqrt{\beta_0^2 + [(\beta_{M2}^2 - \beta_{G0}^2) + \beta_r^2] + \beta_m^2 + \beta_f^2} \quad \text{(C.4)}$$

Derivation of mass uncertainty, β_m

In-service differences from design assumptions, including mass of the isolated superstructure and its distribution in plan, could alter the horizontal displacement response of the isolation system. However, the changes are expected to be very small because a) much of the reactor building mass is reinforced concrete, for which the as-built construction should closely follow the design drawings, b) the masses of large pieces of equipment will be included in the numerical model used for analysis, and c) the isolation system will be designed to minimize torsional response. The dispersion in the displacement response associated with uncertainty in the distribution of mass of the isolated superstructure, β_m, is assumed to be 0.05.

Derivation of model fidelity uncertainty, β_f

Per Section 5.4.3.2 of EPRI (2018), model fidelity uncertainty should be in the range of 0.05 to 0.15, noting that the "…former value [= 0.05] is applicable to structures whose responses are dominated by fundamental modes with simple mode shapes..." Because the response of a seismically isolated building will be dominated by its isolated modes, each with simple shape, the model fidelity uncertainty is set here to the bottom of the range, namely, 0.05.

C.2.2.4 Recommendations for β_d

The uncertainty in demand, β_d, per Equation C.4 is

$$\begin{aligned}\beta_d &= \sqrt{\beta_0^2 + (\beta_{M2}^2 - \beta_{G0}^2) + \beta_r^2 + \beta_m^2 + \beta_f^2} \\ &= \sqrt{0.28^2 + (0.14^2) + 0.05^2 + 0.05^2 + 0.05^2} \\ &= 0.33\end{aligned}$$

Table C.6 Ratio of medians, θ_{M2} and θ_{G0}, for different sites and isolation systems, and two levels of shaking, using data from Table C.2 through Table C.4

(a) Eastern United States, North Anna		
Model	θ_{M2}/θ_{G0}, DRS shaking	θ_{M2}/θ_{G0}, 150% DRS shaking
LR_T2Q3	1.1	1.2
LR_T3Q3	1.1	1.2
LR_T4Q3	1.2	1.2
FP_T2Q3	1.2	1.3
FP_T3Q3	1.2	1.3
FP_T4Q3	1.2	1.3
LDR_T2	1.1	1.1
LDR_T3	1.1	1.1
LDR_T4	1.2	1.2
(b) Central and Eastern United States, Vogtle		
Model[1]	θ_{M2}/θ_{G0}, DRS shaking	θ_{M2}/θ_{G0}, 150% DRS shaking
LR_T3Q3	1.2	1.2
LR_T3Q6	1.3	1.2
LR_T4Q3	1.2	1.2
LR_T4Q6	1.2	1.2
FP_T3Q3	1.2	1.2
FP_T3Q6	1.4	1.3
FP_T4Q3	1.2	1.2
FP_T4Q6	1.3	1.3
(c) Western United States, Diablo Canyon		
Model[1]	θ_{M2}/θ_{G0}, DRS shaking	θ_{M2}/θ_{G0}, 150% DRS shaking
LR_T2Q3	1.2	1.2
LR_T2Q6	1.2	1.2
LR_T2Q9	1.2	1.2
LR_T3Q6	1.2	1.2
LR_T3Q9	1.2	1.2
LR_T4Q9	1.2	1.2
FP_T2Q3	1.2	1.2
FP_T2Q6	1.2	1.2
FP_T2Q9	1.2	1.2
FP_T3Q6	1.2	1.2
FP_T3Q9	1.2	1.2
FP_T4Q9	1.2	1.2

C.2.3 Variability in capacity

The two variables associated with capacity in Table C.1 are strength and inelastic energy absorption (or damping). These variables were proposed for conventional reinforced concrete nuclear construction and not for seismically isolated nuclear structures.

The capacity of a seismic isolator and/or a damper, measured in terms of force-displacement hysteresis, is confirmed by prototype testing of each type and size of device planned for construction, and production testing of every device prior to shipment to the construction site. A lower bound on median capacity is established by prototype testing. There may be device-to-device variability, but for an isolation system which is comprised of many devices, the system-level variability is expected to be insignificant. Accordingly, β_c is set equal to 0.05. Variations in mechanical properties are addressed in β_i above.

C.2.4 Composite logarithmic standard deviation, β

The value of the composite dispersion, $\beta = \sqrt{\beta_d^2 + \beta_c^2}$ for all isolation systems, in lieu of project- and site-specific calculations is:

$$\beta = \sqrt{0.33^2 + 0.05^2} = 0.34$$

The recommended default value for β, is based on the calculation above, rounded to the nearest 0.05, namely, β = 0.35. The calculations presented hereafter and in Section 5 use β = 0.35 for all sites and isolation systems, although project- and site-specific derivations of dispersions, such as those presented in this section will likely support the use of a substantially smaller value for a) lightly damped linear isolation systems, and b) non-linear systems on firm soil or rock sites.

C.3 Performance Calculations for Other Seismic Isolation Systems

C.3.1 Introduction

Section 5 of the report presents a process to compute the required median displacement capacity of an isolation system given a user-specified target performance goal. The process was demonstrated for systems 1 and 3 per Table 4.4 and Table 4.5: a 2-second linear system, and a 2-second linear system and nonlinear FVDs, respectively. In this section, results are provided for isolation systems 2, 4, 5, and 6 per Table 4.4 and Table 4.5: a 2-second nonlinear system, a 2-second nonlinear system with nonlinear FVDs, a 3-second nonlinear system, and a 3D linear system composed of spring isolators and 3D viscoelastic dampers, respectively. The horizontal displacement response of the 3D hybrid isolation system shown in Figure 2.3h

would be identical to that of the 2-second nonlinear system and so is not analyzed.

Performance-related calculations are presented for the Clinch River site, and the BC and CD soils described in Section 5.2. Seismic hazard data are presented in Figure 5.4 and Figure 5.8 and are not repeated here.

C.3.2 Supplemental performance calculations

The 2DOF model of Section 4.5 was analyzed per Section 5 to generate seismic displacement demand curves for isolation systems 2, 4, 5, and 6. Figure C.1 presents the demand curves for BC and CD soils, and all six isolation systems. The choice of isolation system has a significant effect on the displacement demand curve, as evident in Figure C.1.

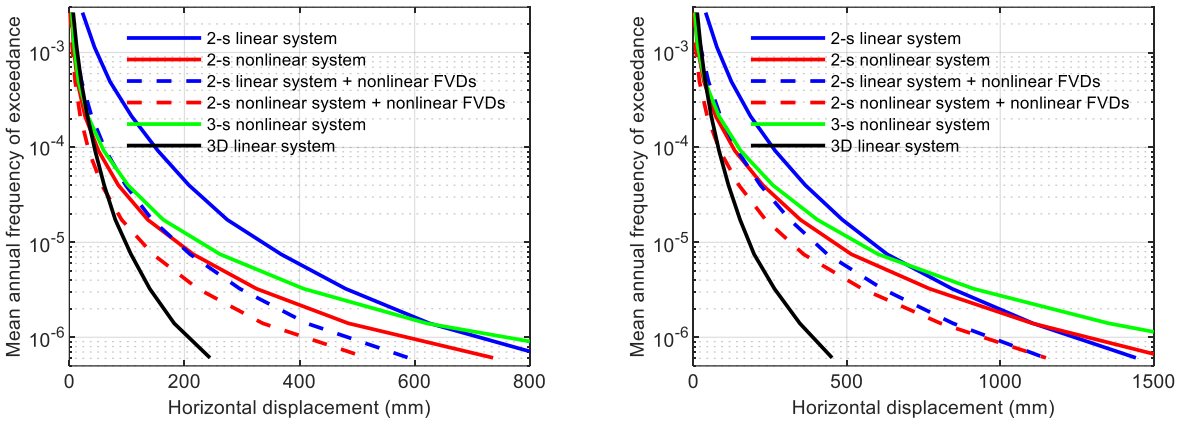

(a) BC soil (b) CD soil

Figure C.1. Displacement demand curves, 6 isolation systems, Clinch River, BC and CD soils

Table C.7 presents risk calculations, including results from Table 5.1. The default composite logarithmic standard deviation, β, of 0.35 is used for the calculations. The median displacement capacities *assumed* for the isolators and dampers are given in the second column of the table, leading to the risk numbers presented in the last two columns. Table C.8 presents the required median displacement capacity of the six isolation systems to achieve different target performance goals at the Clinch River site for BC and CD soils.

C.4 Sensitivity of the Calculated Risk to the Value of β

Values of β smaller than the recommended default of 0.35 might be justified by project- and isolation-system-specific analysis. To understand the impact of the use of a smaller value of β on the calculated risk, the calculations of Section C.3.2 are repeated for β equal to 0.25 and 0.30. Results are presented in

Table C.9 and Table C.10 for isolation systems 1 through 6 as percentage changes from the values calculated using β = 0.35, rounded to the nearest 5%.

The calculated mean annual frequency of unacceptable performance is not affected in a meaningful way by the value of β in the range considered, with appreciable changes only observed for the short period, heavily damped 3D isolation system that could be assigned a β smaller than 0.35 (as β_0 for this system is smaller than 0.28 per Table C.5).

Table C.7. Risk calculations, Clinch River, BC and CD soils, β = 0.35

Isolation system[1]		Median displacement capacity (mm)	MAF of unacceptable performance	
			BC site	CD site
1	2-sec linear system	200	6.6×10^{-5}	2.4×10^{-4}
		250	3.6×10^{-5}	1.5×10^{-4}
2	2-sec nonlinear system	200	1.0×10^{-5}	5.8×10^{-5}
		250	6.5×10^{-6}	4.0×10^{-5}
3	2-sec linear system + nonlinear FVDs	200	1.1×10^{-5}	6.0×10^{-5}
		250	6.3×10^{-6}	3.8×10^{-5}
4	2-sec nonlinear system + nonlinear FVDs	200	4.5×10^{-6}	2.8×10^{-5}
		250	2.7×10^{-6}	1.9×10^{-5}
5	3-sec nonlinear system	300	6.7×10^{-6}	3.6×10^{-5}
		350	4.9×10^{-6}	2.8×10^{-5}
6	3D linear system, $T_{iso,h}$ = 1.1 s	50	9.7×10^{-5}	3.7×10^{-4}
		100	1.5×10^{-5}	8.2×10^{-5}

1. Isolation systems are numbered 1 through 6 per Table 4.4 and Table 4.5

Table C.8. Median displacement capacity, D_{50}, to achieve different TPGs, Clinch River, BC and CD soils, $\beta = 0.35$

		Median displacement capacity[1], D_{50} (mm)					
		BC soil			CD soil		
		Target performance goal			Target performance goal		
Isolation system per Table 4.5[2]		1×10^{-4}	4×10^{-5}	2×10^{-5}	1×10^{-4}	4×10^{-5}	2×10^{-5}
1	2-sec linear system	170	242	310	294	424	542
2	2-sec nonlinear system	54	94	140	140	248	360
3	2-sec linear isolation system + nonlinear FVDs	68	110	152	152	244	334
4	2-sec nonlinear system + nonlinear FVDs	36	62	94	90	162	240
5	3-sec nonlinear system	62	112	168	160	284	416
6	3D linear system, $T_{iso,h} = 1.1$ s	50	70	90	92	132	170

1. The risk calculations for different TPGs presented in this table use the same demand curve: i.e., the curve attached to motions matched to a target spectrum corresponding to a return period of 25,000 (TPG = 4 × 10-5). The risk numbers for TPGs other than 4 × 10-5 are approximate.
2. Isolation systems are numbered 1 through 6 per Table 4.4 and Table 4.5

Table C.9. Risk calculations, Clinch River, BC and CD soils, $\beta = 0.25$, % differences in MAF calculated using $\beta = 0.35$ per Table C.7

Isolation system[1]		Median displacement capacity (mm)	Percentage differences	
			BC site	CD site
1	2-sec linear system	200	-20	-15
		250	-20	-15
2	2-sec nonlinear system	200	-10	-5
		250	-10	-10
3	2-sec linear system + nonlinear FVDs	200	-20	-10
		250	-20	-10
4	2-sec nonlinear system + nonlinear FVDs	200	-15	-5
		250	-15	-10
5	3-sec nonlinear system	300	-10	-5
		350	-10	-10
6	3D linear system, $T_{iso,h} = 1.1$ s	50	-15	-10
		100	-35	-15

1. Isolation systems are numbered 1 through 6 per Table 4.4 and Table 4.5

Table C.10. Risk calculations, Clinch River, BC and CD soils, $\beta = 0.30$, % differences in MAF calculated using $\beta = 0.35$ per Table C.7

Isolation system[1]		Median displacement capacity (mm)	Percentage differences	
			BC site	CD site
1	2-sec linear system	200	-10	-10
		250	-10	-5
2	2-sec nonlinear system	200	-5	-5
		250	-5	-5
3	2-sec linear system + nonlinear FVDs	200	-10	-5
		250	-10	-5
4	2-sec nonlinear system + nonlinear FVDs	200	-5	-5
		250	-10	-5
5	3-sec nonlinear system	300	-5	-5
		350	-5	-5
6	3D linear system, $T_{iso,h}$ = 1.1 s	50	-10	-5
		100	-15	-5

1. Isolation systems are numbered 1 through 6 per Table 4.4 and Table 4.5

C.5 Truncation of the isolation-system fragility function

Figure C.2a presents the displacement demand curve for the 2-second linear isolation system with nonlinear fluid viscous dampers: isolation system 3 per Table 4.4 and Table 4.5, Clinch River site, and BC soil. Figure C.2b and Figure C.2c present a fragility function with a median displacement (θ) of 110 mm and the corresponding risk density plot, respectively. A value of $D_{50} = 110$ mm achieves the TPG of 4×10^{-5} per Table C.8. The bar chart in Figure C.2c enables a reader to disaggregate the total risk into displacement bins, which in turn can be associated with mean annual frequencies of hazard per Figure C.2c.

Production testing of isolators and VDDs per Section 6 requires that the tested units suffer no damage for DB shaking. Recognizing that the isolators and VDDs will have significant margin on no damage (and VDDs must suffer no damage for prototype testing at displacement D_{50}), the fragility functions of Figure C.2b are truncated for the purpose of this calculation at a displacement of $0.67D_{50}$ (= 74 mm), namely, the probability of failure at a displacement less than or equal to 74 mm is zero. Figure C.2d and Figure C.2e present the truncated fragility function and the corresponding risk-density plot.

Figure C.3 presents similar calculations for CD soil, noting that the median displacement capacity required to achieve the TPG at the CD soil site is 244 mm per Table C.8.

Truncating the fragility functions at $0.67D_{50}$ reduces the risk from 4×10^{-5} to 3.6×10^{-5} for both BC and CD soils. For a target performance goal of 4×10^{-5}, the median displacement capacities of 110 mm and 244 mm for BC and CD soils (see Table 5.2), respectively, are reduced to 102 and 225 mm, respectively, if the fragility function is truncated at $0.67D_{50}$.

Although not part of the pathway recommended in this report, truncating the isolation-system fragility function based on the required outcomes of production testing of isolators and VDDs is technically sound.

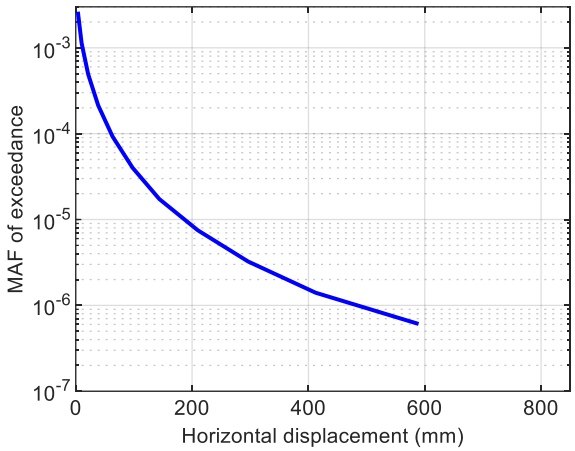

(a) displacement demand curve

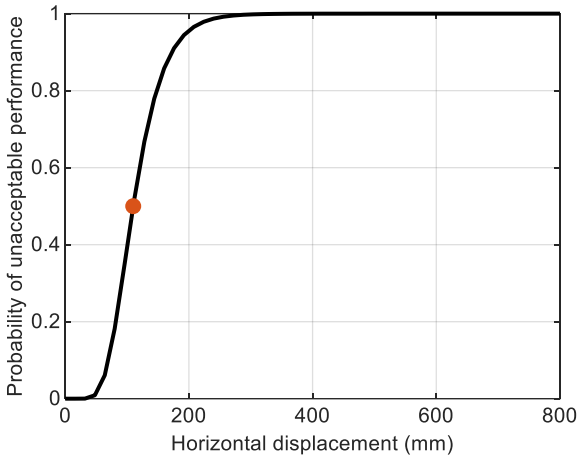

(b) fragility function, 110 mm

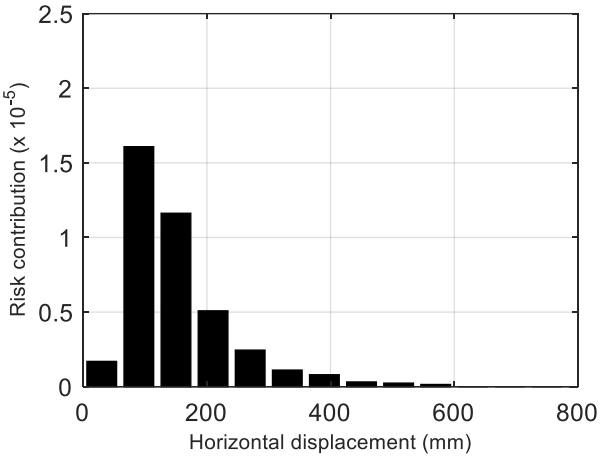

(c) risk density, fragility function of Figure C.2b

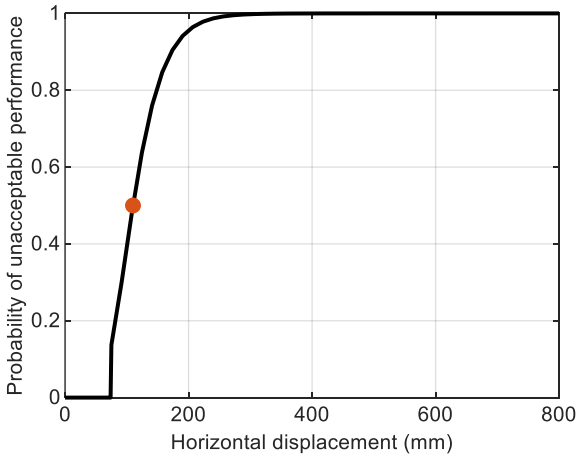

(d) truncated fragility function, $\theta = 110$ mm

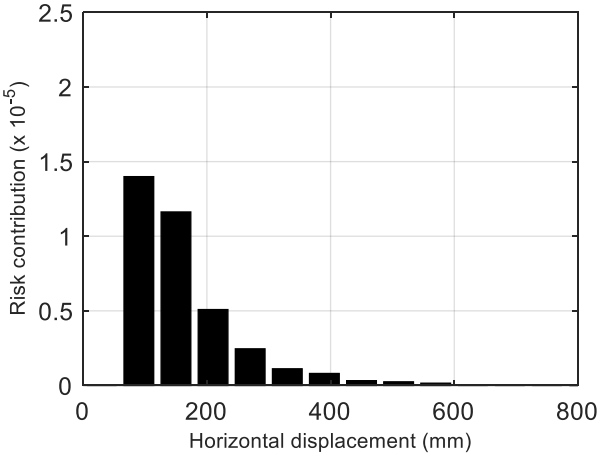

(e) risk density, fragility function of Figure C.2d

Figure C.2. Risk calculations, truncated fragility function, 2-second linear isolation system with nonlinear FVDs, BC soil

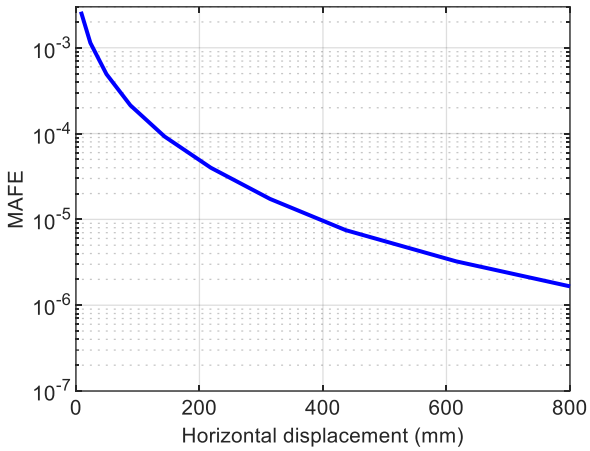

(a) displacement demand curve

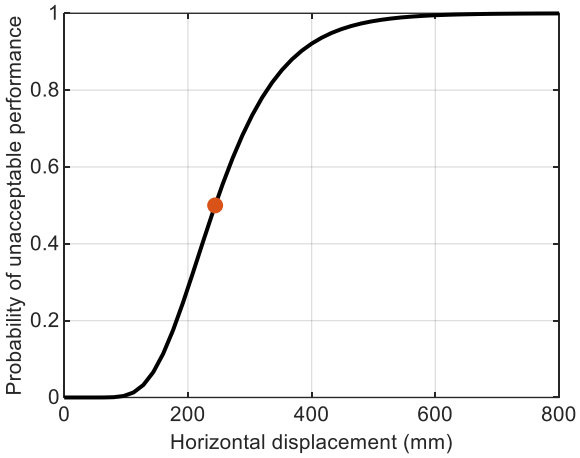

(b) fragility function, $\theta = 244$ mm

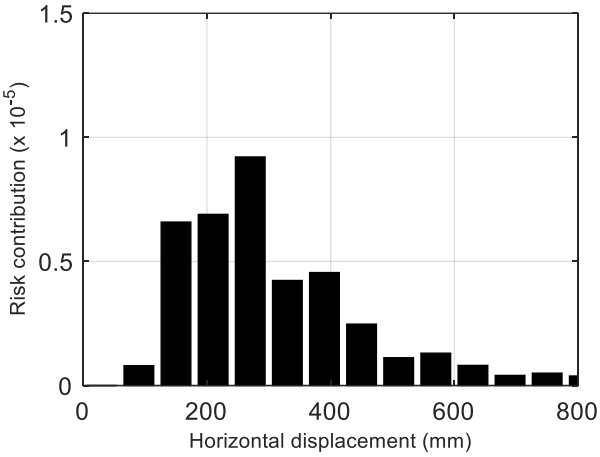

(c) risk density, fragility function of Figure C.3b

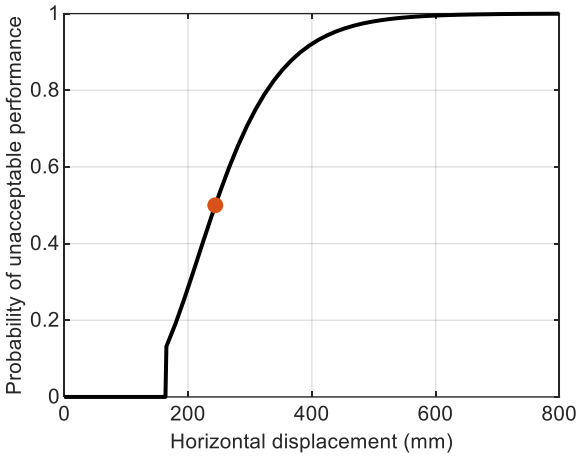

(d) truncated fragility function, $\theta = 244$ mm

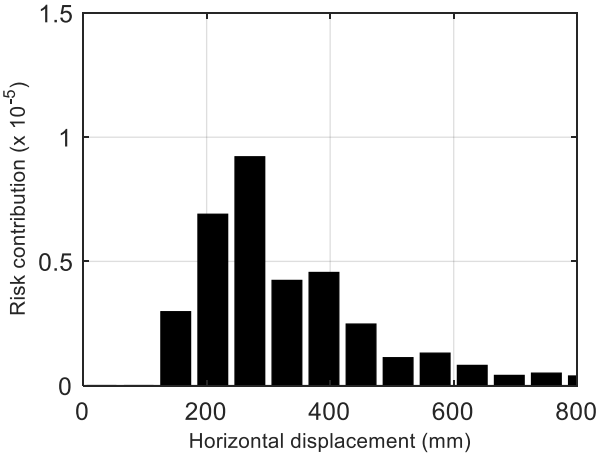

(e) risk density, fragility function of Figure C.3d

Figure C.3. Risk calculations, truncated fragility function, 2-second linear isolation system with nonlinear FVDs, CD soil

C.6 References

American Society of Civil Engineers (ASCE) (2021). "Seismic design criteria for structures, systems, and components in nuclear facilities." ASCE/SEI 43-19, ASCE, Reston, VA.

Baker, J. W., and Cornell, A. C. (2006). "Spectral shape, epsilon and record selection." *Earthquake Engineering and Structural Dynamics*, 35(9), 1077-1095.

Electric Power Research Institute (EPRI) (1994). "Methodology for developing seismic fragilities." TR-103959, EPRI, Palo Alto, CA.

Electric Power Research Institute (EPRI) (2018). "Seismic fragility and seismic margin guidance for seismic probabilistic risk assessments." 3002012994, EPRI, Palo Alto, CA.

Huang, Y.-N., Whittaker, A. S., and Luco, N. (2008). "Maximum spectral demands in the near-fault region." *Earthquake Spectra*, 24(1), 319-341.

Huang, Y. N., Whittaker, A. S., Kennedy, R. P., and Mayes, R. L. (2009). "Assessment of base-isolated nuclear structures for design and beyond-design basis earthquake shaking."MCEER-09-0008, University at Buffalo, Buffalo, NY.

Huang, Y. N., Whittaker, A. S., Kennedy, R. P., and Mayes, R. L. (2013). "Response of base-isolated nuclear structures for design and beyond-design basis earthquake shaking." *Earthquake Engineering and Structural Dynamics*, 42(3), 339-356.

Lal, K. M., Whittaker, A. S., Vahdani, S., Kosbab, B. D., Shirvan, K., and Parsi, S. S. (2024). "Considerations of soil-structure-interaction for seismically isolated nuclear reactor buildings." *MCEER-24-0003*, University at Buffalo, Buffalo, NY

Annex to Appendix C: Derivation of β_0

Table C.11 through Table C.16 present the calculation of the dispersions for isolation systems 1 through 6 of Table 4.4 for BC soil. Table C.17 to Table C.22 present the companion calculations for CD soil. Isolation system 1 is a lightly damped linear system. Isolation systems 3 and 6 are heavily damped linear systems, noting that the model used to analyze system 6 is greatly simplified. Isolation systems 2, 4, and 5 are nonlinear systems.

In each of these tables, the maximum resultant horizontal displacements (units of mm) is listed for each ground motion (GM) and each bin. The second-to-last line in the tables presents the average maximum resultant displacement for each bin. The last line in the tables presents the logarithmic standard deviation of the 30 displacements in the bin.

Table C.11. Calculation of β_0, system 1, 2-second linear system, 5% damping, BC soil

	Bin										
	1	2	3	4	5	6	7	8	9	10	11
GM	Maximum resultant displacement (mm)										
1	17	32	52	80	114	154	204	273	356	464	623
2	20	38	61	93	133	180	237	318	415	541	726
3	17	32	52	79	112	152	200	269	351	457	614
4	20	37	60	92	131	177	234	314	410	534	716
5	20	38	61	93	133	180	237	318	415	540	725
6	19	37	60	91	130	175	231	310	405	527	708
7	19	37	60	92	130	176	232	312	407	530	711
8	18	34	54	83	118	160	211	283	370	482	646
9	21	39	64	98	139	188	248	332	433	564	758
10	17	32	52	79	113	152	201	269	352	458	615
11	18	35	56	85	122	164	217	291	380	495	664
12	20	37	60	92	131	177	234	314	410	534	717
13	20	39	63	96	136	184	243	326	426	555	744
14	18	34	55	84	119	161	212	285	372	484	650
15	19	37	60	91	130	175	231	310	405	527	708
16	19	36	58	88	126	170	224	301	393	512	687
17	20	38	61	94	133	180	238	319	416	542	728
18	17	33	54	82	117	158	208	279	365	475	638
19	23	44	71	109	155	209	276	370	483	630	845
20	18	34	54	83	118	160	211	283	369	481	646
21	17	32	52	80	113	153	202	271	354	461	619
22	22	41	67	103	146	198	261	350	456	595	798
23	17	32	51	78	111	150	198	266	347	452	607
24	18	34	56	85	121	164	217	290	379	494	663
25	17	32	52	79	113	153	202	271	353	460	617
26	21	39	63	97	138	187	246	330	431	562	754
27	23	43	70	106	151	205	270	362	473	616	826
28	18	34	55	85	120	163	215	288	376	490	658
29	23	44	71	108	154	209	275	369	482	628	842
30	20	39	63	96	136	184	243	326	425	554	743
Average	19	36	59	90	128	173	229	307	400	521	700
β_0	0.10	0.10	0.10	0.10	0.10	0.10	0.10	0.10	0.10	0.10	0.10

Table C.12. Calculation of β_0, system 2, 2-second sliding system, BC soil

	Bin										
	1	2	3	4	5	6	7	8	9	10	11
GM	Maximum resultant displacement (mm)										
1	4	6	13	31	56	94	143	211	304	435	623
2	4	7	10	29	62	107	164	244	346	481	682
3	3	7	12	21	34	53	81	121	183	317	522
4	3	5	12	26	49	86	141	222	329	471	681
5	2	5	14	28	49	79	119	173	246	358	566
6	3	6	12	26	47	73	112	179	268	388	570
7	2	4	9	17	37	63	96	170	274	411	657
8	3	5	11	21	38	65	105	175	259	391	590
9	3	6	15	30	57	94	149	228	332	468	683
10	5	9	16	26	37	48	81	136	218	331	501
11	3	6	12	25	41	77	126	200	300	444	657
12	2	5	11	24	47	77	117	167	251	382	585
13	2	9	18	24	40	79	135	215	316	441	681
14	5	8	19	35	57	81	102	130	195	300	469
15	3	7	15	24	41	68	113	183	278	406	604
16	4	6	7	14	29	56	98	159	233	360	560
17	3	5	8	18	33	61	103	170	259	396	650
18	4	7	9	16	33	59	98	160	243	357	528
19	3	8	13	24	51	84	135	209	325	490	743
20	3	7	13	21	37	72	114	166	225	331	528
21	4	7	10	20	31	45	75	133	207	321	511
22	3	5	9	19	34	55	87	147	272	444	706
23	2	5	11	22	37	50	74	129	217	337	510
24	4	6	9	19	38	70	120	193	287	411	609
25	3	5	11	21	46	85	138	221	323	450	631
26	4	7	14	24	36	50	78	126	193	333	573
27	3	5	12	23	46	80	125	198	332	541	843
28	3	5	8	17	36	60	112	199	310	449	647
29	4	5	10	20	40	72	123	198	296	438	677
30	3	6	8	17	44	86	142	220	316	436	622
Ave	3	6	12	23	42	71	114	179	271	404	614
β_0	0.23	0.19	0.24	0.21	0.19	0.22	0.21	0.20	0.18	0.15	0.13

Table C.13. Calculation of β_0, system 3, 2-second linear system with FVDs, BC soil

	Bin										
	1	2	3	4	5	6	7	8	9	10	11
GM	Maximum resultant displacement (mm)										
1	4	10	22	38	62	94	135	193	267	363	508
2	3	10	23	44	73	111	160	229	316	431	601
3	3	8	15	24	38	57	83	121	175	250	375
4	4	11	23	42	68	102	148	212	295	405	571
5	4	12	24	42	65	94	133	186	254	344	482
6	3	9	19	34	57	88	130	188	265	367	520
7	2	6	15	28	46	69	104	158	231	328	474
8	3	6	13	26	47	75	111	164	235	330	472
9	4	11	23	39	60	94	139	203	285	393	555
10	3	7	14	27	46	71	108	162	231	324	463
11	4	10	19	32	49	79	119	179	257	361	519
12	3	10	21	37	60	89	127	183	259	362	519
13	3	8	20	37	63	98	143	206	286	388	540
14	4	11	20	32	47	69	98	139	196	280	407
15	4	8	15	30	52	82	123	182	258	357	507
16	2	6	14	27	44	70	103	149	207	298	438
17	2	7	14	28	49	77	116	171	241	335	476
18	3	8	17	31	49	74	110	162	230	319	454
19	3	8	18	33	54	83	122	184	268	383	558
20	3	7	14	29	51	79	114	161	218	289	397
21	3	8	14	22	36	56	86	133	194	276	405
22	3	8	16	27	44	67	98	146	220	326	492
23	3	7	14	23	37	62	97	148	214	302	435
24	3	7	16	30	52	84	124	182	258	357	506
25	3	8	20	40	69	106	154	220	303	409	566
26	3	8	16	26	41	62	90	131	186	259	396
27	3	10	21	38	61	91	129	183	253	354	506
28	2	7	16	28	47	78	121	183	262	367	522
29	3	9	19	34	57	88	129	188	266	370	532
30	2	8	19	37	62	95	138	199	278	382	539
Ave	3	8	18	32	53	82	120	175	247	344	491
β_0	0.20	0.18	0.19	0.19	0.19	0.18	0.17	0.16	0.15	0.13	0.12

Table C.14. Calculation of β_0, system 4, 2-second sliding system with FVDs, BC soil

	Bin										
	1	2	3	4	5	6	7	8	9	10	11
GM	Maximum resultant displacement (mm)										
1	1	4	8	18	36	62	97	154	229	330	484
2	2	5	7	14	32	64	110	177	265	384	564
3	2	5	10	18	29	43	62	91	133	191	284
4	1	4	9	18	34	58	94	151	234	348	526
5	1	4	10	20	37	61	95	145	211	294	428
6	1	4	9	16	29	50	79	124	192	290	445
7	1	3	6	11	21	39	66	106	159	240	406
8	1	3	6	14	25	38	63	104	171	267	407
9	2	4	8	17	32	56	95	152	236	350	526
10	3	7	11	19	31	45	59	92	144	224	365
11	1	4	8	19	33	50	73	119	193	297	462
12	1	4	8	14	29	53	86	134	197	281	417
13	2	6	12	22	31	45	81	140	223	337	508
14	2	6	13	25	44	67	93	127	165	217	324
15	1	3	10	19	30	45	69	116	186	287	450
16	1	4	7	10	18	31	56	96	158	244	370
17	2	3	6	10	21	38	62	106	173	269	421
18	1	4	8	12	21	39	66	105	165	253	395
19	2	5	11	18	29	51	86	135	204	303	486
20	1	4	8	15	26	36	67	118	183	268	382
21	2	6	8	13	25	39	55	78	122	200	329
22	1	3	6	13	24	42	63	98	148	221	381
23	1	4	7	16	28	43	61	84	118	206	348
24	2	5	7	12	23	40	68	119	195	299	460
25	1	3	6	13	24	47	87	149	235	355	534
26	2	4	11	18	31	45	64	92	135	202	312
27	1	4	9	17	30	53	87	139	207	301	470
28	1	3	7	13	23	38	64	102	180	295	479
29	1	4	8	14	27	46	76	127	202	306	469
30	1	3	8	13	21	45	85	146	227	338	505
Ave	1	4	8	16	28	47	76	121	186	280	431
β_0	0.26	0.23	0.22	0.23	0.20	0.19	0.19	0.20	0.20	0.19	0.17

Table C.15. Calculation of β_0, system 5, 3-second sliding system, BC soil

	Bin										
	1	2	3	4	5	6	7	8	9	10	11
GM	Maximum resultant displacement (mm)										
1	4	6	14	34	63	104	153	223	321	501	806
2	4	9	14	31	72	121	198	323	490	711	1040
3	3	10	16	27	44	70	103	149	244	390	642
4	3	5	14	33	60	102	163	255	375	541	789
5	2	5	15	30	55	91	141	215	320	466	693
6	3	7	12	27	49	85	137	206	329	536	916
7	3	5	10	19	43	72	112	167	234	366	670
8	3	6	12	28	52	75	133	242	404	632	993
9	4	7	14	28	52	92	147	246	398	600	901
10	5	9	16	26	37	58	114	211	338	503	741
11	4	7	14	32	66	110	171	276	421	619	922
12	2	6	12	29	61	107	166	279	436	641	941
13	2	10	24	36	49	102	179	290	437	619	890
14	6	8	19	37	65	99	125	157	229	352	573
15	3	7	18	30	50	86	137	226	353	530	808
16	5	7	8	15	36	74	126	217	351	535	824
17	3	6	8	18	34	58	91	153	269	454	768
18	4	9	10	20	38	73	127	228	394	640	1009
19	3	9	17	34	64	85	114	158	278	447	718
20	3	8	15	25	39	72	129	217	339	522	788
21	5	9	12	24	40	62	89	156	249	372	549
22	3	6	10	26	46	78	124	187	279	451	739
23	3	6	13	28	53	87	129	192	275	438	760
24	4	6	11	19	36	68	118	220	372	582	893
25	3	6	12	27	53	102	175	285	437	645	975
26	4	9	18	30	46	67	104	165	262	402	615
27	3	5	12	26	53	97	160	252	384	566	864
28	3	5	9	21	47	80	135	220	338	507	754
29	4	6	13	25	45	80	132	196	273	431	708
30	3	7	9	19	47	91	147	238	356	517	770
Ave	3	7	13	27	50	85	136	218	340	517	802
β_0	0.26	0.21	0.26	0.22	0.20	0.19	0.19	0.21	0.21	0.19	0.16

Table C.16. Calculation of β_0, system 6, 3D viscoelastic system, BC soil

	Bin										
	1	2	3	4	5	6	7	8	9	10	11
GM	Maximum resultant displacement (mm)										
1	6	12	19	29	41	56	74	99	129	168	225
2	7	12	20	31	44	59	79	105	137	179	240
3	5	9	14	22	31	42	55	74	96	125	168
4	6	11	19	28	40	55	72	97	126	165	221
5	6	11	17	26	37	50	66	89	116	151	203
6	7	14	23	35	50	68	89	120	156	203	273
7	5	10	16	24	34	46	61	81	106	139	186
8	6	12	19	29	41	55	73	98	127	166	223
9	6	12	20	31	43	59	77	104	136	177	237
10	5	10	16	25	35	47	62	83	109	142	190
11	7	13	20	31	44	60	79	106	138	180	242
12	5	9	15	22	32	43	57	76	100	130	174
13	5	9	15	23	33	45	60	80	104	136	182
14	6	11	18	27	38	52	68	92	120	156	209
15	6	12	19	29	41	55	73	97	127	165	222
16	5	9	15	22	32	43	57	76	99	129	174
17	5	10	15	24	34	45	60	80	105	137	183
18	5	10	17	26	36	49	65	87	114	148	199
19	6	12	19	30	42	57	76	101	132	172	231
20	5	10	16	25	35	48	63	85	111	144	193
21	4	8	14	21	29	40	53	71	92	120	161
22	5	9	15	23	33	45	59	80	104	135	181
23	5	9	15	23	33	45	59	79	104	135	181
24	5	10	17	25	36	49	64	86	113	147	197
25	5	10	16	25	35	48	63	84	110	144	193
26	5	9	15	23	33	45	59	80	104	136	182
27	6	12	19	29	41	56	73	99	129	168	225
28	5	10	16	25	35	47	62	84	109	142	191
29	6	12	19	30	42	57	75	101	132	172	231
30	5	10	16	25	35	47	63	84	109	143	191
Ave	6	11	17	26	37	50	67	89	116	152	204
β_0	0.13	0.13	0.13	0.13	0.13	0.13	0.13	0.13	0.13	0.13	0.13

Table C.17. Calculation of β_0, system 1, 2-second linear system, 5% damping, CD soil

	Bin										
	1	2	3	4	5	6	7	8	9	10	11
GM	Maximum resultant displacement (mm)										
1	29	56	91	136	195	267	355	462	616	808	1054
2	30	58	93	140	200	274	365	474	633	831	1083
3	32	61	98	147	211	289	384	500	667	875	1141
4	32	62	100	150	214	293	390	507	677	889	1158
5	37	71	115	173	247	339	450	586	782	1026	1338
6	37	71	116	173	248	340	452	588	785	1030	1343
7	33	64	103	155	221	303	403	524	700	919	1197
8	33	63	101	152	218	298	397	516	689	904	1178
9	29	55	89	133	191	261	347	452	603	791	1032
10	36	69	112	168	240	329	438	569	760	997	1300
11	35	68	110	164	235	322	428	557	744	976	1272
12	30	57	92	137	197	269	358	466	622	816	1064
13	38	72	117	176	252	345	459	597	797	1045	1363
14	29	55	89	134	192	262	349	454	606	795	1037
15	41	78	126	189	270	370	492	640	855	1122	1462
16	37	70	113	170	244	334	444	577	771	1011	1319
17	34	65	105	158	226	310	412	536	716	939	1223
18	32	61	99	148	212	290	386	502	670	879	1146
19	37	70	113	170	244	334	444	577	771	1011	1318
20	34	65	105	157	225	308	410	533	712	934	1217
21	29	56	91	136	195	268	356	463	618	811	1057
22	34	64	104	156	223	305	406	528	705	925	1206
23	31	59	96	144	206	283	376	489	653	856	1116
24	37	70	114	171	244	334	445	578	772	1013	1321
25	30	58	94	140	201	275	366	476	636	834	1088
26	29	56	91	137	196	268	357	464	619	812	1059
27	33	63	102	153	218	299	398	518	691	907	1182
28	40	76	123	185	264	362	482	627	837	1097	1430
29	31	60	96	145	207	284	377	491	655	859	1120
30	34	65	105	158	226	310	412	536	716	939	1224
Ave	33	64	103	155	222	304	405	526	703	922	1202
β_0	0.10	0.10	0.10	0.10	0.10	0.10	0.10	0.10	0.10	0.10	0.10

Table C.18. Calculation of β_0, system 2, 2-second sliding system, CD soil

	Bin										
	1	2	3	4	5	6	7	8	9	10	11
GM	Maximum resultant displacement (mm)										
1	5	13	43	88	145	221	314	435	638	884	1194
2	4	8	25	62	126	217	329	465	654	880	1204
3	6	19	45	83	136	210	304	431	618	851	1146
4	4	13	36	77	137	216	314	443	630	867	1175
5	3	7	22	55	109	177	264	390	663	1020	1493
6	4	9	30	70	138	228	340	481	697	1016	1438
7	3	7	20	46	98	180	287	422	617	890	1342
8	4	11	23	49	85	143	215	329	567	922	1361
9	3	8	19	30	58	107	182	320	520	775	1152
10	4	7	17	38	103	197	306	467	726	1048	1456
11	5	20	50	95	160	246	356	493	699	982	1346
12	4	11	34	71	120	194	286	397	546	731	1061
13	3	9	28	63	139	238	360	515	741	1031	1408
14	6	16	26	33	64	108	201	325	510	740	1028
15	6	24	53	105	178	278	405	566	800	1096	1478
16	4	10	40	92	164	258	377	523	760	1052	1422
17	4	12	29	57	108	198	326	488	715	991	1334
18	3	5	14	33	74	136	241	376	572	821	1202
19	4	9	24	62	114	183	275	421	644	935	1326
20	4	14	35	63	98	128	165	282	523	896	1425
21	3	12	41	88	151	229	315	421	591	821	1122
22	3	5	16	33	65	141	260	410	630	916	1286
23	4	10	26	52	90	143	235	370	580	849	1199
24	3	10	27	53	92	187	329	507	750	1043	1404
25	5	10	27	56	112	190	288	413	595	828	1138
26	3	11	23	49	85	161	259	381	555	853	1244
27	3	9	25	60	107	176	281	424	637	899	1226
28	4	14	35	71	129	227	348	560	861	1235	1708
29	2	6	13	42	97	190	306	440	626	854	1148
30	4	7	19	49	95	157	251	377	585	881	1279
Ave	4	11	29	61	113	189	291	429	642	920	1291
β_0	0.22	0.36	0.36	0.33	0.28	0.24	0.21	0.16	0.13	0.12	0.11

Table C.19. Calculation of β_0, system 3, 2-second linear system with FVDs, CD soil

	Bin										
	1	2	3	4	5	6	7	8	9	10	11
GM	Maximum resultant displacement (mm)										
1	7	23	49	85	133	194	270	364	500	673	895
2	7	22	46	79	125	193	277	383	534	724	968
3	9	24	50	87	138	206	291	398	552	748	1000
4	8	23	47	84	136	202	284	388	543	741	996
5	7	22	46	80	126	185	260	354	490	665	894
6	7	20	41	76	129	199	288	402	569	784	1064
7	6	18	40	72	118	179	257	358	508	701	953
8	6	16	31	52	87	131	188	263	375	540	764
9	5	12	27	50	81	123	175	253	378	541	757
10	4	16	37	69	117	182	265	370	522	716	965
11	12	32	62	105	162	237	331	451	623	842	1126
12	9	26	52	88	137	200	278	377	518	697	927
13	6	18	40	75	129	202	295	414	588	811	1102
14	5	11	25	49	88	142	214	307	442	617	843
15	10	30	61	107	169	252	358	490	683	930	1249
16	9	29	62	109	171	252	352	476	653	876	1161
17	6	16	36	65	113	185	275	390	556	766	1038
18	4	13	30	56	94	153	229	327	470	656	898
19	8	24	48	83	129	189	268	373	530	736	1007
20	7	18	34	54	78	110	168	246	358	502	719
21	9	27	56	95	146	210	290	389	531	711	944
22	4	11	23	46	83	138	212	307	450	637	883
23	7	16	34	65	108	166	239	331	465	634	851
24	7	18	34	59	105	174	264	382	557	783	1075
25	6	17	41	76	123	184	260	354	490	666	896
26	6	16	33	58	98	155	227	318	450	617	832
27	6	20	42	76	126	193	280	391	552	757	1021
28	8	21	45	78	130	199	286	395	554	757	1020
29	4	12	32	65	114	179	260	361	508	692	930
30	5	16	34	60	97	147	216	307	442	621	860
Ave	7	20	41	73	120	182	262	364	513	705	955
β_0	0.28	0.29	0.26	0.23	0.21	0.19	0.18	0.16	0.15	0.14	0.13

Table C.20. Calculation of β_0, system 4, 2-second sliding system with FVDs, CD soil

	Bin										
	1	2	3	4	5	6	7	8	9	10	11
GM	Maximum resultant displacement (mm)										
1	2	7	20	51	98	162	245	350	503	697	941
2	2	6	15	36	76	135	214	335	512	737	1025
3	2	9	27	56	98	158	237	341	500	714	995
4	2	7	20	47	91	151	236	347	508	719	1003
5	2	6	13	32	68	126	201	297	439	622	864
6	3	5	13	37	74	135	227	347	526	759	1066
7	2	5	13	28	55	105	180	284	442	651	932
8	2	7	17	33	57	94	143	220	336	488	719
9	2	5	12	25	42	65	114	184	287	460	735
10	2	6	10	21	42	98	181	294	466	683	968
11	2	10	31	66	119	191	285	407	586	816	1116
12	2	5	17	45	88	147	224	325	474	660	897
13	2	4	12	34	71	126	225	357	552	805	1141
14	3	10	20	33	43	71	111	184	325	521	786
15	2	10	33	68	122	200	305	442	649	918	1270
16	2	5	19	53	109	188	292	424	618	865	1181
17	2	6	18	37	67	112	171	295	492	751	1082
18	2	3	8	17	38	79	137	217	375	585	866
19	2	5	11	35	78	136	209	304	449	658	964
20	1	7	22	44	77	117	159	209	262	424	662
21	2	7	21	53	105	175	262	371	523	706	954
22	1	4	9	17	36	64	113	206	367	593	895
23	2	5	15	33	59	101	156	246	389	578	824
24	1	4	15	37	66	105	158	268	467	735	1093
25	3	9	17	36	67	118	201	308	462	657	917
26	1	6	17	32	60	100	154	249	402	600	855
27	2	7	14	32	70	123	192	294	461	688	996
28	1	6	20	44	80	138	219	344	530	770	1145
29	1	4	9	20	43	93	173	291	469	691	971
30	2	5	11	24	55	100	162	242	383	579	856
Ave	2	6	17	38	72	124	196	299	458	671	957
β_0	0.24	0.30	0.35	0.35	0.33	0.30	0.27	0.23	0.21	0.18	0.15

Table C.21. Calculation of β_0, system 5, 3-second sliding system, CD soil

	Bin										
	1	2	3	4	5	6	7	8	9	10	11
GM	Maximum resultant displacement (mm)										
1	5	15	49	94	143	219	332	482	705	1031	1490
2	4	9	31	85	160	259	384	540	767	1093	1548
3	6	21	50	99	165	264	390	559	868	1330	1942
4	5	15	44	92	162	256	375	527	755	1060	1457
5	4	7	24	65	144	257	407	603	896	1275	1763
6	4	10	36	74	135	230	347	509	754	1250	1902
7	3	7	24	59	113	203	322	477	753	1106	1553
8	4	12	28	54	92	149	224	419	774	1258	1903
9	3	9	21	43	67	131	230	358	578	910	1376
10	4	9	18	38	104	203	328	493	739	1163	1786
11	5	22	57	115	200	315	459	637	930	1324	1886
12	5	12	40	83	156	264	397	567	830	1190	1666
13	3	10	30	71	132	211	308	445	675	1051	1539
14	7	17	26	37	77	157	286	440	637	986	1451
15	6	26	54	112	198	310	445	627	905	1268	1784
16	5	10	47	113	207	327	475	664	939	1299	1797
17	4	12	33	69	114	194	341	538	819	1178	1628
18	3	7	16	38	110	213	342	504	768	1139	1632
19	4	10	23	69	137	229	344	494	731	1033	1420
20	4	13	32	65	108	150	218	365	577	841	1278
21	4	11	44	100	179	281	407	568	818	1171	1662
22	4	6	17	37	67	122	204	363	630	997	1492
23	4	11	30	60	103	165	271	405	625	958	1451
24	4	10	27	58	104	160	279	419	633	972	1398
25	6	13	27	59	103	216	383	596	907	1303	1809
26	3	11	23	50	82	143	260	446	734	1102	1572
27	4	12	27	67	120	198	306	448	720	1088	1569
28	4	15	43	88	164	266	434	657	982	1401	1955
29	3	7	15	42	96	215	348	511	748	1067	1601
30	5	8	20	56	108	172	257	394	636	979	1401
Ave	4	12	32	70	128	216	337	502	761	1127	1624
β_0	0.23	0.35	0.37	0.35	0.30	0.26	0.23	0.18	0.14	0.12	0.11

Table C.22. Calculation of β_0, system 6, 3D viscoelastic system, CD soil

	Bin										
	1	2	3	4	5	6	7	8	9	10	11
GM	Maximum resultant displacement (mm)										
1	12	23	38	57	81	111	148	193	257	338	440
2	10	19	30	46	65	89	119	155	206	271	353
3	13	25	40	60	87	119	158	205	274	359	468
4	11	21	34	51	73	100	133	173	231	303	395
5	10	18	30	45	64	88	117	152	203	266	346
6	11	20	33	49	70	96	128	167	223	292	381
7	11	21	33	50	72	98	131	170	227	298	388
8	9	17	27	40	57	79	105	136	182	238	311
9	9	18	29	43	61	84	112	145	194	254	331
10	9	17	28	41	59	81	108	140	187	245	320
11	13	25	41	61	88	120	160	208	278	365	476
12	11	21	34	51	72	99	132	172	229	301	392
13	14	26	42	63	90	124	165	214	286	375	489
14	9	16	27	40	57	78	104	136	181	237	310
15	16	30	49	73	105	144	191	248	332	435	567
16	13	25	40	60	86	117	156	203	271	355	463
17	10	20	32	48	69	94	125	162	217	284	371
18	8	15	24	36	51	70	94	122	163	214	278
19	10	19	31	47	67	92	122	159	212	279	363
20	11	20	33	49	70	96	128	167	222	292	380
21	13	24	39	59	84	115	153	199	266	349	455
22	8	15	24	35	50	69	92	120	160	209	273
23	10	20	32	49	69	95	127	165	220	288	376
24	10	19	30	45	65	89	119	154	206	270	352
25	10	19	30	45	65	89	118	154	205	269	351
26	9	17	28	42	61	83	110	144	192	251	328
27	9	17	28	42	61	83	110	144	192	251	328
28	11	21	33	50	72	98	131	170	227	298	389
29	9	17	27	41	58	80	106	138	184	242	315
30	9	17	27	40	58	79	105	137	182	239	312
Ave	10	20	32	49	70	95	127	165	220	289	377
β_0	0.17	0.17	0.17	0.17	0.17	0.17	0.17	0.17	0.17	0.17	0.17

APPENDIX D
GENERATING A SEISMIC DISPLACEMENT DEMAND CURVE

D.1 Purpose

This appendix builds on Section 5 and provides information on the selection of ground motion intensities to support response-history analysis and performance calculations (Section D.2), and the generation of a displacement demand curve for a specific isolation system (Section D.3). An alternate approach for generating a displacement demand curve is presented in Section D.4. Section D.5 presents the rationale behind the use of 11 ground motions for analysis as recommended in Section 5.2.2.

D.2 Selecting Ground Motion Intensities

A site, soil class, and TPG are assumed to illustrate the selection of ground motion intensities for response-history analysis: soil BC, Clinch River, and 4×10^{-5} (=1/25,000), respectively. The UHRS for the Clinch River site, a BC soil, and a return period of 25,000 years (the reciprocal of the TPG), used also for the analyses in Section 5, is presented in Figure D.1. The 30 sets of two horizontal component, spectrally matched ground motions, used in Section 5, are adopted herein.

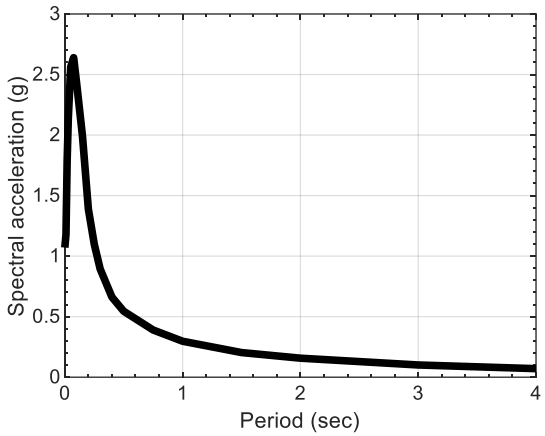

Figure D.1. Uniform hazard response spectra, BC soil, Clinch River

Figure D.2 presents the 2-second seismic hazard curve for BC soil at Clinch River. Note that the ticks on the vertical scale of the plot are in a base-10 log scale, termed log scale hereafter. The 2-second hazard curve is chosen here for ground-motion scaling because longer period, 2D seismic isolation systems are a focus of this report. (Prior studies (Yu *et al.* 2018) make clear that risk outcomes are not sensitive to the choice of period attached to the seismic hazard curve, which is 2 seconds here.) The logarithm of the TPG

is marked on the vertical axis of the plot and the corresponding spectral acceleration is marked as SA_{TPG} on the horizontal axis.

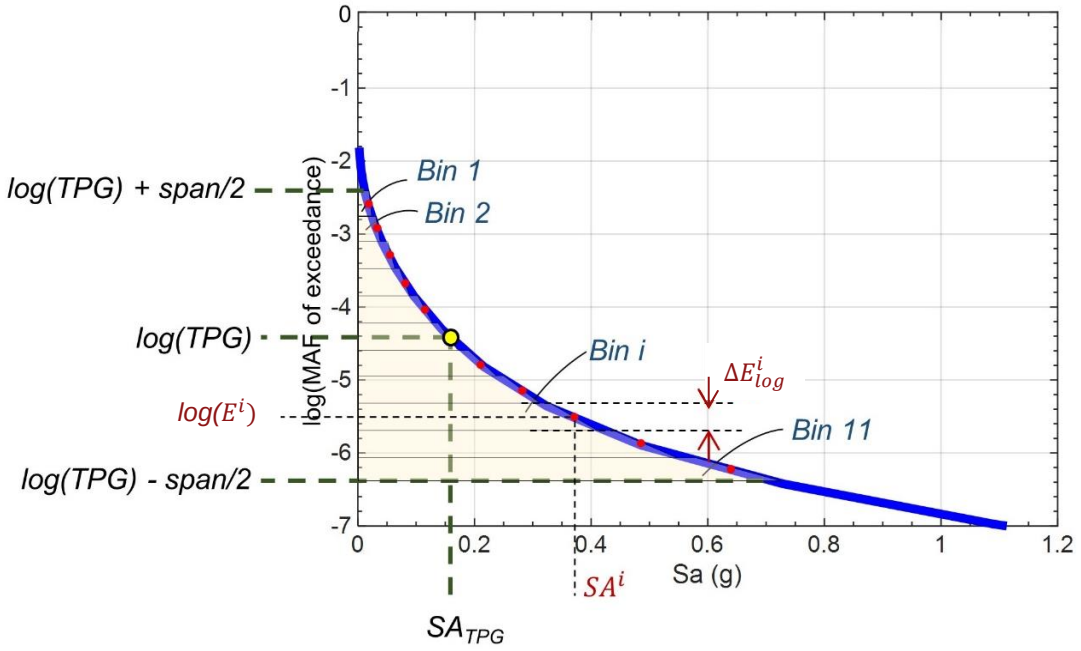

Figure D.2. 2-second hazard curve, BC soil, calculation of scale factors for return periods other than 25000 years, TPG = 4×10^{-5}

This section answers two questions: 1) what *span* of return periods in log space, around the TPG, should be considered for analysis? and 2) how many ground motion intensities (*bins*) should be considered to accurately capture the risk? See Figure C.2 where a *span* of 4 decades and eleven *bins* of equal width in log space on the vertical scale are shown. The boundaries of the eleven bins are defined by twelve equally spaced points in the closed interval *[log(TPG) - span/2, log(TPG) + span/2]*, such that the width of each bin is 0.364 (=span/11=4/11) in log space. For this example, log (TPG) = -4.4, log (TPG) - span/2 = -4.4 - 4/2 = -6.4, and $10^{-6.4} = 4 \times 10^{-7}$, as shown in the figure.

Table D.1 presents the data associated with the bins shown in Figure D.2. To explain the data presented in the table, bin 4 is considered here. The boundaries of the bin on the MAFE axis, in log space, are defined by -3.48 and -3.85. The center of the bin on the MAFE axis in log space is then defined by the average of -3.48 and -3.85, that is, -3.67. The width of a bin on the MAFE axis in linear space is denoted as ΔE^i. For $i = 4$, ΔE^i is obtained by subtracting $10^{-3.85}$ from $10^{-3.48}$. Similarly, for bin 6, the boundaries are defined by -4.21 and -4.57 in log space and the center of the bin on the MAFE axis in log space is the average of -

4.21 and -4.57, that is -4.40. (Bin 6 is centered on the TPG. The logarithm of 4×10^{-5} is -4.40.) The MAFE and the 2-second spectral acceleration associated with the i^{th}-bin, denoted E^i and SA^i, respectively, in Figure C.2, are read from the plot at the center of the i^{th}-bin in log space (red dots in Figure D.2).

Table D.1. Defining eleven bins on the 2-second hazard curve of Figure D.2

Bin number	Bin boundaries, MAFE, log space	MAFE at center of bin, log space	Width of bin, MAF, linear space	2-second spectral acceleration at center of bin (g)	Scale factor for motions
1	(-2.39, -2.76)	-2.58	2.27×10^{-3}	0.02	0.13
2	(-2.76, -3.12)	-2.94	9.82×10^{-4}	0.03	0.19
3	(-3.12, -3.48)	-3.31	4.25×10^{-4}	0.05	0.31
4	(-3.48, -3.85)	-3.67	1.84×10^{-4}	0.08	0.50
5	(-3.85, -4.21)	-4.03	7.97×10^{-5}	0.12	0.75
6	(-4.21, -4.57)	-4.40	3.45×10^{-5}	0.16	1.00
7	(-4.57, -4.94)	-4.76	1.49×10^{-5}	0.21	1.31
8	(-4.94, -5.30)	-5.13	6.46×10^{-6}	0.28	1.75
9	(-5.30, -5.67)	-5.49	2.80×10^{-6}	0.36	2.25
10	(-5.67, -6.03)	-5.85	1.21×10^{-6}	0.47	2.94
11	(-6.03, -6.39)	-6.22	5.24×10^{-7}	0.63	3.94

There are options for scaling ground motions to E^i for response-history analysis of the 2DOF model of the isolation system to produce a displacement demand curve, including: 1) use one spectral shape appropriate for the 4 decades in frequency space, and amplitude scale the motions generated for TPG shaking for the ith-bin by SA^i / SA_{TPG}, and 2) characterize spectral space by decade, generate sets of two-component ground motions (i.e., H1, H2) for use in each decade, and scale the motions in each bin to E^i. Option 1 is sufficient for these example calculations because the displacement response of the isolation system is dependent on spectral demands in a narrow frequency band. Thirty sets of motions (i.e., more than 11) are used for the analysis described below for the reason given in Section 5.2.2.

Risk calculations are made for three combinations of span and number of bins for Systems 2 (2-second nonlinear) and 5 (3-second nonlinear) per Table 4.4, considering BC and CD soil, respectively. The three combinations of span and number of bins are 3 and 11, 4 and 11, and 5 and 21. (The choice of an odd number for the number of bins is only for reasons of presentation as it ensures that one bin is centered at

the TPG; see Figure D.2 where 11 bins are shown, and the 6th bin is centered on TPG.) The three chosen combinations represent increasing levels of computational effort, with the first and the third combinations being the least and the most computationally expensive, respectively. The first combination (span = 3, and number of bins = 11) represents a narrow range of MAFE on the 2-second hazard curve and a fine discretization in terms of ground motion intensities chosen for analysis, whereas the third combination (span = 5, and number of bins = 21) represents a wide range of MAFE and a very fine discretization in terms of ground motion intensities.

Table D.2 presents risk results for the two isolation systems on two different soils and the three combinations of span and number of bins described above. Displacements calculated using spectrally matched motions are increased by a factor of 1.2 to address variability in horizontal shaking about the geometric mean and in isolator and damper properties per Section 5 and Appendix C. Calculations are presented for isolation systems with different median displacement capacities. The recommended default composite logarithmic standard deviation per Section 5 and Appendix C is used here, namely, $\beta = 0.35$. The benchmark is combination 3, although it must be noted that uncertainty drives seismic hazard calculations for small MAFE, and that the risk number for combination 3 is likely no truer than that for combination 2.

The risk numbers presented in Table D.2 indicate that the first combination of span and number of bins (i.e., span = 3, bins = 11) results in values smaller than those resulting from combination 3 (span = 5, bins = 21). However, the differences in risk calculated using combinations 2 and 3 are negligible.

Table D.2. Risk calculations, three combinations of span and bins, two isolation systems, $\beta = 0.35$

Isolation system	Median displacement capacity	MAF of unacceptable performance[1]		
		Combination 1 (span = 3, bins = 11)	Combination 2 (span = 4, bins = 11)	Combination 3 (span = 5, bins = 21)
System 2, 2-second nonlinear, BC soil	200 mm	8.9×10^{-6} (-11%)	1.0×10^{-5} (0%)	1.0×10^{-5}
	250 mm	5.3×10^{-6} (-22%)	6.5×10^{-6} (-4%)	6.8×10^{-6}
System 5, 3-second nonlinear, CD soil	300 mm	3.5×10^{-5} (-3%)	3.6×10^{-5} (0%)	3.6×10^{-5}
	350 mm	2.6×10^{-6} (-7%)	2.8×10^{-6} (0%)	2.8×10^{-6}

1. Values in parenthesis indicate differences with respect to results from Combination 3

Risk calculations should be performed using eleven bins of ground motions, spanning 4 decades of MAFE in log space, of equal width in log space.

D.3 Adjustments to the Seismic Displacement Demand Curve

The analysis performed in this report to generate a seismic displacement demand curve is analogous to set G0 per Huang *et al.* (2013), namely, analysis of a best estimate model of an isolation system using ground motions spectrally matched to a geometric mean spectrum. Adjustments are made to this displacement demand curve to address, in part, variability in ground shaking around the geometric mean (see the discussion in Section A.4) and in the properties of the isolation system. The other part of the variability is addressed via the logarithmic standard deviation assigned to the fragility function, as noted in Appendix C.2.2.2 and it is characterized by β_r.

The displacement demand curve generated using spectrally matched motions is increased by the average value of the ratio $\theta_{M2} / \theta_{G0}$ across Table C.2 through Table C.4, as summarized in Table C.6. The average value of the ratio is 1.2 and it is recommended for use in generating all seismic displacement demand curves.

D.4 An Alternate Approach for Generating a Seismic Displacement Demand Curve

The recommended approach to generate a seismic displacement demand curve is described in the preceding sections of this appendix. That approach is referred to as Approach 1 in this subsection. Section 3.5 of this report recommends the use of 11 sets of three-component ground motions to compute the median

displacement at each of 11 intensity levels. If 11 sets of motions are used, the dispersion associated with analysis using spectrally matched horizontal motions, β_0, should be set equal to 0.28, as described in Section C.2.2.2. An alternate approach for generating a displacement demand curve is described herein, and referred to as Approach 2. Approach 2 involves analysis using 30 sets of ground motions per intensity level, such that the results of the analyses can be used to generate a displacement demand curve that directly accounts for the dispersion in displacements associated with the use of spectrally matched horizontal motions (β_0). The procedure to derive such a demand curve is described below.

Eleven (= *i*) bins of 30 ground motions are used to generate the displacement demand curve. Displacements calculated using spectrally matched motions are increased by a factor of 1.2 to address variability in horizontal shaking about the geometric mean and in isolator and damper properties, as described in Section D.3. The maximum horizontal displacements corresponding to the *i*th bin are arranged as a 30 × 1 vector, D^i, where *i* = 1 to 11. The vector D^i has elements d_j^i organized in increasing order, where *j* denotes the index of the ground motion (*j* = 1 to 30) organized such that d_1^i and d_{30}^i are the minimum and maximum displacements in the *i*th bin, respectively. Each bin is associated with a MAFE (i.e., the ordinate of the red dot at the center of each bin in Figure D.2). The MAFE associated with the *i*th bin and the width of the bin in the linear space are denoted E^i and ΔE^i, respectively. Approach 2 involves tagging each displacement, d_j^i, with a mean annual frequency of occurrence given by $\Delta E_j^i = \Delta E^i / n_{gm}$, where n_{gm} is the number of ground motions in a bin (= 30 here). The displacement demand curve is then defined at a multiple query displacement points that lie within the range d_{30}^1 to d_1^{11} such that the MAFE associated with a particular query displacement d_{query} is the summation of the mean annual frequencies of occurrence associated with displacement data points greater than d_{query} across all bins. Enough (e.g., 20) query displacements are chosen, and the associated MAFE are calculated to generate a smooth displacement demand curve[26]. Figure D.3 illustrates the steps involved in Approach 2.

[26] The maximum and the minimum displacements in the first and the last bin are d_{30}^1 and d_1^{11}, respectively. Reliable information on exceedance frequencies is not available outside this range.

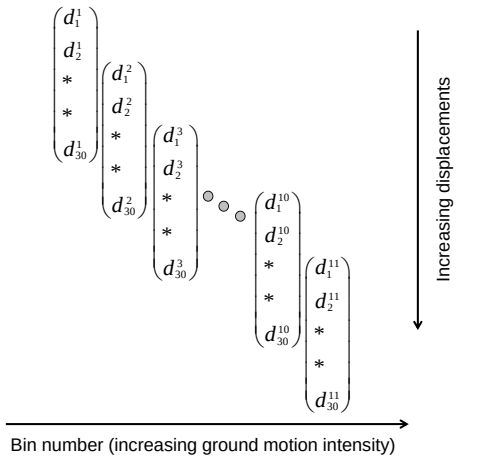

(a) step 1: results of response-history analysis

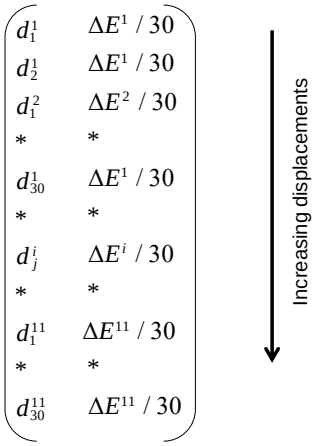

b) step 2: associating each displacement with a mean annual frequency of occurrence

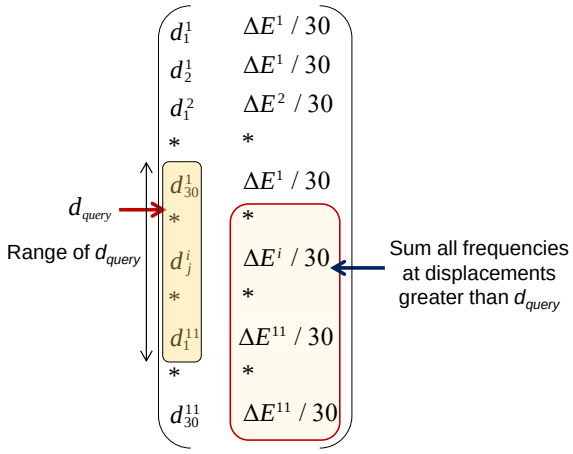

(c) step 3: calculating the annual frequency of exceedance for a chosen displacement, d_{query}

Figure D.3. Defining a displacement demand curve using results of response-history analysis, Approach 2

Because the demand curve generated using Approach 2 directly accounts for the dispersion associated with using spectrally matched horizontal motions, β_0 can be set equal to 0 in the calculation of β_d per Section C.2.2.4. That is,

$$\beta_d = \sqrt{\beta_0^2 + (\beta_{M2}^2 - \beta_{G0}^2) + \beta_r^2 + \beta_m^2 + \beta_f^2}$$

$$= \sqrt{0^2 + (0.14^2) + 0.05^2 + 0.05^2 + 0.05^2}$$

$$= 0.17$$

Thus, the composite logarithmic standard deviation per Section C.2.4 that should be used in performance calculations adopting Approach 2 is[27]:

$$\beta = \sqrt{\beta_d{}^2 + \beta_c{}^2}$$

$$= \sqrt{0.17^2 + 0.05^2}$$

$$= 0.18$$

Figure D.4 and Figure D.5 presents displacement demand curves for three isolation systems generated using the two approaches for BC and CD soils, respectively, and the Clinch River site, as introduced previously. Calculations are presented for isolation systems with median displacement capacities of 200 mm and 250 mm. A composite log standard deviation (β) of 0.35 and 0.18 for Approaches 1 and 2, respectively, is used here. Table D.3 presents the corresponding risk calculations, with Approach 1 serving as a benchmark. The risk estimates from the two approaches do not differ significantly, but those from Approach 1 are higher. Therefore, either approach could be used, but Approach 1 is simpler and is thus recommended.

[27] The value of $\beta = 0.18$ could be rounded to the nearest 0.05 per Approach 1, namely, to 0.20, but 0.18 is used for the calculations presented herein.

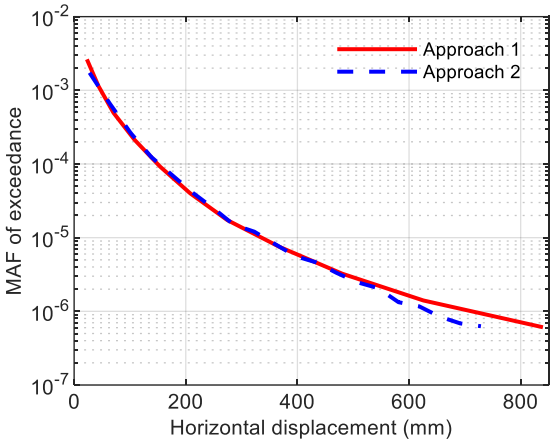

(a) 2-sec linear system

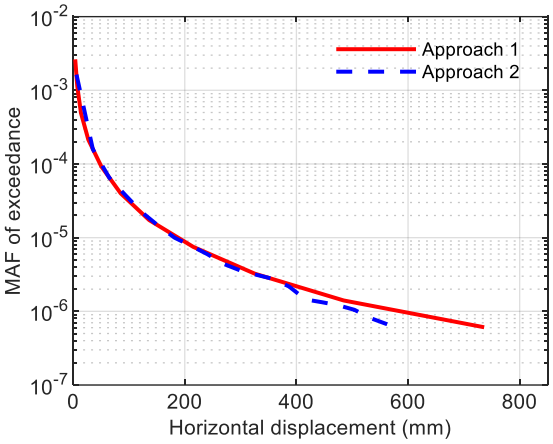

(b) 2-sec nonlinear system

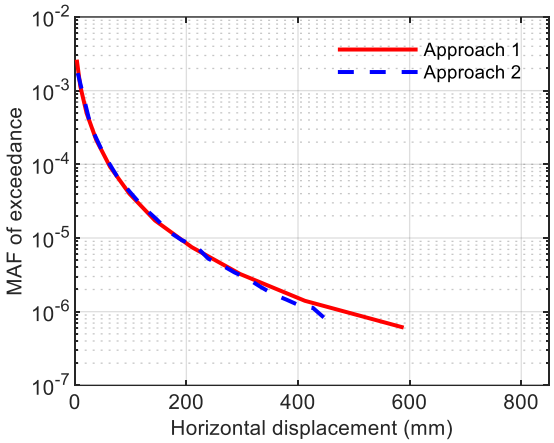

(c) 2-second linear system + nonlinear FVDs

Figure D.4. Comparison of displacement demand curves generated using Approaches 1 and 2, BC soil

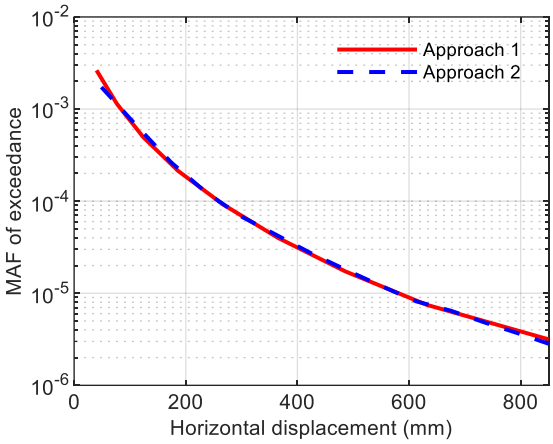

(a) 2-sec linear system

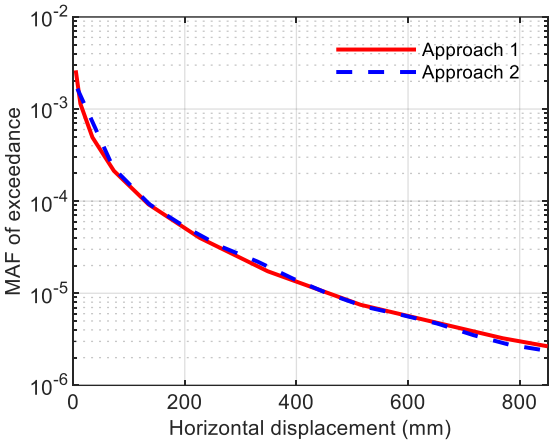

(b) 2-sec nonlinear system

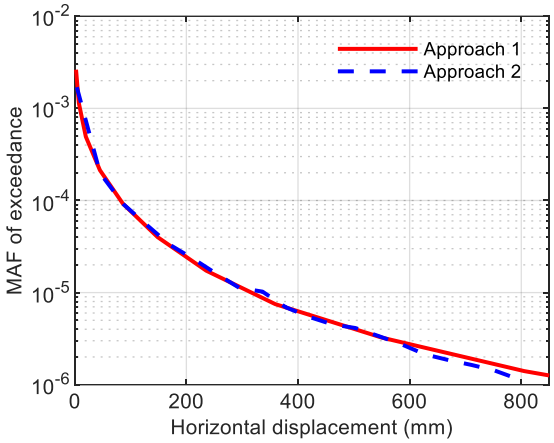

(c) 2-second nonlinear system + nonlinear FVDs

Figure D.5. Comparison of displacement demand curves generated using Approaches 1 and 2, CD soil

Table D.3. Performance calculations using two approaches for generating demand curve, Clinch River, BC soil, $\beta = 0.35$ for Approach 1 and 0.18 for Approach 2

(a) BC soil

	Median displacement capacity (mm)	MAF of unacceptable performance		Percent difference
		Approach 1	Approach 2	
2-sec linear isolation system	200	6.6×10^{-5}	5.4×10^{-5}	24
	250	3.7×10^{-5}	2.8×10^{-5}	32
2-second sliding isolation system	200	1.0×10^{-5}	8.4×10^{-4}	21
	250	6.5×10^{-6}	5.1×10^{-6}	27
2-sec linear isolation system +. nonlinear FVDs	200	1.1×10^{-5}	8.6×10^{-6}	26
	250	6.3×10^{-6}	4.6×10^{-6}	35

(b) CD soil

2-sec linear isolation system	200	2.4×10^{-4}	2.1×10^{-4}	14
	250	1.5×10^{-4}	1.2×10^{-4}	21
2-second sliding isolation system	200	5.8×10^{-5}	5.4×10^{-5}	7
	250	4.0×10^{-5}	3.7×10^{-5}	7
2-sec nonlinear system + nonlinear FVDs	200	2.8×10^{-5}	2.6×10^{-5}	10
	250	1.9×10^{-5}	1.6×10^{-5}	13

D.5 Rationale for Using Eleven Sets of Ground Motions per Intensity Level

Appendix C of Huang *et al*. (2008) presents a detailed discussion on the number of ground motions, *n*, that should be used in an intensity-based assessment to bound the *median* displacement response with a given level of confidence. Huang *et al*. (2008) notes that the number *n* is a function of the required accuracy of the response (e.g., 1 ± *X* of the *true* value) and the required confidence in the estimate (e.g., *Z*%). Both *X* and *Z* are related to the dispersion in the displacement response (β_0 per Appendix C of this report). Equation C.8 in Huang *et al*. relates *n*, *X*, *Z*, and β_0 and is reproduced below:

$$n \approx \left(\frac{\Phi^{-1}\left(1-\frac{\alpha}{2}\right)\beta_0}{X} \right)^2$$

where Φ^{-1} is the inverse standard normal distribution and α is equal to $1-Z\%$. Estimates of β_0 for different isolation systems were presented in Table C.5. On average, β_0 = 0.18 across all isolation systems and the two soil types considered in this report. (The largest of all β_0 values in Table C.5 was used in the derivation of dispersions.) Using β_0 =0.18, X = 0.1 (i.e., selecting the bounds as ± 10% of the true value), and Z = 90% (i.e., 90% confidence in the 1 ± *X* interval), *n* = 11. Thus, using 11 sets of motions ensures a 90% confidence that the obtained median response is within 10% of the true value.

D.6 References

Huang, Y.-N., Whittaker, A. S., and Luco, N. (2008). "Performance assessment of conventional and base-isolated nuclear power plants for earthquake and blast loadings." *MCEER-08-0019*, University at Buffalo, Buffalo, NY

Huang, Y. N., Whittaker, A. S., Kennedy, R. P., and Mayes, R. L. (2013). "Response of base-isolated nuclear structures for design and beyond-design basis earthquake shaking." *Earthquake Engineering and Structural Dynamics*, 42(3), 339-356.

Yu, C. C., Bolisetti, C., Coleman, J. L., Kosbab, B., Whittaker, A. S. (2018). "Using seismic isolation to reduce risk and capital cost of safety-related nuclear structures." *Nuclear Engineering and Design*, 326, 268-284.

APPENDIX E
ISOLATION SYSTEM OPTIONS

E.1 Introduction

The purpose of this appendix is to illustrate isolation-system options available to engineers and analysts, and how a system could be selected for a nuclear power plant. The isolation system provides flexibility in either the two horizontal directions (2D systems) or three directions (3D systems), all between the basemat and the foundation. The flexibility increases the fundamental period of the reactor building in the direction of isolation, which substantially reduces earthquake-induced accelerations on the superstructure, accompanied by an increase in displacements across the isolation plane, as described in Figure 4.3. Viscous damping can be added to the isolation system to control displacements.

The reactor building and internal equipment presented in Section 4.2 and shaking for the Clinch River site described in Appendix A, are used to illustrate the opportunities and tradeoffs associated with the choice of a base isolation system. Cost is not addressed. The building is assumed to be supported by 17 identical isolators below the basemat, as shown in Figure 4.4. Multiple seismic isolation solutions are considered, and some include nonlinear fluid viscous dampers located per Figure 4.4b—four dampers along each horizontal axis. None of the isolation systems were optimized, which is a project-specific activity.

The numerical model of the isolated building and the equipment presented in Section 4 is used for response-history analysis. Tri-directional inputs at two levels of ground shaking intensity are used to highlight outcomes of choosing one isolation system over another. The isolation system is simulated using link elements, as described in Section 4.4. No attempt is made in this appendix to achieve a TPG for either the isolation system or the supported equipment.

Sections E.2.2 provides sample results and preliminary observations for isolation-system displacements, peak in-structure accelerations and acceleration response spectra, and forces in shear walls. Such information would be used to design isolators and dampers, safety-related equipment, and shear walls, respectively. Acceleration responses are compared in Section E.2.3 for systems 1 through 7.

E.2 Dynamic Analysis

E.2.1 Introduction

Response-history analysis of the finite element model is performed using SAP2000 (CSI 2020) for the seven isolation systems identified in Section 4.4, namely:

1. 2D, 2-second linear system
2. 2D, 2-second nonlinear system
3. 2D, 2-second linear system + 1D nonlinear FVDs
4. 2D, 2-second nonlinear system + 1D nonlinear FVDs
5. 2D, 3-second nonlinear system
6. 3D linear system + viscoelastic dampers
7. 3D isolation system composed of 2D 2-second nonlinear isolators, and vertically guided spring isolators and 1D nonlinear FVDs

where the 2D nonlinear systems could be composed of either sliding bearings or LR bearings.

Thirty sets of input motions spectrally matched to the 25,000-year UHRS at the Clinch River site for soil CD shown in Figure E.1 are used for the analysis. Per Figure E.1, the geomean, horizontal, peak ground acceleration (PGA) is 1 g, and the vertical PGA is 0.67 g. Detailed information on the generation of the ground motion time series is presented in Appendix A. The spectrally matched motions are also amplitude scaled by a factor of 0.5 (50% UHRS), and both shaking levels, 50% and 100% UHRS, are used for the dynamic analysis. The PGAs for the two shaking levels in the horizontal and vertical directions (H, V) are (0.5 g, 0.33 g) and (1 g, 0.67 g). The MAFE for the 100% UHRS is 4×10^{-5} (reciprocal of 25,000 years), and that for 50% UHRS is approximately 10^{-4}, per the horizontal PGA hazard curves shown in Figure A.1 for the CD site. Parenthetically, 10^{-4} and 4×10^{-5} are the TPGs per ASCE/SEI 43-19 (ASCE 2021) for Seismic Design Categories 3 and 4, respectively.

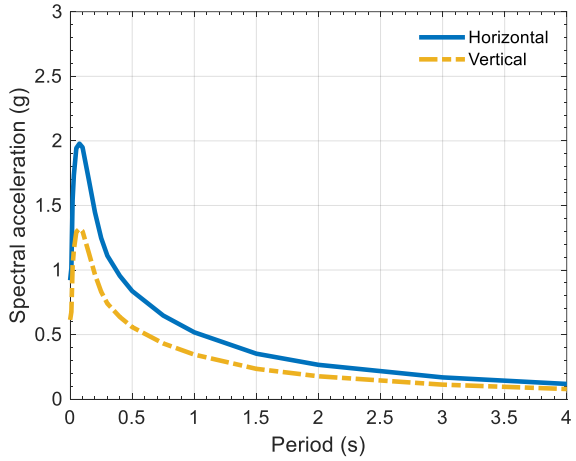

Figure E.1. UHRS for 25,000 years, geomean horizontal and vertical shaking, V/H=0.67, Clinch River site, CD site, 5% of critical damping (repeating Figure A.3)

Section E.2.2 provides sample results and preliminary observations for isolation-system displacements, in-structure accelerations, and response spectra of the reactor building. These responses are compared in Section E.2.3 for systems 1 through 7.

E.2.2 Sample results and observations

Horizontal response data are presented in three formats in this section and Section E.2.3. Resultant horizontal isolation-system displacement and floor acceleration for a given input motion are computed at each time step in a response-history analysis (i.e., $r(t) = \sqrt{x(t)^2 + y(t)^2}$), and the maximum value for all time steps is used for subsequent calculations. Geometric mean (or geomean; Sa_{geo}) acceleration response spectra are computed frequency by frequency as $Sa_{geo} = \sqrt{Sa_x \cdot Sa_y}$. SRSS acceleration response spectra are computed frequency by frequency as $Sa_{SRSS} = \sqrt{Sa_x^{\,2} + Sa_y^{\,2}}$.

Figure E.2 presents *x*, *y*, geomean, and SRSS spectra on the basemat for one input motion and isolation system. The ordinates of the geomean spectrum lay between those of the *x* and *y* spectra. The ordinates of the SRSS spectra are greater than those of the x and y spectra.

All subsequent horizontal acceleration response spectra in this appendix are geomean, to present a composite of the responses in the *x* and *y* directions. Isolation-system displacements and accelerations on the building and equipment are reported in the three translational directions, for the seven systems and two shaking levels. The geomean horizontal and vertical PGAs of the inputs for the two shaking levels are (H, V) = (0.5 g, 0.33 g) and (1 g, 0.67 g).

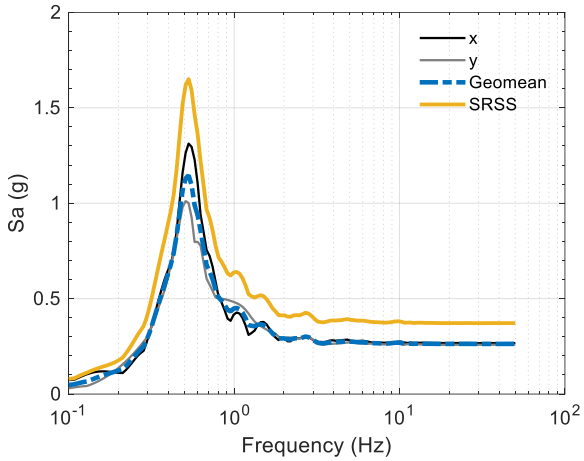

Figure E.2. Acceleration spectra (Sa), *x*-directional, *y*-directional, and geomean, and SRSS, one input motion, center of the basemat, system 1, 5% of critical damping, horizontal PGA=1 g, vertical PGA = 0.67 g

Table E.1 presents the means of the maximum horizontal displacements for the 30 inputs and the two shaking levels. The displacements along the two principal axes (*x* and *y*; 2nd and 3rd columns) for each isolation system are essentially identical. The resultant of the two components is calculated at each time step, as noted above, and the mean of the 30 maxima is presented in the 4th column. For the linear systems 1 and 6, the *x*, *y*, and resultant displacements are doubled as the shaking intensity is increased from 0.5 g to 1 g. For the nonlinear systems (2, 3, 4, 5, and 7), the percentage increase in the displacements with the doubling of the input is more significant; the 1.0-g displacements are 2.5 to 3.6 times their 0.5-g counterparts.

The gravity-load vertical displacement of the 3D isolation systems 6 and 7 is 40 mm (in compression)—a design decision that is a function of the frequency of the vertical isolation system. For these two systems, the mean maximum vertical displacements generated by the vertical inputs at the two shaking intensities are less than 21 mm, and so no uplift occurs. The vertical displacements of the five 2D systems are small due to their high vertical stiffness (and thus short period: 0.03 second (36 Hz) and 0.04 second (26 Hz) per Table 4.5).

Table E.1. Mean maximum horizontal isolation-system displacements, units of mm, 30 inputs, seven isolation systems per Section E.2.1

(a) PGA = 0.5 g

Isolation system	*x*	*y*	Resultant
1	128	128	152
2	46	47	58
3	59	59	71
4	28	29	36
5	52	53	67
6	39	39	48
7	45	46	57

(b) PGA = 1.0 g

1	256	257	304
2	152	152	191
3	150	151	182
4	99	100	124
5	175	177	218
6	79	79	96
7	151	150	189

Accelerations and in-structure spectra are monitored at the locations listed below, and identified in Figure E.3, to enable a comparison of results for different isolation systems:

- A: center of the basemat, at the point of support of the reactor vessel
- B: center of the reactor head, at the point of support of head-mounted equipment
- C: 10 Hz oscillator mounted on the reactor head
- D: 20 Hz oscillator mounted on the reactor head
- E: upper support of RVACS, inside of shield wall
- F: center of the head to the reactor shield structure
- G: point of attachment of the bridge crane on the steel frame

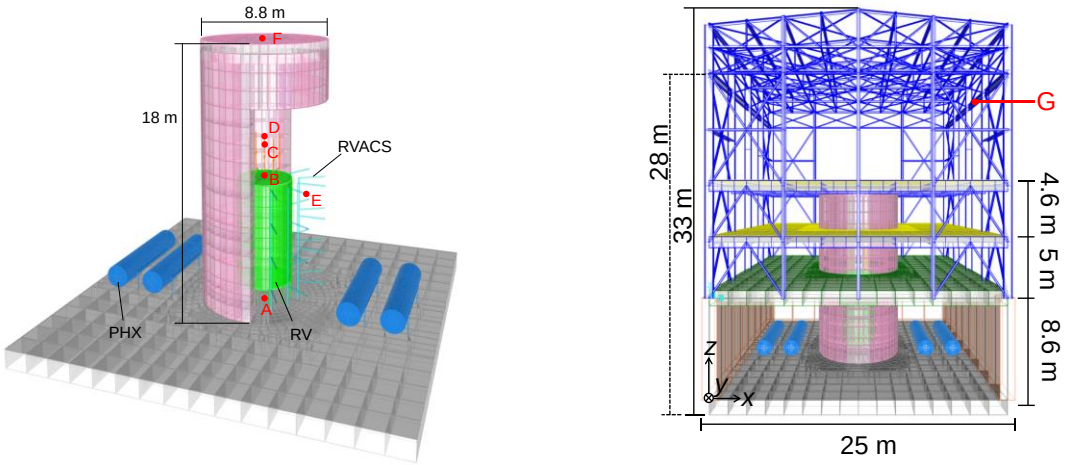

(a) basemat, reactor shield, and equipment, x-z perspective view (part of reactor shield removed)

(b) building, x-z perspective view (reinforced concrete wall on the +y face removed from view)

Figure E.3. Finite element model of the reactor building, response-monitoring locations (A through G) identified using red dots

Table E.2 and Table E.3 present the mean maximum horizontal and vertical accelerations, respectively, for the 30 inputs, two shaking levels, seven systems, and seven monitoring locations. As the shaking intensity increases from PGA = 0.5 g to PGA = 1 g, the acceleration at each monitoring location doubles for the two linear systems (1 and 6), but not for the five nonlinear systems, for which the trends are obscured by a) the coupled dynamics of the building and the equipment, b) the bilinear response of the isolators, and c) the nonlinear response of the dampers. Per Table E.2, all of the maximum accelerations on the basemat (location A) are substantially smaller than the PGA: between 0.11 g and 0.19 g (0.23 g and 0.41 g) for PGA = 0.5 g (1 g). Comparisons of the 7 systems are provided in Section E.2.3.

Figure E.4 presents the mean of 30, 5% damped, geomean horizontal and vertical response spectra (Sa) at the center of the basemat (location A) and the reactor head (location B), for the seven systems and a PGA of 1 g. The spectra in Figure E.4 are plotted to 50 Hz. Per Figure E.4a, for frequencies greater than 5 Hz, which are often associated with equipment, the spectral accelerations on the basemat are generally less than one-half of the PGA. Some of the spectral peaks in Figure E.4a are associated with the lateral frequencies of the isolation systems (0.5 Hz for systems 1, 2, 3, and 7, 0.9 Hz for system 6), coupled vertical-horizontal response of the isolation system (2.5 Hz for systems 6 and 7; 20 Hz and 30 Hz for systems 2, 4, and 5) and building response (10 Hz). The spectral peaks in Figure E.4b are at the lateral frequencies of the isolation system and around 12 Hz, which is the lateral frequency of the reactor vessel.

In Figure E.4c, the spectral peaks for systems 6 and 7 are at the vertical frequencies of the isolation systems, namely, 2.5 Hz. (Greater reductions in spectral acceleration at 2.5 Hz could be achieved for system 7 by increasing either the number of vertical dampers per isolator from 1 to 2 or C_d for each vertical damper.)

Per Table A.1, the vertical (and horizontal) UHRS ordinate peaks between 10 Hz and 20 Hz, and the ordinates are essentially constant in that range. Per Section 4.4.3, much of the vertical mass in the isolated building is associated with modes around 18 Hz for the linear isolation systems 1 and 3 (=58%) and around 20 Hz for the bilinear isolation systems 2, 4, and 5 (=43%). The spectral peaks at 18 and 20 Hz in Figure E.4c and Figure E.4d for systems 1 to 5 are a consequence of significant modal response at the peak of the vertical ground motion spectrum. (Such responses could be substantially reduced by adjusting the vertical stiffness of the isolators, adding damping in the vertical direction, or vertically isolating per systems 6 and 7.) For frequencies greater than 5 Hz, the vertical spectral demands for systems 6 and 7 are less than those for the other systems.

Table E.4 presents the peak ordinate of the mean of 30 geomean horizontal spectra over a frequency range of 5 Hz to 50 Hz, for the two shaking levels, seven systems, and seven monitoring locations. (Five to 50 Hz is chosen here as a range for equipment qualification.) Using location B, system 4, and a horizontal PGA=1 g as an example, the spectral acceleration presented in Table E.4b is 1.51 g, which is the peak ordinate of the red dash-dotted line shown in Figure E.4b.

Table E.2. Mean maximum horizontal acceleration, resultant of the two components, units of g, 30 inputs, seven locations, seven isolation systems per Section E.2.1

(a) Horizontal PGA = 0.5 g, vertical PGA = 0.33 g

Isolation system	A	B	C	D	E	F	G
1	0.16	0.16	0.17	0.16	0.16	0.16	0.68
2	0.16	0.20	0.87	0.44	0.17	0.25	0.81
3	0.11	0.15	0.53	0.32	0.11	0.15	0.71
4	0.19	0.27	1.20	0.58	0.17	0.32	0.92
5	0.15	0.19	0.87	0.42	0.14	0.24	0.80
6	0.18	0.20	0.42	0.26	0.19	0.25	0.37
7	0.15	0.18	0.98	0.36	0.12	0.18	0.40

(b) Horizontal PGA = 1.0 g, vertical PGA = 0.67 g

1	0.31	0.31	0.35	0.32	0.32	0.32	1.37
2	0.41	0.44	1.65	1.08	0.44	0.57	1.36
3	0.23	0.26	0.72	0.44	0.23	0.26	1.36
4	0.37	0.42	1.80	0.98	0.38	0.52	1.51
5	0.27	0.31	1.28	0.74	0.30	0.41	1.33
6	0.35	0.41	0.84	0.52	0.38	0.49	0.73
7	0.28	0.29	1.17	0.47	0.26	0.31	0.51

Table E.3. Mean maximum vertical accelerations, units of g, 30 inputs, seven locations, seven isolation systems per Section E.2.1

(a) Horizontal PGA = 0.5 g, vertical PGA = 0.33 g

Isolation system	A	B	C	D	E	F	G
1	0.38	0.45	0.45	0.45	0.56	0.63	1.23
2	0.33	0.40	0.40	0.40	0.52	0.63	1.31
3	0.36	0.44	0.44	0.44	0.54	0.62	1.28
4	0.33	0.40	0.40	0.40	0.52	0.63	1.31
5	0.33	0.40	0.40	0.40	0.52	0.63	1.30
6	0.27	0.27	0.27	0.27	0.27	0.27	0.30
7	0.24	0.24	0.24	0.24	0.23	0.23	0.30

(b) Horizontal PGA = 1.0 g, vertical PGA = 0.67 g

1	0.75	0.91	0.91	0.91	1.11	1.27	2.45
2	0.70	0.90	0.90	0.90	1.03	1.27	2.64
3	0.73	0.87	0.87	0.87	1.08	1.24	2.57
4	0.68	0.89	0.89	0.89	1.02	1.26	2.63
5	0.70	0.88	0.88	0.88	1.03	1.26	2.62
6	0.53	0.53	0.53	0.53	0.53	0.54	0.59
7	0.53	0.53	0.53	0.53	0.51	0.52	0.58

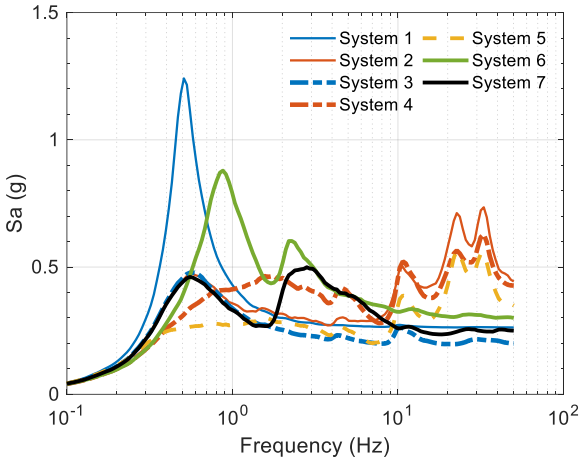

(a) basemat, location A, geomean horizontal

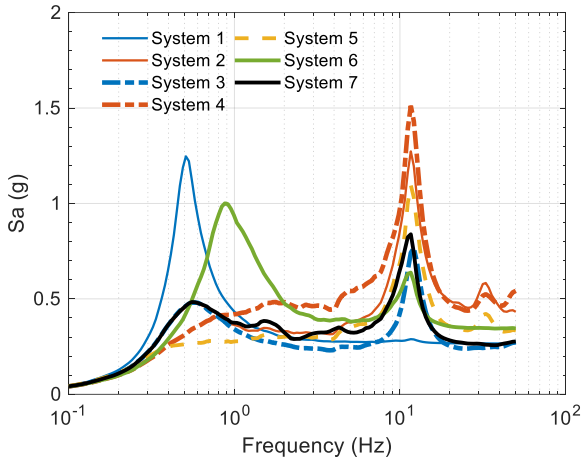

(b) reactor head, location B, geomean horizontal

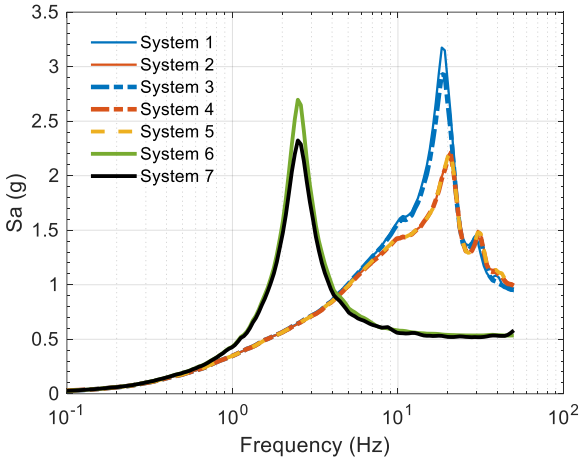

(c) basemat, location A, vertical

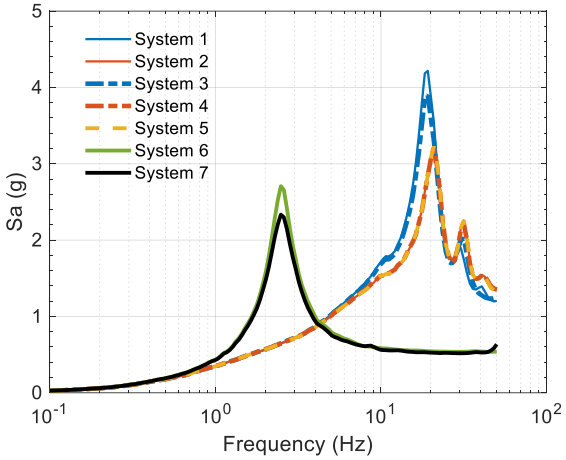

(d) reactor head, location B, vertical

Figure E.4. Mean acceleration spectra (Sa) for the 30 inputs, two locations, seven isolation systems per Section E.2.1, 5% of critical damping, horizontal PGA=1 g, vertical PGA = 0.67 g

Table E.4. Maximum of the mean geomean horizontal spectral acceleration, 5 Hz to 50 Hz, units of g, 30 inputs, seven locations, seven isolation systems per Section E.2.1

(a) Horizontal PGA = 0.5 g, vertical PGA = 0.33 g

Isolation system	A	B	C	D	E	F	G
1	0.14	0.14	0.33	0.17	0.16	0.16	0.79
2	0.27	0.76	4.40	1.76	0.31	0.92	1.45
3	0.18	0.58	2.48	1.40	0.14	0.56	1.08
4	0.36	1.05	5.79	2.48	0.42	1.17	1.77
5	0.26	0.75	4.32	1.77	0.29	0.90	1.42
6	0.19	0.32	1.97	0.65	0.18	0.27	0.46
7	0.39	0.69	5.37	1.57	0.26	0.46	1.15

(b) Horizontal PGA = 1.0 g, vertical PGA = 0.67 g

1	0.27	0.29	0.66	0.34	0.32	0.31	1.57
2	0.73	1.27	7.65	3.00	1.01	1.58	2.41
3	0.27	0.77	3.27	1.84	0.25	0.72	1.76
4	0.63	1.51	8.54	3.55	0.81	1.68	2.64
5	0.56	1.10	6.34	2.59	0.69	1.30	2.25
6	0.39	0.64	3.93	1.29	0.36	0.54	0.92
7	0.39	0.84	6.00	1.92	0.28	0.55	1.13

Shear walls are key components of the seismic force-resisting system in all NPPs. These walls may be required to provide functional confinement for some advanced and micro reactor designs, requiring earthquake-induced damage to be minimal and crack widths to be small. To gage the effect of isolation-system choice on the seismic response of the isolated superstructure, net shearing forces V, in both the x and y directions, in the two safety-related perimeter walls (normal to the y and x directions, respectively), immediately above the basemat, are reported. Table E.5 presents mean maximum shearing forces in kN (rounded to the nearest 100), % of the reactive building weight W = 8920 tonnes, and average in-plane shear stress τ in the MPa. The presented results in the two directions are similar for each system and shaking level. Note that the limiting design shear stress per ACI 318-19 (2019) is 2.62 MPa (= 380 psi) for 4000 psi concrete. The in-plane shear stress is computed by dividing a half of the reported shearing force ($0.5V$; two walls in each direction) by the wall length (25 m) and thickness (1.2 m), where the wall thickness was sized here for protection against wind-borne missiles. All in-plane shear stresses presented in Table E.5 are significantly less than the limiting design value of 2.62 MPa per ACI 318-19 (2019), making clear that no

seismic penalty is incurred for the construction of the shear walls in the reactor building, if isolated with any of the seven systems considered here.

Data such as that presented in Figure E.4 and Table E.2 through Table E.4 could inform the design of equipment and guide the selection of an isolation system. Alternate outcomes from those presented above will result from analysis of different a) buildings and equipment, b) seismic hazard and soil type, and c) isolation systems (e.g., 2D 3-second linear, 2D 2-second bilinear (lead-rubber), 2D 2-second bilinear (sliding) with alternate 1D nonlinear fluid viscous dampers, 3D hybrid isolation system with vertically guided spring isolators and alternate 1D nonlinear fluid viscous dampers).

The goal of the above presentation was to make clear that isolation systems have different attributes (e.g., larger isolation-system displacements versus smaller accelerations in equipment). Knowledge of equipment capacities and clearance of the isolated building from adjacent construction, among other factors, may lead an analyst to choose one isolation system over others, supported by analysis such as that presented above. The cost of the isolation system and the supporting substructure may too be a consideration.

Section E.2.3 compares responses of different isolation systems, again, not with the goal of recommending one system over others but rather to provide some insight to a reader with limited experience in the design of seismic isolation systems.

Table E.5. Mean maximum shearing forces in perimeter walls, 30 inputs, seven isolation systems per Section E.2.1

(a) Horizontal PGA = 0.5 g, vertical PGA = 0.33 g

	x			*y*		
Isolation system	V (kN)	$\%W$	τ (MPa)	V (kN)	$\%W$	τ (MPa)
1	6,400	7	0.11	6,400	7	0.11
2	5,500	6	0.09	5,500	6	0.09
3	4,500	5	0.08	4,500	5	0.08
4	6,300	7	0.11	6,400	7	0.11
5	4,700	5	0.08	4,700	5	0.08
6	7,900	9	0.13	8,100	9	0.13
7	5,300	6	0.09	5,300	6	0.09

(b) Horizontal PGA = 1.0 g, vertical PGA = 0.67 g

1	12,800	15	0.21	12,800	15	0.21
2	12,400	14	0.21	12,900	15	0.21
3	9,300	11	0.16	9,300	11	0.15
4	11,300	13	0.19	11,500	13	0.19
5	8,500	10	0.14	8,900	10	0.15
6	15,800	18	0.26	16,100	18	0.27
7	11,000	13	0.18	10,800	12	0.18

E.2.3 Comparison between responses for different isolation systems

Some of the responses of the isolated buildings are compared below for systems 1 through 7 using the data presented in Table E.1, Table E.2 and Table E.3. Spectra for the 7 systems are extracted from Figure E.4 to enable the comparison. The shaking is represented by horizontal PGA = 1 g and vertical PGA = 0.67 g, unless noted otherwise.

System 1 versus system 2

Systems 1 and 2 are 2-sec linear and nonlinear systems, respectively. The maximum horizontal displacement of the nonlinear system is substantially smaller than that of the linear isolation system. This outcome is expected because the equivalent viscous damping in a bilinear isolation system (system 2) at small displacements is much greater than 5% (system 1). The peak horizontal accelerations for system 2 at all 7 monitoring locations are equal to or greater than those for system 1. Figure E.5 presents the mean of

the 30 geomean spectra at the center of the basemat (location A) and the reactor head (location B) for the two systems, horizontal PGA=1 g, and 5% of critical damping. The spectral demands for system 2 are greater than those for system 1 for frequencies higher than 1.5 Hz at both monitoring locations. For system 1, the spectra at locations A and B are essentially identical, both of which peak at the isolation-system frequency of 0.5 Hz. For system 2, the basemat spectrum peaks at 0.5 Hz (the frequency associated with sliding of the isolation system) and between 10 and 30 Hz. The spectrum at location B, the reactor head, peaks for system 2 at the first mode frequency of the reactor vessel (= 12 Hz), which amplifies the horizontal acceleration at location C, 10-Hz oscillator on the reactor head.

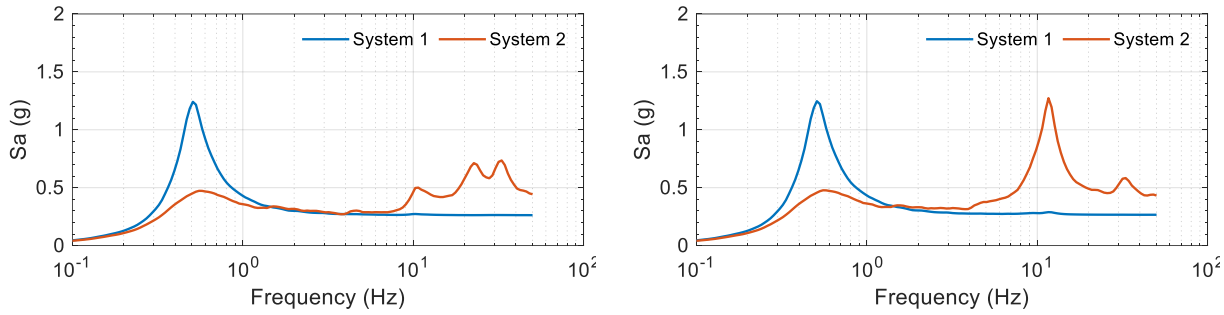

(a) basemat, location A (b) reactor head, location B

Figure E.5. Mean acceleration spectra (Sa) for the 30 inputs, geomean horizontal, two locations, systems 1 and 2, 5% of critical damping, horizontal PGA=1 g, vertical PGA = 0.67 g

System 1 versus system 3

System 3 is composed of the 2-sec linear isolators of system 1 and nonlinear FVDs. The addition of the dampers reduces the isolation-system displacements by a factor of approximately 1.6. The peak horizontal accelerations are reduced at locations A, B, E, F, and G by the addition of the dampers, but are increased at the remaining 2 monitoring locations: 10-Hz and 20-Hz oscillators on the reactor head (C and D). Figure E.6 presents the mean of the 30 geomean spectra at the center of the basemat (location A) and the reactor head (location B) for the two systems. Per Figure E.6, the dampers reduce the spectral demand on the basemat (location A) for frequencies ranging between 0.1 and 50 Hz. On the reactor head, the dampers suppress the acceleration at the isolation frequency (= 0.5 Hz) but increase the spectral demand for frequencies between 8 and 19 Hz. The mean maximum aggregate force in the 17 isolators is 23,000 kN and 13,000 kN for systems 1 and 3, respectively, in each horizontal direction. The mean maximum aggregate force in the 4 dampers along a horizontal axis in system 3 is 4,300 kN.

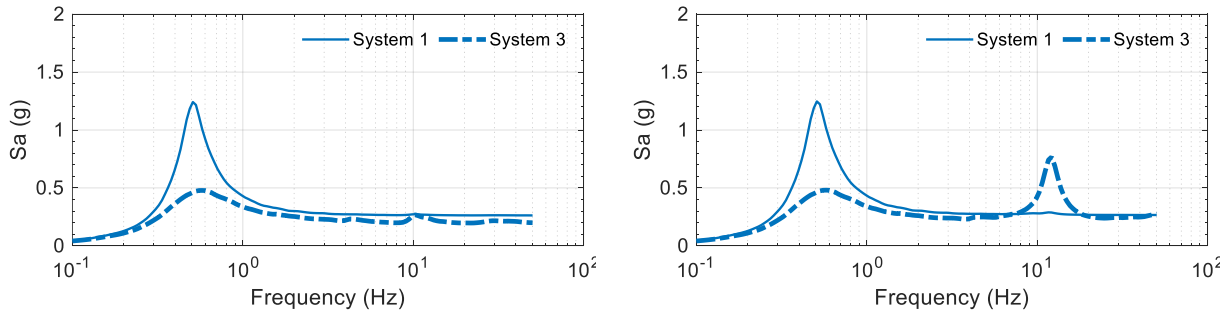

(a) basemat, location A (b) reactor head, location B

Figure E.6. Mean acceleration spectra (Sa) for the 30 inputs, geomean horizontal, two locations, systems 1 and 3, 5% of critical damping, horizontal PGA=1 g, vertical PGA = 0.67 g

System 2 versus system 4

The addition of nonlinear FVDs to system 2 (resulting in system 4) reduces the already small horizontal displacements by a factor of approximately 1.6. Maximum accelerations are generally smaller for system 4. Figure E.7 presents the mean of the 30 geomean spectra at locations A and B for the two systems. The secant stiffness on the bilinear *F-u* relationship, namely K_{eff} of Figure 4.6, is a function of the horizontal displacement, which changes at each time step for a given input. The value of K_{eff} is similar to the first-slope stiffness, K_1, at a small displacement, and similar to $K_{iso,h}$ at a large displacement. The frequencies associated with K_1 and $K_{iso,h}$ are 4 and 0.5 Hz, respectively. The change in K_{eff}, between K_1 and $K_{iso,h}$, affects spectral shape, as evident in Figure E.7. The isolation-system displacement for system 4 is small (= 99 mm), and so the effect of K_1 on the spectral shape is greater than for system 2. Accordingly, the spectral ordinate for system 4 is smaller at 0.5 Hz (associated with $K_{iso,h}$) at both locations A and B. The first spectral peak on the basemat shifts from 0.5 Hz (system 2) to 2 Hz (system 4) because the isolation-system displacements are smaller for system 4. The mean maximum aggregate force in the 17 isolators is 22,000 kN (23,000 kN) and 17,000 kN (17,000 kN) for systems 2 and 4, respectively, in the *x* (*y*) direction. The mean maximum aggregate force in the 4 *x*- (*y*-) directional VDDs in system 4 is 3,900 kN (4,000 kN).

System 2 versus system 5

Systems 2 and 5 are composed of nonlinear isolators with $T_{iso,h}$ = 2 and 3 seconds, respectively. The mean maximum horizontal isolation-system displacements increase with $T_{iso,h}$. The mean maximum horizontal accelerations at the seven monitoring locations for system 5 are equal to or less than that for system 2.

Figure E.8 presents the mean of the 30 geomean spectra at locations A and B for systems 2 and 5. The spectral demands are smaller for the 3-second sliding isolation system.

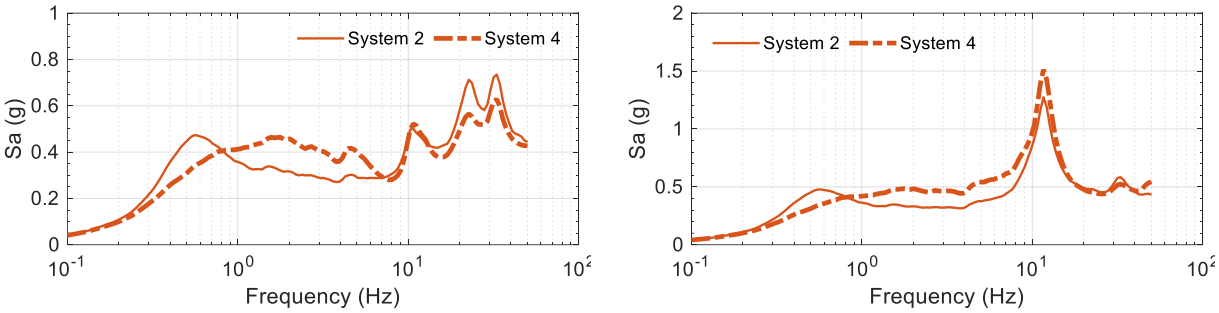

(a) basemat, location A (b) reactor head, location B

Figure E.7. Mean acceleration spectra (Sa) for the 30 inputs, geomean horizontal, two locations, systems 2 and 4, 5% of critical damping, horizontal PGA=1 g, vertical PGA = 0.67 g

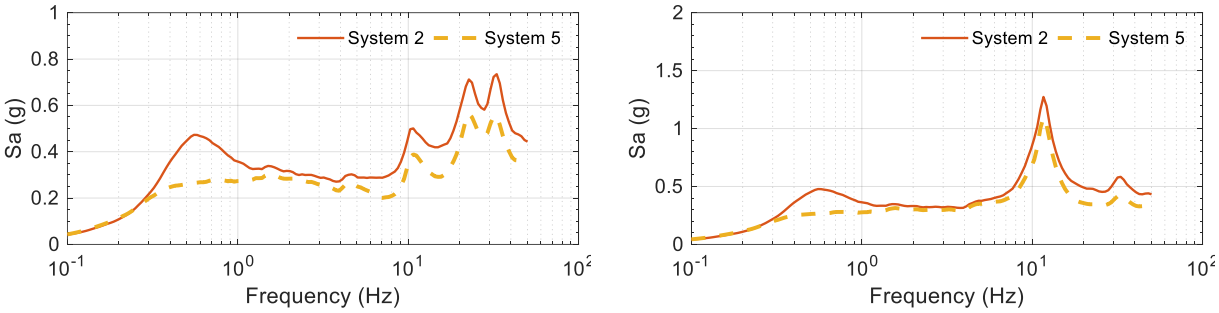

(a) basemat, location A (b) reactor head, location B

Figure E.8. Mean acceleration spectra (Sa) for the 30 inputs, geomean horizontal, two locations, systems 2 and 5, 5% of critical damping, horizontal PGA=1 g, vertical PGA = 0.67 g

System 1 versus system 6

System 1 is a 2D linear system with $T_{iso,h} = 2$ seconds. System 6 is a 3D linear system with $T_{iso,h} = 1.1$ seconds and $T_{iso,v} = 0.4$ second. Because the horizontal period of system 6 is less than that for system 1 and is more heavily damped than system 1, the isolation-system displacement is much smaller. Conversely, the peak horizontal accelerations at all monitoring locations except for G are greater for system 6. Location G is a point of attachment of the bridge crane to the steel frame, where the horizontal response is affected by a breathing mode that is excited by the vertical shaking. The peak horizontal acceleration at location G is much smaller for system 6 because vertical isolation is provided, and the breathing mode is suppressed.

The peak vertical accelerations at all monitoring locations are smaller for system 6. Figure E.9 presents the mean of the 30 geomean horizontal and vertical spectra at locations A and B for systems 1 and 6. The horizontal spectral demands for system 6 are greater than those for system 1 at the two locations for frequencies between 0.7 and 50 Hz, but the vertical spectral demands are substantially smaller for frequencies between 4 and 50 Hz. Note that the horizontal spectral demands for both systems are less than the input horizontal PGA (= 1 g) for frequencies greater than 1 Hz.

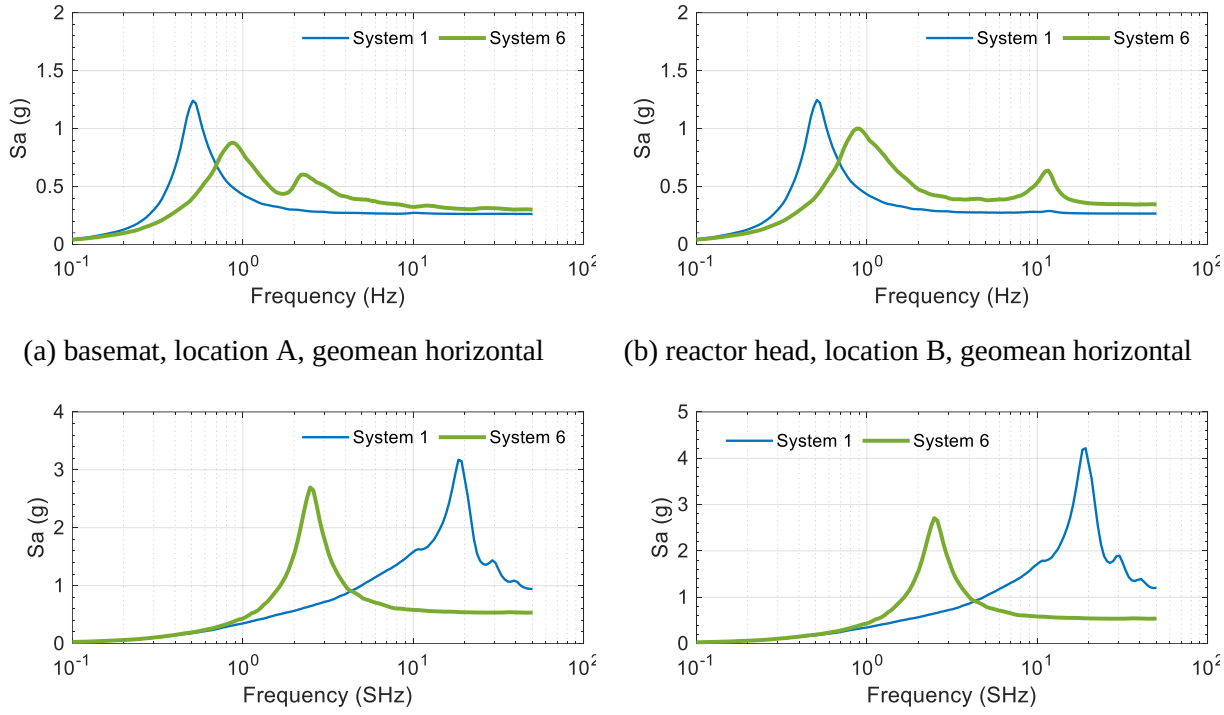

(a) basemat, location A, geomean horizontal

(b) reactor head, location B, geomean horizontal

(c) basemat, location A, vertical

(d) reactor head, location B, vertical

Figure E.9. Mean acceleration spectra (Sa) for the 30 inputs, two locations, systems 1 and 6, 5% of critical damping, horizontal PGA=1 g, vertical PGA = 1 g

System 2 versus system 7

System 7 uses the 2-sec nonlinear isolators of system 2 in the horizontal plane, and 0.4-sec guided spring isolators and nonlinear FVDs for isolation in the vertical direction. The horizontal displacements of systems 2 and 7 are virtually identical, which is an expected outcome. The peak vertical accelerations are smaller in system 7 because it is isolated and damped in that direction. The peak horizontal accelerations are generally smaller for system 7 because these responses are related to Q for the sliding isolators (see Figure 4.6), which is a function of the instantaneous vertical load, namely, gravity ± earthquake loading. (The amplitude

of the vertical earthquake shaking is mitigated by the vertical isolation system that forms part of system 7, reducing the variation in Q and the transmitted acceleration.)

Figure E.10 presents the mean of the 30 geomean horizontal and vertical spectra at the center of the basemat (location A) and the reactor head (location B) for the two systems. The fluctuations in the vertical load (i.e., gravity ± earthquake) on the sliding isolators, which affects Q and in turn the horizontal response, is associated with the vertical isolation frequency of 2.5 Hz. Accordingly, the horizontal spectrum on the basemat (location A) for system 7 peaks at both 0.5 and 2.5 Hz, which are the horizontal and vertical isolation frequencies, respectively. The horizontal spectral demands on the reactor head for system 7 are equal to or smaller than those for system 2. The vertical spectra for system 7 peak at the isolation frequency of 2.5 Hz (=1/$T_{iso,v}$), and the spectral demands are lower than those for system 2 for frequencies higher than 4 Hz, at both locations A and B. The peaks in the vertical spectra for system 2, evident in Figure E.10c and d, result from the alignment of vertical frequencies of the isolated building with the peak ordinates of the vertical UHRS, as noted in Section E.2.2.

E.3 Closing Remarks

The mechanical properties of the seven isolation systems considered here vary widely and so it is not surprising that peak horizontal and vertical displacements and accelerations, for the same seismic inputs, do too. All seven isolation systems considered here could be used to base isolate a reactor building. The cost of the isolation system is not addressed but is not expected to be significant, as a fraction of the construction cost, and likely of the same order or less than that of the conventional substructure supporting the isolation system.

The major challenge to choosing an isolation system is the identification of building design constraints, which are termed design spaces in Parsi *et al.* (2020). Possible building design constraints include:

- A standardized reactor building and equipment, of a design certified by the USNRC for prescribed inputs described by horizontal and vertical acceleration response spectra
- Maximum horizontal clearance to adjacent construction
- Maximum horizontal and vertical accelerations of previously qualified safety-class equipment (e.g., reactor vessels, head-mounted equipment such as control-rod drive mechanisms and pumps)

Once building design constraints are established, alternate isolation systems can be investigated for a given site and seismic hazard. The goal of this appendix was to illustrate tradeoffs between in-structure accelerations of building framing and equipment, and displacements of the isolation system. The merits of

adding FVDs to the isolation system were identified, with positive, albeit different outcomes for use with linear and nonlinear 2D isolation systems. Three-dimensional isolation systems, either proprietary (system 6) or customized (system 7) are effective at mitigating the effects of vertical earthquake shaking, which may be more damaging than horizontal shaking for some equipment and reactor geometries.

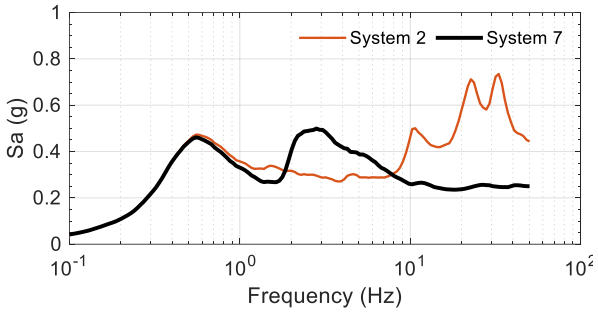

(a) basemat, location A, geomean horizontal

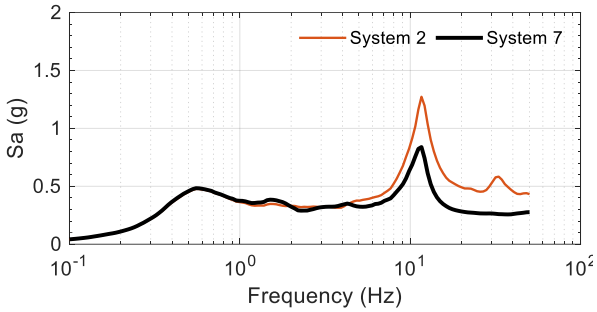

(b) reactor head, location B, geomean horizontal

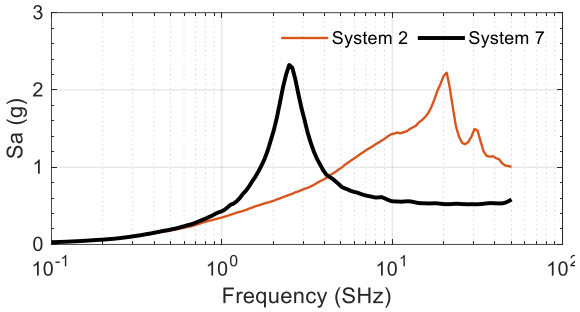

(c) basemat, location A, vertical

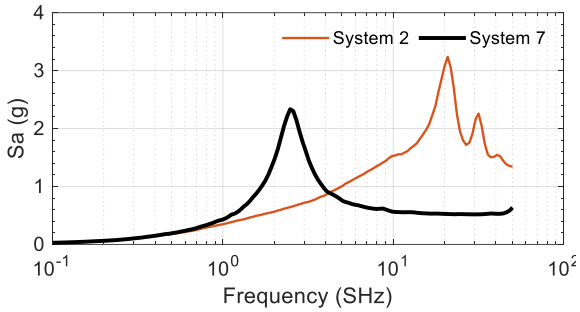

(d) reactor head, location B, vertical

Figure E.10. Mean acceleration spectra (Sa) for the 30 inputs, two locations, systems 2 and 7, 5% of critical damping, horizontal PGA=1 g, vertical PGA = 0.67 g

E.4 References

American Concrete Institute (ACI) (2019). "Building code requirements for structural concrete and commentary." *ACI 318-19*, ACI, Farmington Hills, IL.

American Society of Civil Engineers (ASCE) (2021). "Seismic design criteria for structures, systems, and components in nuclear facilities." *ASCE/SEI 43-19*, ASCE, Reston, VA.

Computers and Structures (CSI) (2020). "SAP2000 Version 22.1.0." CSI, Walnut Creek, CA.

Parsi, S.S., Lal, K.M., Shirvan, K., Kosbab, B.D., Cohen, M., Kirchman, P., and Whittaker, A.S. (2020). "Equipment-level seismic protective systems for advanced nuclear reactors." *Proceedings, 17th World Conference on Earthquake Engineering (WCEE)*, Sendai, Japan.

APPENDIX F
CONSIDERATIONS FOR INSPECTIONS, TESTS, ANALYSES, AND ACCEPTANCE CRITERIA

F.1 Introduction

A combined license (COL) issued under 10 CFR Part 52 enables a licensee to construct a NPP and to operate it once construction is complete if certain standards identified in the COL are satisfied. These standards are called Inspections, Tests, Analyses, and Acceptance Criteria (ITAAC). As required by 10 CFR 52.97(b), the ITAAC identified in the COL are necessary and sufficient, when successfully completed by the licensee, to provide reasonable assurance that the facility has been constructed and will operate in conformity with the COL, the provisions of the Atomic Energy Act of 1954, as amended, and the rules and regulations of the US Nuclear Regulatory Commission (NRC). Generally speaking, a COL includes the ITAAC submitted in the COL application and any ITAAC from referenced early site permits and standard design certifications.

The overriding purpose of ITAAC is to give the regulator and the public confidence that a nuclear plant licensed under 10 CFR Part 52 was built following the information reviewed and approved by the NRC. The ITAAC identify key attributes promised by the design description used by the NRC to make their safety determination.

F.2 Intersection of ITACC and Seismic Isolation Devices

The Westinghouse AP1000 Design Control Document, Rev. 19, Tier 1, Section 3.3 – Non-System Based Design Descriptions and ITAAC – Buildings (USNRC 2011) provides one framework to accommodate inspections, tests, analyses, and/or acceptance criteria for seismic isolation systems and associated components. Because seismic isolators and VDDs would be part of the Seismic Category I structure in an isolated NPP, much of the content in Section 3.3 of the AP1000 Design Control Document would already be directly applicable.

Table 3.3-6 of USNRC (2011), Inspections, Tests, Analyses, and Acceptance Criteria would have addressed the seismic isolation system (if included in the AP1000) via ITAAC 2.a.i.d for the design of the seismic isolation system and ITAAC 13 for sufficient separation of the isolated building from adjacent construction, to enable its unrestricted motion during earthquake shaking.

If details on the seismic isolation system (i.e., seismic isolators and VDDs) and associated components are to be included in both the Tier 1 design description (e.g., Section 3.3 of USNRC (2011)) and as an ITAAC,

the design of the seismic isolation system must be completed before any details are added to the ITAAC. Any change to Tier 1 content after issuance of a COL requires the approval of a regulation exemption by the Presidentially appointed Commissioners, which is increases project risk, cost, and construction schedule beyond changes that can be approved alone by the NRC staff. The process described in Section 5 of this topical report could be used to establish the minimum required clearances between an isolated building and any adjacent construction, to be confirmed via ITAAC. Lessons learned from recent nuclear builds in the US have made clear the importance of not imposing tolerances and dimensional constraints on civil structures components tighter than those effectively used in non-nuclear construction, and this applies to components attached to or supporting isolators and VDDs. One pathway would be to specify the number of each type of isolator and/or VDD, and provide a marking plan for their installation, so that the Acceptance Criteria could be objectively satisfied and easily checked by the NRC resident inspectors. What must be avoided for seismic isolation systems and associated components is a table of ITAAC information that would require detailed surveys and precision measurement equipment, which would add a significant burden of increased construction time and cost but with no improvement in construction quality and operational performance under operational and extreme loadings.

F.3 Considerations for Technical Specifications related to Seismic Base Isolation Equipment

As required by 10 CFR 50.36, a nuclear plant licensee must provide technical specifications as part the license application and these technical specifications will become an attachment to the license when it is granted. Technical specifications define the limits of plant operation to ensure that the plant is operated within the boundaries established by the Safety Analysis and establish requirements for items such as safety limits, limiting safety system settings, limiting control settings, limiting conditions for operation, surveillance requirements, design features, and administrative controls.

Based upon industry examples, such as the Westinghouse AP1000 Standard Technical Specifications (STS) presented in NUREG-2194 Volume 1 (USNRC 2024), a seismic isolation system (i.e., seismic isolators and VDDs) and associated components need not be explicitly addressed in a plant's Technical Specifications. For example, the AP1000 STS does not generally address non-active (i.e., passive) structural elements and all the seismic isolators and VDDs introduced in this report are passive. In practice, structural elements forming Seismic Category I structures, which would like include seismic isolators and VDDs if deployed, will generally be monitored under one or more ongoing plant engineering programs such as a structural monitoring program or an aging management program associated with a planned and/or issued license renewal.

F.4 References

US Nuclear Regulatory Commission (USNRC) (2011). "Westinghouse AP1000 Design Control Document, Rev. 19, Tier 1, Section 3.3 – Non-system based design descriptions and ITAAC – buildings." *(ML11171A319)*, Rockville, MD.

US Nuclear Regulatory Commission (USNRC) (2024). "Standard technical specifications, Westinghouse Advanced Passive 1000 (AP1000) plants." *NUREG-2194, Vol. 1, Rev 1. (ML24026A214)*, Rockville, MD.

APPENDIX G
MUSINGS ON SELECTING A TARGET PERFORMANCE GOAL FOR A SEISMIC ISOLATION SYSTEM

G.1 Introduction

Ideally, the risk target for a seismic isolation system supporting a reactor building should be based on a Level 3 seismic probabilistic risk assessment[28] (SPRA) of the plant, but these are not yet available for advanced and micro reactors. However, the mean annual frequencies assigned to the surrogates for seismic core damage and seismic large early release frequency for advanced and micro reactors are anticipated to be smaller than those values attached to the large light water reactors (LLWRs) in the current US operating fleet because the new designs will take advantage of:

- Smaller inventories of radioactive material compared to LLWRs,
- Use of accident-tolerant fuel, and/or
- Operation at or near atmospheric pressure.

For advanced and micro reactor designs relying upon inherent features and or passive systems for safety, the internal event frequencies for the advanced-reactor surrogates for core damage and large early release may be notably lower than those for large LWRs. If the internal event frequencies of a reactor design are sufficiently low, the risk profile may be shifted such that external hazards, such as earthquakes and extreme winds, will be the dominant contributors to the core damage and large-early-release frequencies.

Sections G.2 and G.3 describe possible pathways to select a target performance goal for a seismic isolation system in the absence of a level 3 PRA. Section G.2 treats the seismic isolation system as an SSC (structure, system, and component) per ANS standards and ASCE/SEI 43-19 (ASCE 2021). Section G.3 enables an order-of-magnitude, *preliminary* estimate to be made of the target performance goal (TPG) for an isolation system, wherein much of the plant-level risk is assigned to the isolation system because the implementation of an isolation system substantially reduces seismic demands on SSCs in the superstructure, reducing the mean annual frequency of core damage and large early release, or their advanced-reactor surrogates, due to failure of superstructure SSCs. Section G.3 is not intended to replace a level 3 PRA.

[28] https://www.nrc.gov/about-nrc/regulatory/risk-informed/pra.html

G.2 Isolation System Treated as an SSC

One product of a seismic probabilistic risk assessment of an isolated reactor building will be the assignment of a seismic design category (SDC) or a TPG to the isolation system, treating it no differently than any other SSC in the nuclear power plant. Per Table 1-1 of ASCE /SEI 43-19 (ASCE 2021), reproduced below as Table G.1, the assigned SDC determines the level of ground shaking used to design the SSC per consensus standards such as those promulgated by the American Society of Civil Engineers (for isolators and dampers), the American Concrete Institute (for reinforced and prestressed concrete), the American Institute for Steel Construction (structural steel), and the American Society of Mechanical Engineers (mechanical components such as reactor vessels).

A SDC maps to a TPG, P_F, which is expressed as a mean annual frequency (MAF) of unacceptable performance, where performance is user specified. Although convenient and traditional, it is not necessary to attach an SDC to the isolation system, because Section 5 of this report accommodates any value of the TPG.

Parenthetically, the TPG assigned to the isolation system should generally equal or be smaller than that for all SSCs in the isolated reactor building. For example, if the highest SDC assigned to an SSC in the isolated reactor building is 3, the TPG assigned to the isolation system shall be no greater than 1×10^{-4} (or SDC 3). To do otherwise would require analysis of the isolated building for more intense shaking than that used to size the isolation system that protects the supported SSCs.

Table G.1. Seismic design categories per ASCE/SEI Standard 43-19, adapted from Table 1-1 in ASCE (2021)

	Seismic design category			
	2	3	4	5
Target performance goal	4×10^{-4}	1×10^{-4}	4×10^{-5}	1×10^{-5}
DBE response spectrum or acceleration time series	SF × UHRS; Chapter 2 in ASCE 43			

G.3 Target Performance Goal for an Isolation System Based on Quantitative Health Objectives

G.3.1 Introduction

One pathway to establishing a risk target for a seismic isolation system is to base the value on an acceptable plant-level risk, which can be determined by Level 1 (frequency of accidents that cause damage to the reactor core—that is, core damage frequency), Level 2 (frequency of accidents that release radionuclides from the reactor building), and Level 3 (consequences of the release of radionuclides) Probabilistic Risk

Assessments[29](PRAs). Level 3 PRAs for advanced and micro reactors are not yet available. An alternate, interim pathway is presented below, building on an NRC-accepted approach for LLWRs, but recognizing the attributes of many advanced and micro reactors and setting aside worst-case scenarios. The discussion presented below is not intended to replace a Level 3 PRA but rather to enable the calculation of a preliminary estimate of a target performance goal for a seismic isolation system.

In 2002, the USNRC published Appendix C, Quantitative Guidelines from the Framework for Risk-Informing 10 CFR Part 50[30] (USNRC 2002). The guidelines introduce quantitative health objectives (QHOs) and describe them as the basis for judging the effectiveness of NRC regulations, which at the time addressed LLWRs only. The guidelines write "Unfortunately, the QHOs are difficult to apply in making risk-informed changes to the [then] existing regulations. Therefore, the following two numerical objectives were adopted in Regulatory Guide 1.174 (NRC 1998) as surrogates for the two QHOs:

- A core damage frequency (CDF) of $<10^{-4}$ per year as a surrogate for the latent cancer QHO [$= 2 \times 10^{-6}$ per year]
- A large early release frequency (LERF) of $<10^{-5}$ per year as a surrogate for the early fatality QHO [$= 5 \times 10^{-7}$ per year]

Appendix C in USNRC (2002) demonstrates how the two goals were derived from the QHOs. Results presented below utilize the process presented in Appendix C of USNRC (2002) to derive a risk target for a seismic isolation system, noting that the advanced and micro reactors have numerous safety attributes (e.g., one or more of accident tolerant fuels, non-water coolants, low operating pressures, much less nuclear fuel, and passive safety systems) that the LLWRs considered in the development of Appendix C in USNRC (2002) were not equipped with (e.g., Surry Unit 1, referenced in NUREG/CR-4551 (USNRC 1993), a 855 MWe Westinghouse Pressurized Water Reactor, operating license May 1972).

The QHOs provide quantitative guidelines in terms of the risk of radiation exposure to public. Mubayi and Youngblood (2019) reflected on the QHOs, acknowledged zero fatalities attributed to the release of radioactive materials from the 2011 Fukushima Daichi accident, noted that the Fukushima outcomes would have satisfied the NRC health-related safety goals, but did not propose changes to the QHOs.

[29] https://www.nrc.gov/about-nrc/regulatory/risk-informed/pra.html

[30] https://www.nrc.gov/docs/ML0221/ML022120663.pdf

The calculations presented below provide a starting point for analyzing and designing an isolation system for an advanced or micro reactor by providing an order of magnitude estimate for the seismic risk target for an isolation system.

G.3.2 Latent cancer fatality QHO

Appendix C.3 in USNRC (2002) notes that "Even at a densely populated US site, if the plant's core damage frequency is 10^{-4} or less, the latent cancer fatality QHO is generally met with no credit for containment." Core damage can be associated with internally initiated accident sequences (e.g., for Surry 1, station blackout, loss of coolant accidents, anticipated transients without scram, other transients, and steam generator tube rupture) and externally initiated accident sequences (e.g., seismic, fire). Other external event sources were excluded from the Surry 1 analysis because of the low frequency of the initiating event (i.e., aircraft (accidental) crashes, hurricanes, tornadoes, external flooding).

The individual latent risk (ILR) is calculated, per Equation 6 of Appendix C in USNRC (2002), as the product of the CDF (considering open containment) and the conditional probability of an individual becoming a latent cancer fatality (CPLF). Values for CPLF were reported for LLWRs in NUREG 1150. A Surry value for CPLF of 4×10^{-3} was used for calculations, corresponding to a large opening in containment and a very large release. Such worst-case scenarios are extraordinarily unlikely in a passively safe advanced reactor incorporating accident tolerant fuels, non-water coolants, and operating near atmospheric pressure, and enclosed by a robust reinforced concrete confinement structure, designed to resist wind-borne missiles impacting at high velocity. Per Appendix C in USNRC (2002), the individual latent risk corresponding to a CDF = 10^{-4} per year is 4×10^{-7} per year and substantially smaller, by a factor of 5, than the latent cancer QHO (2×10^{-6}). Put differently, if the core damage frequency = 5×10^{-4} per year, ILR = $5 \times 4 \times 10^{-7}$ per year = 2×10^{-6} per year = latent cancer fatality QHO.

Setting aside the attributes of advanced and micro reactors identified previously, accepting the unrealistic worst-case scenarios, and ignoring the smaller volumes of nuclear fuel in advanced reactors, the total CDF in an isolated advanced reactor, if less than 5×10^{-4} would achieve the latent cancer QHO. Unlike LLWRs in the operating fleet, the CDF surrogates for many advanced reactors, associated with internally initiated events, are orders of magnitude smaller than those associated with externally initiated events such as earthquakes and fires and can be ignored for preliminary risk calculations. Accordingly, the CDF for externally initiated events is set equal to the total CDF. For an advanced reactor sited beyond a flood zone, and equally weighting CDF due to seismic and fire, the seismic CDF for an isolated advanced reactor should

be no greater than 2.5×10^{-4}, with significant increases possible if the worst-case scenarios are replaced by realistic scenarios backed by risk assessment.

Possible contributors to the seismic CDF in an isolated advanced reactor are 1) failures of structures, systems, and components (SSCs) above the basemat, computed using traditional PRA techniques, and 2) failure of the isolation system to serve its intended function. The implementation of seismic isolation can drastically reduce earthquake demands on structures, systems, and components, and the risk of their failure (Huang *et al.*, 2008). If core damage due to failure of SSCs can be limited to 1×10^{-4}, the seismic risk target for the isolation system, to achieve the latent fatality QHO, need to be no less than 1.5×10^{-4} ($=2.5 \times 10^{-4} - 1 \times 10^{-4}$) , even if the volume of nuclear material at risk is identical to that in a LLWR.

Based on these arguments, a *preliminary* seismic risk target for an isolation system in an advanced or micro reactor building, based on the latent fatality QHO, could be taken as 1.5×10^{-4}.

G.3.3 Early fatality QHO

Appendix C.4 in USNRC (2002) notes that "The early fatality QHO is more restrictive than the latent cancer QHO. If the plant's LERF is 10^{-5} or less, the early fatality QHO is generally met." The concept of large early release was attached to large light water reactors (i.e., PWRs and BWRs), with a relatively large inventory of traditional nuclear fuel contained in a pressurized reactor. In contrast, many advanced and micro reactors use smaller volumes of accident tolerant fuels, non-water coolants, and operate at near atmospheric pressure, making a release on the scale of a legacy nuclear reactor impossible.

Equation 2 in Appendix C.2 in USNRC (2002), and Equations 7 and 8 in Appendix C.4 in USNRC (2002), provide a process to derive a limiting value of LERF and CDF given an early fatality QHO, or individual early risk (IER) of 5×10^{-7}.

The IER is taken as the product of the conditional probability of an individual becoming a prompt (or early) fatality (CPEF) and the frequency of a large early release capable of causing early fatalities (LERF), summed across all accident sequences. Assuming one accident sequence (e.g., seismic) dominates early fatality risk and LERF, LERF can be calculated as the product of the CDF and the conditional large early release probability (CLERP) for that accident sequence. Herein, it is assumed that the LERF for internal initiating events for advanced reactors is negligible for the purpose of risk calculations and the dominant external initiating event, in terms of LERF, is earthquake shaking. Fire is another external initiating event, but it is assumed here that confinement will not be meaningfully breached by fire and the core will not be damaged.

The calculation of Appendix C.4 in USNRC (2002) for large light water reactors assumed the worst case (and unrealizable) scenarios of a) open containment, and b) "all of the conditions necessary for a large early release", and CLERP was set equal to 1.0. Accordingly, core damage was assumed therein to translate directly to a large early release, namely, CDF = LERF.

For advanced and micro nuclear reactors, with their fuel types and *small* fuel volumes, coolants, and operating pressures identified above, passive safety features, and a functional reinforced concrete building envelope (confinement), sized at a minimum for wind-borne missile impact, CLERP is set equal here to 0.25 and LERF = $0.25 \times$ CDF.

Values for CPEF do not exist for advanced or micro reactors, released radionuclides, and modern evacuation outcomes. In Appendix C.4 of USNRC (2002), values for CPEF were taken from the Surry report (NUREG/CR-4551) referenced above (USNRC 1993). The reported largest value of CPEF for an internal initiator in Table 4.3-1 of that NUREG/CR is 3×10^{-2}. (The maximum value in Rev 1 of NUREG/CR-4551, column 6, source term SUR-07-02, is 3.73×10^{-2}.) Appendix C.4 reports that this value of CPEF "corresponds to a large opening in containment and a very large release that is assumed to occur early before effective evacuation of the surrounding population", which is another worst-case scenario. (The highest value of CPEF for a seismic initiator using the EPRI hazard description, in Tables 4.3-5 and 4.3-6 is 4.7×10^{-2} for source term SRD-11-2.) Assuming no large openings in the reinforced concrete building envelope, and the attributes of advanced and micro reactors identified previously, a value of 1×10^{-2} is assigned here to CPEF.

If the total seismic CDF is 2×10^{-4}, composed of equal contributions from the isolation system (= 1×10^{-4}) and the SSCs (= 1×10^{-4}) in the isolated building, LERF is $0.25 \times$ CDF per the assumptions above, and CPEF is 1×10^{-2}, IER is equal to $(2 \times 10^{-4}) \times 0.25 \times (1 \times 10^{-2}) = 5 \times 10^{-7}$, which is the early fatality QHO.

Accordingly, to meet the early fatality QHO, a *preliminary* seismic risk target of 1×10^{-4} could be assigned to an isolation system in an advanced or micro reactor building.

G.4 Summary

Sections G.3.2 and G.3.3 present information that could be used to develop a preliminary target performance goal for a seismic isolation system based on the established QHOs: 1.5×10^{-4} for latent fatality and 1×10^{-4} for early fatality. Accordingly, a preliminary target performance goal of 1×10^{-4} could be assigned to an isolation system, meeting both QHOs.

G.5 References

American Society of Civil Engineers (ASCE) (2021). "Seismic design criteria for structures, systems, and components in nuclear facilities." *ASCE/SEI 43-19*, Reston, VA.

Huang, Y. N., Whittaker, A. S., and Luco, N. (2008). "Performance assessment of conventional and base-isolated nuclear power plants for earthquake and blast loadings." *MCEER-09-0019*, University at Buffalo, Buffalo, NY.

Mubayi, V. and Youngblood, R. (2019). “Re-evaluating the current safety goals.” *INL/CON-19-52120-Revision-0,* Idaho National Laboratory, Idaho Falls, ID.

US Nuclear Regulatory Commission (USNRC) (2002). "Appendix C: Quantitative guidelines from the framework for risk-informing 10 CFR part 50." *10 CFR 50.46/GDC 35, Rev. 1*, USNRC, Rockville, MD.

US Nuclear Regulatory Commission (USNRC) (1993).”Evaluation of severe accident risks: methodology for the containment, source term, consequence, and risk integration analyses.” *NUREG/CR-4551*, Rockville, MD.

MCEER Technical Reports

MCEER publishes technical reports on a variety of subjects written by authors funded through MCEER. These reports can be downloaded from the MCEER website at http://www.buffalo.edu/mceer. They can also be requested through NTIS, P.O. Box 1425, Springfield, Virginia 22151. NTIS accession numbers are shown in parenthesis, if available.

NCEER-87-0001 "First-Year Program in Research, Education and Technology Transfer," 3/5/87, (PB88-134275, A04, MF-A01).

NCEER-87-0002 "Experimental Evaluation of Instantaneous Optimal Algorithms for Structural Control," by R.C. Lin, T.T. Soong and A.M. Reinhorn, 4/20/87, (PB88-134341, A04, MF-A01).

NCEER-87-0003 "Experimentation Using the Earthquake Simulation Facilities at University at Buffalo," by A.M. Reinhorn and R.L. Ketter, not available.

NCEER-87-0004 "The System Characteristics and Performance of a Shaking Table," by J.S. Hwang, K.C. Chang and G.C. Lee, 6/1/87, (PB88-134259, A03, MF-A01). This report is available only through NTIS (see address given above).

NCEER-87-0005 "A Finite Element Formulation for Nonlinear Viscoplastic Material Using a Q Model," by O. Gyebi and G. Dasgupta, 11/2/87, (PB88-213764, A08, MF-A01).

NCEER-87-0006 "Symbolic Manipulation Program (SMP) - Algebraic Codes for Two and Three Dimensional Finite Element Formulations," by X. Lee and G. Dasgupta, 11/9/87, (PB88-218522, A05, MF-A01).

NCEER-87-0007 "Instantaneous Optimal Control Laws for Tall Buildings Under Seismic Excitations," by J.N. Yang, A. Akbarpour and P. Ghaemmaghami, 6/10/87, (PB88-134333, A06, MF-A01). This report is only available through NTIS (see address given above).

NCEER-87-0008 "IDARC: Inelastic Damage Analysis of Reinforced Concrete Frame - Shear-Wall Structures," by Y.J. Park, A.M. Reinhorn and S.K. Kunnath, 7/20/87, (PB88-134325, A09, MF-A01). This report is only available through NTIS (see address given above).

NCEER-87-0009 "Liquefaction Potential for New York State: A Preliminary Report on Sites in Manhattan and Buffalo," by M. Budhu, V. Vijayakumar, R.F. Giese and L. Baumgras, 8/31/87, (PB88-163704, A03, MF-A01). This report is available only through NTIS (see address given above).

NCEER-87-0010 "Vertical and Torsional Vibration of Foundations in Inhomogeneous Media," by A.S. Veletsos and K.W. Dotson, 6/1/87, (PB88-134291, A03, MF-A01). This report is only available through NTIS (see address given above).

NCEER-87-0011 "Seismic Probabilistic Risk Assessment and Seismic Margins Studies for Nuclear Power Plants," by Howard H.M. Hwang, 6/15/87, (PB88-134267, A03, MF-A01). This report is only available through NTIS (see address given above).

NCEER-87-0012 "Parametric Studies of Frequency Response of Secondary Systems Under Ground-Acceleration Excitations," by Y. Yong and Y.K. Lin, 6/10/87, (PB88-134309, A03, MF-A01). This report is only available through NTIS (see address given above).

NCEER-87-0013 "Frequency Response of Secondary Systems Under Seismic Excitation," by J.A. HoLung, J. Cai and Y.K. Lin, 7/31/87, (PB88-134317, A05, MF-A01). This report is only available through NTIS (see address given above).

NCEER-87-0014 "Modelling Earthquake Ground Motions in Seismically Active Regions Using Parametric Time Series Methods," by G.W. Ellis and A.S. Cakmak, 8/25/87, (PB88-134283, A08, MF-A01). This report is only available through NTIS (see address given above).

NCEER-87-0015 "Detection and Assessment of Seismic Structural Damage," by E. DiPasquale and A.S. Cakmak, 8/25/87, (PB88-163712, A05, MF-A01). This report is only available through NTIS (see address given above).

NCEER-87-0016 "Pipeline Experiment at Parkfield, California," by J. Isenberg and E. Richardson, 9/15/87, (PB88-163720, A03, MF-A01). This report is available only through NTIS (see address given above).

NCEER-87-0017 "Digital Simulation of Seismic Ground Motion," by M. Shinozuka, G. Deodatis and T. Harada, 8/31/87, (PB88-155197, A04, MF-A01). This report is available only through NTIS (see address given above).

NCEER-87-0018 "Practical Considerations for Structural Control: System Uncertainty, System Time Delay and Truncation of Small Control Forces," J.N. Yang and A. Akbarpour, 8/10/87, (PB88-163738, A08, MF-A01). This report is only available through NTIS (see address given above).

NCEER-87-0019 "Modal Analysis of Nonclassically Damped Structural Systems Using Canonical Transformation," by J.N. Yang, S. Sarkani and F.X. Long, 9/27/87, (PB88-187851, A04, MF-A01).

NCEER-87-0020 "A Nonstationary Solution in Random Vibration Theory," by J.R. Red-Horse and P.D. Spanos, 11/3/87, (PB88-163746, A03, MF-A01).

NCEER-87-0021 "Horizontal Impedances for Radially Inhomogeneous Viscoelastic Soil Layers," by A.S. Veletsos and K.W. Dotson, 10/15/87, (PB88-150859, A04, MF-A01).

NCEER-87-0022 "Seismic Damage Assessment of Reinforced Concrete Members," by Y.S. Chung, C. Meyer and M. Shinozuka, 10/9/87, (PB88-150867, A05, MF-A01). This report is available only through NTIS (see address given above).

NCEER-87-0023 "Active Structural Control in Civil Engineering," by T.T. Soong, 11/11/87, (PB88-187778, A03, MF-A01).

NCEER-87-0024 "Vertical and Torsional Impedances for Radially Inhomogeneous Viscoelastic Soil Layers," by K.W. Dotson and A.S. Veletsos, 12/87, (PB88-187786, A03, MF-A01).

NCEER-87-0025 "Proceedings from the Symposium on Seismic Hazards, Ground Motions, Soil-Liquefaction and Engineering Practice in Eastern North America," October 20-22, 1987, edited by K.H. Jacob, 12/87, (PB88-188115, A23, MF-A01). This report is available only through NTIS (see address given above).

NCEER-87-0026 "Report on the Whittier-Narrows, California, Earthquake of October 1, 1987," by J. Pantelic and A. Reinhorn, 11/87, (PB88-187752, A03, MF-A01). This report is available only through NTIS (see address given above).

NCEER-87-0027 "Design of a Modular Program for Transient Nonlinear Analysis of Large 3-D Building Structures," by S. Srivastav and J.F. Abel, 12/30/87, (PB88-187950, A05, MF-A01). This report is only available through NTIS (see address given above).

NCEER-87-0028 "Second-Year Program in Research, Education and Technology Transfer," 3/8/88, (PB88-219480, A04, MF-A01).

NCEER-88-0001 "Workshop on Seismic Computer Analysis and Design of Buildings With Interactive Graphics," by W. McGuire, J.F. Abel and C.H. Conley, 1/18/88, (PB88-187760, A03, MF-A01). This report is only available through NTIS (see address given above).

NCEER-88-0002 "Optimal Control of Nonlinear Flexible Structures," by J.N. Yang, F.X. Long and D. Wong, 1/22/88, (PB88-213772, A06, MF-A01).

NCEER-88-0003 "Substructuring Techniques in the Time Domain for Primary-Secondary Structural Systems," by G.D. Manolis and G. Juhn, 2/10/88, (PB88-213780, A04, MF-A01).

NCEER-88-0004 "Iterative Seismic Analysis of Primary-Secondary Systems," by A. Singhal, L.D. Lutes and P.D. Spanos, 2/23/88, (PB88-213798, A04, MF-A01).

NCEER-88-0005 "Stochastic Finite Element Expansion for Random Media," by P.D. Spanos and R. Ghanem, 3/14/88, (PB88-213806, A03, MF-A01).

NCEER-88-0006 "Combining Structural Optimization and Structural Control," by F.Y. Cheng and C.P. Pantelides, 1/10/88, (PB88-213814, A05, MF-A01).

NCEER-88-0007 "Seismic Performance Assessment of Code-Designed Structures," by H.H-M. Hwang, J-W. Jaw and H-J. Shau, 3/20/88, (PB88-219423, A04, MF-A01). This report is only available through NTIS (see address given above).

NCEER-88-0008 "Reliability Analysis of Code-Designed Structures Under Natural Hazards," by H.H-M. Hwang, H. Ushiba and M. Shinozuka, 2/29/88, (PB88-229471, A07, MF-A01). This report is only available through NTIS (see address given above).

NCEER-88-0009 "Seismic Fragility Analysis of Shear Wall Structures," by J-W Jaw and H.H-M. Hwang, 4/30/88, (PB89-102867, A04, MF-A01).

NCEER-88-0010 "Base Isolation of a Multi-Story Building Under a Harmonic Ground Motion - A Comparison of Performances of Various Systems," by F-G Fan, G. Ahmadi and I.G. Tadjbakhsh, 5/18/88, (PB89-122238, A06, MF-A01). This report is only available through NTIS (see address given above).

NCEER-88-0011 "Seismic Floor Response Spectra for a Combined System by Green's Functions," by F.M. Lavelle, L.A. Bergman and P.D. Spanos, 5/1/88, (PB89-102875, A03, MF-A01).

NCEER-88-0012 "A New Solution Technique for Randomly Excited Hysteretic Structures," by G.Q. Cai and Y.K. Lin, 5/16/88, (PB89-102883, A03, MF-A01).

NCEER-88-0013 "A Study of Radiation Damping and Soil-Structure Interaction Effects in the Centrifuge," by K. Weissman, supervised by J.H. Prevost, 5/24/88, (PB89-144703, A06, MF-A01).

NCEER-88-0014 "Parameter Identification and Implementation of a Kinematic Plasticity Model for Frictional Soils," by J.H. Prevost and D.V. Griffiths, not available.

NCEER-88-0015 "Two- and Three- Dimensional Dynamic Finite Element Analyses of the Long Valley Dam," by D.V. Griffiths and J.H. Prevost, 6/17/88, (PB89-144711, A04, MF-A01).

NCEER-88-0016 "Damage Assessment of Reinforced Concrete Structures in Eastern United States," by A.M. Reinhorn, M.J. Seidel, S.K. Kunnath and Y.J. Park, 6/15/88, (PB89-122220, A04, MF-A01). This report is only available through NTIS (see address given above).

NCEER-88-0017 "Dynamic Compliance of Vertically Loaded Strip Foundations in Multilayered Viscoelastic Soils," by S. Ahmad and A.S.M. Israil, 6/17/88, (PB89-102891, A04, MF-A01).

NCEER-88-0018 "An Experimental Study of Seismic Structural Response With Added Viscoelastic Dampers," by R.C. Lin, Z. Liang, T.T. Soong and R.H. Zhang, 6/30/88, (PB89-122212, A05, MF-A01). This report is available only through NTIS (see address given above).

NCEER-88-0019 "Experimental Investigation of Primary - Secondary System Interaction," by G.D. Manolis, G. Juhn and A.M. Reinhorn, 5/27/88, (PB89-122204, A04, MF-A01).

NCEER-88-0020 "A Response Spectrum Approach For Analysis of Nonclassically Damped Structures," by J.N. Yang, S. Sarkani and F.X. Long, 4/22/88, (PB89-102909, A04, MF-A01).

NCEER-88-0021 "Seismic Interaction of Structures and Soils: Stochastic Approach," by A.S. Veletsos and A.M. Prasad, 7/21/88, (PB89-122196, A04, MF-A01). This report is only available through NTIS (see address given above).

NCEER-88-0022 "Identification of the Serviceability Limit State and Detection of Seismic Structural Damage," by E. DiPasquale and A.S. Cakmak, 6/15/88, (PB89-122188, A05, MF-A01). This report is available only through NTIS (see address given above).

NCEER-88-0023 "Multi-Hazard Risk Analysis: Case of a Simple Offshore Structure," by B.K. Bhartia and E.H. Vanmarcke, 7/21/88, (PB89-145213, A05, MF-A01).

NCEER-88-0024 "Automated Seismic Design of Reinforced Concrete Buildings," by Y.S. Chung, C. Meyer and M. Shinozuka, 7/5/88, (PB89-122170, A06, MF-A01). This report is available only through NTIS (see address given above).

NCEER-88-0025 "Experimental Study of Active Control of MDOF Structures Under Seismic Excitations," by L.L. Chung, R.C. Lin, T.T. Soong and A.M. Reinhorn, 7/10/88, (PB89-122600, A04, MF-A01).

NCEER-88-0026 "Earthquake Simulation Tests of a Low-Rise Metal Structure," by J.S. Hwang, K.C. Chang, G.C. Lee and R.L. Ketter, 8/1/88, (PB89-102917, A04, MF-A01).

NCEER-88-0027 "Systems Study of Urban Response and Reconstruction Due to Catastrophic Earthquakes," by F. Kozin and H.K. Zhou, 9/22/88, (PB90-162348, A04, MF-A01).

NCEER-88-0028 "Seismic Fragility Analysis of Plane Frame Structures," by H.H-M. Hwang and Y.K. Low, 7/31/88, (PB89-131445, A06, MF-A01).

NCEER-88-0029 "Response Analysis of Stochastic Structures," by A. Kardara, C. Bucher and M. Shinozuka, 9/22/88, (PB89-174429, A04, MF-A01).

NCEER-88-0030 "Nonnormal Accelerations Due to Yielding in a Primary Structure," by D.C.K. Chen and L.D. Lutes, 9/19/88, (PB89-131437, A04, MF-A01).

NCEER-88-0031 "Design Approaches for Soil-Structure Interaction," by A.S. Veletsos, A.M. Prasad and Y. Tang, 12/30/88, (PB89-174437, A03, MF-A01). This report is available only through NTIS (see address given above).

NCEER-88-0032 "A Re-evaluation of Design Spectra for Seismic Damage Control," by C.J. Turkstra and A.G. Tallin, 11/7/88, (PB89-145221, A05, MF-A01).

NCEER-88-0033 "The Behavior and Design of Noncontact Lap Splices Subjected to Repeated Inelastic Tensile Loading," by V.E. Sagan, P. Gergely and R.N. White, 12/8/88, (PB89-163737, A08, MF-A01).

NCEER-88-0034 "Seismic Response of Pile Foundations," by S.M. Mamoon, P.K. Banerjee and S. Ahmad, 11/1/88, (PB89-145239, A04, MF-A01).

NCEER-88-0035 "Modeling of R/C Building Structures With Flexible Floor Diaphragms (IDARC2)," by A.M. Reinhorn, S.K. Kunnath and N. Panahshahi, 9/7/88, (PB89-207153, A07, MF-A01).

NCEER-88-0036 "Solution of the Dam-Reservoir Interaction Problem Using a Combination of FEM, BEM with Particular Integrals, Modal Analysis, and Substructuring," by C-S. Tsai, G.C. Lee and R.L. Ketter, 12/31/88, (PB89-207146, A04, MF-A01).

NCEER-88-0037 "Optimal Placement of Actuators for Structural Control," by F.Y. Cheng and C.P. Pantelides, 8/15/88, (PB89-162846, A05, MF-A01).

NCEER-88-0038 "Teflon Bearings in Aseismic Base Isolation: Experimental Studies and Mathematical Modeling," by A. Mokha, M.C. Constantinou and A.M. Reinhorn, 12/5/88, (PB89-218457, A10, MF-A01). This report is available only through NTIS (see address given above).

NCEER-88-0039 "Seismic Behavior of Flat Slab High-Rise Buildings in the New York City Area," by P. Weidlinger and M. Ettouney, 10/15/88, (PB90-145681, A04, MF-A01).

NCEER-88-0040 "Evaluation of the Earthquake Resistance of Existing Buildings in New York City," by P. Weidlinger and M. Ettouney, 10/15/88, not available.

NCEER-88-0041 "Small-Scale Modeling Techniques for Reinforced Concrete Structures Subjected to Seismic Loads," by W. Kim, A. El-Attar and R.N. White, 11/22/88, (PB89-189625, A05, MF-A01).

NCEER-88-0042 "Modeling Strong Ground Motion from Multiple Event Earthquakes," by G.W. Ellis and A.S. Cakmak, 10/15/88, (PB89-174445, A03, MF-A01).

NCEER-88-0043 "Nonstationary Models of Seismic Ground Acceleration," by M. Grigoriu, S.E. Ruiz and E. Rosenblueth, 7/15/88, (PB89-189617, A04, MF-A01).

NCEER-88-0044 "SARCF User's Guide: Seismic Analysis of Reinforced Concrete Frames," by Y.S. Chung, C. Meyer and M. Shinozuka, 11/9/88, (PB89-174452, A08, MF-A01).

NCEER-88-0045 "First Expert Panel Meeting on Disaster Research and Planning," edited by J. Pantelic and J. Stoyle, 9/15/88, (PB89-174460, A05, MF-A01).

NCEER-88-0046 "Preliminary Studies of the Effect of Degrading Infill Walls on the Nonlinear Seismic Response of Steel Frames," by C.Z. Chrysostomou, P. Gergely and J.F. Abel, 12/19/88, (PB89-208383, A05, MF-A01).

NCEER-88-0047 "Reinforced Concrete Frame Component Testing Facility - Design, Construction, Instrumentation and Operation," by S.P. Pessiki, C. Conley, T. Bond, P. Gergely and R.N. White, 12/16/88, (PB89-174478, A04, MF-A01).

NCEER-89-0001 "Effects of Protective Cushion and Soil Compliancy on the Response of Equipment Within a Seismically Excited Building," by J.A. HoLung, 2/16/89, (PB89-207179, A04, MF-A01).

NCEER-89-0002 "Statistical Evaluation of Response Modification Factors for Reinforced Concrete Structures," by H.H-M. Hwang and J-W. Jaw, 2/17/89, (PB89-207187, A05, MF-A01).

NCEER-89-0003 "Hysteretic Columns Under Random Excitation," by G-Q. Cai and Y.K. Lin, 1/9/89, (PB89-196513, A03, MF-A01).

NCEER-89-0004 "Experimental Study of `Elephant Foot Bulge' Instability of Thin-Walled Metal Tanks," by Z-H. Jia and R.L. Ketter, 2/22/89, (PB89-207195, A03, MF-A01).

NCEER-89-0005 "Experiment on Performance of Buried Pipelines Across San Andreas Fault," by J. Isenberg, E. Richardson and T.D. O'Rourke, 3/10/89, (PB89-218440, A04, MF-A01). This report is available only through NTIS (see address given above).

NCEER-89-0006 "A Knowledge-Based Approach to Structural Design of Earthquake-Resistant Buildings," by M. Subramani, P. Gergely, C.H. Conley, J.F. Abel and A.H. Zaghw, 1/15/89, (PB89-218465, A06, MF-A01).

NCEER-89-0007 "Liquefaction Hazards and Their Effects on Buried Pipelines," by T.D. O'Rourke and P.A. Lane, 2/1/89, (PB89-218481, A09, MF-A01).

NCEER-89-0008 "Fundamentals of System Identification in Structural Dynamics," by H. Imai, C-B. Yun, O. Maruyama and M. Shinozuka, 1/26/89, (PB89-207211, A04, MF-A01).

NCEER-89-0009 "Effects of the 1985 Michoacan Earthquake on Water Systems and Other Buried Lifelines in Mexico," by A.G. Ayala and M.J. O'Rourke, 3/8/89, (PB89-207229, A06, MF-A01).

NCEER-89-R010 "NCEER Bibliography of Earthquake Education Materials," by K.E.K. Ross, Second Revision, 9/1/89, (PB90-125352, A05, MF-A01). This report is replaced by NCEER-92-0018.

NCEER-89-0011 "Inelastic Three-Dimensional Response Analysis of Reinforced Concrete Building Structures (IDARC-3D), Part I - Modeling," by S.K. Kunnath and A.M. Reinhorn, 4/17/89, (PB90-114612, A07, MF-A01). This report is available only through NTIS (see address given above).

NCEER-89-0012 "Recommended Modifications to ATC-14," by C.D. Poland and J.O. Malley, 4/12/89, (PB90-108648, A15, MF-A01).

NCEER-89-0013 "Repair and Strengthening of Beam-to-Column Connections Subjected to Earthquake Loading," by M. Corazao and A.J. Durrani, 2/28/89, (PB90-109885, A06, MF-A01).

NCEER-89-0014 "Program EXKAL2 for Identification of Structural Dynamic Systems," by O. Maruyama, C-B. Yun, M. Hoshiya and M. Shinozuka, 5/19/89, (PB90-109877, A09, MF-A01).

NCEER-89-0015 "Response of Frames With Bolted Semi-Rigid Connections, Part I - Experimental Study and Analytical Predictions," by P.J. DiCorso, A.M. Reinhorn, J.R. Dickerson, J.B. Radziminski and W.L. Harper, 6/1/89, not available.

NCEER-89-0016 "ARMA Monte Carlo Simulation in Probabilistic Structural Analysis," by P.D. Spanos and M.P. Mignolet, 7/10/89, (PB90-109893, A03, MF-A01).

NCEER-89-P017 "Preliminary Proceedings from the Conference on Disaster Preparedness - The Place of Earthquake Education in Our Schools," Edited by K.E.K. Ross, 6/23/89, (PB90-108606, A03, MF-A01).

NCEER-89-0017 "Proceedings from the Conference on Disaster Preparedness - The Place of Earthquake Education in Our Schools," Edited by K.E.K. Ross, 12/31/89, (PB90-207895, A012, MF-A02). This report is available only through NTIS (see address given above).

NCEER-89-0018 "Multidimensional Models of Hysteretic Material Behavior for Vibration Analysis of Shape Memory Energy Absorbing Devices, by E.J. Graesser and F.A. Cozzarelli, 6/7/89, (PB90-164146, A04, MF-A01).

NCEER-89-0019 "Nonlinear Dynamic Analysis of Three-Dimensional Base Isolated Structures (3D-BASIS)," by S. Nagarajaiah, A.M. Reinhorn and M.C. Constantinou, 8/3/89, (PB90-161936, A06, MF-A01). This report has been replaced by NCEER-93-0011.

NCEER-89-0020 "Structural Control Considering Time-Rate of Control Forces and Control Rate Constraints," by F.Y. Cheng and C.P. Pantelides, 8/3/89, (PB90-120445, A04, MF-A01).

NCEER-89-0021 "Subsurface Conditions of Memphis and Shelby County," by K.W. Ng, T-S. Chang and H-H.M. Hwang, 7/26/89, (PB90-120437, A03, MF-A01).

NCEER-89-0022 "Seismic Wave Propagation Effects on Straight Jointed Buried Pipelines," by K. Elhmadi and M.J. O'Rourke, 8/24/89, (PB90-162322, A10, MF-A02).

NCEER-89-0023 "Workshop on Serviceability Analysis of Water Delivery Systems," edited by M. Grigoriu, 3/6/89, (PB90-127424, A03, MF-A01).

NCEER-89-0024 "Shaking Table Study of a 1/5 Scale Steel Frame Composed of Tapered Members," by K.C. Chang, J.S. Hwang and G.C. Lee, 9/18/89, (PB90-160169, A04, MF-A01).

NCEER-89-0025 "DYNA1D: A Computer Program for Nonlinear Seismic Site Response Analysis - Technical Documentation," by Jean H. Prevost, 9/14/89, (PB90-161944, A07, MF-A01). This report is available only through NTIS (see address given above).

NCEER-89-0026 "1:4 Scale Model Studies of Active Tendon Systems and Active Mass Dampers for Aseismic Protection," by A.M. Reinhorn, T.T. Soong, R.C. Lin, Y.P. Yang, Y. Fukao, H. Abe and M. Nakai, 9/15/89, (PB90-173246, A10, MF-A02). This report is available only through NTIS (see address given above).

NCEER-89-0027 "Scattering of Waves by Inclusions in a Nonhomogeneous Elastic Half Space Solved by Boundary Element Methods," by P.K. Hadley, A. Askar and A.S. Cakmak, 6/15/89, (PB90-145699, A07, MF-A01).

NCEER-89-0028 "Statistical Evaluation of Deflection Amplification Factors for Reinforced Concrete Structures," by H.H.M. Hwang, J-W. Jaw and A.L. Ch'ng, 8/31/89, (PB90-164633, A05, MF-A01).

NCEER-89-0029 "Bedrock Accelerations in Memphis Area Due to Large New Madrid Earthquakes," by H.H.M. Hwang, C.H.S. Chen and G. Yu, 11/7/89, (PB90-162330, A04, MF-A01).

NCEER-89-0030 "Seismic Behavior and Response Sensitivity of Secondary Structural Systems," by Y.Q. Chen and T.T. Soong, 10/23/89, (PB90-164658, A08, MF-A01).

NCEER-89-0031 "Random Vibration and Reliability Analysis of Primary-Secondary Structural Systems," by Y. Ibrahim, M. Grigoriu and T.T. Soong, 11/10/89, (PB90-161951, A04, MF-A01).

NCEER-89-0032 "Proceedings from the Second U.S. - Japan Workshop on Liquefaction, Large Ground Deformation and Their Effects on Lifelines, September 26-29, 1989," Edited by T.D. O'Rourke and M. Hamada, 12/1/89, (PB90-209388, A22, MF-A03).

NCEER-89-0033 "Deterministic Model for Seismic Damage Evaluation of Reinforced Concrete Structures," by J.M. Bracci, A.M. Reinhorn, J.B. Mander and S.K. Kunnath, 9/27/89, (PB91-108803, A06, MF-A01).

NCEER-89-0034 "On the Relation Between Local and Global Damage Indices," by E. DiPasquale and A.S. Cakmak, 8/15/89, (PB90-173865, A05, MF-A01).

NCEER-89-0035 "Cyclic Undrained Behavior of Nonplastic and Low Plasticity Silts," by A.J. Walker and H.E. Stewart, 7/26/89, (PB90-183518, A10, MF-A01).

NCEER-89-0036 "Liquefaction Potential of Surficial Deposits in the City of Buffalo, New York," by M. Budhu, R. Giese and L. Baumgrass, 1/17/89, (PB90-208455, A04, MF-A01).

NCEER-89-0037 "A Deterministic Assessment of Effects of Ground Motion Incoherence," by A.S. Veletsos and Y. Tang, 7/15/89, (PB90-164294, A03, MF-A01).

NCEER-89-0038 "Workshop on Ground Motion Parameters for Seismic Hazard Mapping," July 17-18, 1989, edited by R.V. Whitman, 12/1/89, (PB90-173923, A04, MF-A01).

NCEER-89-0039 "Seismic Effects on Elevated Transit Lines of the New York City Transit Authority," by C.J. Costantino, C.A. Miller and E. Heymsfield, 12/26/89, (PB90-207887, A06, MF-A01).

NCEER-89-0040 "Centrifugal Modeling of Dynamic Soil-Structure Interaction," by K. Weissman, Supervised by J.H. Prevost, 5/10/89, (PB90-207879, A07, MF-A01).

NCEER-89-0041 "Linearized Identification of Buildings With Cores for Seismic Vulnerability Assessment," by I-K. Ho and A.E. Aktan, 11/1/89, (PB90-251943, A07, MF-A01).

NCEER-90-0001 "Geotechnical and Lifeline Aspects of the October 17, 1989 Loma Prieta Earthquake in San Francisco," by T.D. O'Rourke, H.E. Stewart, F.T. Blackburn and T.S. Dickerman, 1/90, (PB90-208596, A05, MF-A01).

NCEER-90-0002 "Nonnormal Secondary Response Due to Yielding in a Primary Structure," by D.C.K. Chen and L.D. Lutes, 2/28/90, (PB90-251976, A07, MF-A01).

NCEER-90-0003 "Earthquake Education Materials for Grades K-12," by K.E.K. Ross, 4/16/90, (PB91-251984, A05, MF-A05). This report has been replaced by NCEER-92-0018.

NCEER-90-0004 "Catalog of Strong Motion Stations in Eastern North America," by R.W. Busby, 4/3/90, (PB90-251984, A05, MF-A01).

NCEER-90-0005 "NCEER Strong-Motion Data Base: A User Manual for the GeoBase Release (Version 1.0 for the Sun3)," by P. Friberg and K. Jacob, 3/31/90 (PB90-258062, A04, MF-A01).

NCEER-90-0006 "Seismic Hazard Along a Crude Oil Pipeline in the Event of an 1811-1812 Type New Madrid Earthquake," by H.H.M. Hwang and C-H.S. Chen, 4/16/90, (PB90-258054, A04, MF-A01).

NCEER-90-0007 "Site-Specific Response Spectra for Memphis Sheahan Pumping Station," by H.H.M. Hwang and C.S. Lee, 5/15/90, (PB91-108811, A05, MF-A01).

NCEER-90-0008 "Pilot Study on Seismic Vulnerability of Crude Oil Transmission Systems," by T. Ariman, R. Dobry, M. Grigoriu, F. Kozin, M. O'Rourke, T. O'Rourke and M. Shinozuka, 5/25/90, (PB91-108837, A06, MF-A01).

NCEER-90-0009 "A Program to Generate Site Dependent Time Histories: EQGEN," by G.W. Ellis, M. Srinivasan and A.S. Cakmak, 1/30/90, (PB91-108829, A04, MF-A01).

NCEER-90-0010 "Active Isolation for Seismic Protection of Operating Rooms," by M.E. Talbott, Supervised by M. Shinozuka, 6/8/9, (PB91-110205, A05, MF-A01).

NCEER-90-0011 "Program LINEARID for Identification of Linear Structural Dynamic Systems," by C-B. Yun and M. Shinozuka, 6/25/90, (PB91-110312, A08, MF-A01).

NCEER-90-0012 "Two-Dimensional Two-Phase Elasto-Plastic Seismic Response of Earth Dams," by A.N. Yiagos, Supervised by J.H. Prevost, 6/20/90, (PB91-110197, A13, MF-A02).

NCEER-90-0013 "Secondary Systems in Base-Isolated Structures: Experimental Investigation, Stochastic Response and Stochastic Sensitivity," by G.D. Manolis, G. Juhn, M.C. Constantinou and A.M. Reinhorn, 7/1/90, (PB91-110320, A08, MF-A01).

NCEER-90-0014 "Seismic Behavior of Lightly-Reinforced Concrete Column and Beam-Column Joint Details," by S.P. Pessiki, C.H. Conley, P. Gergely and R.N. White, 8/22/90, (PB91-108795, A11, MF-A02).

NCEER-90-0015 "Two Hybrid Control Systems for Building Structures Under Strong Earthquakes," by J.N. Yang and A. Danielians, 6/29/90, (PB91-125393, A04, MF-A01).

NCEER-90-0016 "Instantaneous Optimal Control with Acceleration and Velocity Feedback," by J.N. Yang and Z. Li, 6/29/90, (PB91-125401, A03, MF-A01).

NCEER-90-0017 "Reconnaissance Report on the Northern Iran Earthquake of June 21, 1990," by M. Mehrain, 10/4/90, (PB91-125377, A03, MF-A01).

NCEER-90-0018 "Evaluation of Liquefaction Potential in Memphis and Shelby County," by T.S. Chang, P.S. Tang, C.S. Lee and H. Hwang, 8/10/90, (PB91-125427, A09, MF-A01).

NCEER-90-0019 "Experimental and Analytical Study of a Combined Sliding Disc Bearing and Helical Steel Spring Isolation System," by M.C. Constantinou, A.S. Mokha and A.M. Reinhorn, 10/4/90, (PB91-125385, A06, MF-A01). This report is available only through NTIS (see address given above).

NCEER-90-0020 "Experimental Study and Analytical Prediction of Earthquake Response of a Sliding Isolation System with a Spherical Surface," by A.S. Mokha, M.C. Constantinou and A.M. Reinhorn, 10/11/90, (PB91-125419, A05, MF-A01).

NCEER-90-0021 "Dynamic Interaction Factors for Floating Pile Groups," by G. Gazetas, K. Fan, A. Kaynia and E. Kausel, 9/10/90, (PB91-170381, A05, MF-A01).

NCEER-90-0022 "Evaluation of Seismic Damage Indices for Reinforced Concrete Structures," by S. Rodriguez-Gomez and A.S. Cakmak, 9/30/90, PB91-171322, A06, MF-A01).

NCEER-90-0023 "Study of Site Response at a Selected Memphis Site," by H. Desai, S. Ahmad, E.S. Gazetas and M.R. Oh, 10/11/90, (PB91-196857, A03, MF-A01).

NCEER-90-0024 "A User's Guide to Strongmo: Version 1.0 of NCEER's Strong-Motion Data Access Tool for PCs and Terminals," by P.A. Friberg and C.A.T. Susch, 11/15/90, (PB91-171272, A03, MF-A01).

NCEER-90-0025 "A Three-Dimensional Analytical Study of Spatial Variability of Seismic Ground Motions," by L-L. Hong and A.H.-S. Ang, 10/30/90, (PB91-170399, A09, MF-A01).

NCEER-90-0026 "MUMOID User's Guide - A Program for the Identification of Modal Parameters," by S. Rodriguez-Gomez and E. DiPasquale, 9/30/90, (PB91-171298, A04, MF-A01).

NCEER-90-0027 "SARCF-II User's Guide - Seismic Analysis of Reinforced Concrete Frames," by S. Rodriguez-Gomez, Y.S. Chung and C. Meyer, 9/30/90, (PB91-171280, A05, MF-A01).

NCEER-90-0028 "Viscous Dampers: Testing, Modeling and Application in Vibration and Seismic Isolation," by N. Makris and M.C. Constantinou, 12/20/90 (PB91-190561, A06, MF-A01).

NCEER-90-0029 "Soil Effects on Earthquake Ground Motions in the Memphis Area," by H. Hwang, C.S. Lee, K.W. Ng and T.S. Chang, 8/2/90, (PB91-190751, A05, MF-A01).

NCEER-91-0001 "Proceedings from the Third Japan-U.S. Workshop on Earthquake Resistant Design of Lifeline Facilities and Countermeasures for Soil Liquefaction, December 17-19, 1990," edited by T.D. O'Rourke and M. Hamada, 2/1/91, (PB91-179259, A99, MF-A04).

NCEER-91-0002 "Physical Space Solutions of Non-Proportionally Damped Systems," by M. Tong, Z. Liang and G.C. Lee, 1/15/91, (PB91-179242, A04, MF-A01).

NCEER-91-0003 "Seismic Response of Single Piles and Pile Groups," by K. Fan and G. Gazetas, 1/10/91, (PB92-174994, A04, MF-A01).

NCEER-91-0004 "Damping of Structures: Part 1 - Theory of Complex Damping," by Z. Liang and G. Lee, 10/10/91, (PB92-197235, A12, MF-A03).

NCEER-91-0005 "3D-BASIS - Nonlinear Dynamic Analysis of Three Dimensional Base Isolated Structures: Part II," by S. Nagarajaiah, A.M. Reinhorn and M.C. Constantinou, 2/28/91, (PB91-190553, A07, MF-A01). This report has been replaced by NCEER-93-0011.

NCEER-91-0006 "A Multidimensional Hysteretic Model for Plasticity Deforming Metals in Energy Absorbing Devices," by E.J. Graesser and F.A. Cozzarelli, 4/9/91, (PB92-108364, A04, MF-A01).

NCEER-91-0007 "A Framework for Customizable Knowledge-Based Expert Systems with an Application to a KBES for Evaluating the Seismic Resistance of Existing Buildings," by E.G. Ibarra-Anaya and S.J. Fenves, 4/9/91, (PB91-210930, A08, MF-A01).

NCEER-91-0008 "Nonlinear Analysis of Steel Frames with Semi-Rigid Connections Using the Capacity Spectrum Method," by G.G. Deierlein, S-H. Hsieh, Y-J. Shen and J.F. Abel, 7/2/91, (PB92-113828, A05, MF-A01).

NCEER-91-0009 "Earthquake Education Materials for Grades K-12," by K.E.K. Ross, 4/30/91, (PB91-212142, A06, MF-A01). This report has been replaced by NCEER-92-0018.

NCEER-91-0010 "Phase Wave Velocities and Displacement Phase Differences in a Harmonically Oscillating Pile," by N. Makris and G. Gazetas, 7/8/91, (PB92-108356, A04, MF-A01).

NCEER-91-0011 "Dynamic Characteristics of a Full-Size Five-Story Steel Structure and a 2/5 Scale Model," by K.C. Chang, G.C. Yao, G.C. Lee, D.S. Hao and Y.C. Yeh," 7/2/91, (PB93-116648, A06, MF-A02).

NCEER-91-0012 "Seismic Response of a 2/5 Scale Steel Structure with Added Viscoelastic Dampers," by K.C. Chang, T.T. Soong, S-T. Oh and M.L. Lai, 5/17/91, (PB92-110816, A05, MF-A01).

NCEER-91-0013 "Earthquake Response of Retaining Walls; Full-Scale Testing and Computational Modeling," by S. Alampalli and A-W.M. Elgamal, 6/20/91, not available.

NCEER-91-0014 "3D-BASIS-M: Nonlinear Dynamic Analysis of Multiple Building Base Isolated Structures," by P.C. Tsopelas, S. Nagarajaiah, M.C. Constantinou and A.M. Reinhorn, 5/28/91, (PB92-113885, A09, MF-A02).

NCEER-91-0015 "Evaluation of SEAOC Design Requirements for Sliding Isolated Structures," by D. Theodossiou and M.C. Constantinou, 6/10/91, (PB92-114602, A11, MF-A03).

NCEER-91-0016 "Closed-Loop Modal Testing of a 27-Story Reinforced Concrete Flat Plate-Core Building," by H.R. Somaprasad, T. Toksoy, H. Yoshiyuki and A.E. Aktan, 7/15/91, (PB92-129980, A07, MF-A02).

NCEER-91-0017 "Shake Table Test of a 1/6 Scale Two-Story Lightly Reinforced Concrete Building," by A.G. El-Attar, R.N. White and P. Gergely, 2/28/91, (PB92-222447, A06, MF-A02).

NCEER-91-0018 "Shake Table Test of a 1/8 Scale Three-Story Lightly Reinforced Concrete Building," by A.G. El-Attar, R.N. White and P. Gergely, 2/28/91, (PB93-116630, A08, MF-A02).

NCEER-91-0019 "Transfer Functions for Rigid Rectangular Foundations," by A.S. Veletsos, A.M. Prasad and W.H. Wu, 7/31/91, not available.

NCEER-91-0020 "Hybrid Control of Seismic-Excited Nonlinear and Inelastic Structural Systems," by J.N. Yang, Z. Li and A. Danielians, 8/1/91, (PB92-143171, A06, MF-A02).

NCEER-91-0021 "The NCEER-91 Earthquake Catalog: Improved Intensity-Based Magnitudes and Recurrence Relations for U.S. Earthquakes East of New Madrid," by L. Seeber and J.G. Armbruster, 8/28/91, (PB92-176742, A06, MF-A02).

NCEER-91-0022 "Proceedings from the Implementation of Earthquake Planning and Education in Schools: The Need for Change - The Roles of the Changemakers," by K.E.K. Ross and F. Winslow, 7/23/91, (PB92-129998, A12, MF-A03).

NCEER-91-0023 "A Study of Reliability-Based Criteria for Seismic Design of Reinforced Concrete Frame Buildings," by H.H.M. Hwang and H-M. Hsu, 8/10/91, (PB92-140235, A09, MF-A02).

NCEER-91-0024 "Experimental Verification of a Number of Structural System Identification Algorithms," by R.G. Ghanem, H. Gavin and M. Shinozuka, 9/18/91, (PB92-176577, A18, MF-A04).

NCEER-91-0025 "Probabilistic Evaluation of Liquefaction Potential," by H.H.M. Hwang and C.S. Lee," 11/25/91, (PB92-143429, A05, MF-A01).

NCEER-91-0026 "Instantaneous Optimal Control for Linear, Nonlinear and Hysteretic Structures - Stable Controllers," by J.N. Yang and Z. Li, 11/15/91, (PB92-163807, A04, MF-A01).

NCEER-91-0027 "Experimental and Theoretical Study of a Sliding Isolation System for Bridges," by M.C. Constantinou, A. Kartoum, A.M. Reinhorn and P. Bradford, 11/15/91, (PB92-176973, A10, MF-A03).

NCEER-92-0001 "Case Studies of Liquefaction and Lifeline Performance During Past Earthquakes, Volume 1: Japanese Case Studies," Edited by M. Hamada and T. O'Rourke, 2/17/92, (PB92-197243, A18, MF-A04).

NCEER-92-0002 "Case Studies of Liquefaction and Lifeline Performance During Past Earthquakes, Volume 2: United States Case Studies," Edited by T. O'Rourke and M. Hamada, 2/17/92, (PB92-197250, A20, MF-A04).

NCEER-92-0003 "Issues in Earthquake Education," Edited by K. Ross, 2/3/92, (PB92-222389, A07, MF-A02).

NCEER-92-0004 "Proceedings from the First U.S. - Japan Workshop on Earthquake Protective Systems for Bridges," Edited by I.G. Buckle, 2/4/92, (PB94-142239, A99, MF-A06).

NCEER-92-0005 "Seismic Ground Motion from a Haskell-Type Source in a Multiple-Layered Half-Space," A.P. Theoharis, G. Deodatis and M. Shinozuka, 1/2/92, not available.

NCEER-92-0006 "Proceedings from the Site Effects Workshop," Edited by R. Whitman, 2/29/92, (PB92-197201, A04, MF-A01).

NCEER-92-0007 "Engineering Evaluation of Permanent Ground Deformations Due to Seismically-Induced Liquefaction," by M.H. Baziar, R. Dobry and A-W.M. Elgamal, 3/24/92, (PB92-222421, A13, MF-A03).

NCEER-92-0008 "A Procedure for the Seismic Evaluation of Buildings in the Central and Eastern United States," by C.D. Poland and J.O. Malley, 4/2/92, (PB92-222439, A20, MF-A04).

NCEER-92-0009 "Experimental and Analytical Study of a Hybrid Isolation System Using Friction Controllable Sliding Bearings," by M.Q. Feng, S. Fujii and M. Shinozuka, 5/15/92, (PB93-150282, A06, MF-A02).

NCEER-92-0010 "Seismic Resistance of Slab-Column Connections in Existing Non-Ductile Flat-Plate Buildings," by A.J. Durrani and Y. Du, 5/18/92, (PB93-116812, A06, MF-A02).

NCEER-92-0011 "The Hysteretic and Dynamic Behavior of Brick Masonry Walls Upgraded by Ferrocement Coatings Under Cyclic Loading and Strong Simulated Ground Motion," by H. Lee and S.P. Prawel, 5/11/92, not available.

NCEER-92-0012 "Study of Wire Rope Systems for Seismic Protection of Equipment in Buildings," by G.F. Demetriades, M.C. Constantinou and A.M. Reinhorn, 5/20/92, (PB93-116655, A08, MF-A02).

NCEER-92-0013 "Shape Memory Structural Dampers: Material Properties, Design and Seismic Testing," by P.R. Witting and F.A. Cozzarelli, 5/26/92, (PB93-116663, A05, MF-A01).

NCEER-92-0014 "Longitudinal Permanent Ground Deformation Effects on Buried Continuous Pipelines," by M.J. O'Rourke, and C. Nordberg, 6/15/92, (PB93-116671, A08, MF-A02).

NCEER-92-0015 "A Simulation Method for Stationary Gaussian Random Functions Based on the Sampling Theorem," by M. Grigoriu and S. Balopoulou, 6/11/92, (PB93-127496, A05, MF-A01).

NCEER-92-0016 "Gravity-Load-Designed Reinforced Concrete Buildings: Seismic Evaluation of Existing Construction and Detailing Strategies for Improved Seismic Resistance," by G.W. Hoffmann, S.K. Kunnath, A.M. Reinhorn and J.B. Mander, 7/15/92, (PB94-142007, A08, MF-A02).

NCEER-92-0017 "Observations on Water System and Pipeline Performance in the Limón Area of Costa Rica Due to the April 22, 1991 Earthquake," by M. O'Rourke and D. Ballantyne, 6/30/92, (PB93-126811, A06, MF-A02).

NCEER-92-0018 "Fourth Edition of Earthquake Education Materials for Grades K-12," Edited by K.E.K. Ross, 8/10/92, (PB93-114023, A07, MF-A02).

NCEER-92-0019 "Proceedings from the Fourth Japan-U.S. Workshop on Earthquake Resistant Design of Lifeline Facilities and Countermeasures for Soil Liquefaction," Edited by M. Hamada and T.D. O'Rourke, 8/12/92, (PB93-163939, A99, MF-E11).

NCEER-92-0020 "Active Bracing System: A Full Scale Implementation of Active Control," by A.M. Reinhorn, T.T. Soong, R.C. Lin, M.A. Riley, Y.P. Wang, S. Aizawa and M. Higashino, 8/14/92, (PB93-127512, A06, MF-A02).

NCEER-92-0021 "Empirical Analysis of Horizontal Ground Displacement Generated by Liquefaction-Induced Lateral Spreads," by S.F. Bartlett and T.L. Youd, 8/17/92, (PB93-188241, A06, MF-A02).

NCEER-92-0022 "IDARC Version 3.0: Inelastic Damage Analysis of Reinforced Concrete Structures," by S.K. Kunnath, A.M. Reinhorn and R.F. Lobo, 8/31/92, (PB93-227502, A07, MF-A02).

NCEER-92-0023 "A Semi-Empirical Analysis of Strong-Motion Peaks in Terms of Seismic Source, Propagation Path and Local Site Conditions, by M. Kamiyama, M.J. O'Rourke and R. Flores-Berrones, 9/9/92, (PB93-150266, A08, MF-A02).

NCEER-92-0024 "Seismic Behavior of Reinforced Concrete Frame Structures with Nonductile Details, Part I: Summary of Experimental Findings of Full Scale Beam-Column Joint Tests," by A. Beres, R.N. White and P. Gergely, 9/30/92, (PB93-227783, A05, MF-A01).

NCEER-92-0025 "Experimental Results of Repaired and Retrofitted Beam-Column Joint Tests in Lightly Reinforced Concrete Frame Buildings," by A. Beres, S. El-Borgi, R.N. White and P. Gergely, 10/29/92, (PB93-227791, A05, MF-A01).

NCEER-92-0026 "A Generalization of Optimal Control Theory: Linear and Nonlinear Structures," by J.N. Yang, Z. Li and S. Vongchavalitkul, 11/2/92, (PB93-188621, A05, MF-A01).

NCEER-92-0027 "Seismic Resistance of Reinforced Concrete Frame Structures Designed Only for Gravity Loads: Part I - Design and Properties of a One-Third Scale Model Structure," by J.M. Bracci, A.M. Reinhorn and J.B. Mander, 12/1/92, (PB94-104502, A08, MF-A02).

NCEER-92-0028 "Seismic Resistance of Reinforced Concrete Frame Structures Designed Only for Gravity Loads: Part II - Experimental Performance of Subassemblages," by L.E. Aycardi, J.B. Mander and A.M. Reinhorn, 12/1/92, (PB94-104510, A08, MF-A02).

NCEER-92-0029 "Seismic Resistance of Reinforced Concrete Frame Structures Designed Only for Gravity Loads: Part III - Experimental Performance and Analytical Study of a Structural Model," by J.M. Bracci, A.M. Reinhorn and J.B. Mander, 12/1/92, (PB93-227528, A09, MF-A01).

NCEER-92-0030 "Evaluation of Seismic Retrofit of Reinforced Concrete Frame Structures: Part I - Experimental Performance of Retrofitted Subassemblages," by D. Choudhuri, J.B. Mander and A.M. Reinhorn, 12/8/92, (PB93-198307, A07, MF-A02).

NCEER-92-0031 "Evaluation of Seismic Retrofit of Reinforced Concrete Frame Structures: Part II - Experimental Performance and Analytical Study of a Retrofitted Structural Model," by J.M. Bracci, A.M. Reinhorn and J.B. Mander, 12/8/92, (PB93-198315, A09, MF-A03).

NCEER-92-0032 "Experimental and Analytical Investigation of Seismic Response of Structures with Supplemental Fluid Viscous Dampers," by M.C. Constantinou and M.D. Symans, 12/21/92, (PB93-191435, A10, MF-A03). This report is available only through NTIS (see address given above).

NCEER-92-0033 "Reconnaissance Report on the Cairo, Egypt Earthquake of October 12, 1992," by M. Khater, 12/23/92, (PB93-188621, A03, MF-A01).

NCEER-92-0034 "Low-Level Dynamic Characteristics of Four Tall Flat-Plate Buildings in New York City," by H. Gavin, S. Yuan, J. Grossman, E. Pekelis and K. Jacob, 12/28/92, (PB93-188217, A07, MF-A02).

NCEER-93-0001 "An Experimental Study on the Seismic Performance of Brick-Infilled Steel Frames With and Without Retrofit," by J.B. Mander, B. Nair, K. Wojtkowski and J. Ma, 1/29/93, (PB93-227510, A07, MF-A02).

NCEER-93-0002 "Social Accounting for Disaster Preparedness and Recovery Planning," by S. Cole, E. Pantoja and V. Razak, 2/22/93, (PB94-142114, A12, MF-A03).

NCEER-93-0003 "Assessment of 1991 NEHRP Provisions for Nonstructural Components and Recommended Revisions," by T.T. Soong, G. Chen, Z. Wu, R-H. Zhang and M. Grigoriu, 3/1/93, (PB93-188639, A06, MF-A02).

NCEER-93-0004 "Evaluation of Static and Response Spectrum Analysis Procedures of SEAOC/UBC for Seismic Isolated Structures," by C.W. Winters and M.C. Constantinou, 3/23/93, (PB93-198299, A10, MF-A03).

NCEER-93-0005 "Earthquakes in the Northeast - Are We Ignoring the Hazard? A Workshop on Earthquake Science and Safety for Educators," edited by K.E.K. Ross, 4/2/93, (PB94-103066, A09, MF-A02).

NCEER-93-0006 "Inelastic Response of Reinforced Concrete Structures with Viscoelastic Braces," by R.F. Lobo, J.M. Bracci, K.L. Shen, A.M. Reinhorn and T.T. Soong, 4/5/93, (PB93-227486, A05, MF-A02).

NCEER-93-0007 "Seismic Testing of Installation Methods for Computers and Data Processing Equipment," by K. Kosar, T.T. Soong, K.L. Shen, J.A. HoLung and Y.K. Lin, 4/12/93, (PB93-198299, A07, MF-A02).

NCEER-93-0008 "Retrofit of Reinforced Concrete Frames Using Added Dampers," by A. Reinhorn, M. Constantinou and C. Li, not available.

NCEER-93-0009 "Seismic Behavior and Design Guidelines for Steel Frame Structures with Added Viscoelastic Dampers," by K.C. Chang, M.L. Lai, T.T. Soong, D.S. Hao and Y.C. Yeh, 5/1/93, (PB94-141959, A07, MF-A02).

NCEER-93-0010 "Seismic Performance of Shear-Critical Reinforced Concrete Bridge Piers," by J.B. Mander, S.M. Waheed, M.T.A. Chaudhary and S.S. Chen, 5/12/93, (PB93-227494, A08, MF-A02).

NCEER-93-0011 "3D-BASIS-TABS: Computer Program for Nonlinear Dynamic Analysis of Three Dimensional Base Isolated Structures," by S. Nagarajaiah, C. Li, A.M. Reinhorn and M.C. Constantinou, 8/2/93, (PB94-141819, A09, MF-A02).

NCEER-93-0012 "Effects of Hydrocarbon Spills from an Oil Pipeline Break on Ground Water," by O.J. Helweg and H.H.M. Hwang, 8/3/93, (PB94-141942, A06, MF-A02).

NCEER-93-0013 "Simplified Procedures for Seismic Design of Nonstructural Components and Assessment of Current Code Provisions," by M.P. Singh, L.E. Suarez, E.E. Matheu and G.O. Maldonado, 8/4/93, (PB94-141827, A09, MF-A02).

NCEER-93-0014 "An Energy Approach to Seismic Analysis and Design of Secondary Systems," by G. Chen and T.T. Soong, 8/6/93, (PB94-142767, A11, MF-A03).

NCEER-93-0015 "Proceedings from School Sites: Becoming Prepared for Earthquakes - Commemorating the Third Anniversary of the Loma Prieta Earthquake," Edited by F.E. Winslow and K.E.K. Ross, 8/16/93, (PB94-154275, A16, MF-A02).

NCEER-93-0016 "Reconnaissance Report of Damage to Historic Monuments in Cairo, Egypt Following the October 12, 1992 Dahshur Earthquake," by D. Sykora, D. Look, G. Croci, E. Karaesmen and E. Karaesmen, 8/19/93, (PB94-142221, A08, MF-A02).

NCEER-93-0017 "The Island of Guam Earthquake of August 8, 1993," by S.W. Swan and S.K. Harris, 9/30/93, (PB94-141843, A04, MF-A01).

NCEER-93-0018 "Engineering Aspects of the October 12, 1992 Egyptian Earthquake," by A.W. Elgamal, M. Amer, K. Adalier and A. Abul-Fadl, 10/7/93, (PB94-141983, A05, MF-A01).

NCEER-93-0019 "Development of an Earthquake Motion Simulator and its Application in Dynamic Centrifuge Testing," by I. Krstelj, Supervised by J.H. Prevost, 10/23/93, (PB94-181773, A-10, MF-A03).

NCEER-93-0020 "NCEER-Taisei Corporation Research Program on Sliding Seismic Isolation Systems for Bridges: Experimental and Analytical Study of a Friction Pendulum System (FPS)," by M.C. Constantinou, P. Tsopelas, Y-S. Kim and S. Okamoto, 11/1/93, (PB94-142775, A08, MF-A02).

NCEER-93-0021 "Finite Element Modeling of Elastomeric Seismic Isolation Bearings," by L.J. Billings, Supervised by R. Shepherd, 11/8/93, not available.

NCEER-93-0022 "Seismic Vulnerability of Equipment in Critical Facilities: Life-Safety and Operational Consequences," by K. Porter, G.S. Johnson, M.M. Zadeh, C. Scawthorn and S. Eder, 11/24/93, (PB94-181765, A16, MF-A03).

NCEER-93-0023 "Hokkaido Nansei-oki, Japan Earthquake of July 12, 1993, by P.I. Yanev and C.R. Scawthorn, 12/23/93, (PB94-181500, A07, MF-A01).

NCEER-94-0001 "An Evaluation of Seismic Serviceability of Water Supply Networks with Application to the San Francisco Auxiliary Water Supply System," by I. Markov, Supervised by M. Grigoriu and T. O'Rourke, 1/21/94, (PB94-204013, A07, MF-A02).

NCEER-94-0002 "NCEER-Taisei Corporation Research Program on Sliding Seismic Isolation Systems for Bridges: Experimental and Analytical Study of Systems Consisting of Sliding Bearings, Rubber Restoring Force Devices and Fluid Dampers," Volumes I and II, by P. Tsopelas, S. Okamoto, M.C. Constantinou, D. Ozaki and S. Fujii, 2/4/94, (PB94-181740, A09, MF-A02 and PB94-181757, A12, MF-A03).

NCEER-94-0003 "A Markov Model for Local and Global Damage Indices in Seismic Analysis," by S. Rahman and M. Grigoriu, 2/18/94, (PB94-206000, A12, MF-A03).

NCEER-94-0004 "Proceedings from the NCEER Workshop on Seismic Response of Masonry Infills," edited by D.P. Abrams, 3/1/94, (PB94-180783, A07, MF-A02).

NCEER-94-0005 "The Northridge, California Earthquake of January 17, 1994: General Reconnaissance Report," edited by J.D. Goltz, 3/11/94, (PB94-193943, A10, MF-A03).

NCEER-94-0006 "Seismic Energy Based Fatigue Damage Analysis of Bridge Columns: Part I - Evaluation of Seismic Capacity," by G.A. Chang and J.B. Mander, 3/14/94, (PB94-219185, A11, MF-A03).

NCEER-94-0007 "Seismic Isolation of Multi-Story Frame Structures Using Spherical Sliding Isolation Systems," by T.M. Al-Hussaini, V.A. Zayas and M.C. Constantinou, 3/17/94, (PB94-193745, A09, MF-A02).

NCEER-94-0008 "The Northridge, California Earthquake of January 17, 1994: Performance of Highway Bridges," edited by I.G. Buckle, 3/24/94, (PB94-193851, A06, MF-A02).

NCEER-94-0009 "Proceedings of the Third U.S.-Japan Workshop on Earthquake Protective Systems for Bridges," edited by I.G. Buckle and I. Friedland, 3/31/94, (PB94-195815, A99, MF-A06).

NCEER-94-0010 "3D-BASIS-ME: Computer Program for Nonlinear Dynamic Analysis of Seismically Isolated Single and Multiple Structures and Liquid Storage Tanks," by P.C. Tsopelas, M.C. Constantinou and A.M. Reinhorn, 4/12/94, (PB94-204922, A09, MF-A02).

NCEER-94-0011 "The Northridge, California Earthquake of January 17, 1994: Performance of Gas Transmission Pipelines," by T.D. O'Rourke and M.C. Palmer, 5/16/94, (PB94-204989, A05, MF-A01).

NCEER-94-0012 "Feasibility Study of Replacement Procedures and Earthquake Performance Related to Gas Transmission Pipelines," by T.D. O'Rourke and M.C. Palmer, 5/25/94, (PB94-206638, A09, MF-A02).

NCEER-94-0013 "Seismic Energy Based Fatigue Damage Analysis of Bridge Columns: Part II - Evaluation of Seismic Demand," by G.A. Chang and J.B. Mander, 6/1/94, (PB95-18106, A08, MF-A02).

NCEER-94-0014 "NCEER-Taisei Corporation Research Program on Sliding Seismic Isolation Systems for Bridges: Experimental and Analytical Study of a System Consisting of Sliding Bearings and Fluid Restoring Force/Damping Devices," by P. Tsopelas and M.C. Constantinou, 6/13/94, (PB94-219144, A10, MF-A03).

NCEER-94-0015 "Generation of Hazard-Consistent Fragility Curves for Seismic Loss Estimation Studies," by H. Hwang and J-R. Huo, 6/14/94, (PB95-181996, A09, MF-A02).

NCEER-94-0016 "Seismic Study of Building Frames with Added Energy-Absorbing Devices," by W.S. Pong, C.S. Tsai and G.C. Lee, 6/20/94, (PB94-219136, A10, A03).

NCEER-94-0017 "Sliding Mode Control for Seismic-Excited Linear and Nonlinear Civil Engineering Structures," by J. Yang, J. Wu, A. Agrawal and Z. Li, 6/21/94, (PB95-138483, A06, MF-A02).

NCEER-94-0018 "3D-BASIS-TABS Version 2.0: Computer Program for Nonlinear Dynamic Analysis of Three Dimensional Base Isolated Structures," by A.M. Reinhorn, S. Nagarajaiah, M.C. Constantinou, P. Tsopelas and R. Li, 6/22/94, (PB95-182176, A08, MF-A02).

NCEER-94-0019 "Proceedings of the International Workshop on Civil Infrastructure Systems: Application of Intelligent Systems and Advanced Materials on Bridge Systems," Edited by G.C. Lee and K.C. Chang, 7/18/94, (PB95-252474, A20, MF-A04).

NCEER-94-0020 "Study of Seismic Isolation Systems for Computer Floors," by V. Lambrou and M.C. Constantinou, 7/19/94, (PB95-138533, A10, MF-A03).

NCEER-94-0021 "Proceedings of the U.S.-Italian Workshop on Guidelines for Seismic Evaluation and Rehabilitation of Unreinforced Masonry Buildings," Edited by D.P. Abrams and G.M. Calvi, 7/20/94, (PB95-138749, A13, MF-A03).

NCEER-94-0022 "NCEER-Taisei Corporation Research Program on Sliding Seismic Isolation Systems for Bridges: Experimental and Analytical Study of a System Consisting of Lubricated PTFE Sliding Bearings and Mild Steel Dampers," by P. Tsopelas and M.C. Constantinou, 7/22/94, (PB95-182184, A08, MF-A02).

NCEER-94-0023 "Development of Reliability-Based Design Criteria for Buildings Under Seismic Load," by Y.K. Wen, H. Hwang and M. Shinozuka, 8/1/94, (PB95-211934, A08, MF-A02).

NCEER-94-0024 "Experimental Verification of Acceleration Feedback Control Strategies for an Active Tendon System," by S.J. Dyke, B.F. Spencer, Jr., P. Quast, M.K. Sain, D.C. Kaspari, Jr. and T.T. Soong, 8/29/94, (PB95-212320, A05, MF-A01).

NCEER-94-0025 "Seismic Retrofitting Manual for Highway Bridges," Edited by I.G. Buckle and I.F. Friedland, published by the Federal Highway Administration (PB95-212676, A15, MF-A03).

NCEER-94-0026 "Proceedings from the Fifth U.S.-Japan Workshop on Earthquake Resistant Design of Lifeline Facilities and Countermeasures Against Soil Liquefaction," Edited by T.D. O'Rourke and M. Hamada, 11/7/94, (PB95-220802, A99, MF-E08).

NCEER-95-0001 "Experimental and Analytical Investigation of Seismic Retrofit of Structures with Supplemental Damping: Part 1 - Fluid Viscous Damping Devices," by A.M. Reinhorn, C. Li and M.C. Constantinou, 1/3/95, (PB95-266599, A09, MF-A02).

NCEER-95-0002 "Experimental and Analytical Study of Low-Cycle Fatigue Behavior of Semi-Rigid Top-And-Seat Angle Connections," by G. Pekcan, J.B. Mander and S.S. Chen, 1/5/95, (PB95-220042, A07, MF-A02).

NCEER-95-0003 "NCEER-ATC Joint Study on Fragility of Buildings," by T. Anagnos, C. Rojahn and A.S. Kiremidjian, 1/20/95, (PB95-220026, A06, MF-A02).

NCEER-95-0004 "Nonlinear Control Algorithms for Peak Response Reduction," by Z. Wu, T.T. Soong, V. Gattulli and R.C. Lin, 2/16/95, (PB95-220349, A05, MF-A01).

NCEER-95-0005 "Pipeline Replacement Feasibility Study: A Methodology for Minimizing Seismic and Corrosion Risks to Underground Natural Gas Pipelines," by R.T. Eguchi, H.A. Seligson and D.G. Honegger, 3/2/95, (PB95-252326, A06, MF-A02).

NCEER-95-0006 "Evaluation of Seismic Performance of an 11-Story Frame Building During the 1994 Northridge Earthquake," by F. Naeim, R. DiSulio, K. Benuska, A. Reinhorn and C. Li, not available.

NCEER-95-0007 "Prioritization of Bridges for Seismic Retrofitting," by N. Basöz and A.S. Kiremidjian, 4/24/95, (PB95-252300, A08, MF-A02).

NCEER-95-0008 "Method for Developing Motion Damage Relationships for Reinforced Concrete Frames," by A. Singhal and A.S. Kiremidjian, 5/11/95, (PB95-266607, A06, MF-A02).

NCEER-95-0009 "Experimental and Analytical Investigation of Seismic Retrofit of Structures with Supplemental Damping: Part II - Friction Devices," by C. Li and A.M. Reinhorn, 7/6/95, (PB96-128087, A11, MF-A03).

NCEER-95-0010 "Experimental Performance and Analytical Study of a Non-Ductile Reinforced Concrete Frame Structure Retrofitted with Elastomeric Spring Dampers," by G. Pekcan, J.B. Mander and S.S. Chen, 7/14/95, (PB96-137161, A08, MF-A02).

NCEER-95-0011 "Development and Experimental Study of Semi-Active Fluid Damping Devices for Seismic Protection of Structures," by M.D. Symans and M.C. Constantinou, 8/3/95, (PB96-136940, A23, MF-A04).

NCEER-95-0012 "Real-Time Structural Parameter Modification (RSPM): Development of Innervated Structures," by Z. Liang, M. Tong and G.C. Lee, 4/11/95, (PB96-137153, A06, MF-A01).

NCEER-95-0013 "Experimental and Analytical Investigation of Seismic Retrofit of Structures with Supplemental Damping: Part III - Viscous Damping Walls," by A.M. Reinhorn and C. Li, 10/1/95, (PB96-176409, A11, MF-A03).

NCEER-95-0014 "Seismic Fragility Analysis of Equipment and Structures in a Memphis Electric Substation," by J-R. Huo and H.H.M. Hwang, 8/10/95, (PB96-128087, A09, MF-A02).

NCEER-95-0015 "The Hanshin-Awaji Earthquake of January 17, 1995: Performance of Lifelines," Edited by M. Shinozuka, 11/3/95, (PB96-176383, A15, MF-A03).

NCEER-95-0016 "Highway Culvert Performance During Earthquakes," by T.L. Youd and C.J. Beckman, available as NCEER-96-0015.

NCEER-95-0017 "The Hanshin-Awaji Earthquake of January 17, 1995: Performance of Highway Bridges," Edited by I.G. Buckle, 12/1/95, not available.

NCEER-95-0018 "Modeling of Masonry Infill Panels for Structural Analysis," by A.M. Reinhorn, A. Madan, R.E. Valles, Y. Reichmann and J.B. Mander, 12/8/95, (PB97-110886, MF-A01, A06).

NCEER-95-0019 "Optimal Polynomial Control for Linear and Nonlinear Structures," by A.K. Agrawal and J.N. Yang, 12/11/95, (PB96-168737, A07, MF-A02).

NCEER-95-0020 "Retrofit of Non-Ductile Reinforced Concrete Frames Using Friction Dampers," by R.S. Rao, P. Gergely and R.N. White, 12/22/95, (PB97-133508, A10, MF-A02).

NCEER-95-0021 "Parametric Results for Seismic Response of Pile-Supported Bridge Bents," by G. Mylonakis, A. Nikolaou and G. Gazetas, 12/22/95, (PB97-100242, A12, MF-A03).

NCEER-95-0022 "Kinematic Bending Moments in Seismically Stressed Piles," by A. Nikolaou, G. Mylonakis and G. Gazetas, 12/23/95, (PB97-113914, MF-A03, A13).

NCEER-96-0001 "Dynamic Response of Unreinforced Masonry Buildings with Flexible Diaphragms," by A.C. Costley and D.P. Abrams," 10/10/96, (PB97-133573, MF-A03, A15).

NCEER-96-0002 "State of the Art Review: Foundations and Retaining Structures," by I. Po Lam, not available.

NCEER-96-0003 "Ductility of Rectangular Reinforced Concrete Bridge Columns with Moderate Confinement," by N. Wehbe, M. Saiidi, D. Sanders and B. Douglas, 11/7/96, (PB97-133557, A06, MF-A02).

NCEER-96-0004 "Proceedings of the Long-Span Bridge Seismic Research Workshop," edited by I.G. Buckle and I.M. Friedland, not available.

NCEER-96-0005 "Establish Representative Pier Types for Comprehensive Study: Eastern United States," by J. Kulicki and Z. Prucz, 5/28/96, (PB98-119217, A07, MF-A02).

NCEER-96-0006 "Establish Representative Pier Types for Comprehensive Study: Western United States," by R. Imbsen, R.A. Schamber and T.A. Osterkamp, 5/28/96, (PB98-118607, A07, MF-A02).

NCEER-96-0007 "Nonlinear Control Techniques for Dynamical Systems with Uncertain Parameters," by R.G. Ghanem and M.I. Bujakov, 5/27/96, (PB97-100259, A17, MF-A03).

NCEER-96-0008 "Seismic Evaluation of a 30-Year Old Non-Ductile Highway Bridge Pier and Its Retrofit," by J.B. Mander, B. Mahmoodzadegan, S. Bhadra and S.S. Chen, 5/31/96, (PB97-110902, MF-A03, A10).

NCEER-96-0009 "Seismic Performance of a Model Reinforced Concrete Bridge Pier Before and After Retrofit," by J.B. Mander, J.H. Kim and C.A. Ligozio, 5/31/96, (PB97-110910, MF-A02, A10).

NCEER-96-0010 "IDARC2D Version 4.0: A Computer Program for the Inelastic Damage Analysis of Buildings," by R.E. Valles, A.M. Reinhorn, S.K. Kunnath, C. Li and A. Madan, 6/3/96, (PB97-100234, A17, MF-A03).

NCEER-96-0011 "Estimation of the Economic Impact of Multiple Lifeline Disruption: Memphis Light, Gas and Water Division Case Study," by S.E. Chang, H.A. Seligson and R.T. Eguchi, 8/16/96, (PB97-133490, A11, MF-A03).

NCEER-96-0012 "Proceedings from the Sixth Japan-U.S. Workshop on Earthquake Resistant Design of Lifeline Facilities and Countermeasures Against Soil Liquefaction, Edited by M. Hamada and T. O'Rourke, 9/11/96, (PB97-133581, A99, MF-A06).

NCEER-96-0013 "Chemical Hazards, Mitigation and Preparedness in Areas of High Seismic Risk: A Methodology for Estimating the Risk of Post-Earthquake Hazardous Materials Release," by H.A. Seligson, R.T. Eguchi, K.J. Tierney and K. Richmond, 11/7/96, (PB97-133565, MF-A02, A08).

NCEER-96-0014 "Response of Steel Bridge Bearings to Reversed Cyclic Loading," by J.B. Mander, D-K. Kim, S.S. Chen and G.J. Premus, 11/13/96, (PB97-140735, A12, MF-A03).

NCEER-96-0015 "Highway Culvert Performance During Past Earthquakes," by T.L. Youd and C.J. Beckman, 11/25/96, (PB97-133532, A06, MF-A01).

NCEER-97-0001 "Evaluation, Prevention and Mitigation of Pounding Effects in Building Structures," by R.E. Valles and A.M. Reinhorn, 2/20/97, (PB97-159552, A14, MF-A03).

NCEER-97-0002 "Seismic Design Criteria for Bridges and Other Highway Structures," by C. Rojahn, R. Mayes, D.G. Anderson, J. Clark, J.H. Hom, R.V. Nutt and M.J. O'Rourke, 4/30/97, (PB97-194658, A06, MF-A03).

NCEER-97-0003 "Proceedings of the U.S.-Italian Workshop on Seismic Evaluation and Retrofit," Edited by D.P. Abrams and G.M. Calvi, 3/19/97, (PB97-194666, A13, MF-A03).

NCEER-97-0004 "Investigation of Seismic Response of Buildings with Linear and Nonlinear Fluid Viscous Dampers," by A.A. Seleemah and M.C. Constantinou, 5/21/97, (PB98-109002, A15, MF-A03).

NCEER-97-0005 "Proceedings of the Workshop on Earthquake Engineering Frontiers in Transportation Facilities," edited by G.C. Lee and I.M. Friedland, 8/29/97, (PB98-128911, A25, MR-A04).

NCEER-97-0006 "Cumulative Seismic Damage of Reinforced Concrete Bridge Piers," by S.K. Kunnath, A. El-Bahy, A. Taylor and W. Stone, 9/2/97, (PB98-108814, A11, MF-A03).

NCEER-97-0007 "Structural Details to Accommodate Seismic Movements of Highway Bridges and Retaining Walls," by R.A. Imbsen, R.A. Schamber, E. Thorkildsen, A. Kartoum, B.T. Martin, T.N. Rosser and J.M. Kulicki, 9/3/97, (PB98-108996, A09, MF-A02).

NCEER-97-0008 "A Method for Earthquake Motion-Damage Relationships with Application to Reinforced Concrete Frames," by A. Singhal and A.S. Kiremidjian, 9/10/97, (PB98-108988, A13, MF-A03).

NCEER-97-0009 "Seismic Analysis and Design of Bridge Abutments Considering Sliding and Rotation," by K. Fishman and R. Richards, Jr., 9/15/97, (PB98-108897, A06, MF-A02).

NCEER-97-0010 "Proceedings of the FHWA/NCEER Workshop on the National Representation of Seismic Ground Motion for New and Existing Highway Facilities," edited by I.M. Friedland, M.S. Power and R.L. Mayes, 9/22/97, (PB98-128903, A21, MF-A04).

NCEER-97-0011 "Seismic Analysis for Design or Retrofit of Gravity Bridge Abutments," by K.L. Fishman, R. Richards, Jr. and R.C. Divito, 10/2/97, (PB98-128937, A08, MF-A02).

NCEER-97-0012 "Evaluation of Simplified Methods of Analysis for Yielding Structures," by P. Tsopelas, M.C. Constantinou, C.A. Kircher and A.S. Whittaker, 10/31/97, (PB98-128929, A10, MF-A03).

NCEER-97-0013 "Seismic Design of Bridge Columns Based on Control and Repairability of Damage," by C-T. Cheng and J.B. Mander, 12/8/97, (PB98-144249, A11, MF-A03).

NCEER-97-0014 "Seismic Resistance of Bridge Piers Based on Damage Avoidance Design," by J.B. Mander and C-T. Cheng, 12/10/97, (PB98-144223, A09, MF-A02).

NCEER-97-0015 “Seismic Response of Nominally Symmetric Systems with Strength Uncertainty,” by S. Balopoulou and M. Grigoriu, 12/23/97, (PB98-153422, A11, MF-A03).

NCEER-97-0016 “Evaluation of Seismic Retrofit Methods for Reinforced Concrete Bridge Columns,” by T.J. Wipf, F.W. Klaiber and F.M. Russo, 12/28/97, (PB98-144215, A12, MF-A03).

NCEER-97-0017 “Seismic Fragility of Existing Conventional Reinforced Concrete Highway Bridges,” by C.L. Mullen and A.S. Cakmak, 12/30/97, (PB98-153406, A08, MF-A02).

NCEER-97-0018 “Loss Asssessment of Memphis Buildings,” edited by D.P. Abrams and M. Shinozuka, 12/31/97, (PB98-144231, A13, MF-A03).

NCEER-97-0019 “Seismic Evaluation of Frames with Infill Walls Using Quasi-static Experiments,” by K.M. Mosalam, R.N. White and P. Gergely, 12/31/97, (PB98-153455, A07, MF-A02).

NCEER-97-0020 “Seismic Evaluation of Frames with Infill Walls Using Pseudo-dynamic Experiments,” by K.M. Mosalam, R.N. White and P. Gergely, 12/31/97, (PB98-153430, A07, MF-A02).

NCEER-97-0021 “Computational Strategies for Frames with Infill Walls: Discrete and Smeared Crack Analyses and Seismic Fragility,” by K.M. Mosalam, R.N. White and P. Gergely, 12/31/97, (PB98-153414, A10, MF-A02).

NCEER-97-0022 “Proceedings of the NCEER Workshop on Evaluation of Liquefaction Resistance of Soils,” edited by T.L. Youd and I.M. Idriss, 12/31/97, (PB98-155617, A15, MF-A03).

MCEER-98-0001 “Extraction of Nonlinear Hysteretic Properties of Seismically Isolated Bridges from Quick-Release Field Tests,” by Q. Chen, B.M. Douglas, E.M. Maragakis and I.G. Buckle, 5/26/98, (PB99-118838, A06, MF-A01).

MCEER-98-0002 “Methodologies for Evaluating the Importance of Highway Bridges,” by A. Thomas, S. Eshenaur and J. Kulicki, 5/29/98, (PB99-118846, A10, MF-A02).

MCEER-98-0003 “Capacity Design of Bridge Piers and the Analysis of Overstrength,” by J.B. Mander, A. Dutta and P. Goel, 6/1/98, (PB99-118853, A09, MF-A02).

MCEER-98-0004 “Evaluation of Bridge Damage Data from the Loma Prieta and Northridge, California Earthquakes,” by N. Basoz and A. Kiremidjian, 6/2/98, (PB99-118861, A15, MF-A03).

MCEER-98-0005 “Screening Guide for Rapid Assessment of Liquefaction Hazard at Highway Bridge Sites,” by T. L. Youd, 6/16/98, (PB99-118879, A06, not available on microfiche).

MCEER-98-0006 “Structural Steel and Steel/Concrete Interface Details for Bridges,” by P. Ritchie, N. Kauhl and J. Kulicki, 7/13/98, (PB99-118945, A06, MF-A01).

MCEER-98-0007 “Capacity Design and Fatigue Analysis of Confined Concrete Columns,” by A. Dutta and J.B. Mander, 7/14/98, (PB99-118960, A14, MF-A03).

MCEER-98-0008 “Proceedings of the Workshop on Performance Criteria for Telecommunication Services Under Earthquake Conditions,” edited by A.J. Schiff, 7/15/98, (PB99-118952, A08, MF-A02).

MCEER-98-0009 “Fatigue Analysis of Unconfined Concrete Columns,” by J.B. Mander, A. Dutta and J.H. Kim, 9/12/98, (PB99-123655, A10, MF-A02).

MCEER-98-0010 “Centrifuge Modeling of Cyclic Lateral Response of Pile-Cap Systems and Seat-Type Abutments in Dry Sands,” by A.D. Gadre and R. Dobry, 10/2/98, (PB99-123606, A13, MF-A03).

MCEER-98-0011 “IDARC-BRIDGE: A Computational Platform for Seismic Damage Assessment of Bridge Structures,” by A.M. Reinhorn, V. Simeonov, G. Mylonakis and Y. Reichman, 10/2/98, (PB99-162919, A15, MF-A03).

MCEER-98-0012 “Experimental Investigation of the Dynamic Response of Two Bridges Before and After Retrofitting with Elastomeric Bearings,” by D.A. Wendichansky, S.S. Chen and J.B. Mander, 10/2/98, (PB99-162927, A15, MF-A03).

MCEER-98-0013 “Design Procedures for Hinge Restrainers and Hinge Sear Width for Multiple-Frame Bridges,” by R. Des Roches and G.L. Fenves, 11/3/98, (PB99-140477, A13, MF-A03).

MCEER-98-0014 “Response Modification Factors for Seismically Isolated Bridges,” by M.C. Constantinou and J.K. Quarshie, 11/3/98, (PB99-140485, A14, MF-A03).

MCEER-98-0015 “Proceedings of the U.S.-Italy Workshop on Seismic Protective Systems for Bridges,” edited by I.M. Friedland and M.C. Constantinou, 11/3/98, (PB2000-101711, A22, MF-A04).

MCEER-98-0016 “Appropriate Seismic Reliability for Critical Equipment Systems: Recommendations Based on Regional Analysis of Financial and Life Loss,” by K. Porter, C. Scawthorn, C. Taylor and N. Blais, 11/10/98, (PB99-157265, A08, MF-A02).

MCEER-98-0017 “Proceedings of the U.S. Japan Joint Seminar on Civil Infrastructure Systems Research,” edited by M. Shinozuka and A. Rose, 11/12/98, (PB99-156713, A16, MF-A03).

MCEER-98-0018 “Modeling of Pile Footings and Drilled Shafts for Seismic Design,” by I. PoLam, M. Kapuskar and D. Chaudhuri, 12/21/98, (PB99-157257, A09, MF-A02).

MCEER-99-0001 "Seismic Evaluation of a Masonry Infilled Reinforced Concrete Frame by Pseudodynamic Testing," by S.G. Buonopane and R.N. White, 2/16/99, (PB99-162851, A09, MF-A02).

MCEER-99-0002 "Response History Analysis of Structures with Seismic Isolation and Energy Dissipation Systems: Verification Examples for Program SAP2000," by J. Scheller and M.C. Constantinou, 2/22/99, (PB99-162869, A08, MF-A02).

MCEER-99-0003 "Experimental Study on the Seismic Design and Retrofit of Bridge Columns Including Axial Load Effects," by A. Dutta, T. Kokorina and J.B. Mander, 2/22/99, (PB99-162877, A09, MF-A02).

MCEER-99-0004 "Experimental Study of Bridge Elastomeric and Other Isolation and Energy Dissipation Systems with Emphasis on Uplift Prevention and High Velocity Near-source Seismic Excitation," by A. Kasalanati and M. C. Constantinou, 2/26/99, (PB99-162885, A12, MF-A03).

MCEER-99-0005 "Truss Modeling of Reinforced Concrete Shear-flexure Behavior," by J.H. Kim and J.B. Mander, 3/8/99, (PB99-163693, A12, MF-A03).

MCEER-99-0006 "Experimental Investigation and Computational Modeling of Seismic Response of a 1:4 Scale Model Steel Structure with a Load Balancing Supplemental Damping System," by G. Pekcan, J.B. Mander and S.S. Chen, 4/2/99, (PB99-162893, A11, MF-A03).

MCEER-99-0007 "Effect of Vertical Ground Motions on the Structural Response of Highway Bridges," by M.R. Button, C.J. Cronin and R.L. Mayes, 4/10/99, (PB2000-101411, A10, MF-A03).

MCEER-99-0008 "Seismic Reliability Assessment of Critical Facilities: A Handbook, Supporting Documentation, and Model Code Provisions," by G.S. Johnson, R.E. Sheppard, M.D. Quilici, S.J. Eder and C.R. Scawthorn, 4/12/99, (PB2000-101701, A18, MF-A04).

MCEER-99-0009 "Impact Assessment of Selected MCEER Highway Project Research on the Seismic Design of Highway Structures," by C. Rojahn, R. Mayes, D.G. Anderson, J.H. Clark, D'Appolonia Engineering, S. Gloyd and R.V. Nutt, 4/14/99, (PB99-162901, A10, MF-A02).

MCEER-99-0010 "Site Factors and Site Categories in Seismic Codes," by R. Dobry, R. Ramos and M.S. Power, 7/19/99, (PB2000-101705, A08, MF-A02).

MCEER-99-0011 "Restrainer Design Procedures for Multi-Span Simply-Supported Bridges," by M.J. Randall, M. Saiidi, E. Maragakis and T. Isakovic, 7/20/99, (PB2000-101702, A10, MF-A02).

MCEER-99-0012 "Property Modification Factors for Seismic Isolation Bearings," by M.C. Constantinou, P. Tsopelas, A. Kasalanati and E. Wolff, 7/20/99, (PB2000-103387, A11, MF-A03).

MCEER-99-0013 "Critical Seismic Issues for Existing Steel Bridges," by P. Ritchie, N. Kauhl and J. Kulicki, 7/20/99, (PB2000-101697, A09, MF-A02).

MCEER-99-0014 "Nonstructural Damage Database," by A. Kao, T.T. Soong and A. Vender, 7/24/99, (PB2000-101407, A06, MF-A01).

MCEER-99-0015 "Guide to Remedial Measures for Liquefaction Mitigation at Existing Highway Bridge Sites," by H.G. Cooke and J. K. Mitchell, 7/26/99, (PB2000-101703, A11, MF-A03).

MCEER-99-0016 "Proceedings of the MCEER Workshop on Ground Motion Methodologies for the Eastern United States," edited by N. Abrahamson and A. Becker, 8/11/99, (PB2000-103385, A07, MF-A02).

MCEER-99-0017 "Quindío, Colombia Earthquake of January 25, 1999: Reconnaissance Report," by A.P. Asfura and P.J. Flores, 10/4/99, (PB2000-106893, A06, MF-A01).

MCEER-99-0018 "Hysteretic Models for Cyclic Behavior of Deteriorating Inelastic Structures," by M.V. Sivaselvan and A.M. Reinhorn, 11/5/99, (PB2000-103386, A08, MF-A02).

MCEER-99-0019 "Proceedings of the 7th U.S.- Japan Workshop on Earthquake Resistant Design of Lifeline Facilities and Countermeasures Against Soil Liquefaction," edited by T.D. O'Rourke, J.P. Bardet and M. Hamada, 11/19/99, (PB2000-103354, A99, MF-A06).

MCEER-99-0020 "Development of Measurement Capability for Micro-Vibration Evaluations with Application to Chip Fabrication Facilities," by G.C. Lee, Z. Liang, J.W. Song, J.D. Shen and W.C. Liu, 12/1/99, (PB2000-105993, A08, MF-A02).

MCEER-99-0021 "Design and Retrofit Methodology for Building Structures with Supplemental Energy Dissipating Systems," by G. Pekcan, J.B. Mander and S.S. Chen, 12/31/99, (PB2000-105994, A11, MF-A03).

MCEER-00-0001 "The Marmara, Turkey Earthquake of August 17, 1999: Reconnaissance Report," edited by C. Scawthorn; with major contributions by M. Bruneau, R. Eguchi, T. Holzer, G. Johnson, J. Mander, J. Mitchell, W. Mitchell, A. Papageorgiou, C. Scaethorn, and G. Webb, 3/23/00, (PB2000-106200, A11, MF-A03).

MCEER-00-0002 "Proceedings of the MCEER Workshop for Seismic Hazard Mitigation of Health Care Facilities," edited by G.C. Lee, M. Ettouney, M. Grigoriu, J. Hauer and J. Nigg, 3/29/00, (PB2000-106892, A08, MF-A02).

MCEER-00-0003 "The Chi-Chi, Taiwan Earthquake of September 21, 1999: Reconnaissance Report," edited by G.C. Lee and C.H. Loh, with major contributions by G.C. Lee, M. Bruneau, I.G. Buckle, S.E. Chang, P.J. Flores, T.D. O'Rourke, M. Shinozuka, T.T. Soong, C-H. Loh, K-C. Chang, Z-J. Chen, J-S. Hwang, M-L. Lin, G-Y. Liu, K-C. Tsai, G.C. Yao and C-L. Yen, 4/30/00, (PB2001-100980, A10, MF-A02).

MCEER-00-0004 "Seismic Retrofit of End-Sway Frames of Steel Deck-Truss Bridges with a Supplemental Tendon System: Experimental and Analytical Investigation," by G. Pekcan, J.B. Mander and S.S. Chen, 7/1/00, (PB2001-100982, A10, MF-A02).

MCEER-00-0005 "Sliding Fragility of Unrestrained Equipment in Critical Facilities," by W.H. Chong and T.T. Soong, 7/5/00, (PB2001-100983, A08, MF-A02).

MCEER-00-0006 "Seismic Response of Reinforced Concrete Bridge Pier Walls in the Weak Direction," by N. Abo-Shadi, M. Saiidi and D. Sanders, 7/17/00, (PB2001-100981, A17, MF-A03).

MCEER-00-0007 "Low-Cycle Fatigue Behavior of Longitudinal Reinforcement in Reinforced Concrete Bridge Columns," by J. Brown and S.K. Kunnath, 7/23/00, (PB2001-104392, A08, MF-A02).

MCEER-00-0008 "Soil Structure Interaction of Bridges for Seismic Analysis," I. PoLam and H. Law, 9/25/00, (PB2001-105397, A08, MF-A02).

MCEER-00-0009 "Proceedings of the First MCEER Workshop on Mitigation of Earthquake Disaster by Advanced Technologies (MEDAT-1), edited by M. Shinozuka, D.J. Inman and T.D. O'Rourke, 11/10/00, (PB2001-105399, A14, MF-A03).

MCEER-00-0010 "Development and Evaluation of Simplified Procedures for Analysis and Design of Buildings with Passive Energy Dissipation Systems, Revision 01," by O.M. Ramirez, M.C. Constantinou, C.A. Kircher, A.S. Whittaker, M.W. Johnson, J.D. Gomez and C. Chrysostomou, 11/16/01, (PB2001-105523, A23, MF-A04).

MCEER-00-0011 "Dynamic Soil-Foundation-Structure Interaction Analyses of Large Caissons," by C-Y. Chang, C-M. Mok, Z-L. Wang, R. Settgast, F. Waggoner, M.A. Ketchum, H.M. Gonnermann and C-C. Chin, 12/30/00, (PB2001-104373, A07, MF-A02).

MCEER-00-0012 "Experimental Evaluation of Seismic Performance of Bridge Restrainers," by A.G. Vlassis, E.M. Maragakis and M. Saiid Saiidi, 12/30/00, (PB2001-104354, A09, MF-A02).

MCEER-00-0013 "Effect of Spatial Variation of Ground Motion on Highway Structures," by M. Shinozuka, V. Saxena and G. Deodatis, 12/31/00, (PB2001-108755, A13, MF-A03).

MCEER-00-0014 "A Risk-Based Methodology for Assessing the Seismic Performance of Highway Systems," by S.D. Werner, C.E. Taylor, J.E. Moore, II, J.S. Walton and S. Cho, 12/31/00, (PB2001-108756, A14, MF-A03).

MCEER-01-0001 “Experimental Investigation of P-Delta Effects to Collapse During Earthquakes,” by D. Vian and M. Bruneau, 6/25/01, (PB2002-100534, A17, MF-A03).

MCEER-01-0002 “Proceedings of the Second MCEER Workshop on Mitigation of Earthquake Disaster by Advanced Technologies (MEDAT-2),” edited by M. Bruneau and D.J. Inman, 7/23/01, (PB2002-100434, A16, MF-A03).

MCEER-01-0003 “Sensitivity Analysis of Dynamic Systems Subjected to Seismic Loads,” by C. Roth and M. Grigoriu, 9/18/01, (PB2003-100884, A12, MF-A03).

MCEER-01-0004 “Overcoming Obstacles to Implementing Earthquake Hazard Mitigation Policies: Stage 1 Report,” by D.J. Alesch and W.J. Petak, 12/17/01, (PB2002-107949, A07, MF-A02).

MCEER-01-0005 “Updating Real-Time Earthquake Loss Estimates: Methods, Problems and Insights,” by C.E. Taylor, S.E. Chang and R.T. Eguchi, 12/17/01, (PB2002-107948, A05, MF-A01).

MCEER-01-0006 “Experimental Investigation and Retrofit of Steel Pile Foundations and Pile Bents Under Cyclic Lateral Loadings,” by A. Shama, J. Mander, B. Blabac and S. Chen, 12/31/01, (PB2002-107950, A13, MF-A03).

MCEER-02-0001 “Assessment of Performance of Bolu Viaduct in the 1999 Duzce Earthquake in Turkey” by P.C. Roussis, M.C. Constantinou, M. Erdik, E. Durukal and M. Dicleli, 5/8/02, (PB2003-100883, A08, MF-A02).

MCEER-02-0002 “Seismic Behavior of Rail Counterweight Systems of Elevators in Buildings,” by M.P. Singh, Rildova and L.E. Suarez, 5/27/02. (PB2003-100882, A11, MF-A03).

MCEER-02-0003 “Development of Analysis and Design Procedures for Spread Footings,” by G. Mylonakis, G. Gazetas, S. Nikolaou and A. Chauncey, 10/02/02, (PB2004-101636, A13, MF-A03, CD-A13).

MCEER-02-0004 “Bare-Earth Algorithms for Use with SAR and LIDAR Digital Elevation Models,” by C.K. Huyck, R.T. Eguchi and B. Houshmand, 10/16/02, (PB2004-101637, A07, CD-A07).

MCEER-02-0005 "Review of Energy Dissipation of Compression Members in Concentrically Braced Frames," by K.Lee and M. Bruneau, 10/18/02, (PB2004-101638, A10, CD-A10).

MCEER-03-0001 "Experimental Investigation of Light-Gauge Steel Plate Shear Walls for the Seismic Retrofit of Buildings" by J. Berman and M. Bruneau, 5/2/03, (PB2004-101622, A10, MF-A03, CD-A10).

MCEER-03-0002 "Statistical Analysis of Fragility Curves," by M. Shinozuka, M.Q. Feng, H. Kim, T. Uzawa and T. Ueda, 6/16/03, (PB2004-101849, A09, CD-A09).

MCEER-03-0003 "Proceedings of the Eighth U.S.-Japan Workshop on Earthquake Resistant Design f Lifeline Facilities and Countermeasures Against Liquefaction," edited by M. Hamada, J.P. Bardet and T.D. O'Rourke, 6/30/03, (PB2004-104386, A99, CD-A99).

MCEER-03-0004 "Proceedings of the PRC-US Workshop on Seismic Analysis and Design of Special Bridges," edited by L.C. Fan and G.C. Lee, 7/15/03, (PB2004-104387, A14, CD-A14).

MCEER-03-0005 "Urban Disaster Recovery: A Framework and Simulation Model," by S.B. Miles and S.E. Chang, 7/25/03, (PB2004-104388, A07, CD-A07).

MCEER-03-0006 "Behavior of Underground Piping Joints Due to Static and Dynamic Loading," by R.D. Meis, M. Maragakis and R. Siddharthan, 11/17/03, (PB2005-102194, A13, MF-A03, CD-A00).

MCEER-04-0001 "Experimental Study of Seismic Isolation Systems with Emphasis on Secondary System Response and Verification of Accuracy of Dynamic Response History Analysis Methods," by E. Wolff and M. Constantinou, 1/16/04 (PB2005-102195, A99, MF-E08, CD-A00).

MCEER-04-0002 "Tension, Compression and Cyclic Testing of Engineered Cementitious Composite Materials," by K. Kesner and S.L. Billington, 3/1/04, (PB2005-102196, A08, CD-A08).

MCEER-04-0003 "Cyclic Testing of Braces Laterally Restrained by Steel Studs to Enhance Performance During Earthquakes," by O.C. Celik, J.W. Berman and M. Bruneau, 3/16/04, (PB2005-102197, A13, MF-A03, CD-A00).

MCEER-04-0004 "Methodologies for Post Earthquake Building Damage Detection Using SAR and Optical Remote Sensing: Application to the August 17, 1999 Marmara, Turkey Earthquake," by C.K. Huyck, B.J. Adams, S. Cho, R.T. Eguchi, B. Mansouri and B. Houshmand, 6/15/04, (PB2005-104888, A10, CD-A00).

MCEER-04-0005 "Nonlinear Structural Analysis Towards Collapse Simulation: A Dynamical Systems Approach," by M.V. Sivaselvan and A.M. Reinhorn, 6/16/04, (PB2005-104889, A11, MF-A03, CD-A00).

MCEER-04-0006 "Proceedings of the Second PRC-US Workshop on Seismic Analysis and Design of Special Bridges," edited by G.C. Lee and L.C. Fan, 6/25/04, (PB2005-104890, A16, CD-A00).

MCEER-04-0007 "Seismic Vulnerability Evaluation of Axially Loaded Steel Built-up Laced Members," by K. Lee and M. Bruneau, 6/30/04, (PB2005-104891, A16, CD-A00).

MCEER-04-0008 "Evaluation of Accuracy of Simplified Methods of Analysis and Design of Buildings with Damping Systems for Near-Fault and for Soft-Soil Seismic Motions," by E.A. Pavlou and M.C. Constantinou, 8/16/04, (PB2005-104892, A08, MF-A02, CD-A00).

MCEER-04-0009 "Assessment of Geotechnical Issues in Acute Care Facilities in California," by M. Lew, T.D. O'Rourke, R. Dobry and M. Koch, 9/15/04, (PB2005-104893, A08, CD-A00).

MCEER-04-0010 "Scissor-Jack-Damper Energy Dissipation System," by A.N. Sigaher-Boyle and M.C. Constantinou, 12/1/04 (PB2005-108221).

MCEER-04-0011 "Seismic Retrofit of Bridge Steel Truss Piers Using a Controlled Rocking Approach," by M. Pollino and M. Bruneau, 12/20/04 (PB2006-105795).

MCEER-05-0001 "Experimental and Analytical Studies of Structures Seismically Isolated with an Uplift-Restraint Isolation System," by P.C. Roussis and M.C. Constantinou, 1/10/05 (PB2005-108222).

MCEER-05-0002 "A Versatile Experimentation Model for Study of Structures Near Collapse Applied to Seismic Evaluation of Irregular Structures," by D. Kusumastuti, A.M. Reinhorn and A. Rutenberg, 3/31/05 (PB2006-101523).

MCEER-05-0003 "Proceedings of the Third PRC-US Workshop on Seismic Analysis and Design of Special Bridges," edited by L.C. Fan and G.C. Lee, 4/20/05, (PB2006-105796).

MCEER-05-0004 "Approaches for the Seismic Retrofit of Braced Steel Bridge Piers and Proof-of-Concept Testing of an Eccentrically Braced Frame with Tubular Link," by J.W. Berman and M. Bruneau, 4/21/05 (PB2006-101524).

MCEER-05-0005 "Simulation of Strong Ground Motions for Seismic Fragility Evaluation of Nonstructural Components in Hospitals," by A. Wanitkorkul and A. Filiatrault, 5/26/05 (PB2006-500027).

MCEER-05-0006 "Seismic Safety in California Hospitals: Assessing an Attempt to Accelerate the Replacement or Seismic Retrofit of Older Hospital Facilities," by D.J. Alesch, L.A. Arendt and W.J. Petak, 6/6/05 (PB2006-105794).

MCEER-05-0007 "Development of Seismic Strengthening and Retrofit Strategies for Critical Facilities Using Engineered Cementitious Composite Materials," by K. Kesner and S.L. Billington, 8/29/05 (PB2006-111701).

MCEER-05-0008 "Experimental and Analytical Studies of Base Isolation Systems for Seismic Protection of Power Transformers," by N. Murota, M.Q. Feng and G-Y. Liu, 9/30/05 (PB2006-111702).

MCEER-05-0009 "3D-BASIS-ME-MB: Computer Program for Nonlinear Dynamic Analysis of Seismically Isolated Structures," by P.C. Tsopelas, P.C. Roussis, M.C. Constantinou, R. Buchanan and A.M. Reinhorn, 10/3/05 (PB2006-111703).

MCEER-05-0010 "Steel Plate Shear Walls for Seismic Design and Retrofit of Building Structures," by D. Vian and M. Bruneau, 12/15/05 (PB2006-111704).

MCEER-05-0011 "The Performance-Based Design Paradigm," by M.J. Astrella and A. Whittaker, 12/15/05 (PB2006-111705).

MCEER-06-0001 "Seismic Fragility of Suspended Ceiling Systems," H. Badillo-Almaraz, A.S. Whittaker, A.M. Reinhorn and G.P. Cimellaro, 2/4/06 (PB2006-111706).

MCEER-06-0002 "Multi-Dimensional Fragility of Structures," by G.P. Cimellaro, A.M. Reinhorn and M. Bruneau, 3/1/06 (PB2007-106974, A09, MF-A02, CD A00).

MCEER-06-0003 "Built-Up Shear Links as Energy Dissipators for Seismic Protection of Bridges," by P. Dusicka, A.M. Itani and I.G. Buckle, 3/15/06 (PB2006-111708).

MCEER-06-0004 "Analytical Investigation of the Structural Fuse Concept," by R.E. Vargas and M. Bruneau, 3/16/06 (PB2006-111709).

MCEER-06-0005 "Experimental Investigation of the Structural Fuse Concept," by R.E. Vargas and M. Bruneau, 3/17/06 (PB2006-111710).

MCEER-06-0006 "Further Development of Tubular Eccentrically Braced Frame Links for the Seismic Retrofit of Braced Steel Truss Bridge Piers," by J.W. Berman and M. Bruneau, 3/27/06 (PB2007-105147).

MCEER-06-0007 "REDARS Validation Report," by S. Cho, C.K. Huyck, S. Ghosh and R.T. Eguchi, 8/8/06 (PB2007-106983).

MCEER-06-0008 "Review of Current NDE Technologies for Post-Earthquake Assessment of Retrofitted Bridge Columns," by J.W. Song, Z. Liang and G.C. Lee, 8/21/06 (PB2007-106984).

MCEER-06-0009 "Liquefaction Remediation in Silty Soils Using Dynamic Compaction and Stone Columns," by S. Thevanayagam, G.R. Martin, R. Nashed, T. Shenthan, T. Kanagalingam and N. Ecemis, 8/28/06 (PB2007-106985).

MCEER-06-0010 "Conceptual Design and Experimental Investigation of Polymer Matrix Composite Infill Panels for Seismic Retrofitting," by W. Jung, M. Chiewanichakorn and A.J. Aref, 9/21/06 (PB2007-106986).

MCEER-06-0011 "A Study of the Coupled Horizontal-Vertical Behavior of Elastomeric and Lead-Rubber Seismic Isolation Bearings," by G.P. Warn and A.S. Whittaker, 9/22/06 (PB2007-108679).

MCEER-06-0012 "Proceedings of the Fourth PRC-US Workshop on Seismic Analysis and Design of Special Bridges: Advancing Bridge Technologies in Research, Design, Construction and Preservation," Edited by L.C. Fan, G.C. Lee and L. Ziang, 10/12/06 (PB2007-109042).

MCEER-06-0013 "Cyclic Response and Low Cycle Fatigue Characteristics of Plate Steels," by P. Dusicka, A.M. Itani and I.G. Buckle, 11/1/06 06 (PB2007-106987).

MCEER-06-0014 "Proceedings of the Second US-Taiwan Bridge Engineering Workshop," edited by W.P. Yen, J. Shen, J-Y. Chen and M. Wang, 11/15/06 (PB2008-500041).

MCEER-06-0015 "User Manual and Technical Documentation for the REDARS™ Import Wizard," by S. Cho, S. Ghosh, C.K. Huyck and S.D. Werner, 11/30/06 (PB2007-114766).

MCEER-06-0016 "Hazard Mitigation Strategy and Monitoring Technologies for Urban and Infrastructure Public Buildings: Proceedings of the China-US Workshops," edited by X.Y. Zhou, A.L. Zhang, G.C. Lee and M. Tong, 12/12/06 (PB2008-500018).

MCEER-07-0001 "Static and Kinetic Coefficients of Friction for Rigid Blocks," by C. Kafali, S. Fathali, M. Grigoriu and A.S. Whittaker, 3/20/07 (PB2007-114767).

MCEER-07-0002 "Hazard Mitigation Investment Decision Making: Organizational Response to Legislative Mandate," by L.A. Arendt, D.J. Alesch and W.J. Petak, 4/9/07 (PB2007-114768).

MCEER-07-0003 "Seismic Behavior of Bidirectional-Resistant Ductile End Diaphragms with Unbonded Braces in Straight or Skewed Steel Bridges," by O. Celik and M. Bruneau, 4/11/07 (PB2008-105141).

MCEER-07-0004 "Modeling Pile Behavior in Large Pile Groups Under Lateral Loading," by A.M. Dodds and G.R. Martin, 4/16/07(PB2008-105142).

MCEER-07-0005 "Experimental Investigation of Blast Performance of Seismically Resistant Concrete-Filled Steel Tube Bridge Piers," by S. Fujikura, M. Bruneau and D. Lopez-Garcia, 4/20/07 (PB2008-105143).

MCEER-07-0006 "Seismic Analysis of Conventional and Isolated Liquefied Natural Gas Tanks Using Mechanical Analogs," by I.P. Christovasilis and A.S. Whittaker, 5/1/07, not available.

MCEER-07-0007 "Experimental Seismic Performance Evaluation of Isolation/Restraint Systems for Mechanical Equipment – Part 1: Heavy Equipment Study," by S. Fathali and A. Filiatrault, 6/6/07 (PB2008-105144).

MCEER-07-0008 "Seismic Vulnerability of Timber Bridges and Timber Substructures," by A.A. Sharma, J.B. Mander, I.M. Friedland and D.R. Allicock, 6/7/07 (PB2008-105145).

MCEER-07-0009 "Experimental and Analytical Study of the XY-Friction Pendulum (XY-FP) Bearing for Bridge Applications," by C.C. Marin-Artieda, A.S. Whittaker and M.C. Constantinou, 6/7/07 (PB2008-105191).

MCEER-07-0010 "Proceedings of the PRC-US Earthquake Engineering Forum for Young Researchers," Edited by G.C. Lee and X.Z. Qi, 6/8/07 (PB2008-500058).

MCEER-07-0011 "Design Recommendations for Perforated Steel Plate Shear Walls," by R. Purba and M. Bruneau, 6/18/07, (PB2008-105192).

MCEER-07-0012 "Performance of Seismic Isolation Hardware Under Service and Seismic Loading," by M.C. Constantinou, A.S. Whittaker, Y. Kalpakidis, D.M. Fenz and G.P. Warn, 8/27/07, (PB2008-105193).

MCEER-07-0013 "Experimental Evaluation of the Seismic Performance of Hospital Piping Subassemblies," by E.R. Goodwin, E. Maragakis and A.M. Itani, 9/4/07, (PB2008-105194).

MCEER-07-0014 "A Simulation Model of Urban Disaster Recovery and Resilience: Implementation for the 1994 Northridge Earthquake," by S. Miles and S.E. Chang, 9/7/07, (PB2008-106426).

MCEER-07-0015 "Statistical and Mechanistic Fragility Analysis of Concrete Bridges," by M. Shinozuka, S. Banerjee and S-H. Kim, 9/10/07, (PB2008-106427).

MCEER-07-0016 "Three-Dimensional Modeling of Inelastic Buckling in Frame Structures," by M. Schachter and AM. Reinhorn, 9/13/07, (PB2008-108125).

MCEER-07-0017 "Modeling of Seismic Wave Scattering on Pile Groups and Caissons," by I. Po Lam, H. Law and C.T. Yang, 9/17/07 (PB2008-108150).

MCEER-07-0018 "Bridge Foundations: Modeling Large Pile Groups and Caissons for Seismic Design," by I. Po Lam, H. Law and G.R. Martin (Coordinating Author), 12/1/07 (PB2008-111190).

MCEER-07-0019 "Principles and Performance of Roller Seismic Isolation Bearings for Highway Bridges," by G.C. Lee, Y.C. Ou, Z. Liang, T.C. Niu and J. Song, 12/10/07 (PB2009-110466).

MCEER-07-0020 "Centrifuge Modeling of Permeability and Pinning Reinforcement Effects on Pile Response to Lateral Spreading," by L.L Gonzalez-Lagos, T. Abdoun and R. Dobry, 12/10/07 (PB2008-111191).

MCEER-07-0021 "Damage to the Highway System from the Pisco, Perú Earthquake of August 15, 2007," by J.S. O'Connor, L. Mesa and M. Nykamp, 12/10/07, (PB2008-108126).

MCEER-07-0022 "Experimental Seismic Performance Evaluation of Isolation/Restraint Systems for Mechanical Equipment – Part 2: Light Equipment Study," by S. Fathali and A. Filiatrault, 12/13/07 (PB2008-111192).

MCEER-07-0023 "Fragility Considerations in Highway Bridge Design," by M. Shinozuka, S. Banerjee and S.H. Kim, 12/14/07 (PB2008-111193).

MCEER-07-0024 "Performance Estimates for Seismically Isolated Bridges," by G.P. Warn and A.S. Whittaker, 12/30/07 (PB2008-112230).

MCEER-08-0001 "Seismic Performance of Steel Girder Bridge Superstructures with Conventional Cross Frames," by L.P. Carden, A.M. Itani and I.G. Buckle, 1/7/08, (PB2008-112231).

MCEER-08-0002 "Seismic Performance of Steel Girder Bridge Superstructures with Ductile End Cross Frames with Seismic Isolators," by L.P. Carden, A.M. Itani and I.G. Buckle, 1/7/08 (PB2008-112232).

MCEER-08-0003 "Analytical and Experimental Investigation of a Controlled Rocking Approach for Seismic Protection of Bridge Steel Truss Piers," by M. Pollino and M. Bruneau, 1/21/08 (PB2008-112233).

MCEER-08-0004 "Linking Lifeline Infrastructure Performance and Community Disaster Resilience: Models and Multi-Stakeholder Processes," by S.E. Chang, C. Pasion, K. Tatebe and R. Ahmad, 3/3/08 (PB2008-112234).

MCEER-08-0005 "Modal Analysis of Generally Damped Linear Structures Subjected to Seismic Excitations," by J. Song, Y-L. Chu, Z. Liang and G.C. Lee, 3/4/08 (PB2009-102311).

MCEER-08-0006 "System Performance Under Multi-Hazard Environments," by C. Kafali and M. Grigoriu, 3/4/08 (PB2008-112235).

MCEER-08-0007 "Mechanical Behavior of Multi-Spherical Sliding Bearings," by D.M. Fenz and M.C. Constantinou, 3/6/08 (PB2008-112236).

MCEER-08-0008 "Post-Earthquake Restoration of the Los Angeles Water Supply System," by T.H.P. Tabucchi and R.A. Davidson, 3/7/08 (PB2008-112237).

MCEER-08-0009 "Fragility Analysis of Water Supply Systems," by A. Jacobson and M. Grigoriu, 3/10/08 (PB2009-105545).

MCEER-08-0010 "Experimental Investigation of Full-Scale Two-Story Steel Plate Shear Walls with Reduced Beam Section Connections," by B. Qu, M. Bruneau, C-H. Lin and K-C. Tsai, 3/17/08 (PB2009-106368).

MCEER-08-0011 "Seismic Evaluation and Rehabilitation of Critical Components of Electrical Power Systems," S. Ersoy, B. Feizi, A. Ashrafi and M. Ala Saadeghvaziri, 3/17/08 (PB2009-105546).

MCEER-08-0012 "Seismic Behavior and Design of Boundary Frame Members of Steel Plate Shear Walls," by B. Qu and M. Bruneau, 4/26/08 . (PB2009-106744).

MCEER-08-0013 "Development and Appraisal of a Numerical Cyclic Loading Protocol for Quantifying Building System Performance," by A. Filiatrault, A. Wanitkorkul and M. Constantinou, 4/27/08 (PB2009-107906).

MCEER-08-0014 "Structural and Nonstructural Earthquake Design: The Challenge of Integrating Specialty Areas in Designing Complex, Critical Facilities," by W.J. Petak and D.J. Alesch, 4/30/08 (PB2009-107907).

MCEER-08-0015 "Seismic Performance Evaluation of Water Systems," by Y. Wang and T.D. O'Rourke, 5/5/08 (PB2009-107908).

MCEER-08-0016 "Seismic Response Modeling of Water Supply Systems," by P. Shi and T.D. O'Rourke, 5/5/08 (PB2009-107910).

MCEER-08-0017 "Numerical and Experimental Studies of Self-Centering Post-Tensioned Steel Frames," by D. Wang and A. Filiatrault, 5/12/08 (PB2009-110479).

MCEER-08-0018 "Development, Implementation and Verification of Dynamic Analysis Models for Multi-Spherical Sliding Bearings," by D.M. Fenz and M.C. Constantinou, 8/15/08 (PB2009-107911).

MCEER-08-0019 "Performance Assessment of Conventional and Base Isolated Nuclear Power Plants for Earthquake Blast Loadings," by Y.N. Huang, A.S. Whittaker and N. Luco, 10/28/08 (PB2009-107912).

MCEER-08-0020 "Remote Sensing for Resilient Multi-Hazard Disaster Response – Volume I: Introduction to Damage Assessment Methodologies," by B.J. Adams and R.T. Eguchi, 11/17/08 (PB2010-102695).

MCEER-08-0021 "Remote Sensing for Resilient Multi-Hazard Disaster Response – Volume II: Counting the Number of Collapsed Buildings Using an Object-Oriented Analysis: Case Study of the 2003 Bam Earthquake," by L. Gusella, C.K. Huyck and B.J. Adams, 11/17/08 (PB2010-100925).

MCEER-08-0022 "Remote Sensing for Resilient Multi-Hazard Disaster Response – Volume III: Multi-Sensor Image Fusion Techniques for Robust Neighborhood-Scale Urban Damage Assessment," by B.J. Adams and A. McMillan, 11/17/08 (PB2010-100926).

MCEER-08-0023 "Remote Sensing for Resilient Multi-Hazard Disaster Response – Volume IV: A Study of Multi-Temporal and Multi-Resolution SAR Imagery for Post-Katrina Flood Monitoring in New Orleans," by A. McMillan, J.G. Morley, B.J. Adams and S. Chesworth, 11/17/08 (PB2010-100927).

MCEER-08-0024 "Remote Sensing for Resilient Multi-Hazard Disaster Response – Volume V: Integration of Remote Sensing Imagery and VIEWS^{TM} Field Data for Post-Hurricane Charley Building Damage Assessment," by J.A. Womble, K. Mehta and B.J. Adams, 11/17/08 (PB2009-115532).

MCEER-08-0025 "Building Inventory Compilation for Disaster Management: Application of Remote Sensing and Statistical Modeling," by P. Sarabandi, A.S. Kiremidjian, R.T. Eguchi and B. J. Adams, 11/20/08 (PB2009-110484).

MCEER-08-0026 "New Experimental Capabilities and Loading Protocols for Seismic Qualification and Fragility Assessment of Nonstructural Systems," by R. Retamales, G. Mosqueda, A. Filiatrault and A. Reinhorn, 11/24/08 (PB2009-110485).

MCEER-08-0027 "Effects of Heating and Load History on the Behavior of Lead-Rubber Bearings," by I.V. Kalpakidis and M.C. Constantinou, 12/1/08 (PB2009-115533).

MCEER-08-0028 "Experimental and Analytical Investigation of Blast Performance of Seismically Resistant Bridge Piers," by S.Fujikura and M. Bruneau, 12/8/08 (PB2009-115534).

MCEER-08-0029 "Evolutionary Methodology for Aseismic Decision Support," by Y. Hu and G. Dargush, 12/15/08.

MCEER-08-0030 "Development of a Steel Plate Shear Wall Bridge Pier System Conceived from a Multi-Hazard Perspective," by D. Keller and M. Bruneau, 12/19/08 (PB2010-102696).

MCEER-09-0001 "Modal Analysis of Arbitrarily Damped Three-Dimensional Linear Structures Subjected to Seismic Excitations," by Y.L. Chu, J. Song and G.C. Lee, 1/31/09 (PB2010-100922).

MCEER-09-0002 "Air-Blast Effects on Structural Shapes," by G. Ballantyne, A.S. Whittaker, A.J. Aref and G.F. Dargush, 2/2/09 (PB2010-102697).

MCEER-09-0003 "Water Supply Performance During Earthquakes and Extreme Events," by A.L. Bonneau and T.D. O'Rourke, 2/16/09 (PB2010-100923).

MCEER-09-0004 "Generalized Linear (Mixed) Models of Post-Earthquake Ignitions," by R.A. Davidson, 7/20/09 (PB2010-102698).

MCEER-09-0005 "Seismic Testing of a Full-Scale Two-Story Light-Frame Wood Building: NEESWood Benchmark Test," by I.P. Christovasilis, A. Filiatrault and A. Wanitkorkul, 7/22/09 (PB2012-102401).

MCEER-09-0006 "IDARC2D Version 7.0: A Program for the Inelastic Damage Analysis of Structures," by A.M. Reinhorn, H. Roh, M. Sivaselvan, S.K. Kunnath, R.E. Valles, A. Madan, C. Li, R. Lobo and Y.J. Park, 7/28/09 (PB2010-103199).

MCEER-09-0007 "Enhancements to Hospital Resiliency: Improving Emergency Planning for and Response to Hurricanes," by D.B. Hess and L.A. Arendt, 7/30/09 (PB2010-100924).

MCEER-09-0008 "Assessment of Base-Isolated Nuclear Structures for Design and Beyond-Design Basis Earthquake Shaking," by Y.N. Huang, A.S. Whittaker, R.P. Kennedy and R.L. Mayes, 8/20/09 (PB2010-102699).

MCEER-09-0009 "Quantification of Disaster Resilience of Health Care Facilities," by G.P. Cimellaro, C. Fumo, A.M Reinhorn and M. Bruneau, 9/14/09 (PB2010-105384).

MCEER-09-0010 "Performance-Based Assessment and Design of Squat Reinforced Concrete Shear Walls," by C.K. Gulec and A.S. Whittaker, 9/15/09 (PB2010-102700).

MCEER-09-0011 "Proceedings of the Fourth US-Taiwan Bridge Engineering Workshop," edited by W.P. Yen, J.J. Shen, T.M. Lee and R.B. Zheng, 10/27/09 (PB2010-500009).

MCEER-09-0012 "Proceedings of the Special International Workshop on Seismic Connection Details for Segmental Bridge Construction," edited by W. Phillip Yen and George C. Lee, 12/21/09 (PB2012-102402).

MCEER-10-0001 "Direct Displacement Procedure for Performance-Based Seismic Design of Multistory Woodframe Structures," by W. Pang and D. Rosowsky, 4/26/10 (PB2012-102403).

MCEER-10-0002 "Simplified Direct Displacement Design of Six-Story NEESWood Capstone Building and Pre-Test Seismic Performance Assessment," by W. Pang, D. Rosowsky, J. van de Lindt and S. Pei, 5/28/10 (PB2012-102404).

MCEER-10-0003 "Integration of Seismic Protection Systems in Performance-Based Seismic Design of Woodframed Structures," by J.K. Shinde and M.D. Symans, 6/18/10 (PB2012-102405).

MCEER-10-0004 "Modeling and Seismic Evaluation of Nonstructural Components: Testing Frame for Experimental Evaluation of Suspended Ceiling Systems," by A.M. Reinhorn, K.P. Ryu and G. Maddaloni, 6/30/10 (PB2012-102406).

MCEER-10-0005 "Analytical Development and Experimental Validation of a Structural-Fuse Bridge Pier Concept," by S. El-Bahey and M. Bruneau, 10/1/10 (PB2012-102407).

MCEER-10-0006 "A Framework for Defining and Measuring Resilience at the Community Scale: The PEOPLES Resilience Framework," by C.S. Renschler, A.E. Frazier, L.A. Arendt, G.P. Cimellaro, A.M. Reinhorn and M. Bruneau, 10/8/10 (PB2012-102408).

MCEER-10-0007 "Impact of Horizontal Boundary Elements Design on Seismic Behavior of Steel Plate Shear Walls," by R. Purba and M. Bruneau, 11/14/10 (PB2012-102409).

MCEER-10-0008 "Seismic Testing of a Full-Scale Mid-Rise Building: The NEESWood Capstone Test," by S. Pei, J.W. van de Lindt, S.E. Pryor, H. Shimizu, H. Isoda and D.R. Rammer, 12/1/10 (PB2012-102410).

MCEER-10-0009 "Modeling the Effects of Detonations of High Explosives to Inform Blast-Resistant Design," by P. Sherkar, A.S. Whittaker and A.J. Aref, 12/1/10 (PB2012-102411).

MCEER-10-0010 "L'Aquila Earthquake of April 6, 2009 in Italy: Rebuilding a Resilient City to Withstand Multiple Hazards," by G.P. Cimellaro, I.P. Christovasilis, A.M. Reinhorn, A. De Stefano and T. Kirova, 12/29/10.

MCEER-11-0001 "Numerical and Experimental Investigation of the Seismic Response of Light-Frame Wood Structures," by I.P. Christovasilis and A. Filiatrault, 8/8/11 (PB2012-102412).

MCEER-11-0002 "Seismic Design and Analysis of a Precast Segmental Concrete Bridge Model," by M. Anagnostopoulou, A. Filiatrault and A. Aref, 9/15/11.

MCEER-11-0003 'Proceedings of the Workshop on Improving Earthquake Response of Substation Equipment," Edited by A.M. Reinhorn, 9/19/11 (PB2012-102413).

MCEER-11-0004 "LRFD-Based Analysis and Design Procedures for Bridge Bearings and Seismic Isolators," by M.C. Constantinou, I. Kalpakidis, A. Filiatrault and R.A. Ecker Lay, 9/26/11.

MCEER-11-0005 "Experimental Seismic Evaluation, Model Parameterization, and Effects of Cold-Formed Steel-Framed Gypsum Partition Walls on the Seismic Performance of an Essential Facility," by R. Davies, R. Retamales, G. Mosqueda and A. Filiatrault, 10/12/11.

MCEER-11-0006 "Modeling and Seismic Performance Evaluation of High Voltage Transformers and Bushings," by A.M. Reinhorn, K. Oikonomou, H. Roh, A. Schiff and L. Kempner, Jr., 10/3/11.

MCEER-11-0007 "Extreme Load Combinations: A Survey of State Bridge Engineers," by G.C. Lee, Z. Liang, J.J. Shen and J.S. O'Connor, 10/14/11.

MCEER-12-0001 "Simplified Analysis Procedures in Support of Performance Based Seismic Design," by Y.N. Huang and A.S. Whittaker.

MCEER-12-0002 "Seismic Protection of Electrical Transformer Bushing Systems by Stiffening Techniques," by M. Koliou, A. Filiatrault, A.M. Reinhorn and N. Oliveto, 6/1/12.

MCEER-12-0003 "Post-Earthquake Bridge Inspection Guidelines," by J.S. O'Connor and S. Alampalli, 6/8/12.

MCEER-12-0004 "Integrated Design Methodology for Isolated Floor Systems in Single-Degree-of-Freedom Structural Fuse Systems," by S. Cui, M. Bruneau and M.C. Constantinou, 6/13/12.

MCEER-12-0005 "Characterizing the Rotational Components of Earthquake Ground Motion," by D. Basu, A.S. Whittaker and M.C. Constantinou, 6/15/12.

MCEER-12-0006 "Bayesian Fragility for Nonstructural Systems," by C.H. Lee and M.D. Grigoriu, 9/12/12.

MCEER-12-0007 "A Numerical Model for Capturing the In-Plane Seismic Response of Interior Metal Stud Partition Walls," by R.L. Wood and T.C. Hutchinson, 9/12/12.

MCEER-12-0008 "Assessment of Floor Accelerations in Yielding Buildings," by J.D. Wieser, G. Pekcan, A.E. Zaghi, A.M. Itani and E. Maragakis, 10/5/12.

MCEER-13-0001 "Experimental Seismic Study of Pressurized Fire Sprinkler Piping Systems," by Y. Tian, A. Filiatrault and G. Mosqueda, 4/8/13.

MCEER-13-0002 "Enhancing Resource Coordination for Multi-Modal Evacuation Planning," by D.B. Hess, B.W. Conley and C.M. Farrell, 2/8/13.

MCEER-13-0003 "Seismic Response of Base Isolated Buildings Considering Pounding to Moat Walls," by A. Masroor and G. Mosqueda, 2/26/13.

MCEER-13-0004 "Seismic Response Control of Structures Using a Novel Adaptive Passive Negative Stiffness Device," by D.T.R. Pasala, A.A. Sarlis, S. Nagarajaiah, A.M. Reinhorn, M.C. Constantinou and D.P. Taylor, 6/10/13.

MCEER-13-0005 "Negative Stiffness Device for Seismic Protection of Structures," by A.A. Sarlis, D.T.R. Pasala, M.C. Constantinou, A.M. Reinhorn, S. Nagarajaiah and D.P. Taylor, 6/12/13.

MCEER-13-0006 "Emilia Earthquake of May 20, 2012 in Northern Italy: Rebuilding a Resilient Community to Withstand Multiple Hazards," by G.P. Cimellaro, M. Chiriatti, A.M. Reinhorn and L. Tirca, June 30, 2013.

MCEER-13-0007 "Precast Concrete Segmental Components and Systems for Accelerated Bridge Construction in Seismic Regions," by A.J. Aref, G.C. Lee, Y.C. Ou and P. Sideris, with contributions from K.C. Chang, S. Chen, A. Filiatrault and Y. Zhou, June 13, 2013.

MCEER-13-0008 "A Study of U.S. Bridge Failures (1980-2012)," by G.C. Lee, S.B. Mohan, C. Huang and B.N. Fard, June 15, 2013.

MCEER-13-0009 "Development of a Database Framework for Modeling Damaged Bridges," by G.C. Lee, J.C. Qi and C. Huang, June 16, 2013.

MCEER-13-0010 "Model of Triple Friction Pendulum Bearing for General Geometric and Frictional Parameters and for Uplift Conditions," by A.A. Sarlis and M.C. Constantinou, July 1, 2013.

MCEER-13-0011 "Shake Table Testing of Triple Friction Pendulum Isolators under Extreme Conditions," by A.A. Sarlis, M.C. Constantinou and A.M. Reinhorn, July 2, 2013.

MCEER-13-0012 "Theoretical Framework for the Development of MH-LRFD," by G.C. Lee (coordinating author), H.A Capers, Jr., C. Huang, J.M. Kulicki, Z. Liang, T. Murphy, J.J.D. Shen, M. Shinozuka and P.W.H. Yen, July 31, 2013.

MCEER-13-0013 "Seismic Protection of Highway Bridges with Negative Stiffness Devices," by N.K.A. Attary, M.D. Symans, S. Nagarajaiah, A.M. Reinhorn, M.C. Constantinou, A.A. Sarlis, D.T.R. Pasala, and D.P. Taylor, September 3, 2014.

MCEER-14-0001 "Simplified Seismic Collapse Capacity-Based Evaluation and Design of Frame Buildings with and without Supplemental Damping Systems," by M. Hamidia, A. Filiatrault, and A. Aref, May 19, 2014.

MCEER-14-0002 "Comprehensive Analytical Seismic Fragility of Fire Sprinkler Piping Systems," by Siavash Soroushian, Emmanuel "Manos" Maragakis, Arash E. Zaghi, Alicia Echevarria, Yuan Tian and Andre Filiatrault, August 26, 2014.

MCEER-14-0003 "Hybrid Simulation of the Seismic Response of a Steel Moment Frame Building Structure through Collapse," by M. Del Carpio Ramos, G. Mosqueda and D.G. Lignos, October 30, 2014.

MCEER-14-0004 "Blast and Seismic Resistant Concrete-Filled Double Skin Tubes and Modified Steel Jacketed Bridge Columns," by P.P. Fouche and M. Bruneau, June 30, 2015.

MCEER-14-0005 "Seismic Performance of Steel Plate Shear Walls Considering Various Design Approaches," by R. Purba and M. Bruneau, October 31, 2014.

MCEER-14-0006 "Air-Blast Effects on Civil Structures," by Jinwon Shin, Andrew S. Whittaker, Amjad J. Aref and David Cormie, October 30, 2014.

MCEER-14-0007 "Seismic Performance Evaluation of Precast Girders with Field-Cast Ultra High Performance Concrete (UHPC) Connections," by G.C. Lee, C. Huang, J. Song, and J. S. O'Connor, July 31, 2014.

MCEER-14-0008 "Post-Earthquake Fire Resistance of Ductile Concrete-Filled Double-Skin Tube Columns," by Reza Imani, Gilberto Mosqueda and Michel Bruneau, December 1, 2014.

MCEER-14-0009 "Cyclic Inelastic Behavior of Concrete Filled Sandwich Panel Walls Subjected to In-Plane Flexure," by Y. Alzeni and M. Bruneau, December 19, 2014.

MCEER-14-0010 "Analytical and Experimental Investigation of Self-Centering Steel Plate Shear Walls," by D.M. Dowden and M. Bruneau, December 19, 2014.

MCEER-15-0001 "Seismic Analysis of Multi-story Unreinforced Masonry Buildings with Flexible Diaphragms," by J. Aleman, G. Mosqueda and A.S. Whittaker, June 12, 2015.

MCEER-15-0002 "Site Response, Soil-Structure Interaction and Structure-Soil-Structure Interaction for Performance Assessment of Buildings and Nuclear Structures," by C. Bolisetti and A.S. Whittaker, June 15, 2015.

MCEER-15-0003 "Stress Wave Attenuation in Solids for Mitigating Impulsive Loadings," by R. Rafiee-Dehkharghani, A.J. Aref and G. Dargush, August 15, 2015.

MCEER-15-0004 "Computational, Analytical, and Experimental Modeling of Masonry Structures," by K.M. Dolatshahi and A.J. Aref, November 16, 2015.

MCEER-15-0005 "Property Modification Factors for Seismic Isolators: Design Guidance for Buildings," by W.J. McVitty and M.C. Constantinou, June 30, 2015.

MCEER-15-0006 "Seismic Isolation of Nuclear Power Plants using Sliding Bearings," by Manish Kumar, Andrew S. Whittaker and Michael C. Constantinou, December 27, 2015.

MCEER-15-0007 "Quintuple Friction Pendulum Isolator Behavior, Modeling and Validation," by Donghun Lee and Michael C. Constantinou, December 28, 2015.

MCEER-15-0008 "Seismic Isolation of Nuclear Power Plants using Elastomeric Bearings," by Manish Kumar, Andrew S. Whittaker and Michael C. Constantinou, December 29, 2015.

MCEER-16-0001 "Experimental, Numerical and Analytical Studies on the Seismic Response of Steel-Plate Concrete (SC) Composite Shear Walls," by Siamak Epackachi and Andrew S. Whittaker, June 15, 2016.

MCEER-16-0002 "Seismic Demand in Columns of Steel Frames," by Lisa Shrestha and Michel Bruneau, June 17, 2016.

MCEER-16-0003 "Development and Evaluation of Procedures for Analysis and Design of Buildings with Fluidic Self-Centering Systems" by Shoma Kitayama and Michael C. Constantinou, July 21, 2016.

MCEER-16-0004 "Real Time Control of Shake Tables for Nonlinear Hysteretic Systems," by Ki Pung Ryu and Andrei M. Reinhorn, October 22, 2016.

MCEER-16-0006 "Seismic Isolation of High Voltage Electrical Power Transformers," by Kostis Oikonomou, Michael C. Constantinou, Andrei M. Reinhorn and Leon Kemper, Jr., November 2, 2016.

MCEER-16-0007 "Open Space Damping System Theory and Experimental Validation," by Erkan Polat and Michael C. Constantinou, December 13, 2016.

MCEER-16-0008 "Seismic Response of Low Aspect Ratio Reinforced Concrete Walls for Buildings and Safety-Related Nuclear Applications," by Bismarck N. Luna and Andrew S. Whittaker.

MCEER-16-0009 "Buckling Restrained Braces Applications for Superstructure and Substructure Protection in Bridges," by Xiaone Wei and Michel Bruneau, December 28, 2016.

MCEER-16-0010 "Procedures and Results of Assessment of Seismic Performance of Seismically Isolated Electrical Transformers with Due Consideration for Vertical Isolation and Vertical Ground Motion Effects," by Shoma Kitayama, Michael C. Constantinou and Donghun Lee, December 31, 2016.

MCEER-17-0001 "Diagonal Tension Field Inclination Angle in Steel Plate Shear Walls," by Yushan Fu, Fangbo Wang and Michel Bruneau, February 10, 2017.

MCEER-17-0002 "Behavior of Steel Plate Shear Walls Subjected to Long Duration Earthquakes," by Ramla Qureshi and Michel Bruneau, September 1, 2017.

MCEER-17-0003 "Response of Steel-plate Concrete (SC) Wall Piers to Combined In-plane and Out-of-plane Seismic Loadings," by Brian Terranova, Andrew S. Whittaker, Siamak Epackachi and Nebojsa Orbovic, July 17, 2017.

MCEER-17-0004 "Design of Reinforced Concrete Panels for Wind-borne Missile Impact," by Brian Terranova, Andrew S. Whittaker and Len Schwer, July 18, 2017.

MCEER-17-0005 "A Simple Strategy for Dynamic Substructuring and its Application to Soil-Foundation-Structure Interaction," by Aikaterini Stefanaki and Metttupalayam V. Sivaselvan, December 15, 2017.

MCEER-17-0006 "Dynamics of Cable Structures: Modeling and Applications," by Nicholas D. Oliveto and Mettupalayam V. Sivaselvan, December 1, 2017.

MCEER-17-0007 "Development and Validation of a Combined Horizontal-Vertical Seismic Isolation System for High-Voltage-Power Transformers," by Donghun Lee and Michael C. Constantinou, November 3, 2017.

MCEER-18-0001 "Reduction of Seismic Acceleration Parameters for Temporary Bridge Design," by Conor Stucki and Michel Bruneau, March 22, 2018.

MCEER-18-0002 "Seismic Response of Low Aspect Ratio Reinforced Concrete Walls," by Bismarck N. Luna, Jonathan P. Rivera, Siamak Epackachi and Andrew S. Whittaker, April 21, 2018.

MCEER-18-0003 "Seismic Damage Assessment of Low Aspect Ratio Reinforced Concrete Shear Walls," by Jonathan P. Rivera, Bismarck N. Luna and Andrew S. Whittaker, April 16, 2018.

MCEER-18-0004 "Seismic Performance Assessment of Seismically Isolated Buildings Designed by the Procedures of ASCE/ SEI 7," by Shoma Kitayama and Michael C. Constantinou, April 14, 2018.

MCEER-19-0001 MCEER-19-0001 "Development and Validation of a Seismic Isolation System for Lightweight Residential Construction," by Huseyin Cisalar and Michael C. Constantinou, March 24, 2019.

MCEER-20-0001 "A Multiscale Study of Reinforced Concrete Shear Walls Subjected to Elevated Temperatures," by Alok Deshpande and Andrew S. Whittaker, June 26, 2020.

MCEER-20-0002 "Further Results on the Assessment of Performance of Seismically Isolated Electrical Transformers," by Shoma Kitayama and Michael C. Constantinou, June 30, 2020.

MCEER-20-0003 "Analytical and Numerical Studies of Seismic Fluid-Structure Interaction in Liquid-Filled Vessels – Revision 01," by Ching-Ching Yu and Andrew S. Whittaker, April 16, 2021.

MCEER-22-0001 "Modeling Triple Friction Pendulum Bearings in Program OpenSees Including Frictional Heating Effects," by Hyun-Myung Kim and Michael C. Constantinou, April 18, 2022.

MCEER-22-0002 "Physical and Numerical Simulations of Seismic Fluid-Structure Interaction in Advanced Nuclear Reactors," by Faizan Ul Haq Mir, Ching-Ching Yu, Andrew S. Whittaker and Michael C. Constantinou, July 8, 2022.

MCEER-22-0003 "Impedance-Matching Control Design for Shake-Table Testing and Model-in-the-Loop Simulations," by Sai Sharath Parsi, Mettupalayam V. Sivaselvan and Andrew S. Whittaker, September 30, 2022.

MCEER-22-0004 "Earthquake-Simulator Experiments of a Model of a Seismically-Isolated, Fluoride-Salt Cooled High-Temperature Reactor," by Faizan Ul Haq Mir, Kaivalya M. Lal, Benjamin D. Kosbab, Nam Nguyen, Brian Song, Matthew Clavelli, Kaniel Z. Tilow and Andrew S. Whittaker, October 24, 2022.

MCEER-23-0001 “Mid-height Seismic Isolation of Tall, Slender Equipment in Advanced Nuclear Power Plants,” by Kaivalya M. Lal, Andrew S. Whittaker and Michael C. Constantinou, February 4, 2023.

MCEER-23-0002 “Development of Performance-based Testing Specifications for Seismic Isolators,” by Hyun-Myung Kim and Michael C. Constantinou, August 18, 2023.

MCEER-24-0001 “Guidelines for Implementing Seismic Base Isolation in Advanced Nuclear Reactors – Revision 01,” by Faizan Ul Haq Mir, Ching-Ching Yu, Benjamin M. Carmichael, Brandon M. Chisholm, Jason Redd, Mohamed M. Talaat, Chandrakanth Bolisetti, and Andrew S. Whittaker, March 7, 2025.

MCEER-24-0002 “Shake Table Testing and Model Development and Validation of a Seismic Isolation System for Lightweight Structures,” by Sebastian Lopez Restrepo and Michael C. Constantinou, August 14, 2024.

MCEER-24-0003 “Considerations of Soil-Structure-Interaction for Seismically Isolated Nuclear Reactor Buildings,” by Kaivalya M. Lal, Andrew S. Whittaker, Shahriar Vahdani, Benjamin D. Kosbab, Koroush Shirvan, and Sai Sharath Parsi, September 5, 2024.

MCEER-24-0004 “Seismic Response of Graphite Block Assemblies in a Horizontal Compact HTGR: Experiments, Numerical Simulations and Analytical Modeling,” by Sai Sharath Parsi, Andrew S. Whittaker, Mettupalayam V. Sivaselvan, Enrique Velez-Lopez, W. Robb Stewart, Kaivalya M. Lal and Koroush Shirvan, November 25, 2024.

MCEER: Earthquake Engineering to Extreme Events

University at Buffalo, The State University of New York
133A Ketter Hall | Buffalo, NY 14260
mceer@buffalo.edu; buffalo.edu/mceer

ISSN 1520-295X